

AD-A239 949



2

NAVAL POSTGRADUATE SCHOOL Monterey, California



DTIC
ELECTE
AUG 27 1991
S B D

THESIS

NUMERICAL INVESTIGATION OF THE
EFFECT OF LEADING EDGE GEOMETRY
ON DYNAMIC STALL OF AIRFOILS

by

Lt. Col. Steven P. Grohsmeyer
September 1990

Thesis Advisor: Dr. J. A. Ekaterinaris
Thesis Co-Advisor: Dr. M. F. Platzer

Approved for public release; distribution is unlimited

91 8 26 010

10

91-08868



UNCLASSIFIED

SECURITY CLASSIFICATION OF THIS PAGE

REPORT DOCUMENTATION PAGE				Form Approved OMB No 0704-0188	
1a REPORT SECURITY CLASSIFICATION Unclassified		1b RESTRICTIVE MARKINGS			
2a SECURITY CLASSIFICATION AUTHORITY		3 DISTRIBUTION/AVAILABILITY OF REPORT			
2b DECLASSIFICATION/DOWNGRADING SCHEDULE		Approved for public release; distribution is unlimited			
4. PERFORMING ORGANIZATION REPORT NUMBER(S)		5 MONITORING ORGANIZATION REPORT NUMBER(S)			
6a NAME OF PERFORMING ORGANIZATION Naval Postgraduate School		6b OFFICE SYMBOL (If applicable) 31	7a NAME OF MONITORING ORGANIZATION Naval Postgraduate School		
6c ADDRESS (City, State, and ZIP Code) Monterey, CA 93943-5000		7b ADDRESS (City, State, and ZIP Code) Monterey, CA 93943-5000			
8a. NAME OF FUNDING / SPONSORING ORGANIZATION		8b OFFICE SYMBOL (If applicable)	9 PROCUREMENT INSTRUMENT IDENTIFICATION NUMBER		
8c ADDRESS (City, State, and ZIP Code)		10 SOURCE OF FUNDING NUMBERS			
		PROGRAM ELEMENT NO	PROJECT NO	TASK NO	WORK UNIT ACCESSION NO
11 TITLE (Include Security Classification) NUMERICAL INVESTIGATION OF THE EFFECT OF LEADING EDGE GEOMETRY ON THE DYNAMIC STALL OF AIRFOILS					
12 PERSONAL AUTHOR(S) GROHMEYER, STEVEN P.					
13a TYPE OF REPORT Master's Thesis		13b TIME COVERED FROM _____ TO _____	14 DATE OF REPORT (Year, Month, Day) 1990 September	15 PAGE COUNT 182	
16 SUPPLEMENTARY NOTATION The views expressed in this thesis are those of the author and do not reflect the official policy or position of the Department of Defence or the U.S. Government.					
17 COSATI CODES			18 SUBJECT TERMS (Continue on reverse if necessary and identify by block number)		
FIELD	GROUP	SUB-GROUP	Dynamic Stall, Oscillating Airfoil, Pitching Airfoil, Leading Edge Geometry, Pressure Gradient		
19 ABSTRACT (Continue on reverse if necessary and identify by block number) The dynamic stall of rapidly pitching and oscillating airfoils is investigated by the numerical solution of the full compressible unsteady two-dimensional Navier-Stokes equations using an alternating-direction-implicit scheme. The flow is assumed to be fully turbulent, and the turbulent stresses are modelled by the Baldwin-Lomax eddy viscosity model. Three airfoils (NACA 0012, NACA 0012-33, and NACA 0012-63) are analyzed for the purpose of examining the influence of leading-edge geometry on unsteady flow separation. It is found that a larger leading edge radius, thicker contouring of the forward part of the airfoil, or increasing reduced frequency results in delaying flow separation and formation of the dynamic stall vortex to a higher angle of attack, yielding higher peak C _L . Within the scope of this study, the pressure gradient encountered by the flow at initial separation is found to be independent of reduced frequency and freestream speed. The critical pressure gradient is dependent on leading edge radius and increases for decreasing leading edge radius.					
20 DISTRIBUTION/AVAILABILITY OF ABSTRACT <input checked="" type="checkbox"/> UNCLASSIFIED/UNLIMITED <input type="checkbox"/> SAME AS PPT <input type="checkbox"/> DTIC USERS			21 ABSTRACT SECURITY CLASSIFICATION Unclassified		
22a NAME OF RESPONSIBLE INDIVIDUAL M.F. Platzer		22b TELEPHONE (Include Area Code) (408)646-2058	22c OFFICE SYMBOL Code 31AAPL		

DD Form 1473, JUN 86

Previous editions are obsolete

SECURITY CLASSIFICATION OF THIS PAGE

S/N 0102-LF-014-6603

UNCLASSIFIED

Approved for public release; distribution is unlimited.

Numerical Investigation of the
Effect of Leading Edge Geometry on
Dynamic Stall of Airfoils

by

Steven P. Grohsmeyer
Lieutenant Colonel, United States Marine Corps
B.S., Illinois Benedictine College, 1973

Submitted in partial fulfillment of the
requirements for the degrees of

AERONAUTICAL ENGINEER

and

MASTER OF SCIENCE IN AERONAUTICAL ENGINEERING

from the

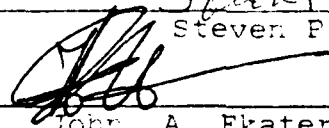
NAVAL POSTGRADUATE SCHOOL
September 1990

Author:

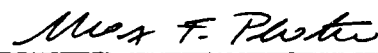


Steven P. Grohsmeyer

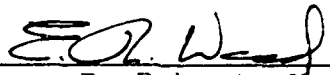
Approved by:



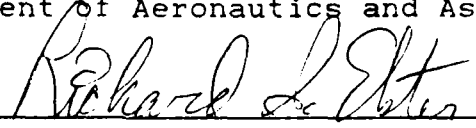
John A. Ekaterinaris, Thesis Advisor



Max F. Platzer, Thesis Co-Advisor



E. Roberts Wood, Chairman,
Department of Aeronautics and Astronautics



Richard S. Elster, Dean of Instruction

ABSTRACT

The dynamic stall of rapidly pitching and oscillating airfoils is investigated by the numerical solution of the full compressible unsteady two-dimensional Navier-Stokes equations using an alternating-direction-implicit scheme. The flow is assumed to be fully turbulent, and the turbulent stresses are modelled by the Baldwin-Lomax eddy viscosity model. Three airfoils (NACA 0012, NACA 0012-33, and NACA 0012-63) are analyzed for the purpose of examining the influence of leading-edge geometry on unsteady flow separation. It is found that a larger leading edge radius, thicker contouring of the forward part of the airfoil, or increasing reduced frequency results in delaying flow separation and formation of the dynamic stall vortex to a higher angle of attack, yielding higher peak C_l . Within the scope of this study, the pressure gradient encountered by the flow at initial separation is found to be independent of reduced frequency and freestream speed. The critical pressure gradient is dependent on leading edge radius and increases for decreasing leading edge radius.

TABLE OF CONTENTS

I.	INTRODUCTION	1
A.	BACKGROUND	1
B.	PURPOSE	5
C.	AIRFOIL SELECTION	6
II.	GOVERNING EQUATIONS	9
A.	CONTINUITY EQUATION	9
B.	THE MOMENTUM (NAVIER-STOKES) EQUATIONS	10
C.	THE ENERGY EQUATION	14
D.	CONSERVATION LAW FORM OF THE GOVERNING EQUATIONS	17
III.	NUMERICAL APPROACH	22
A.	NUMERICAL PROCEDURE	22
B.	THE BEAM-WARMING ALGORITHM	22
C.	THE BALDWIN-LOMAX EDDY-VISCOSITY MODEL	31
D.	BOUNDARY CONDITIONS	33
E.	GRID GENERATION	34
1.	Grid Generation Methods	34
2.	Algebraic Grid Generation Method	35
IV.	RESULTS AND DISCUSSION	40
A.	INVESTIGATION METHOD	40
B.	LIFT BEHAVIOR	43
1.	Harmonically Oscillating Airfoil	43
2.	Rapidly Pitching Airfoil	46

C.	VORTEX FLOW DEVELOPMENT	59
1.	Rapidly Pitching Airfoil	59
2.	Harmonically Oscillating Airfoil	91
D.	REDUCED FREQUENCY EFFECT	96
E.	EFFECT OF FREESTREAM MACH NUMBER	99
F.	PRESSURE GRADIENT AT FLOW SEPARATION	102
V.	CONCLUSIONS AND RECOMMENDATIONS	109
A.	CONCLUSIONS	109
B.	RECOMMENDATIONS	109
	LIST OF REFERENCES	111
	APPENDIX A - USING THE PROGRAM	113
	APPENDIX B - PROGRAM NSE2D.F	121
	APPENDIX C - PROGRAM AIRFGR.F	157
	INITIAL DISTRIBUTION LIST	167

LIST OF TABLES

TABLE 1.	AIRFOIL COORDINATES	7
TABLE 2.	RAPIDLY PITCHING AIRFOIL CASES, $Re = 4 \times 10^6$	40
TABLE 3.	PEAK LIFT COEFFICIENTS	42

LIST OF FIGURES

Figure 1.	Events of Dynamic Stall on NACA 0012 Airfoil	3
Figure 2.	Airfoil Profile Comparison	8
Figure 3.	Forces on a Fluid Element	11
Figure 4.	Strain on a Fluid Element	12
Figure 5.	Energy Fluxes on Fluid Element	15
Figure 6.	Airfoil Grid Unwrapping	36
Figure 7.	N0012 Global Grid	37
Figure 8.	N0012-63 Local Grid	38
Figure 9.	N0012-33 Local Grid	39
Figure 10.	Lift Behavior, NACA 0012, $M=0.3$, $k=0.1$	44
Figure 11.	Lift Behavior, NACA 0012, $M=0.3$, $k=0.2$	45
Figure 12.	Lift Comparison, $M=0.3$, $k=0.01$	47
Figure 13.	Lift Comparison, $M=0.3$, $k=0.02$	48
Figure 14.	Lift Comparison, $M=0.4$, $k=0.01$	49
Figure 15.	Lift Comparison, $M=0.4$, $k=0.02$	50
Figure 16.	Instantaneous Streamlines, NACA 0012, $M=0.4$, $k=0.01$, $\alpha=17^\circ$	54
Figure 17.	Leading Edge Instantaneous Streamlines, NACA 0012, $M=0.4$, $k=0.01$, $\alpha=17^\circ$	55
Figure 18.	Instantaneous Streamlines, NACA 0012-63, $M=0.4$, $k=0.01$, $\alpha=17^\circ$	56
Figure 19.	Leading Edge Instantaneous Streamlines, NACA 0012-63, $M=0.4$, $k=0.01$, $\alpha=17^\circ$	57

Figure 20.	Instantaneous Streamlines, NACA 0012-33, M=0.4, k=0.01, $\alpha=17^\circ$	58
Figure 21.	Velocity Field, NACA 0012-63, M=0.4, k=0.01, $\alpha=14.0^\circ$	62
Figure 22.	Vorticity Contours, NACA 0012-63, M=0.3, k=0.01, $\alpha=14.0^\circ$	63
Figure 23.	Velocity Field, NACA 0012-63, M=0.4, k=0.01, $\alpha=16.0^\circ$	64
Figure 24.	Vorticity Contours, NACA 0012-63, M=0.4, k=0.01, $\alpha=16.0^\circ$	65
Figure 25.	Velocity Field, NACA 0012-63, M=0.4, k=0.01, $\alpha=17.0^\circ$	66
Figure 26.	Vorticity Contours, NACA 0012-63, M=0.3, k=0.01, $\alpha=17.0^\circ$	67
Figure 27.	Velocity Field, NACA 0012-63, M=0.4, k=0.01, $\alpha=18.0^\circ$	68
Figure 28.	Velocity Field, NACA 0012-63, M=0.4, k=0.01, $\alpha=19.0^\circ$	69
Figure 29.	Vorticity Contours, NACA 0012-63, M=0.4, k=0.01, $\alpha=19.0^\circ$	70
Figure 30.	Velocity Field, NACA 0012-63, M=0.4, k=0.01, $\alpha=20.0^\circ$	71
Figure 31.	Vorticity Contours, NACA 0012-63, M=0.3, k=0.01, $\alpha=20.0^\circ$	72
Figure 32.	Velocity Field, NACA 0012-63, M=0.4, k=0.01, $\alpha=21.0^\circ$	73
Figure 33.	Vorticity Contours, NACA 0012-63, M=0.4, k=0.01, $\alpha=21.0^\circ$	74
Figure 34.	Surface Pressure, NACA 0012-63, M=0.4, k=0.01, $\alpha=14.0^\circ$	75
Figure 35.	Surface Pressure, NACA 0012-63, M=0.4, k=0.01, $\alpha=16.0^\circ$	76
Figure 36.	Surface Pressure, NACA 0012-63, M=0.4, k=0.01, $\alpha=17.0^\circ$	77

Figure 37.	Surface Pressure, NACA 0012-63, $M=0.4$, $k=0.01$, $\alpha=18.0^\circ$	78
Figure 38.	Surface Pressure, NACA 0012-63, $M=0.4$, $k=0.01$, $\alpha=19.0^\circ$	79
Figure 39.	Surface Pressure, NACA 0012-63, $M=0.4$, $k=0.01$, $\alpha=20.0^\circ$	80
Figure 40.	Surface Pressure, NACA 0012-63, $M=0.4$, $k=0.01$, $\alpha=21.0^\circ$	81
Figure 41.	Surface Temperature, NACA 0012-63, $M=0.4$, $k=0.01$, $\alpha=14.0^\circ$	82
Figure 42.	Surface Temperature, NACA 0012-63, $M=0.4$, $k=0.01$, $\alpha=16.0^\circ$	83
Figure 43.	Surface Temperature, NACA 0012-63, $M=0.4$, $k=0.01$, $\alpha=17.0^\circ$	84
Figure 44.	Surface Temperature, NACA 0012-63, $M=0.4$, $k=0.01$, $\alpha=18.0^\circ$	85
Figure 45.	Surface Temperature, NACA 0012-63, $M=0.4$, $k=0.01$, $\alpha=19.0^\circ$	86
Figure 46.	Surface Temperature, NACA 0012-63, $M=0.4$, $k=0.01$, $\alpha=20.0^\circ$	87
Figure 47.	Surface Temperature, NACA 0012-63, $M=0.4$, $k=0.01$, $\alpha=21.0^\circ$	88
Figure 48.	Velocity Field, NACA 0012-33, $M=0.3$, $k=0.02$, $\alpha=22.0^\circ$	89
Figure 49.	Vorticity Contours, NACA 0012-33, $M=0.3$, $k=0.02$, $\alpha=22.0^\circ$	90
Figure 50.	Velocity Field, NACA 0012, $M=0.3$, $k=0.1$, $\alpha=15.0^\circ$ downstroke	92
Figure 51.	Velocity Field, NACA 0012, $M=0.3$, $k=0.1$, $\alpha=13.0^\circ$ downstroke	93
Figure 52.	Velocity Field, NACA 0012, $M=0.3$, $k=0.1$, $\alpha=11.0^\circ$ downstroke	94
Figure 53.	Velocity Field, NACA 0012, $M=0.3$, $k=0.1$, $\alpha=10.0^\circ$ downstroke	95

Figure 54.	Reduced Frequency Effect, NACA 0012, $M=0.3$	97
Figure 55.	Reduced Frequency Effect, NACA 0012-33, $M=0.3$	99
Figure 56.	Freestream Speed Effect, NACA 0012, $k=0.02$	100
Figure 57.	Freestream Speed Effect, NACA 0012-33, $k=0.02$	101
Figure 58.	Pressure Gradients, NACA 0012-63	105
Figure 59.	Pressure Gradients, NACA 0012-33	106
Figure 60.	Pressure Gradient Comparison, $M=0.4$, $k=0.01$	107
Figure 61.	Flow Reversal Location, $M=0.4$, $k=0.01$	108

ACKNOWLEDGEMENTS

I would like to acknowledge the instruction and support given by Dr. John Ekaterinaris in the use of advanced numerical computational facilities. In addition, his ability to link aerodynamic theory to the numerical techniques required in this investigation has been invaluable.

Likewise, over the past 18 months, Dr. Max Platzer has provided instruction and valued discussion in a number of areas of aerodynamic theory. In particular, his instruction on the full, unsteady, compressible Navier-Stokes equations and Boundary Layer theory have given me the theoretical background necessary for the completion of this study.

Finally, I would like to thank my wife Janeen for her patience and durability in typing the iterations required for this thesis.

I. INTRODUCTION

A. BACKGROUND

The aeronautical community has been aware of the phenomenon of dynamic stall for several decades. Dynamic stall is characterized by separated flow and shedding of the leading edge vortex from the upper surface of an airfoil which is rapidly pitched to angles of attack beyond the normal stalling angle of attack. The phenomenon results in significant temporary increases and decreases in lift, drag, and moment coefficients.

The scope of this work is the investigation of the phenomenon of dynamic stall for rapidly pitching and oscillating airfoils. The phenomenon of dynamic stall was observed for the first time for flows over the retreating blades of a helicopter. The dynamic stall resulting from the oscillatory motion of the rotor blade is associated with an increase in lift and the development of a severe nose down pitching moment. The effects of dynamic stall are usually undesirable for the helicopter, and where possible special care is taken to reduce its effects by special design of the rotor. On the other hand, interest has recently developed to exploit the increased lift obtained from the rapid pitch-up motion of an airfoil in order to enhance the maneuverability and extend the

flight envelope of the modern fighter aircraft to the high angle of attack regime, or to alleviate retreating blade stall for helicopters utilizing Higher Harmonic Control (HHC).

It is well known that for flow over an airfoil at fixed angle of attack the streamlined airflow is disrupted once a critical angle of attack is exceeded. At stall, the flow over the upper surface of the airfoil separates and the lift drops. It was observed, however, that rapid pitch-up motion of the airfoil delays static stall so that high lift can be maintained for angles of attack beyond the static stall angle.

As the pitch-up angle exceeds the static stalling angle of attack, a thin layer of reversed flow develops in the boundary layer. This reversed flow occurs in two types of stall: trailing edge stall and leading edge stall [Ref. 1]. In trailing edge stall, the reverse flow region begins near the trailing edge and traverses forward; in leading edge stall, the reverse flow region occurs near the suction peak just aft of the leading edge. In both cases, a vortex begins to form near the leading edge region, expands, and moves downstream. The angle of attack at which the vortex is formed depends on airfoil shape, pitch rate, mean angle and amplitude, Mach number, and Reynolds number.

The vortex formed at the leading edge is called the dynamic stall vortex, and moves with a speed of approximately 0.4 freestream speed relative to the airfoil as the pitch-up progresses. Lift, drag, and pitching moment increase signifi-

cantly until the vortex approaches the trailing edge, then drop sharply, but not simultaneously (Figure 1). The unsteady surface pressure increases, and the suction peak appears at different locations along the chord as the dynamic stall vortex moves over the airfoil. Secondary and tertiary vortices may also be present and produce additional suction peaks and fluctuations in airloads.

To date, most theoretical investigations on dynamic stall have focused on the effects of variations of reduced frequency ($k = \dot{\alpha}c/2U_\infty$), angle of attack, free stream speed, and Reynolds number on a particular airfoil shape (usually the NACA 0012 airfoil). McCroskey [Ref. 1] documented the effects of reduced frequency, amplitude and Mach number on different airfoils. These experimental studies demonstrated the large hysteresis in the

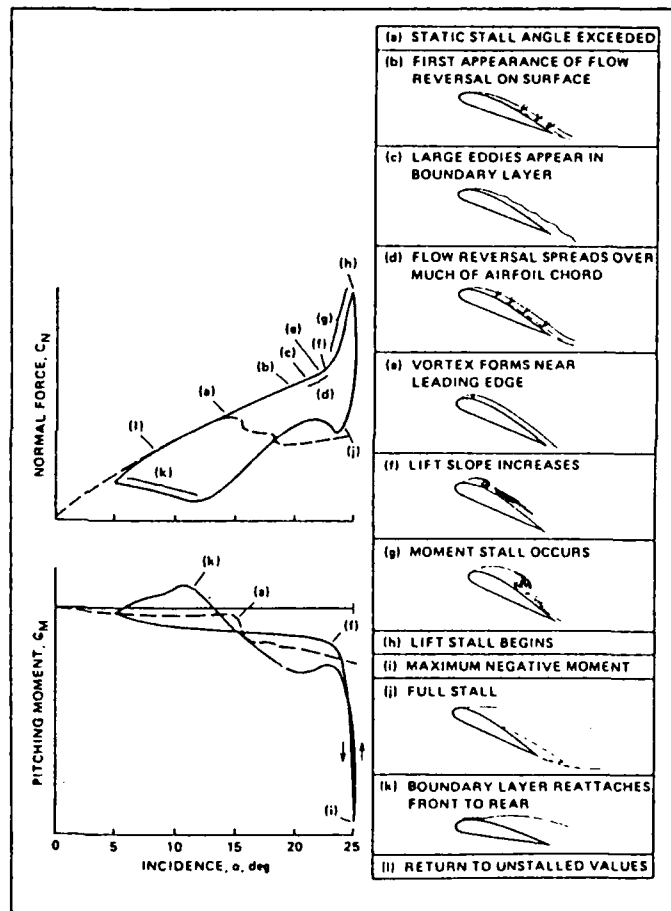


Figure 1. Events of Dynamic Stall on NACA 0012 Airfoil

occurrence of stall of an oscillating airfoil compared to a fixed angle of attack airfoil. McCroskey and Pucci [Ref. 2] identified varying regimes of viscous-inviscid interaction during varying degrees of unsteady flow separation. The conclusion of the experimental studies of Refs. 1 and 2 was that the reduced frequency has a dominant effect on the development and progression of the dynamic stall. Experimental work by Chandrasekhara and Carr [Ref. 3] using the NACA 0012 airfoil showed that a dynamic stall vortex always forms near the leading edge of an oscillating airfoil. Their study also documents the movement of the dynamic stall vortex. Chandrasekhara and Brydges [Ref. 4] documented the effects of increasing amplitude on an oscillating airfoil in both compressible and incompressible flow. They showed that larger amplitudes resulted in vortex retention at higher angles of attack for a given Mach number and reduced frequency.

Progress in computational fluid dynamics has made possible the study of dynamic stall by numerical solution of the unsteady Navier-Stokes equations. Mehta [Ref. 5] demonstrated that Navier-Stokes simulation of the unsteady incompressible flow around the airfoil in oscillatory motion can reproduce the experimentally observed results. Wu et al. [Ref. 6] presented solution procedures based on an integral formulation of the incompressible Navier-Stokes equations for the computation of unsteady flow over airfoils. Beddoes [Ref. 7] and Jang et al. [Ref. 8] presented viscous-inviscid computa-

tion methods for unsteady flows. Sankar and Tang [Ref. 9], Visbal [Ref. 10], and Ekaterinaris [Ref. 11] used ADI (Alternating Direction Implicit) numerical schemes for the solution of the compressible Navier-Stokes equations, and investigated the effects of compressibility on dynamic stall. The numerical solutions for both incompressible and compressible flows showed good agreement with experimental results, and predicted the events of dynamic stalls.

B. PURPOSE

As indicated, the aforementioned studies focused on the variation of flowfield parameters on the dynamic stall of a particular airfoil. The purpose of this study is the systematic investigation of the effect of leading edge geometry on the development of dynamic stall. It is expected that the effect of the leading edge geometry will have a significant effect on both the development of the dynamic stall vortex and its subsequent shedding. This numerical investigation is intended to provide a cost-effective means of quantifying which airfoil parameter variations should be analyzed in more expensive wind-tunnel tests. The numerical investigation of airfoil parameter variations offers the benefit of optimizing the utilization of more costly test facilities.

The investigation is conducted using a numerical solution of the full two-dimensional, Reynolds-averaged Navier-Stokes

Equations, and the Baldwin-Lomax eddy viscosity model of Ref. 16 is used to obtain the turbulent stresses.

C. AIRFOIL SELECTION

Modifications to the NACA 0012 airfoil were made forward of the point of maximum thickness (12% thick at 30%) chord by the method suggested in Ref. 12. The NACA 0012 profile was retained aft of 30% chord for the two new airfoils. In this manner, changes in the flow could be attributed directly to the changes in the forward part of the airfoil. The two airfoils consisted of the NACA 0012-63 and NACA 0012-33 airfoil section forward of 30% chord. The NACA 0012-63 has the same leading edge radius as the NACA 0012 (1.58% chord) but different curvature to the point of maximum thickness. The NACA 0012-33 has a smaller leading edge radius (0.39% chord) with curvature necessary to achieve the same 12% thickness ratio at 30% chord. Airfoil coordinates are provided in Table 1, and the resulting modified profiles are shown in Figure 2.

TABLE 1. AIRFOIL COORDINATES

<u>X/C</u>	<u>N0012</u>	<u>N0012-63</u>	<u>N0012-33</u>
.01	.01701	.01682	.01040
.02	.02360	.02320	.01550
.03	.02842	.02783	.01969
.04	.03232	.03160	.02332
.05	.03555	.03474	.02661
.06	.03840	.03750	.02962
.07	.04090	.03991	.03241
.08	.04313	.04210	.03500
.09	.04505	.04403	.03741
.10	.04681	.04580	.03966
.11	.04842	.04742	.04177
.12	.04990	.04890	.04374
.13	.05123	.05023	.04557
.14	.05242	.05147	.04734
.15	.05345	.05260	.04888
.16	.05441	.05362	.05035
.18	.05610	.05540	.05300
.20	.05742	.05686	.05515
.22	.05840	.05802	.05692
.24	.05903	.05890	.05830
.25	.05943	.05924	.05881
.26	.05964	.05952	.05925
.28	.05992	.05988	.05982
.30	.06000	.06000	.06000
.40	.05803	.05803	.05803
.50	.05294	.05294	.05294
.60	.04563	.04563	.04563
.70	.03664	.03664	.03664
.80	.02623	.02623	.02623
.90	.01448	.01448	.01448
.95	.00807	.00807	.00807
1.00	.00126	.00126	.00126

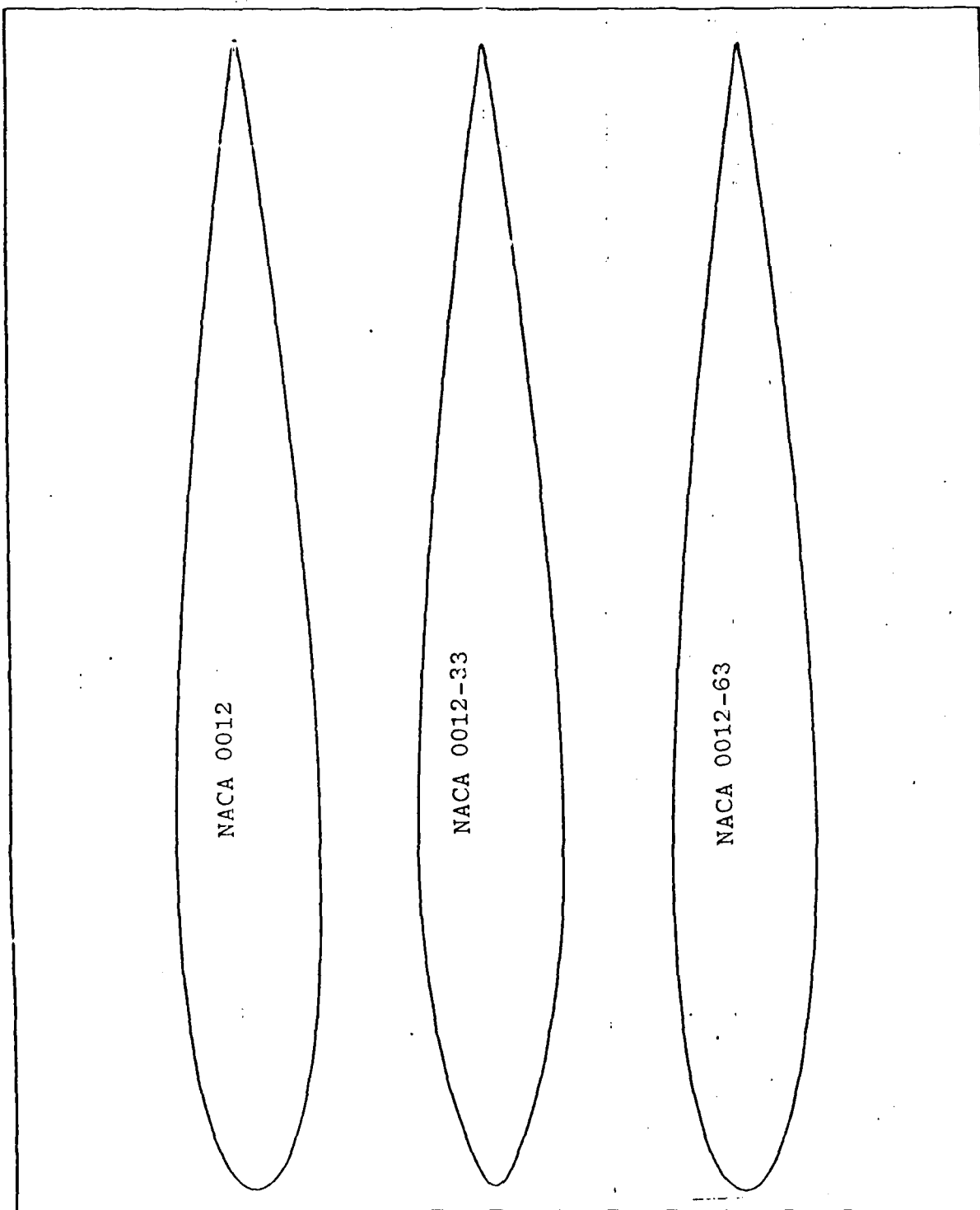


Figure 2. Airfoil Profile Comparison

II. GOVERNING EQUATIONS

The flow of a compressible, viscous fluid satisfies conservation of mass, momentum, and energy. The conservation of mass is expressed by the Continuity Equation, the conservation of momentum by the Navier-Stokes Equations, and the conservation of energy by the Energy Equation. The conservation equations are derived in the following section. The derivation is done in an Eulerian frame of reference.

A. CONTINUITY EQUATION

Consider a control volume in a flow field where flow properties vary with both time and space. Conservation of mass requires that the rate of change of mass inside the control volume equals net mass flux out of the control volume. This is expressed as:

$$\frac{\partial}{\partial t} \iiint_{vol} \rho \, d(vol) + \int_s \rho \vec{V} \cdot d\vec{s} = 0 \quad (1)$$

using Gauss's theorem for a surface integral, Eq. 1 becomes

$$\iiint_{vol} \frac{\partial \rho}{\partial t} \, d(vol) + \iiint_{vol} \nabla \cdot (\rho \vec{V}) \, d(vol) = 0 \quad (2)$$

or,

$$\iiint_{vol} \left[\frac{\partial \rho}{\partial t} + \nabla \cdot (\rho \vec{V}) \right] \, d(vol) = 0 \quad (3)$$

therefore, for an arbitrary control volume,

$$\frac{\partial \rho}{\partial t} + \nabla \cdot (\rho \vec{V}) = 0 \quad (4)$$

for any continuous flow. For a two-dimensional flow, and Cartesian coordinates, Eq. 4 reduces to

$$\frac{\partial \rho}{\partial t} + \frac{\partial(\rho u)}{\partial x} + \frac{\partial(\rho v)}{\partial y} = 0 \quad (5)$$

B. THE MOMENTUM (NAVIER-STOKES) EQUATIONS

Consider a fluid element in a rectangular Cartesian coordinate system. The stresses and pressures are shown in Figure 3, and body forces are neglected. Summation of forces in the x-direction yields:

$$\begin{aligned} F_x &= \rho \, dx \, dy \, dz \, \frac{Du}{Dt} \\ &= [p - (p + \frac{\partial p}{\partial x} dx)] \, dy \, dz + [(\tau_{xx} + \frac{\partial \tau_{xx}}{\partial x} dx) - \tau_{xx}] \, dy \, dz \\ &\quad + [(\tau_{yx} + \frac{\partial \tau_{yx}}{\partial y} dy) - \tau_{yx}] \, dx \, dz + [\tau_{zx} + \frac{\partial \tau_{zx}}{\partial z} dz) - \tau_{zx}] \, dx \, dy \end{aligned} \quad (6)$$

or,

$$\rho \frac{Du}{Dt} = -\frac{\partial p}{\partial x} + \frac{\partial \tau_{xx}}{\partial x} + \frac{\partial \tau_{yx}}{\partial y} + \frac{\partial \tau_{zx}}{\partial z} \quad (7)$$

Similarly, summation of forces in the y- and z- directions yields:

$$\rho \frac{Dv}{Dt} = -\frac{\partial p}{\partial y} + \frac{\partial \tau_{xy}}{\partial x} + \frac{\partial \tau_{yy}}{\partial y} + \frac{\partial \tau_{zy}}{\partial z} \quad (8)$$

$$\rho \frac{Dw}{Dt} = -\frac{\partial p}{\partial z} + \frac{\partial \tau_{xz}}{\partial x} + \frac{\partial \tau_{yz}}{\partial y} + \frac{\partial \tau_{zz}}{\partial z} \quad (9)$$

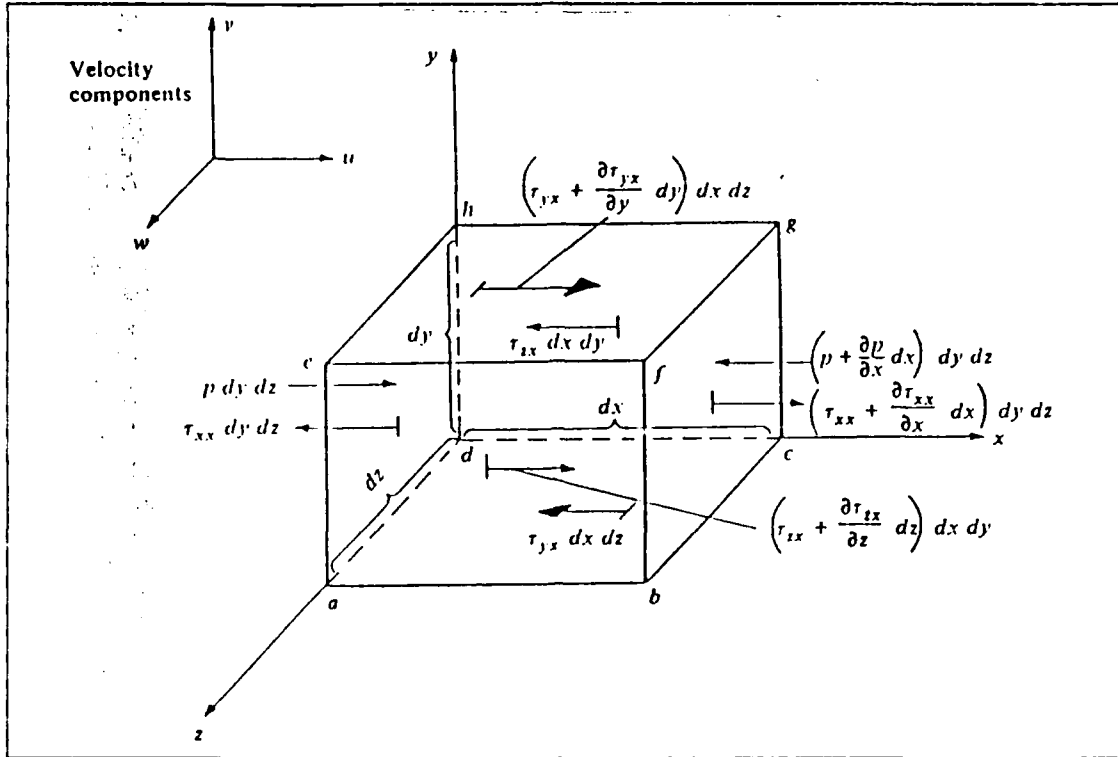


Figure 3. Forces on a Fluid Element

Using the Continuity Equation, the equations expressing the conservation of momentum for a two-dimensional flow are:

$$\frac{\partial(\rho u)}{\partial t} + \frac{\partial}{\partial x}(\rho u^2 + p) + \frac{\partial}{\partial y}(\rho uv) = \frac{\partial \tau_{xx}}{\partial x} + \frac{\partial \tau_{xy}}{\partial y} \quad (10)$$

$$\frac{\partial(\rho v)}{\partial t} + \frac{\partial}{\partial x}(\rho uv) + \frac{\partial}{\partial y}(\rho v^2 + p) = \frac{\partial \tau_{xy}}{\partial x} + \frac{\partial \tau_{yy}}{\partial y} \quad (11)$$

The relation of the viscous stresses τ_{xx} , τ_{yy} , and τ_{xy} to the independent variables is developed in the following discussion.

For a two-dimensional flow in Cartesian coordinates with an infinitesimal fluid element undergoing distortion due to

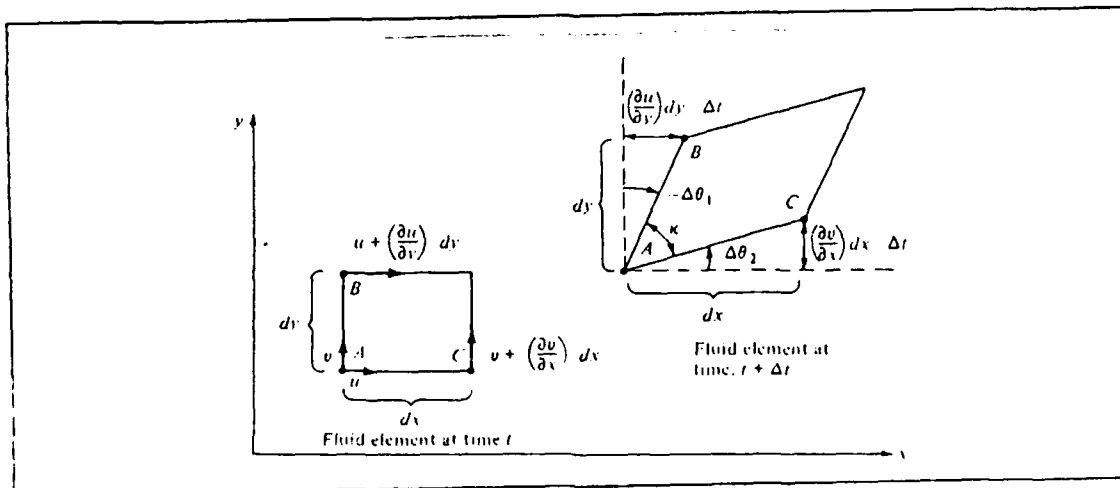


Figure 4. Strain on a Fluid Element

stresses as shown in Figure 4, the angular displacements $\Delta\theta_1$ and $\Delta\theta_2$ are:

$$\Delta\theta_2 = \frac{\partial v}{\partial x} \Delta t \quad \Delta\theta_1 = -\frac{\partial u}{\partial y} \Delta t \quad (12)$$

The strain increment is given by:

$$\Delta K = \Delta\theta_2 - \Delta\theta_1, \quad (13)$$

in the limit, the rate of strain is given by:

$$e_{xy} = \frac{dk}{dt} = \frac{d\theta_2}{dt} - \frac{d\theta_1}{dt} = \frac{\partial v}{\partial x} + \frac{\partial u}{\partial y} \quad (14)$$

Using Newton's Law of Fluid Friction (definition of viscosity),

$$\tau_{1j} = \mu \frac{\partial u_j}{\partial x_j} \quad (15)$$

then the rate of strain caused by the tangential shear stress is given by:

$$\tau_{xy} = \mu \epsilon_{xy} = \mu \left(\frac{\partial v}{\partial x} + \frac{\partial u}{\partial y} \right) \quad (16)$$

For large velocity gradients the normal stresses τ_{xx} and τ_{yy} can be significant and result in a viscous-induced normal force on the fluid element. For example, as documented by Schlichting [Ref. 13], in order for fluid isotropy to be maintained at every point, the principal axes of stress and rate-of-strain must coincide to avoid introducing a preferred rotation direction. With this concept, a normal stress must depend both on its respective component rate of strain as well as the shearing strain rates, with different weighting factors. Choosing the factor 2μ for the component direction factor, which causes Newton's Law of Friction to be satisfied for simple shear, obtain

$$\tau_{xx} = \lambda \left(\frac{\partial u}{\partial x} + \frac{\partial v}{\partial y} \right) + 2\mu \frac{\partial u}{\partial x} \quad (17)$$

$$\tau_{yy} = \lambda \left(\frac{\partial u}{\partial x} + \frac{\partial v}{\partial y} \right) + 2\mu \frac{\partial v}{\partial y} \quad (18)$$

where λ is the shearing stress proportionality factor. Using Stokes's hypothesis, $\lambda = -2/3 \mu$, obtain

$$\begin{aligned}
\tau_{xx} &= \frac{2}{3} \mu \left(2 \frac{\partial u}{\partial x} - \frac{\partial v}{\partial y} \right) \\
\tau_{yy} &= \frac{2}{3} \mu \left(2 \frac{\partial v}{\partial y} - \frac{\partial u}{\partial x} \right) \\
\tau_{xy} &= \mu \left(\frac{\partial v}{\partial x} + \frac{\partial u}{\partial y} \right)
\end{aligned}
\tag{19}$$

C. THE ENERGY EQUATION

Conservation of energy is the manifestation of the First Law of Thermodynamics ($dE = dW + dQ$) to a moving fluid element in rectangular Cartesian coordinates. The First Law of Thermodynamics is applied to a control volume (Figure 5), where the energy fluxes are shown. The rate of change of energy inside the fluid element is equal to the net flux of heat into the element plus the rate of work done on the element by pressure and viscous stress.

The rate of change of energy of the fluid element having an instantaneous internal energy per unit mass e and speed V is

$$\rho \frac{\partial}{\partial t} \left(e + \frac{V^2}{2} \right) dx dy dz
\tag{20}$$

where $V^2 = u^2 + v^2 + w^2$. The heat flux into the fluid element is the sum of external volumetric heating and heat transfer across the surface due to temperature gradients. Assuming no external heat addition, the volumetric heating is zero.

The net heat transferred out of the fluid element due to thermal conduction in the x-direction can be expressed as:

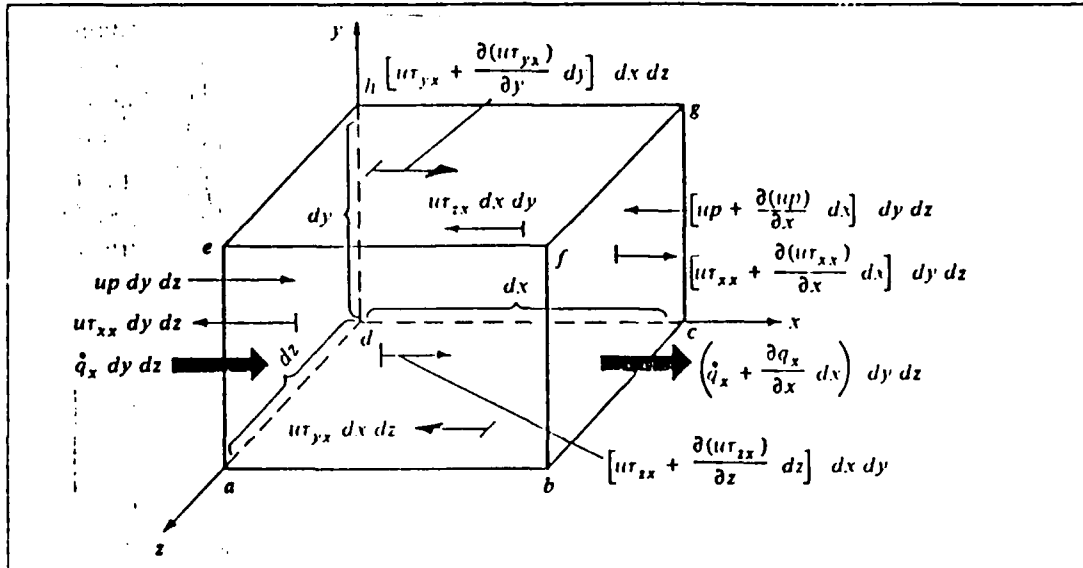


Figure 5. Energy Fluxes on Fluid Element

$$[\dot{q}_x - (\dot{q}_x + \frac{\partial \dot{q}_x}{\partial x} dx)] dy dz = - \frac{\partial \dot{q}_x}{\partial x} dx dy dz \quad (21)$$

Accounting for the y and z directions, the total heat transferred out of the fluid element is:

$$- (\frac{\partial \dot{q}_x}{\partial x} + \frac{\partial \dot{q}_y}{\partial y} + \frac{\partial \dot{q}_z}{\partial z}) dx dy dz = - (\nabla \cdot \vec{q}) dx dy dz \quad (22)$$

where the heat flux is expressed in terms of the temperature gradient according to Fourier's law of heat conduction as

$$\dot{q}_i = -k \frac{\partial T}{\partial x_i} \quad (23)$$

and k is the thermal conductivity, considered constant and independent of temperature.

The rate of work done on the fluid element in the x-direction by pressure and shear stresses is

$$\left[-\frac{\partial(\rho p)}{\partial x} + \frac{\partial(\rho u \tau_{xx})}{\partial x} + \frac{\partial(\rho u \tau_{yx})}{\partial y} + \frac{\partial(\rho u \tau_{zx})}{\partial z} \right] dx dy dz \quad (24)$$

Accounting for the y and z direction pressure and shear stresses, the net rate of work done on the fluid element can be expressed as:

$$\begin{aligned} & [-\nabla \cdot \rho \vec{V} + \frac{\partial(\rho u \tau_{xx})}{\partial x} + \frac{\partial(\rho u \tau_{yx})}{\partial y} + \frac{\partial(\rho u \tau_{zx})}{\partial z} \\ & + \frac{\partial(\rho v \tau_{xy})}{\partial x} + \frac{\partial(\rho v \tau_{yy})}{\partial y} + \frac{\partial(\rho v \tau_{zy})}{\partial z} \\ & + \frac{\partial(\rho w \tau_{xz})}{\partial x} + \frac{\partial(\rho w \tau_{yz})}{\partial y} + \frac{\partial(\rho w \tau_{zz})}{\partial z}] dx dy dz \end{aligned} \quad (25)$$

The complete energy equation for a viscous flow with no external heating can then be expressed as:

$$\begin{aligned} \rho \frac{d}{dt} (e + \frac{1}{2} V^2) = & [-\nabla \cdot \vec{q} - \nabla \cdot \rho \vec{V} \\ & + \frac{\partial(\rho u \tau_{xx})}{\partial x} + \frac{\partial(\rho u \tau_{yx})}{\partial y} + \frac{\partial(\rho u \tau_{zx})}{\partial z} \\ & + \frac{\partial(\rho v \tau_{xy})}{\partial x} + \frac{\partial(\rho v \tau_{yy})}{\partial y} + \frac{\partial(\rho v \tau_{zy})}{\partial z} \\ & + \frac{\partial(\rho w \tau_{xz})}{\partial x} + \frac{\partial(\rho w \tau_{yz})}{\partial y} + \frac{\partial(\rho w \tau_{zz})}{\partial z}] dx dy dz \end{aligned} \quad (26)$$

The two-dimensional compressible viscous flow energy equation reduces to:

$$\begin{aligned} & \rho \frac{d}{dt} (e + \frac{1}{2} V^2) + \frac{\partial}{\partial x} (\rho u) + \frac{\partial}{\partial y} (\rho v) \\ & = \frac{\partial}{\partial x} (\rho u \tau_{xx} + \rho v \tau_{xy} - \dot{q}_x) + \frac{\partial}{\partial y} (\rho u \tau_{yx} + \rho v \tau_{yy} - \dot{q}_y) \end{aligned} \quad (27)$$

Using the continuity equation and setting

$$E = (e + \frac{1}{2} V^2) \rho , \quad (28)$$

the total energy per unit volume, the energy equation becomes

$$\begin{aligned} & \frac{\partial E}{\partial t} + \frac{\partial}{\partial x} [(E+p)u] + \frac{\partial}{\partial y} [(E+p)v] \\ & = \frac{\partial}{\partial x} (u\tau_{xx} + v\tau_{xy} - \dot{q}_x) + \frac{\partial}{\partial y} (u\tau_{xy} + v\tau_{yy} - \dot{q}_y) \end{aligned} \quad (29)$$

where τ_{xx} , τ_{yy} , and τ_{xy} are as previously derived (see Eq. 19).

D. CONSERVATION LAW FORM OF THE GOVERNING EQUATIONS

The conservation law form of the governing equations for the two-dimensional viscous compressible flows can be written as [Ref. 14]

$$\frac{\partial Q}{\partial t} + \frac{\partial F}{\partial x} + \frac{\partial G}{\partial y} = \frac{\partial R}{\partial x} + \frac{\partial S}{\partial y} \quad (30)$$

where Q is the vector of dependent variables, F and G are the inviscid fluxes along the x and y directions, respectively, and R and S are the viscous fluxes along the x and y directions, respectively. These terms are given by:

$$Q = \begin{bmatrix} \rho \\ \rho u \\ \rho v \\ E \end{bmatrix} \quad F = \begin{bmatrix} \rho u \\ \rho u^2 + p \\ \rho uv \\ (E+p)u \end{bmatrix} \quad G = \begin{bmatrix} \rho v \\ \rho uv \\ \rho v^2 + p \\ (E+p)v \end{bmatrix}$$

$$R = \begin{bmatrix} 0 \\ \tau_{xx} \\ \tau_{xy} \\ u\tau_{xx} + v\tau_{xy} - \dot{q}_x \end{bmatrix} \quad S = \begin{bmatrix} 0 \\ \tau_{xy} \\ \tau_{yy} \\ u\tau_{xy} + v\tau_{yy} - \dot{q}_y \end{bmatrix}$$

Non-dimensionalizing the equations with

$$\begin{aligned} x_i^* &= \frac{x_i}{L} & u_i^* &= \frac{u_i}{V_\infty} & \rho^* &= \frac{\rho}{\rho_\infty V_\infty^2} & p^* &= \frac{p}{\rho_\infty V_\infty^2} \\ T^* &= \frac{T}{T_\infty} & \mu^* &= \frac{\mu}{\mu_\infty} & e^* &= \frac{e}{V_\infty^2} & t^* &= \frac{t}{L/V_\infty} \end{aligned}$$

where L is the reference length, and setting

$$Re = \frac{\rho_\infty V_\infty L}{\mu_\infty} \quad (31)$$

the Reynolds number based on the reference length, obtain the non-dimensional form of the conservation law:

$$\frac{\partial Q}{\partial t} + \frac{\partial F}{\partial x} + \frac{\partial G}{\partial y} = \frac{1}{Re} \left(\frac{\partial R}{\partial x} + \frac{\partial S}{\partial y} \right) \quad (32)$$

with non-dimensional variable Q and the inviscid flux terms (F and G) as before, and the viscous terms given by:

$$R = \begin{bmatrix} 0 \\ \tau_{xx} \\ \tau_{xy} \\ u\tau_{xx} + v\tau_{xy} - \frac{\mu}{(\gamma-1)M^2 Pr} \frac{\partial T}{\partial x} \end{bmatrix} \quad (33)$$

$$S = \begin{bmatrix} 0 \\ \tau_{xy} \\ \tau_{yy} \\ u\tau_{xy} + v\tau_{yy} - \frac{\mu}{(\gamma-1)M^2 Pr} \frac{\partial T}{\partial y} \end{bmatrix} \quad (34)$$

Here $Pr = C_p \mu / K$ is the Prandtl number, and $M = |\nabla| / a_\infty$. In order to enable solution of the governing equation for arbitrary geometries, the governing equations are expressed for a curvilinear generalized coordinate system. The curvilinear coordinate system (ξ, η) is linked to the Cartesian coordinate system (x, y) by

$$\xi = \xi(x, y, t), \quad \eta = \eta(x, y, t) \quad (35)$$

The curvilinear coordinate space (ξ, η) is referred to as the computational domain and is linked to the physical domain (x, y) by the non-zero Jacobian of the coordinates transformation

$$J = \frac{\partial(\xi, \eta)}{\partial(x, y)} = \frac{\partial\xi}{\partial x} \frac{\partial\eta}{\partial y} - \frac{\partial\xi}{\partial y} \frac{\partial\eta}{\partial x} = \frac{1}{\frac{\partial x}{\partial\xi} \frac{\partial y}{\partial\eta} - \frac{\partial x}{\partial\eta} \frac{\partial y}{\partial\xi}} \quad (36)$$

It can be shown that the governing equations [Ref. 18] retain the strong conservation law form for a generalized coordinate system. The two-dimensional strong conservation law form for a generalized coordinate system is:

$$\frac{\partial Q}{\partial t} + \frac{\partial F}{\partial\xi} + \frac{\partial G}{\partial\eta} = \frac{1}{Re} \left(\frac{\partial R}{\partial\xi} + \frac{\partial S}{\partial\eta} \right) \quad (37)$$

where

$$Q = \frac{1}{J} \begin{bmatrix} \rho \\ \rho u \\ \rho v \\ E \end{bmatrix} \quad (38)$$

$$F = \frac{1}{J} \begin{bmatrix} \rho U \\ \rho u U + p \frac{\partial \xi}{\partial x} \\ \rho v U + p \frac{\partial \xi}{\partial y} \\ (E+p) U - p \frac{\partial \xi}{\partial t} \end{bmatrix} \quad G = \frac{1}{J} \begin{bmatrix} \rho V \\ \rho u V + p \frac{\partial \eta}{\partial x} \\ \rho v V + p \frac{\partial \eta}{\partial y} \\ (E+p) V - p \frac{\partial \eta}{\partial t} \end{bmatrix} \quad (39, 40)$$

and U and V are the contravariant velocity components along the ξ and η directions, respectively given by:

$$U = \frac{\partial \xi}{\partial t} + u \frac{\partial \xi}{\partial x} + v \frac{\partial \xi}{\partial y} \quad V = \frac{\partial \eta}{\partial t} + u \frac{\partial \eta}{\partial x} + v \frac{\partial \eta}{\partial y} \quad (41, 42)$$

The viscous terms are given by:

$$R = \frac{1}{J} \begin{bmatrix} 0 \\ \tau_{xx} \frac{\partial \xi}{\partial x} + \tau_{xy} \frac{\partial \xi}{\partial y} \\ \tau_{xy} \frac{\partial \xi}{\partial x} + \tau_{yy} \frac{\partial \xi}{\partial y} \\ \left[(u\tau_{xx} + v\tau_{xy} - \frac{\mu}{(\gamma-1)M^2 Pr} \frac{\partial T}{\partial x}) \frac{\partial \xi}{\partial x} \right. \\ \left. + (u\tau_{xy} + v\tau_{yy} - \frac{\mu}{(\gamma-1)m^2 Pr} \frac{\partial T}{\partial y}) \frac{\partial \xi}{\partial y} \right] \end{bmatrix} \quad (43)$$

and

$$S = \frac{1}{J} \begin{bmatrix} 0 \\ \tau_{xx} \frac{\partial \eta}{\partial x} + \tau_{xy} \frac{\partial \eta}{\partial y} \\ \tau_{xy} \frac{\partial \eta}{\partial x} + \tau_{yy} \frac{\partial \eta}{\partial y} \\ \left[(u\tau_{xy} + v\tau_{yy} - \frac{\mu}{(\gamma-1)M^2 Pr} \frac{\partial T}{\partial y}) \frac{\partial \eta}{\partial x} \right. \\ \left. + (u\tau_{xy} + v\tau_{yy} - \frac{\mu}{(\gamma-1)m^2 Pr} \frac{\partial T}{\partial y}) \frac{\partial \eta}{\partial y} \right] \end{bmatrix} \quad (44)$$

III. NUMERICAL APPROACH

A. NUMERICAL PROCEDURE

The strong conservation law form of the two-dimensional Continuity, Navier-Stokes, and Energy Equations in generalized coordinates presented in Chapter II provides a useable format for implementing a numerical solution technique. The numerical method used for the integration of the governing equations is a finite difference numerical scheme based on the Beam-Warming algorithm [Ref. 15]. The viscous terms are retained in both directions in order to enable capturing intense viscous effects encountered in massively separated flow regions at high angles of attack. The turbulent stresses were modeled using the Baldwin-Lomax eddy viscosity model [Ref. 16]. An algebraic C-type grid (157x58) was used for the computations. The boundary conditions were treated explicitly, and the unsteadiness was imposed by the motion of the grid.

B. THE BEAM-WARMING ALGORITHM

The strong conservation law form of the two-dimensional compressible Navier-Stokes equations in the vector notation is as follows:

$$\frac{\partial U}{\partial t} + \frac{\partial E(U)}{\partial x} + \frac{\partial F(U)}{\partial y} = \frac{\partial V_1(U, U_x)}{\partial x} + \frac{\partial V_2(U, U_y)}{\partial x} + \frac{\partial W_1(U, U_x)}{\partial y} + \frac{\partial W_2(U, U_y)}{\partial y} \quad (45)$$

here the vector U , the non-linear inviscid terms E and F , and the viscous terms R and S are given by:

$$U = \begin{bmatrix} \rho \\ \rho u \\ \rho v \\ E_t \end{bmatrix} \quad E(U) = \begin{bmatrix} \rho u \\ \rho u^2 + p \\ \rho uv \\ (E_t + p)u \end{bmatrix} \quad F(U) = \begin{bmatrix} \rho v \\ \rho uv \\ \rho v^2 + p \\ (E_t + p)v \end{bmatrix}$$

$$R = V_1 + V_2 = \begin{bmatrix} 0 \\ \frac{2}{3}\mu(2u_x - v_y) \\ \mu(u_y + v_x) \\ \mu v(u_y + v_x) + \frac{2}{3}\mu u(2u_x - v_y) + kT_x \end{bmatrix} \quad (46)$$

$$S = W_1 + W_2 = \begin{bmatrix} 0 \\ \mu(u_y + v_x) \\ \frac{2}{3}\mu(2v_y - u_x) \\ \mu u(u_y + v_x) + \frac{2}{3}\mu v(2v_y - u_x) + kT_y \end{bmatrix}$$

The Beam-Warming numerical algorithm is an implicit finite difference scheme where the solution is marched in time using the difference formula

$$\Delta^n U = \frac{\theta_1 \Delta t}{1 + \theta_2} \frac{\partial}{\partial t} (\Delta^n U) + \frac{\Delta t}{1 + \theta_2} \frac{\partial}{\partial t} (U^n) + \frac{\theta_2}{1 + \theta_2} \Delta^{n-1} U + O[(\theta_1 - \frac{1}{2} - \theta_2) (\Delta t)^2 + (\Delta t)^3] \quad (47)$$

where $\Delta^n U = U^{n+1} - U^n$. By substituting Eq. (45) into Eq. (47), obtain

$$\begin{aligned} \Delta^n U = & \frac{\theta_1 \Delta t}{1 + \theta_2} \left[\frac{\partial}{\partial x} (-\Delta^n E + \Delta^n V_1 + \Delta^n V_2) + \frac{\partial}{\partial y} (-\Delta^n F + \Delta^n W_1 + \Delta^n W_2) \right] \\ & + \frac{\Delta t}{1 + \theta_2} \left[\frac{\partial}{\partial x} (-E^n + V_1^n + V_2^n) + \frac{\partial}{\partial y} (-F^n + W_1^n + W_2^n) \right] \\ & + \frac{\theta_2}{1 + \theta_2} \Delta^{n-1} U + O \left[\left(\theta_1 - \frac{1}{2} - \theta_2 \right) (\Delta t)^2 + (\Delta t)^3 \right] \end{aligned} \quad (48)$$

The delta terms are linearized using truncated Taylor series expansions, so that:

$$E^{n+1} = E^n + \left(\frac{\partial E}{\partial U} \right)^n (U^{n+1} - U^n) + O[(\Delta t)^2] \quad (49)$$

which can be rewritten as

$$\Delta^n E = [A]^n \Delta^n U + O[(\Delta t)^2] \quad (50)$$

where $[A]$ is the flux Jacobian matrix $\partial E / \partial U$ given by

$$[A] = - \left[\begin{array}{c|ccc} 0 & -1 & 0 & 0 \\ \frac{3-\gamma}{2}u^2 + \frac{1-\gamma}{2}v^2 & (\gamma-3)u & (\gamma-1)v & (1-\gamma) \\ uv & -v & -u & 0 \\ \frac{\gamma E_t u}{\rho} + (1-\gamma)u(u^2+v^2) & -\frac{\gamma E_t}{\rho} + \frac{\gamma-1}{2}(3u^2+v^2) & (\gamma-1)uv & -\gamma u \end{array} \right] \quad (51)$$

In a like manner, $\Delta^n F$ can be linearized as

$$\Delta^n F = [B]^n \Delta^n U + O[(\Delta t)^2] \quad (52)$$

where $[B]$ is the Jacobian matrix $\partial F / \partial U$ given by

$$[B] = - \left[\begin{array}{ccc|ccc} 0 & 0 & -1 & 0 & & \\ uv & -v & -u & 0 & & \\ \frac{3-\gamma}{2}v^2 + \frac{1-\gamma}{2}u^2 & (\gamma-1)u & (\gamma-3)v & 1-\gamma & & \\ \frac{\gamma E_t v}{\rho} + (1-\gamma)v(u^2 + v^2) & (\gamma-1)uv & -\frac{\gamma E_t}{\rho} + \frac{\gamma-1}{2}(3v^2 + u^2) & -\gamma v & & \end{array} \right] \quad (53)$$

The viscous delta term $\Delta^n V_1(U, U_x)$ is linearized by writing

$$\begin{aligned} \Delta^n V_1 &= \left(\frac{\partial V_1}{\partial U} \right)^n \Delta^n U + \left(\frac{\partial V_1}{\partial U_x} \right)^n \Delta^n U_x + O[(\Delta t)^2] \\ &= [P]^n \Delta^n U + [R]^n \Delta^n U_x + O[(\Delta t)^2] \\ &= ([P] - [R_x])^n \Delta^n U + \frac{\partial}{\partial x} ([R]^n \Delta^n U) + O[(\Delta t)^2] \end{aligned} \quad (54)$$

where $[P]$ is the Jacobian $\partial V_1 / \partial U$, $[R]$ is the Jacobian $\partial V_1 / \partial U_x$, and $[R_x] = \partial [R] / \partial x$. These matrices can be written as

$$[P] - [R_x] = -\frac{1}{\rho} \left[\begin{array}{ccc|ccc} 0 & 0 & 0 & 0 & & \\ -u \left(\frac{4}{3} \mu \right)_x & \left(\frac{4}{3} \mu \right)_x & 0 & 0 & & \\ -v \mu_x & 0 & \mu_x & 0 & & \\ -u^2 \left(\frac{4}{3} \mu \right)_x - v^2 \mu_x & u \left(\frac{4}{3} \mu \right)_x & v \mu_x & 0 & & \end{array} \right] \quad (55)$$

$$[R] = \frac{1}{\rho} \left[\begin{array}{ccc|ccc} 0 & 0 & 0 & 0 & & \\ -\frac{4}{3} \mu u & \frac{4}{3} \mu & 0 & 0 & & \\ -\mu v & 0 & \mu & 0 & & \\ -\left(\frac{4}{3} \mu - \frac{k}{c_v} \right) u^2 - \left(\mu - \frac{k}{c_v} \right) v^2 - \frac{k}{c_v} \frac{E_t}{\rho} & \left(\frac{4}{3} \mu - \frac{k}{c_v} \right) u & \left(\mu - \frac{k}{c_v} \right) v & \frac{k}{c_v} & & \end{array} \right] \quad (56)$$

The matrix for $[P]-[R_x]$ is obtained by assuming that μ and k are locally independent of U . In a like manner, $\Delta^n W_2(U, U_y)$ is linearized as

$$\Delta^n W_2 = ([Q] - [S_y])^n \Delta^n U + \frac{\partial}{\partial y} ([S]^n \Delta^n U) + O[(\Delta t)^2] \quad (57)$$

where

$$[Q] - [S_y] = -\frac{1}{\rho} \left[\begin{array}{cc|cc} 0 & 0 & 0 & 0 \\ -u\mu_y & \mu_y & 0 & 0 \\ -v \left(\frac{4}{3} \mu \right)_y & 0 & \left(\frac{4}{3} \mu \right)_y & 0 \\ -v^2 \left(\frac{4}{3} \mu \right)_y - u^2 \mu_y & u\mu_y & v \left(\frac{4}{3} \mu \right)_y & 0 \end{array} \right] \quad (58)$$

and

$$[S] = \frac{1}{\rho} \left[\begin{array}{cc|cc} 0 & 0 & 0 & 0 \\ -\mu u & \mu & 0 & 0 \\ -\frac{4}{3} \mu v & 0 & \frac{4}{3} \mu & 0 \\ -\left(\frac{4}{3} \mu - \frac{k}{c_v} \right) v^2 - \left(\mu - \frac{k}{c_v} \right) u^2 - \frac{k}{c_v} \frac{E_t}{\rho} & \left(\mu - \frac{k}{c_v} \right) u & \left(\frac{4}{3} \mu - \frac{k}{c_v} \right) v & \frac{k}{c_v} \end{array} \right] \quad (59)$$

The cross-derivative terms can be evaluated explicitly without loss of accuracy by noting that

$$\begin{aligned}\Delta^n V^2 &= \Delta^{n-1} V_2 + O[(\Delta t)^2] \\ \Delta^n W^n &= \Delta^{n-1} W_1 + O[(\Delta t)^2]\end{aligned}\tag{60}$$

for a uniform time step Δt . By evaluating the cross-derivative terms in this manner, the block tridiagonal form of the final equations is maintained.

Substituting Eqs. (50), (52), (54), (57), and (59) into Eq. (48) yields

$$\begin{aligned}& \left\{ [I] + \frac{\theta_1 \Delta t}{1 + \theta_2} \left[\frac{\partial}{\partial x} ([A] - [P] + [R_x])^n - \frac{\partial^2}{\partial x^2} [R]^n \right. \right. \\ & \quad \left. \left. + \frac{\partial}{\partial y} ([B] - [Q] + [S_y])^n - \frac{\partial^2}{\partial y^2} [S]^n \right] \right\} \Delta^n U \\ &= \frac{\Delta t}{1 + \theta_2} \left[\frac{\partial}{\partial x} (-E + V_1 + V_2)^n + \frac{\partial}{\partial y} (-F + W_1 + W_2)^n \right] \\ & \quad + \frac{\theta_1 \Delta t}{1 + \theta_2} \left[\frac{\partial}{\partial x} (\Delta^{n-1} V_2) + \frac{\partial}{\partial y} (\Delta^{n-1} W_1) \right] + \frac{\theta_2}{1 + \theta_2} \Delta^{n-1} U \\ & \quad + O \left[\left(\theta_1 - \frac{1}{2} - \theta_2 \right) (\Delta t)^2, (\Delta t)^3 \right]\end{aligned}\tag{61}$$

where $[I]$ is the identity matrix. In Eq. (61), expressions such as

$$\left[\frac{\partial}{\partial x} ([A] - [P] + [R_x])^n \right] \Delta^n U\tag{62}$$

are equivalent to

$$\left[\frac{\partial}{\partial x} ([A] - [P] + [R_x])^n \Delta^n U \right]\tag{63}$$

The left-hand side of Eq. (60) is factorized in the following manner:

$$\begin{aligned} & \left([I] + \frac{\theta_1 \Delta t}{1 + \theta_2} \left[\frac{\partial}{\partial x} ([A] - [P] + [R_x]) \right] n - \frac{\partial^2}{\partial x^2} [R] \right) \\ & \times \left([I] + \frac{\theta_1 \Delta t}{1 + \theta_2} \left[\frac{\partial}{\partial y} ([B] - [Q] + [S_y]) \right] n - \frac{\partial^2}{\partial y^2} [S] \right) \Delta^n U \quad (64) \\ & = LHS(Eq. 60) + O[(\Delta t)^3] \end{aligned}$$

and the final form of the Beam-Warming Algorithm becomes

$$LHS[Eq. (64)] = RHS[Eq. (61)] \quad (65)$$

The partial derivatives in the algorithm are evaluated using second-order accurate central differences.

The Beam-Warming algorithm is implemented in the following manner:

Step 1:

$$\left([I] + \frac{\theta_1 \Delta t}{1 + \theta_2} \left[\frac{\partial}{\partial x} ([A] - [P] + [R_x]) \right] n - \frac{\partial^2}{\partial x^2} [R] \right) \Delta^n U_1 = RHS[61] \quad (66)$$

Step 2:

$$\left([I] + \frac{\theta_1 \Delta t}{1 + \theta_2} \left[\frac{\partial}{\partial y} ([B] - [Q] + [S_y]) \right] n - \frac{\partial^2}{\partial y^2} [S] \right) \Delta^n U = \Delta^n U_1 \quad (67)$$

Step 3:

$$U^{n+1} = U^n + \Delta^n U \quad (68)$$

In Step 1, $\Delta^n U_1$ represents the remaining terms on the left-hand side of Eq. (64). Equations (66) and (67) represent systems of equations which have a block tridiagonal structure.

For the two-dimensional compressible Navier-Stokes equations the block matrices have a dimension of 4x4. Central differencing is used for the second order space derivatives. Dissipation terms for numerical stability are added.

Warming and Beam [Ref. 15] have shown that the algorithm can be simplified by assuming that μ is locally constant so that $\partial\mu/\partial x=0$, $\partial\mu/\partial y=0$. Then $[P]-[R_x]=0$ and $[Q]-[S_y]=0$. Therefore, the algorithm for $\theta_1 = \frac{1}{2}$, $\theta_2 = 0$, implying second order accuracy in time, obtains the following form:

$$[I] + \frac{\Delta t}{2} \left[\frac{\partial}{\partial x} [A]^n - \frac{\partial}{\partial x} [R_x]^n \right] \Delta^n U_1 = RHS \quad (69)$$

$$[I] + \frac{\Delta t}{2} \left[\frac{\partial}{\partial x} [B]^n - \frac{\partial}{\partial y} [S_y]^n \right] \Delta^n U = \Delta^n U_1 \quad (70)$$

In the present work the viscous terms were treated explicitly in order to avoid the expensive computation of the matrices R_x and S_y . The Beam-Warming algorithm with explicit treatment of viscous terms in generalized coordinates (ξ, η) is written as

$$\begin{aligned} & \left([I] + \frac{\Delta t}{2} \left[\frac{\partial}{\partial \xi} A^n + \frac{\partial}{\partial \eta} B^n \right] \right) \Delta U^{n+1} = \\ & \Delta t \left(-\frac{\partial}{\partial \xi} F^n - \frac{\partial}{\partial \eta} G^n + \frac{\partial}{\partial \xi} R^n + \frac{\partial}{\partial \eta} S^n \right) = RHS^n \end{aligned} \quad (71)$$

The algorithm is further simplified by approximately factorizing the LHS(61) or LHS(71) operator in order to avoid integration of the full two-dimensional operator. The factored form of the algorithm is

$$\begin{aligned}
([I] + \frac{\Delta t}{2} \delta_{\xi} A_{i,k}^n) \Delta \bar{U}_{i,k}^{n+1} &= RHS(61)^n \\
([I] + \frac{\Delta t}{2} \delta_{\eta} B_{i,k}^n) \Delta U_{i,k}^{n+1} &= \Delta \bar{U}_{i,k}^{n+1}
\end{aligned}
\tag{72}$$

In practice, implicit algorithms have stability limits due to nonlinearities. In addition, whenever discrete methods are used to compute high Reynolds number viscous behavior, small scales of motion appear which cannot be resolved by the numerics. These scales are brought about by the nonlinear interactions in the convective terms of the momentum equations. In any finite discrete mesh the small scales which cannot be resolved, result eventually in inaccuracy and contamination of the long wavelength, large scale phenomena. In order to dampen the high frequency numerical effects caused by the poor resolution of the small scales, implicit and explicit numerical dissipation is added to complete the algorithm. The numerical dissipation terms introduce an error level that does not interfere with the accuracy and resolution of any physical effects. The dissipation terms used in the present work are the ones suggested by Ref. 15. The complete factorized form of the numerical algorithms with the implicit and explicit dissipation terms is

$$\begin{aligned}
& [I + (\frac{\Delta t}{2}) (\partial_{\xi} A^n + (D_{impl})_{\xi})] \times [I + (\frac{\Delta t}{2}) (\partial_{\eta} B^n + (D_{impl})_{\eta})] \Delta^n Q \\
& = \Delta t (-\partial_{\xi} F^n - \partial_{\eta} G^n + \partial_{\eta} R^n + \partial_{\eta} S^n - \epsilon_{expl} D_n)
\end{aligned}
\tag{73}$$

C. THE BALDWIN-LOMAX EDDY-VISCOSITY MODEL

The Baldwin-Lomax model [Ref. 16] is an algebraic eddy viscosity model for calculating two- and three-dimensional separated flows. As opposed to the classical boundary-layer approximation which assumes zero normal pressure gradient in the boundary layer, thereby neglecting the normal momentum equation, the Baldwin-Lomax Thin Layer model retains the momentum equations and makes no assumptions about the pressure gradient. The advantage of this model arises in application to high Reynolds number, separated turbulent flows, including reverse flow regions. The Baldwin-Lomax model is a two-layer algebraic eddy-viscosity model and avoids the difficulty of finding the edge of the boundary layer. The effects of turbulence are simulated in terms of an eddy viscosity coefficient μ_t , where $\mu + \mu_t$ replaces μ (the physical viscosity coefficient) in the stress terms of the governing equations. In the model, μ_t is given by

$$\mu_t = \begin{cases} (\mu_t)_{inner} & y \leq y_c \\ (\mu_t)_{outer} & y_c > y \end{cases} \quad (74)$$

where y is the normal distance from the wall and y_c is the smallest y where inner and outer values are equal. In the inner region, the Prandtl-Van Driest formula is used:

$$(\mu_t)_{inner} = \rho l^2 |\omega| \quad (75)$$

where $l = ky[1 - \exp(-y^+/A^+)]$ and $|\omega|$ is the magnitude of the vorticity. In two dimensions,

$$|\omega| = \left(\frac{\partial u}{\partial y} - \frac{\partial v}{\partial x} \right) \quad (76)$$

and

$$y^+ = \frac{\rho_w u_{\tau} y}{\mu_w} = \frac{\sqrt{\rho_w \tau_w} y}{\mu_w} \quad (77)$$

The subscript w indicates wall values.

For the outer region

$$(u_t)_{outer} = KC_{cp} \rho F_{WAKE} F_{KLEB}(y) \quad (78)$$

where K , C_{cp} are constants and

$$F_{WAKE} = Y_{MAX} F_{MAX} \quad \text{for boundary layers, or}$$

$$F_{WAKE} = C_{wk} Y_{MAX} u^2_{DIP} / F_{MAX} \quad \text{for wakes and separated boundary layers.}$$

The quantities y_{MAX} and F_{MAX} are determined from

$$F(y) = y|w|[1 - \exp(y^+/A^+)] \quad (79)$$

The exponential term in this equation is set equal to zero for wakes.

F_{MAX} is the maximum values of $F(y)$, which occurs at a value of $y = y_{MAX}$. The function $F_{KLEB}(y)$ is the Klebanoff intermittency factor given by

$$F_{KLEB}(y) = [1 + 5.5 \left(\frac{C_{KLEB} y}{Y_{MAX}} \right)^6]^{-1} \quad (80)$$

The quantity U_{DIF} is the difference between $U = U|_{y=y_{MAX}}$ and minimum total velocity at a fixed flow-wise station:

$$U_{DIF} = (\sqrt{U^2 + V^2})_{y=y_{MAX}} - (\sqrt{U^2 + V^2})_{min} \quad (81)$$

where the second term is zero except in wakes.

In order to achieve agreement with Cebeci [Ref. 17], the values determined for the constants are:

A^+	= 26	k	= 0.4
C_{cp}	= 1.6	K	= 0.0168
C_{KLEB}	= 0.3	Pr	= 0.72
C_{WK}	= 1.0	Pr_t	= 0.9

D. BOUNDARY CONDITIONS

The following boundary conditions were used in the numerical implementation. A non-slip non-penetration boundary condition in terms of the contravariant velocity components was used on the airfoil solid boundary. The unsteady pitching motion was accomplished by rotating the grid about the quarter chord point at pitch rates determined by the desired reduced frequency. The inflow boundary was placed approximately eight chord lengths away from the body surface. Therefore, freestream conditions were specified at the grid inflow boundary. Simple first order extrapolation was used for the flow variables at the outflow boundary. For the wake, averaging of the flow variables on the upper and lower surfaces of the C-grid was used. The velocity on the surface

is given by $u_s = \dot{x} = \omega z$ and $v_s = \dot{z} = -\omega x$. The contravariant velocity components for viscous flow solutions are set equal to 0. Therefore, the non-slip condition in terms of the physical velocity components for moving grid is expressed by

$$\begin{bmatrix} u \\ v \end{bmatrix} = \frac{1}{J} \begin{bmatrix} \eta_y & -\xi_y \\ -\eta_x & \xi_x \end{bmatrix} \begin{bmatrix} \dot{x} \\ \dot{z} \end{bmatrix} \quad (82)$$

E. GRID GENERATION

1. Grid Generation Methods

In order to effectively compute complex flowfields, the physical domain of interest must be discretized with a finite mesh. The requirements of an efficient numerical grid are [Ref. 18]:

1. smooth grid lines so that the transformation derivatives (metrics) are continuous.
2. grid point spacing which varies inversely with expectation of large numerical errors.
3. minimizing grid skewness to avoid large truncation errors.

Several general grid generation techniques exist; among these the most common methods are:

1. Complex Variable methods, where the transformations are at least partly analytic; this method is restricted to two-dimensions.
2. Algebraic methods, usable in two- or three-dimensions.
3. Differential Equation methods, usable in two- or three-dimensions.

The grid generation method used in this study utilized the algebraic grid generation technique because of the computational efficiency and speed it provides.

2. Algebraic Grid Generation Method

The algebraic method used employs known, easily invertible, functions to map arbitrarily shaped regions (in this case, the airfoil contour) into a simpler computational domain. The airfoil surface is unwrapped to form a simple curve in the computational plane as in Figure 6. In the computational domain lines are first drawn normal to this curve, and the grid points in the normal direction are subsequently generated. In the case of airfoil grid generation, consideration must be given for the clustering of grid points near the airfoil in order to adequately resolve the near surface viscous layers. An algebraic function is used to provide a uniform stretching normal to the airfoil in the computational plane. The resulting computational domain grid is wrapped back to the initial physical grid using inverse transformations.

The grid generation program used in this study yielded a 157x58 C-type grid. The program is listed in Appendix C. Grids for the airfoils under consideration are displayed in Figures 7-9. Figure 7 displays the global grid including wake for the NACA 0012 airfoil. Figures 8 and 9 show the body-fitted grid in more detail for the two modified airfoils. Grid clustering near the airfoils is shown for resolving the

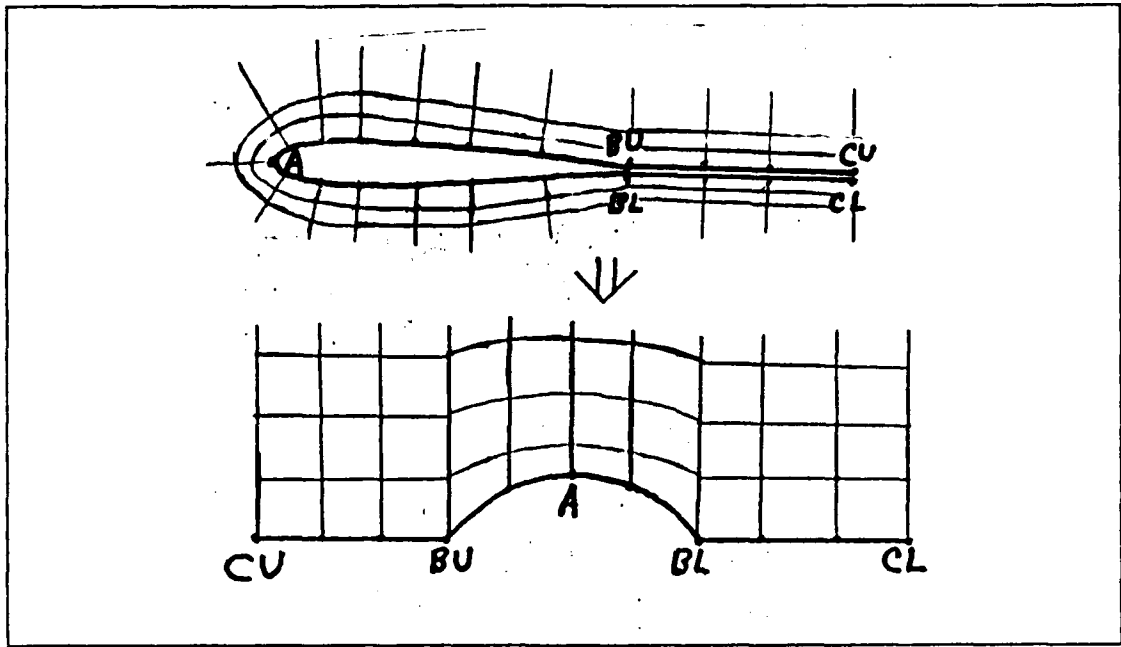


Figure 6. Airfoil Grid Unwrapping

boundary layer flow in turbulent and separated flow conditions.

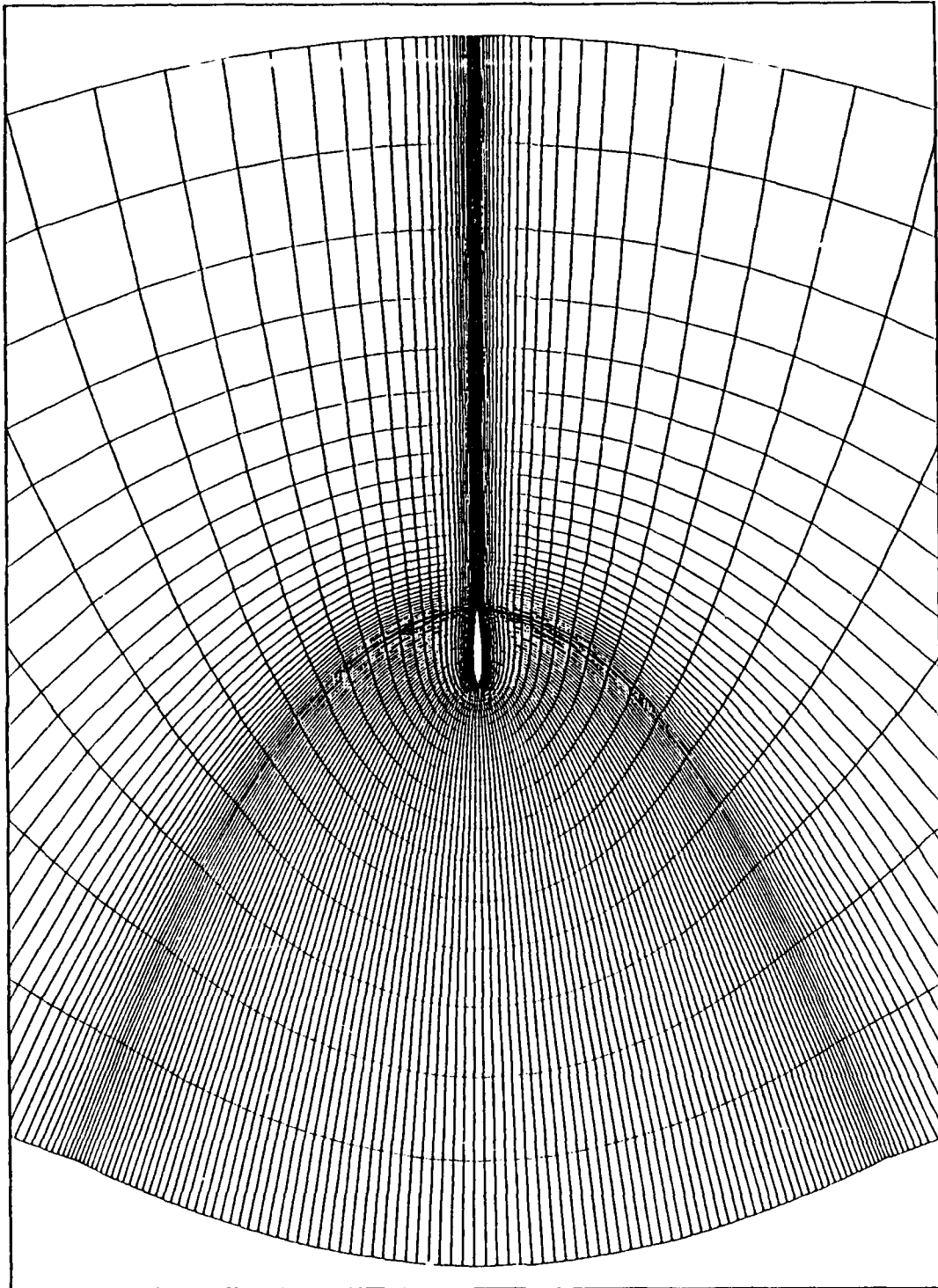


Figure 7. N0012 Global Grid

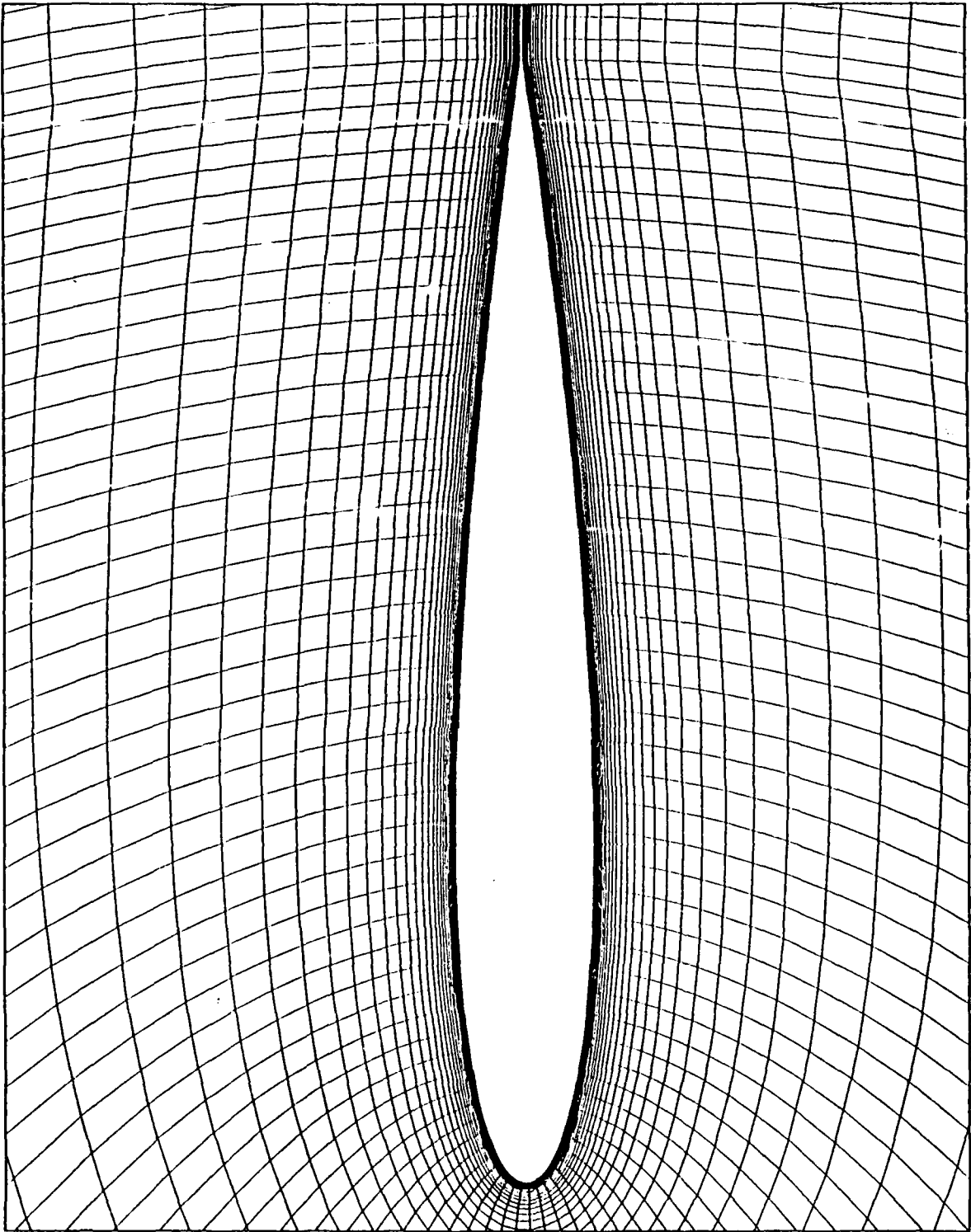


Figure 8. N0012-63 Local Grid

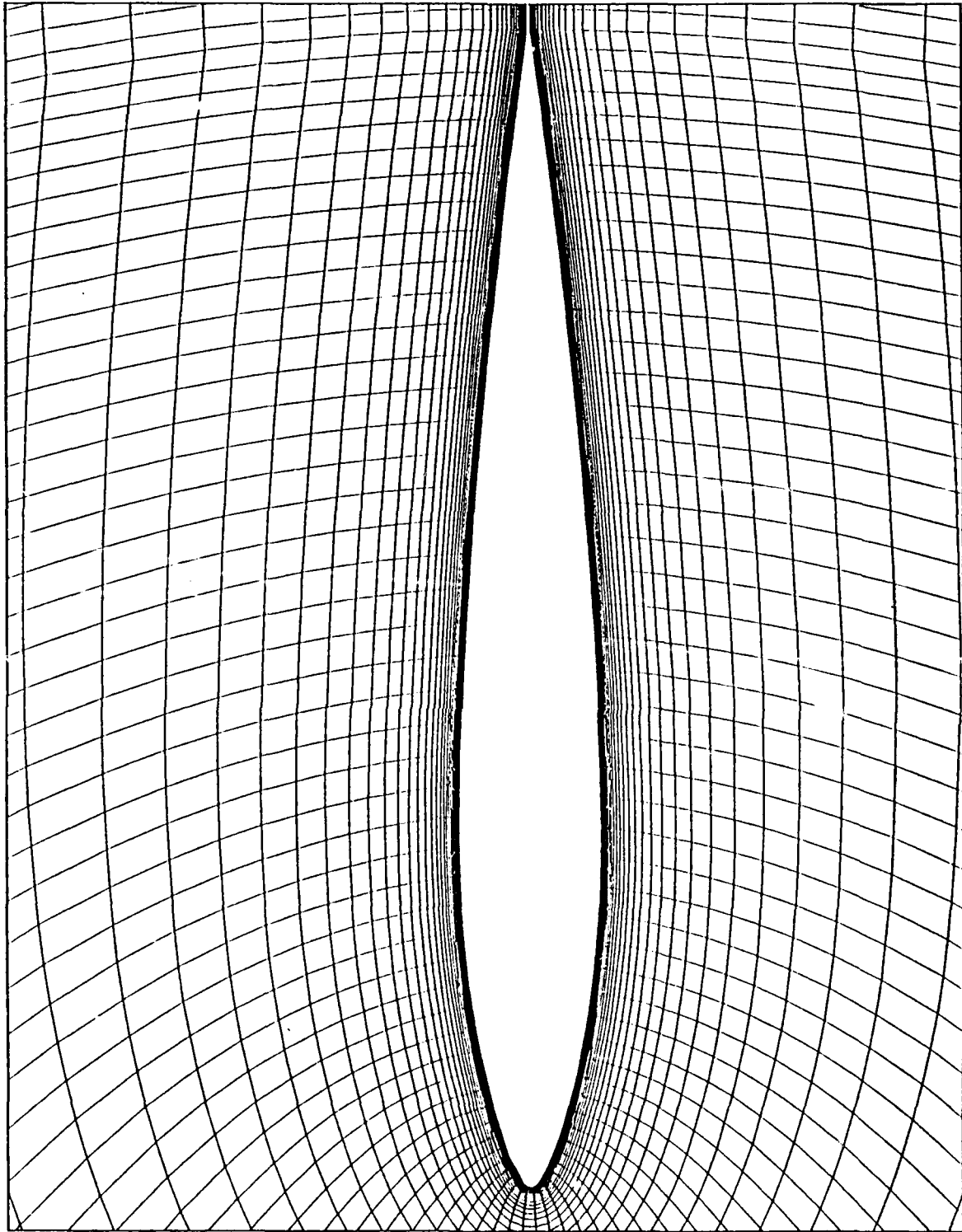


Figure 9. N0012-33 Local Grid

IV. RESULTS AND DISCUSSION

A. INVESTIGATION METHOD

Two-dimensional unsteady flows involving both harmonically oscillating and rapidly pitching (ramp pitch-up) airfoils were investigated. Studies for the oscillatory cases were conducted using the NACA 0012 airfoil in order to enable comparisons with previously conducted experimental measurements. Flows over all three airfoils rapidly pitched from 0° to 30° angle of attack with the reduced frequencies and Mach numbers (shown in Table 2) were subsequently investigated.

TABLE 2. RAPIDLY PITCHING AIRFOIL CASES, $Re = 4 \times 10^6$

AIRFOIL	0.3 Mach		0.4 Mach	
	k=.01	k=.02	k=.01	k=.02
NACA 0012	X	X	X	X
NACA 0012-63	X	X	X	X
NACA 0012-33	X	X	X	X

Solutions for the harmonically oscillating NACA 0012 airfoil were obtained for flows at a freestream Mach number of 0.3, Reynolds number based on the root chord $Re_c = 4 \times 10^6$ and for two reduced frequencies of $k=0.1$ and $k=0.2$. The reduced frequency is defined as $k = \omega c / 2U_\infty$ for the oscillatory case where $\alpha(t) = \alpha_0 + a_1 \sin(\omega t)$. In terms of nondimensional quantities k is given by $k = \omega / 2M_\infty$, and $\dot{\alpha}(t) = a_1 \omega \cos(\omega t)$ is the

instantaneous pitch-up rate which varies during the cycle with $\omega=2kM_\infty$ for a unit chord length. The present computations were conducted for a variation of the angle of attack as $\alpha(t)=10^\circ+6\sin(t)$. Experimental test conditions for the same freestream Mach and Reynolds numbers were for $\alpha(t)=10^\circ+5\sin(t)$. Because the airfoil stalled just at 15° for the experiment, the computed flow for the same conditions did not yield a hysteresis loop. Therefore, as McCroskey suggested, the oscillation was increased by one degree and a hysteresis loop was obtained. The computed lift behavior shown in Figures 10 and 11 exhibits the well-known hysteresis loop of a harmonically oscillating airfoil experiencing dynamic stall. The computation was initiated from a steady-state solution at $\alpha=5^\circ$ and was carried out for two cycles. Figures 10 and 11 display the results of the second cycle from the two-cycle computation.

Flow solutions for a rapidly pitching airfoil were obtained by pitching the airfoil at a constant rate from a zero angle of attack and steady-state flow conditions to an angle of attack of 30° at the desired reduced frequency and freestream Mach number. For the case where ramp motion was imposed, the reduced frequency k is given by $k=\dot{\alpha}c/2U_\infty$ where $\dot{\alpha}$ is the constant pitch-up rate. In terms of nondimensional quantities $k=\omega/2M_\infty$, or $\omega=2kM_\infty=\text{constant}$, and $\alpha(t)=\alpha_0+(\alpha_f-\alpha_0)\omega t$, where in this study $\alpha_0=0^\circ$ and $\alpha_f=30^\circ$ and $\omega=\dot{\alpha}(t)$. A summary of

the computed results for the rapidly pitching airfoils is provided in Table 3.

TABLE 3. PEAK LIFT COEFFICIENTS

AIRFOIL	Mach No.	Reduced Frequency	Peak C_l	Angle of Attack
N0012	0.3	.01	1.90	19.40°
		.02	2.10	23.40°
	0.4	.01	1.97	21.08°
		.02	2.24	25.21°
N0012-63	0.3	.01	1.84	18.50°
		.02	2.09	23.00°
	0.4	.01	1.93	20.60°
		.02	2.22	25.00°
N0012-33	0.3	.01	1.65	15.80°
		.02	1.94	19.60°
	0.4	.01	1.74	17.10°
		.02	2.09	23.15°

A general observation on the computed solution is that the modified NACA 0012-63 airfoil exhibited comparable lift behavior to the baseline NACA 0012 airfoil. A slight angle of attack versus lift curve shift was observed between the two airfoils at all reduced frequency/Mach number combinations. However, for the same flow parameters the NACA 0012-33 airfoil consistently underperformed the larger leading edge radius airfoils. The difference in the unsteady lift behavior with increasing angle of attack resulted from the different flow character at the leading edge region as will be shown later in detail. In the following sections, detailed comparison of the lift behavior of the three airfoils is presented at the various flow conditions. The flow characteristics and the

development and progression of the dynamic stall process are examined. The effects of reduced frequency and freestream Mach number are also discussed.

B. LIFT BEHAVIOR

1. Harmonically Oscillating Airfoil

Although hysteresis loops characteristic of an oscillating airfoil undergoing dynamic stall were observed for reduced frequencies of both 0.1 and 0.2, agreement with experimental results varied. At a reduced frequency of 0.1, the response agreed well with McCroskey's experimental results (Figure 10) during the upstroke. Maximum lift coefficient was 1.52 at an angle of attack of 15.8° . The lift behavior continues to agree well with the experimental data during the upstroke of the hysteresis loop and during the initial part of the downstroke. As the downstroke continues and the flow reattaches, however, the numerical solution displays significantly greater oscillations in lift coefficient compared to experimental data, which were obtained as an average over several cycles of oscillation.

At a reduced frequency of 0.2 (Figure 11), the numerical solution exhibited a much smaller hysteresis loop than the respective experimental data. In this case, maximum lift coefficient in the numerical solution occurred just prior to the downstroke, so that flow reattachment occurred almost

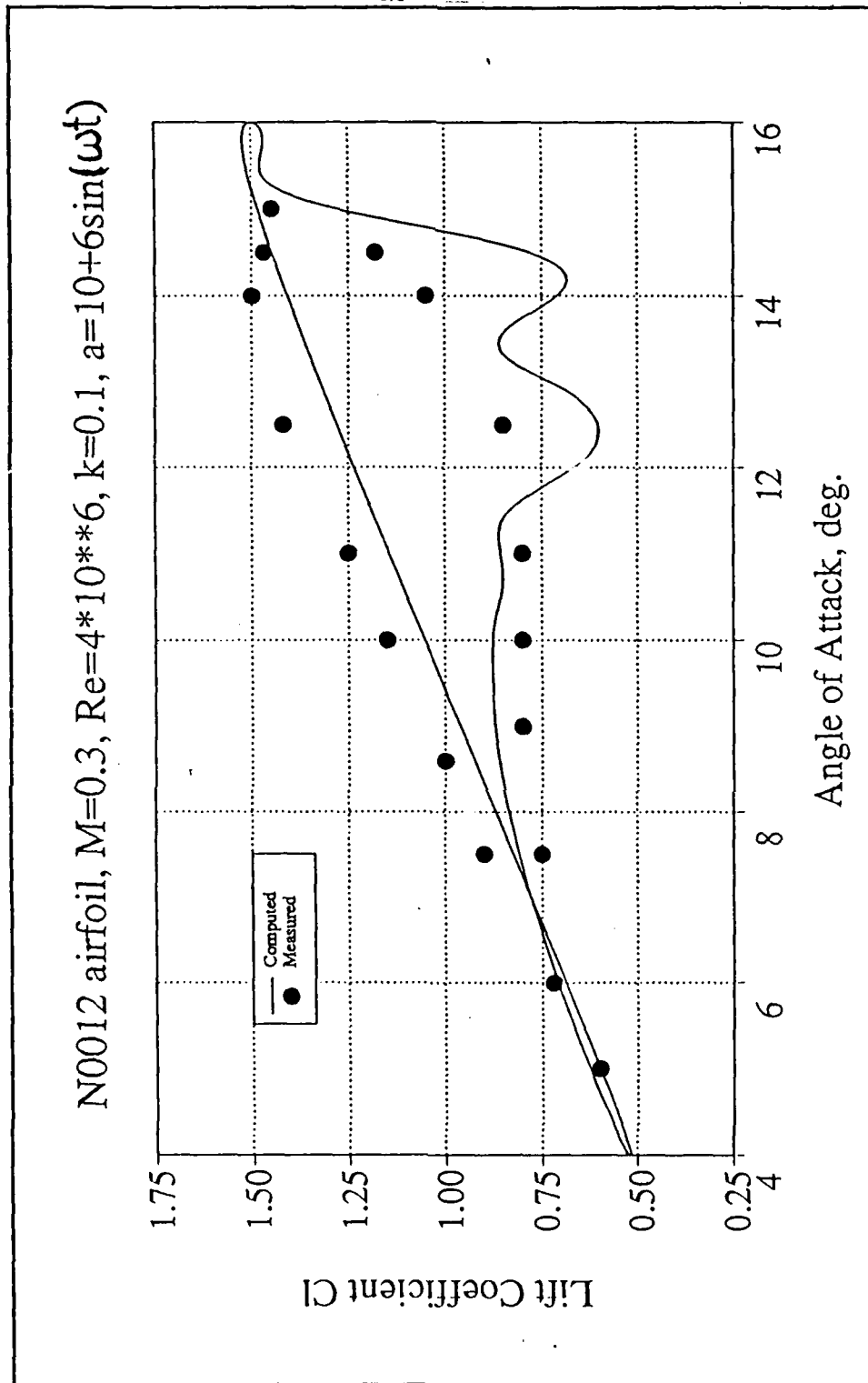


Figure 10. Lift Behavior, NACA 0012, $M=0.3$, $k=0.1$

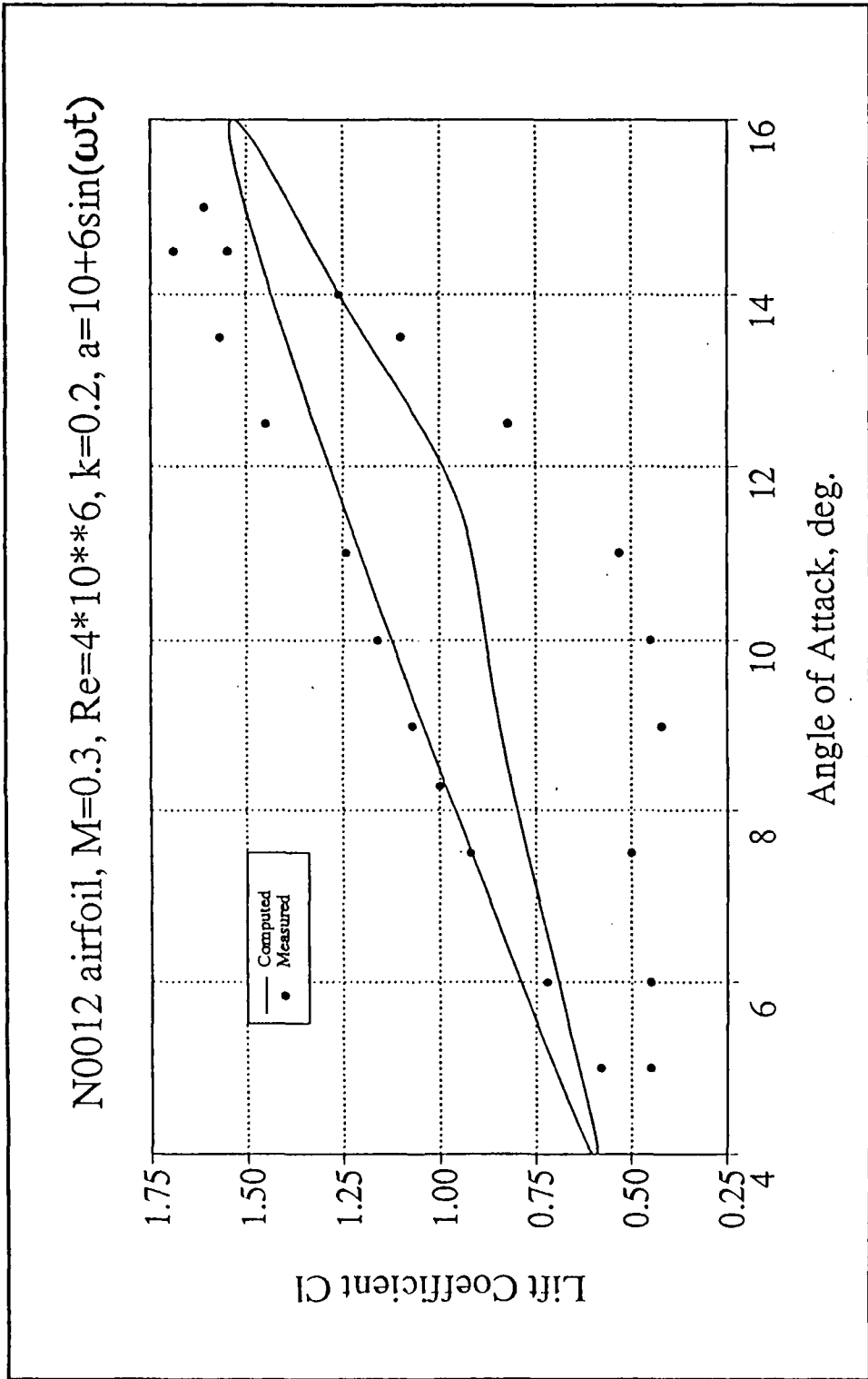


Figure 11. Lift Behavior, NACA 0012, $M=0.3$, $k=0.2$

immediately. Maximum lift coefficient at $k=0.2$ was only slightly higher than at the $k=0.1$ case.

The lack of agreement with experimental data at a reduced frequency of 0.2 and during the flow reattachment process at $k=0.1$ may be indicative of the poor behavior of the eddy-viscosity model (which is suitable for steady flows). Higher values of the reduced frequency resulted in larger discrepancies from the measured lift values.

2. Rapidly Pitching Airfoil

Lift coefficient vs. angle of attack comparison of the three airfoils is presented in Figures 12-15 for the Mach number/reduced frequency combinations listed in Table 2. For the same flow parameters, all three airfoils have nearly the same lift curve slope until the onset of dynamic stall. Along with the aforementioned angle of attack shift of the lift curves between the NACA 0012 and -63 airfoils after stall occurs, the peak lift coefficients for the NACA 0012 airfoil are slightly higher than for the -63 airfoil. The peak lift coefficient for the NACA 0012 occurred 0.2 to 0.9 degrees angle of attack higher than the peak C_l for the -63 airfoil for the same flow conditions. With both airfoils having the same leading edge radius, the small difference in performance may be attributed to the slightly thicker contouring of the forward part of the baseline NACA 0012 airfoil (Table 1).

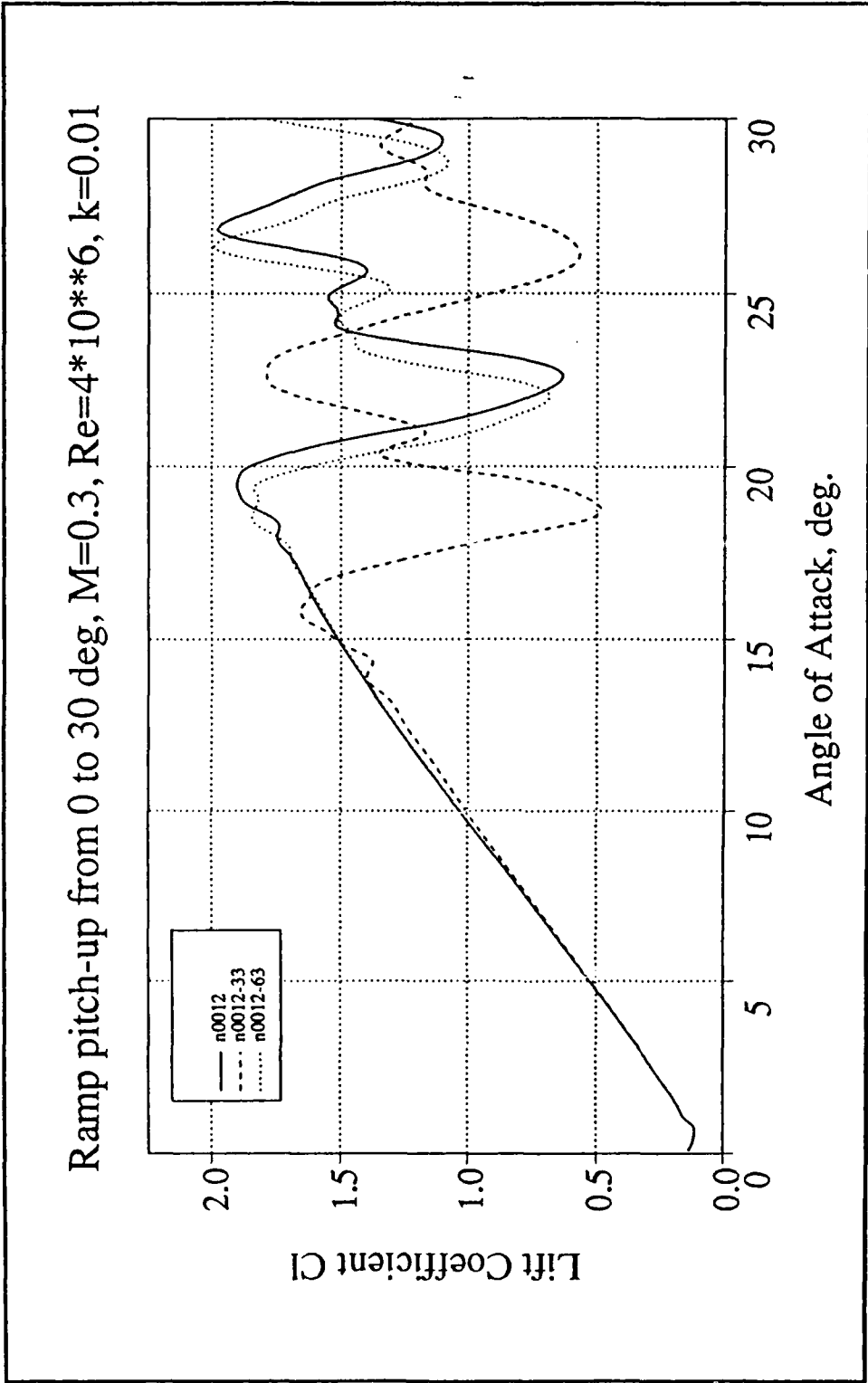


Figure 12. Lift Comparison, $M=0.3$, $k=0.01$

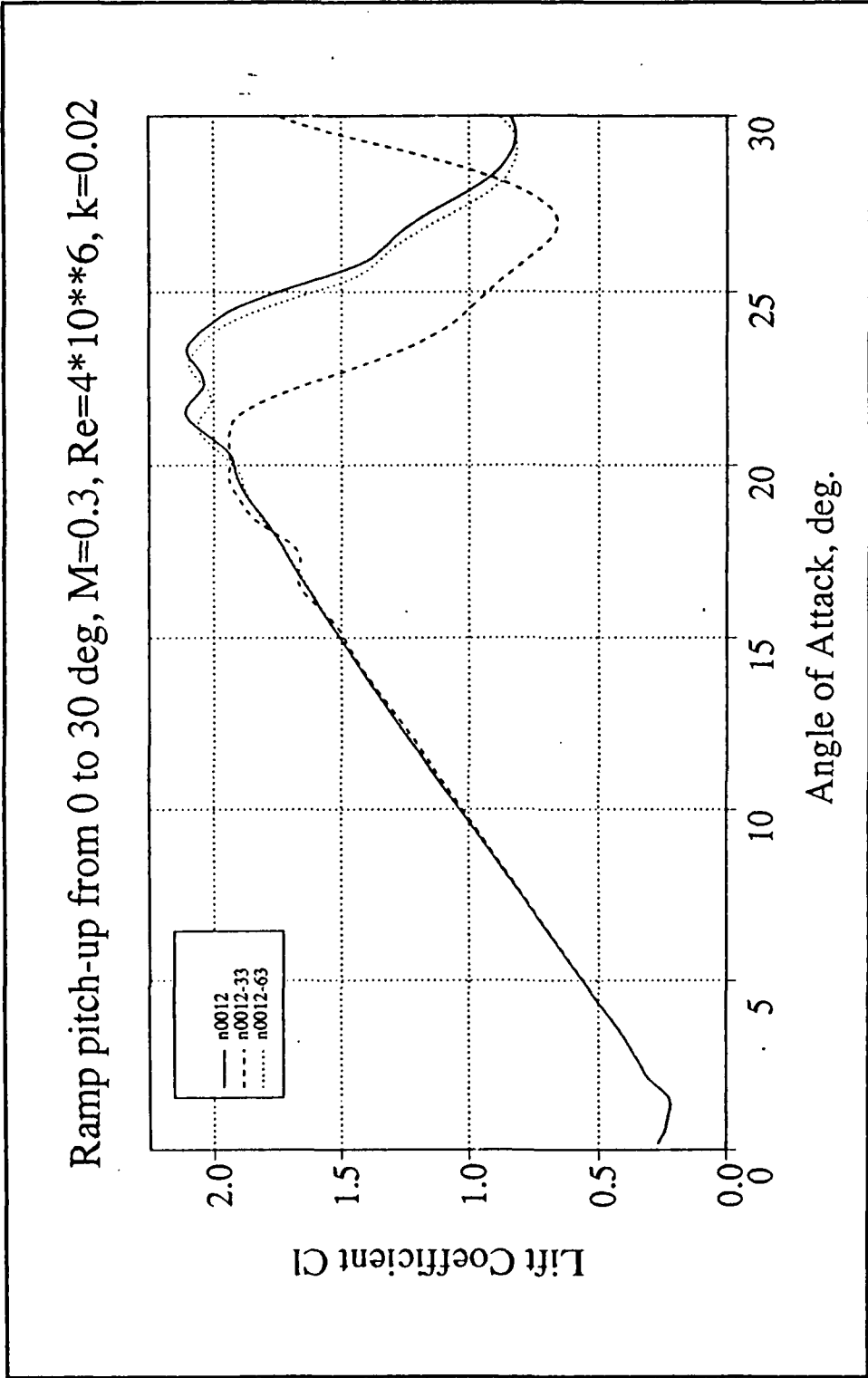


Figure 13. Lift Comparison, $M=0.3$, $k=0.02$

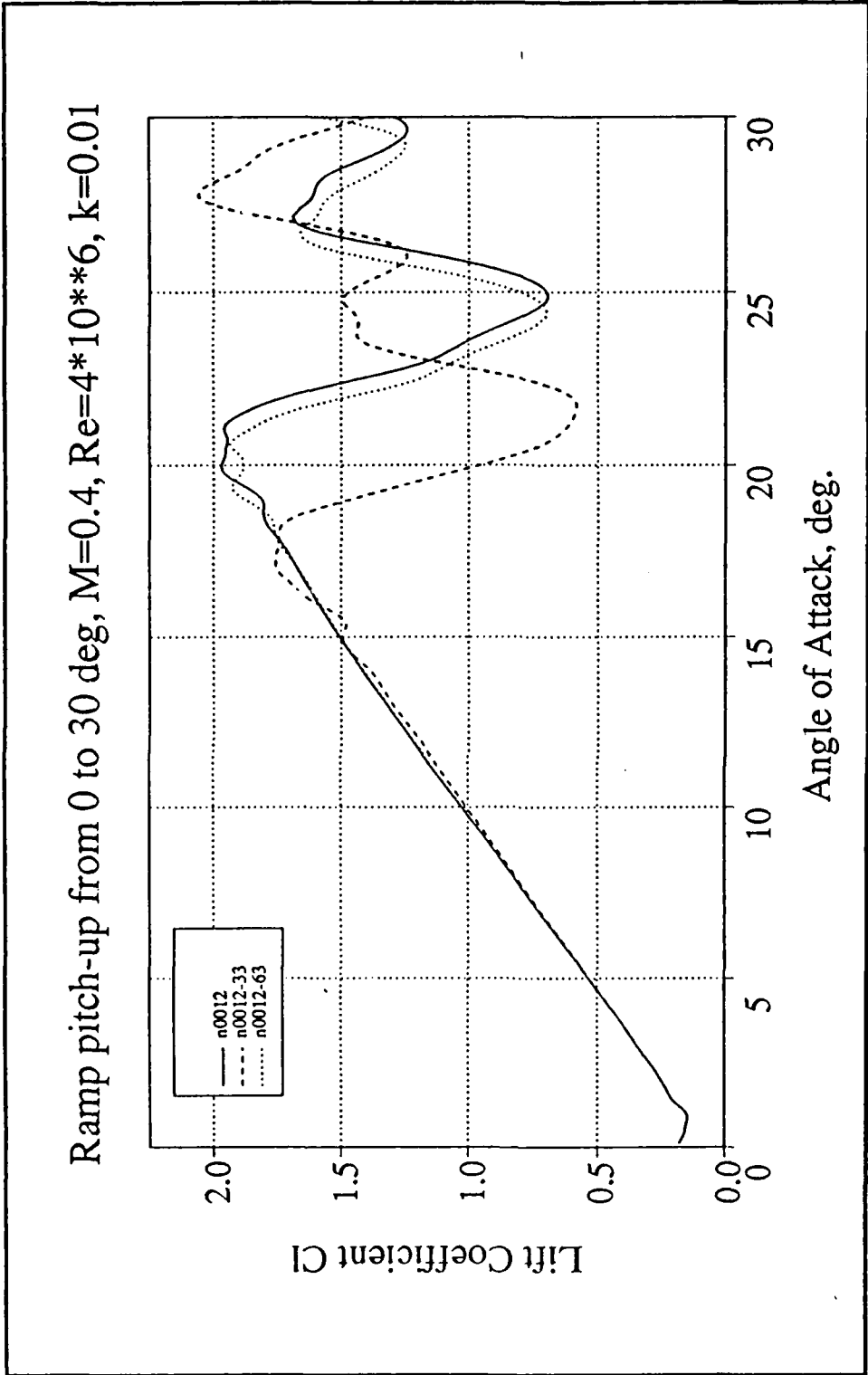


Figure 14. Lift Comparison, $M=0.4$, $k=0.01$

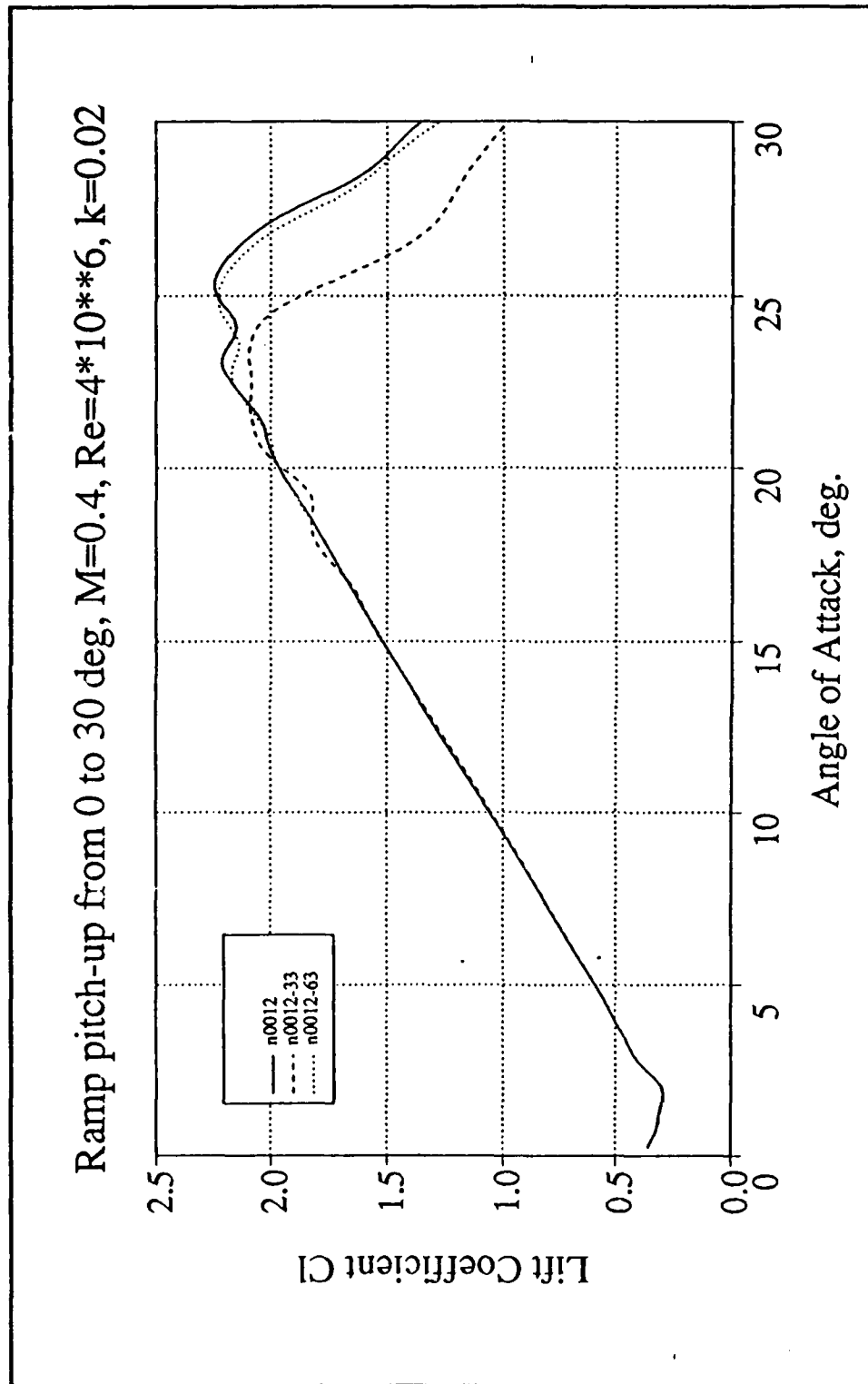


Figure 15. Lift Comparison, $M=0.4$, $k=0.02$

The maximum lift coefficient obtained with the NACA 0012-33 airfoil was lower than that obtained with the other two airfoils and occurred at 1.8 to 4.0 degrees lower angle of attack. At a reduced frequency of $k=0.01$ and freestream Mach number of 0.3, the initial leading edge vortex originated at an angle of attack of 12° for the -33 airfoil. Under the same flow conditions, formation of the vortex occurred at 17° and 16.5° for the baseline 0012 and -63 airfoils, respectively. Similar differences occurred at all other flow conditions investigated. The smaller leading edge radius of the NACA 0012-33 airfoil promoted earlier development of the dynamic stall vortex from the leading edge upper surface.

As will be shown, the dynamic stall vortex originates as a result of the combination of the accelerated flow over the leading edge with the boundary layer reverse flow behind the leading edge. An adverse pressure gradient is encountered by the flow as it passes the suction peak just downstream of the airfoil leading edge. This adverse pressure gradient causes flow deceleration just aft of the suction peak, leading eventually to the boundary layer separating at a critical value of the adverse pressure gradient. The momentum of the flow, however, is increased as the flow accelerates around the leading edge and opposes the tendency of the flow to separate. Eventually, depending on the airfoil shape characteristics, the boundary layer separates, reversed flow occurs, and combines with the freestream to form the leading edge vortex.

As observed in this investigation, the size of the leading edge radius is of primary importance in determining the angle of attack at which the boundary layer separates and rolls to form the dynamic stall vortex. For the same flow parameters and angle of attack during pitch-up, the critical pressure gradient for flow separation occurred earlier on the airfoil with smaller leading edge radius (NACA 0012-33). Stated otherwise, at a given angle of attack during pitch-up, the adverse pressure gradient aft of the suction peak is greater for the smaller leading edge airfoil.

The contouring of the forward part of the airfoil is of secondary importance in alleviating development of the adverse pressure gradient. The effect of contouring is indicated by the slightly earlier development of leading edge reverse flow on the NACA 0012-63 airfoil compared to the baseline 0012 airfoil.

In summary, enlarging the leading edge radius and thickening the contouring of the forward part of the airfoil results in decreasing the adverse pressure gradient encountered by the flow, with resulting delay in separation. This is shown graphically in Figures 16-20 where instantaneous streamlines are shown for the three airfoils at the same 17° angle of attack, 0.4 Mach, and $k=0.01$. Reversed boundary layer flow has just begun on the NACA 0012 airfoil aft of the suction peak, whereas initiation of the dynamic stall vortex has already occurred on the NACA 0012-63 airfoil which has

thinner contouring. The NACA 0012-33 airfoil with the small leading edge radius has a fully developed dynamic stall vortex and is 0.6° angle of attack prior to dynamic stall. A detailed discussion of the vortical flow development follows.

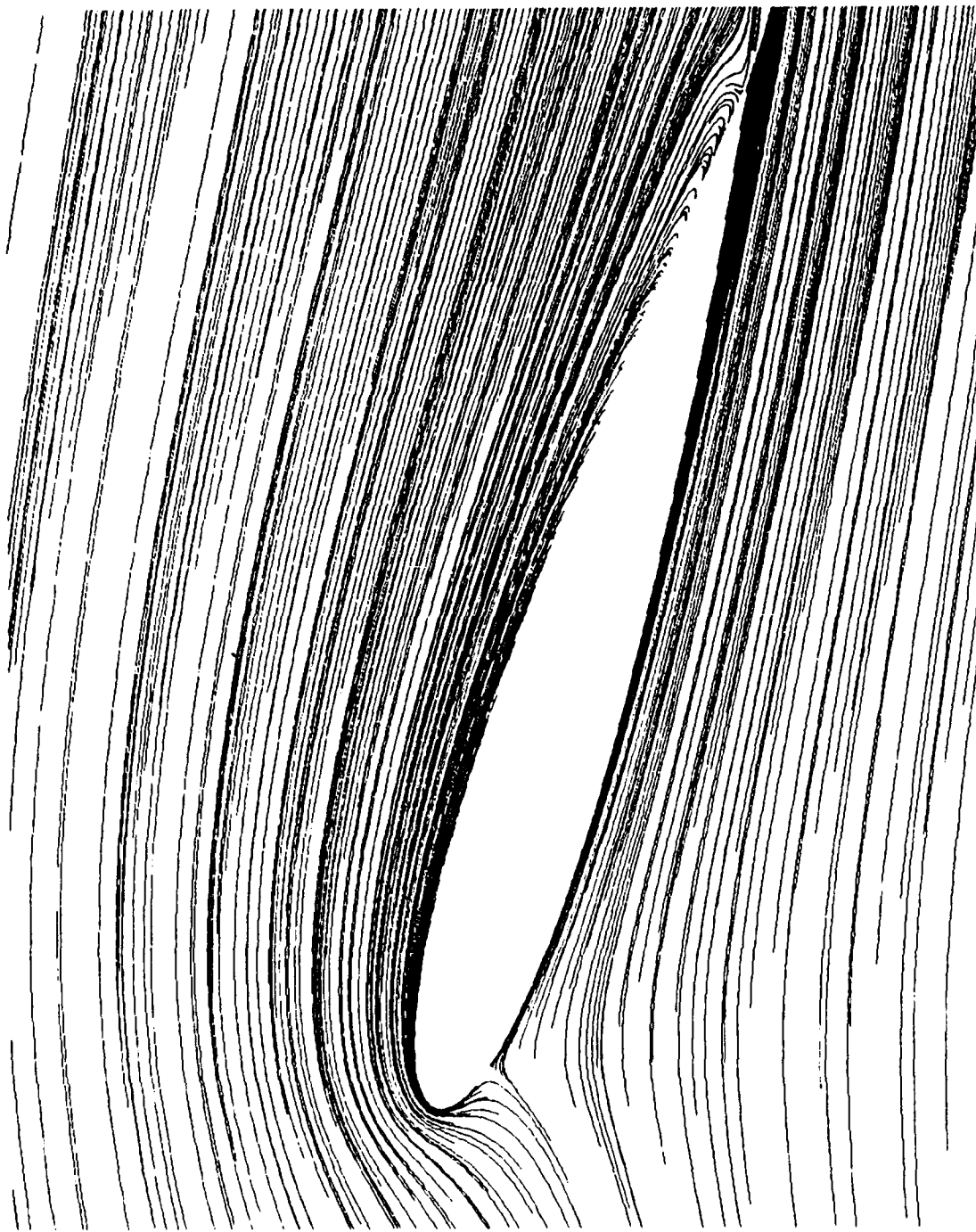


Figure 16. Instantaneous Streamlines, NACA 0012, $M=0.4$,
 $k=0.01$, $\alpha=17^\circ$

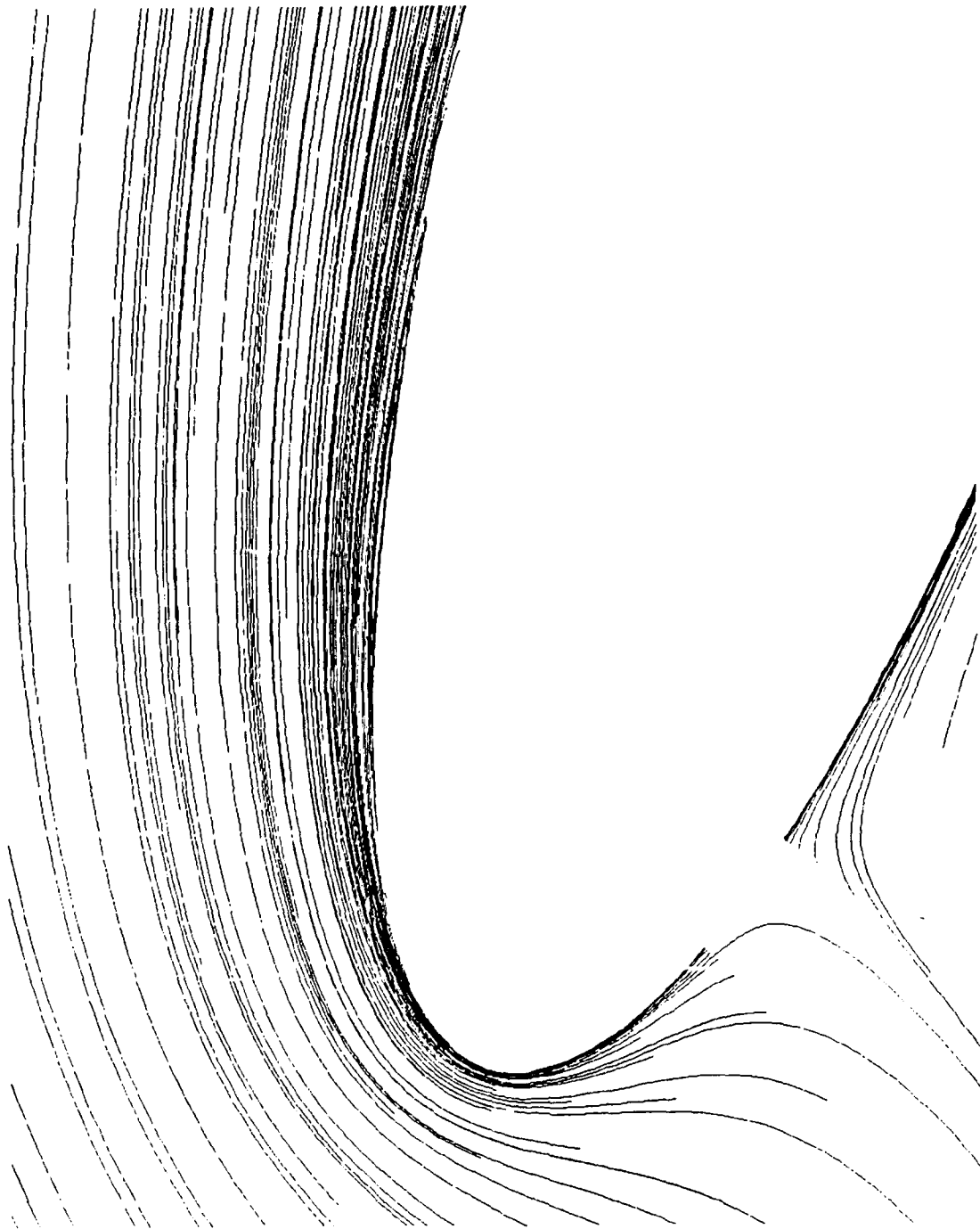


Figure 17. Leading Edge Instantaneous Streamlines, NACA 0012,
 $M=0.4$, $k=0.01$, $\alpha=17^\circ$

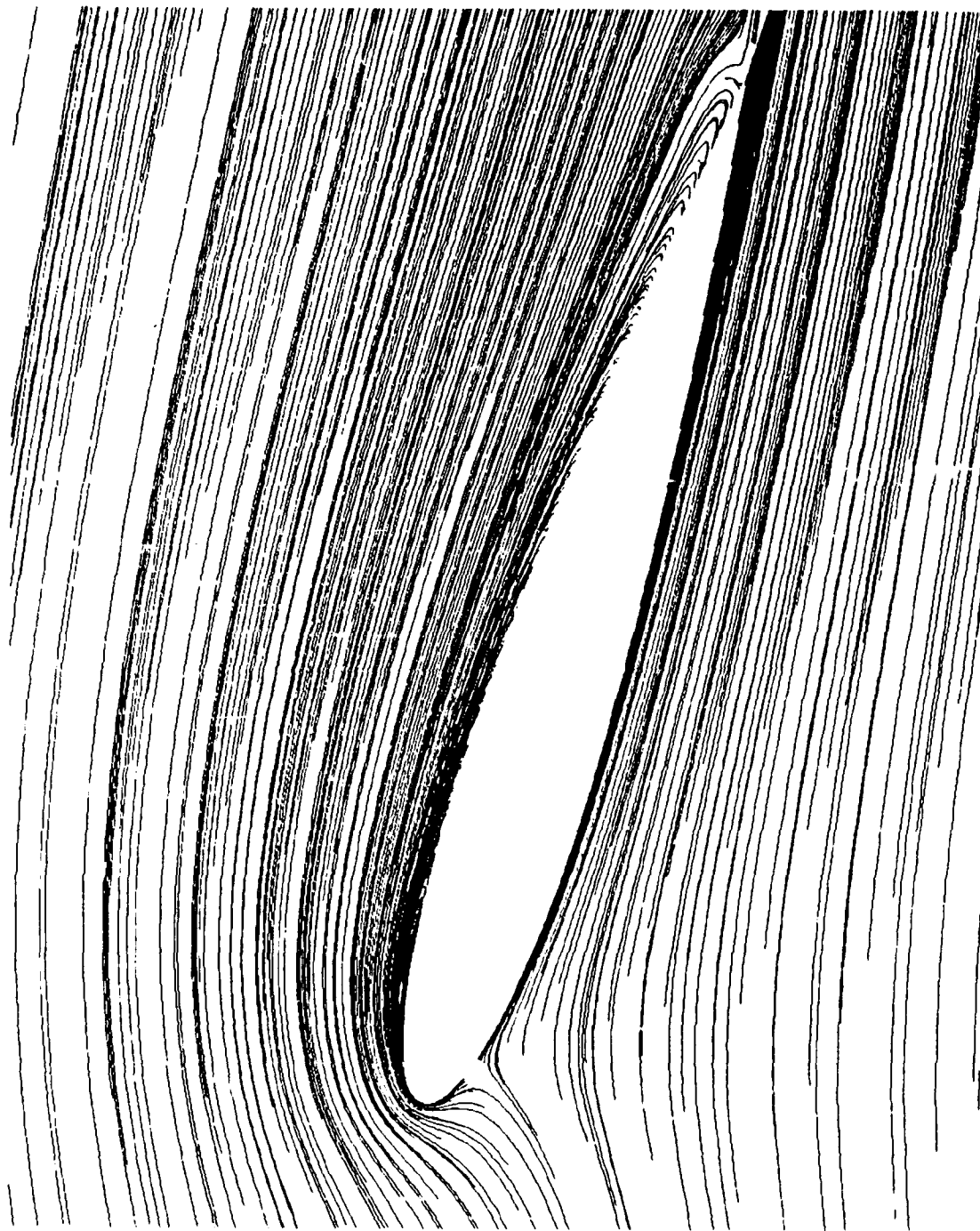


Figure 18. Instantaneous Streamlines, NACA 0012-63, $M=0.4$, $k=0.01$, $\alpha=17^\circ$



Figure 19. Leading Edge Instantaneous Streamlines, NACA 0012-63, $M=0.4$, $k=0.01$, $\alpha=17^\circ$

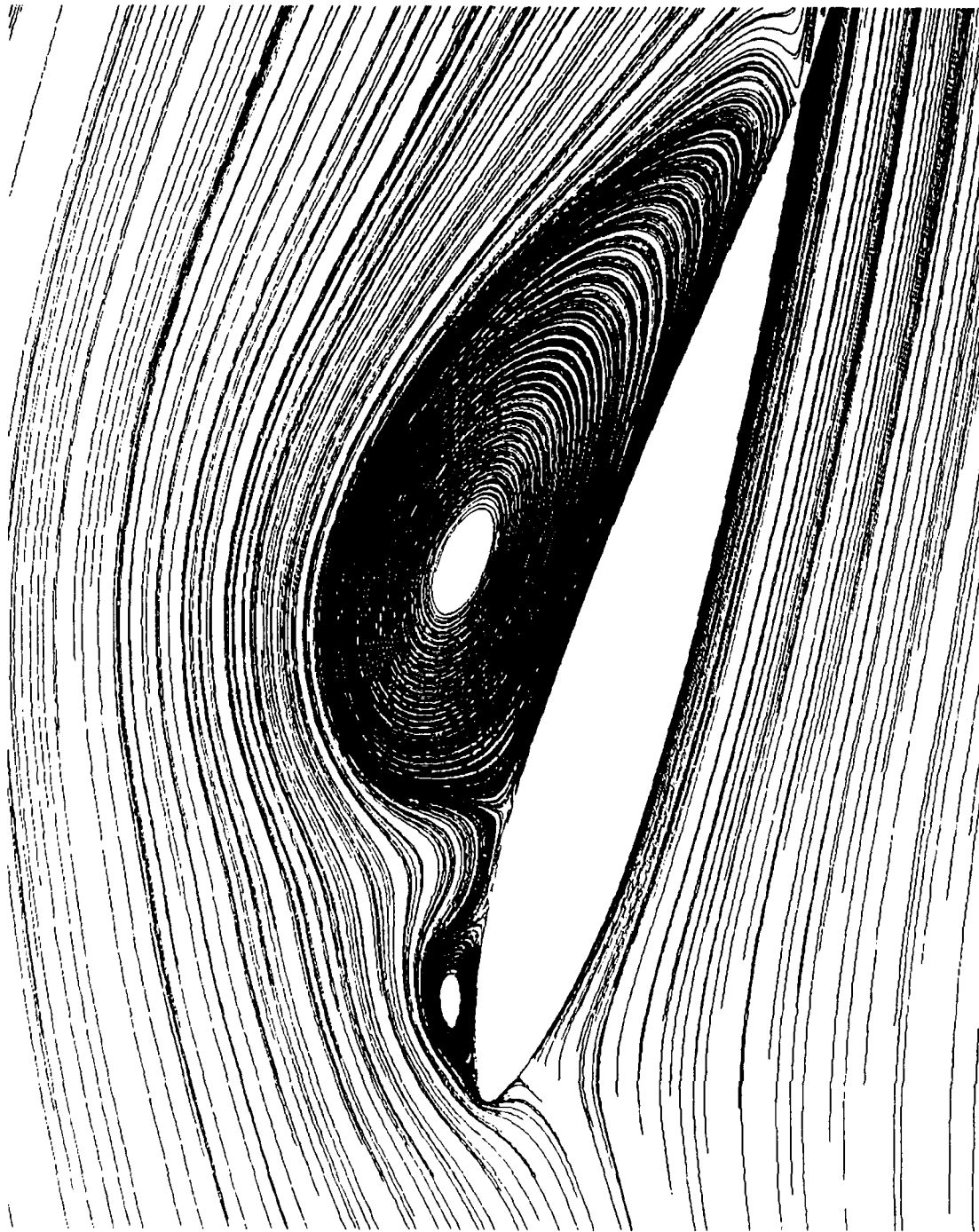


Figure 20. Instantaneous Streamlines, NACA 0012-33, $M=0.4$, $k=0.01$, $\alpha=17^\circ$

C. VORTEX FLOW DEVELOPMENT

1. Rapidly Pitching Airfoil

The development of the vortical flowfield as the angle of attack is increasing follows a consistent, general sequence of events. This sequence of events requires examination of the variation of several flow quantities as angle of attack is increased. Figures 21-33 illustrate the flow development stages using the velocity vector field, the pressure, and vorticity field contours for the NACA 0012-63 airfoil at $M=0.4$ and $k=0.01$. Figures 34-47 display the associated surface pressures and temperatures of the developing flow.

Initially, smooth streamlined flow is observed over the airfoil leading edge (Figures 21-22). As angle of attack increases beyond a certain critical limit depending on pitching rate, freestream Mach number, airfoil shape, and Reynolds number, small reverse flow regions develop on the upper surface aft of the suction peak and forward of the trailing edge due to the adverse pressure gradients encountered by the flow. Figure 23 shows the reversed boundary layer flow near the airfoil surface. Figure 24 displays the developing leading edge vortex.

The developing vortex forms on the upper surface just aft of the leading edge as a result of the combination of the accelerated flow near the suction peak and the reverse flow just aft of the suction peak. It is observed that the dynamic stall vortex initiates as a separated flow bubble, and rapidly

grows in size to form the characteristic leading edge dynamic stall vortical structure as the angle of attack increases. During this initiation process the primary vortex has a oval shape and becomes more rounded as the angle of attack increases. Figure 25 shows the oval dynamic stall vortex taking shape. Figure 26 displays the relative strength of the developing vortex.

The vortex grows in size and strengthens, becoming approximately circular as angle of attack increases, and moves away from the airfoil. Figure 27 shows the development of the vortex as it moves downstream. Passage of the dynamic stall vortex over the airfoil surface induces reverse velocities and significantly contributes to the development of reversed flows. A secondary vortex originates near the leading edge and also grows as angle of attack increases. Figures 28 and 29 show the development of a secondary vortex as the primary vortex moves downstream and promotes reverse flow over the whole upper airfoil surface.

At the trailing edge, flow separation is initiated at approximately the same time as at the leading edge, and a pressure gradient exists between the lower and upper surfaces. The upper surface reverse flow combines with the high pressure flow from the lower surface to form a counter-clockwise vortex at the trailing edge shortly before dynamic stall occurs. Figures 30 and 31 show the developed trailing edge vortex 0.6° angle of attack before peak lift coefficient is obtained. As

the primary vortex grows and moves downstream past approximately 60-70% chord, dynamic stall occurs, usually accompanied by development of a small, tertiary vortex at the leading edge. Figures 32 and 33 display the position of the dynamic stall vortex 0.4° angle of attack after attainment of peak lift coefficient.

By this time, the primary vortex is centered at a distance greater than the airfoil maximum thickness from the airfoil and combines with lower surface high pressure flow to energize the counter-clockwise vortex at the trailing edge.

With further increase in angle of attack, the airfoil enters the deep stall regime, and the freestream flow has no effect on the upper surface flow characteristics. In this case, the aerodynamic behavior of the airfoil is greatly determined by the vortical flow field formed by the shed vortices, and the strength of the vortices themselves determine the flow over the upper surface. Figures 48 and 49 show the NACA 0012-33 airfoil in deep stall at 0.3 Mach, $k=0.02$, $\alpha=22.0^\circ$ and demonstrate that the vortices can combine to form a large vortical region and entrain other secondary flows. In this case a counterclockwise vortex was formed between the paired primary and secondary vortices and the airfoil.

VELOCITY COLORED BY PRESSURE

MACH 0.400
 ALPHA 14.01 DEG
 Re 4.000×10^6
 I-NAME 31.
 GRID 157x58

CONTOUR I FUFIS

0.060000
 0.080000
 0.100000
 0.120000
 0.140000
 0.160000
 0.180000
 0.200000
 0.220000
 0.240000
 0.260000
 0.280000
 0.300000
 0.320000
 0.340000
 0.360000
 0.380000
 0.400000
 0.420000
 0.440000
 0.460000
 0.480000
 0.500000
 0.520000
 0.540000
 0.560000
 0.580000
 0.600000
 0.620000
 0.640000
 0.660000
 0.680000
 0.700000
 0.720000
 0.740000
 0.760000
 0.780000
 0.800000
 0.820000
 0.840000
 0.860000
 0.880000
 0.900000
 0.920000
 0.940000
 0.960000
 0.980000
 1.000000

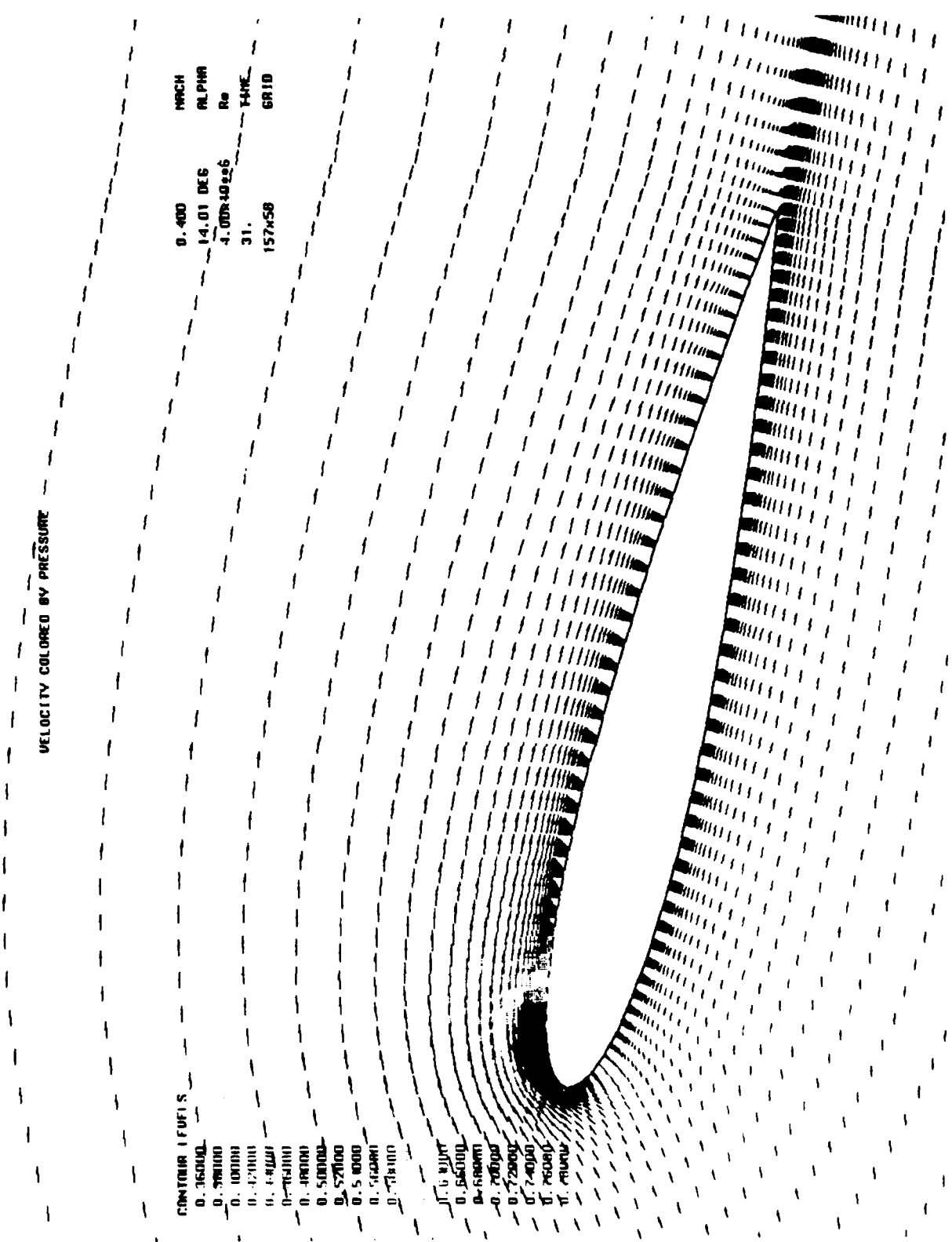


Figure 21. Velocity Field, NACA 0012-63, M=0.4, k=0.01, $\alpha=14.0^\circ$

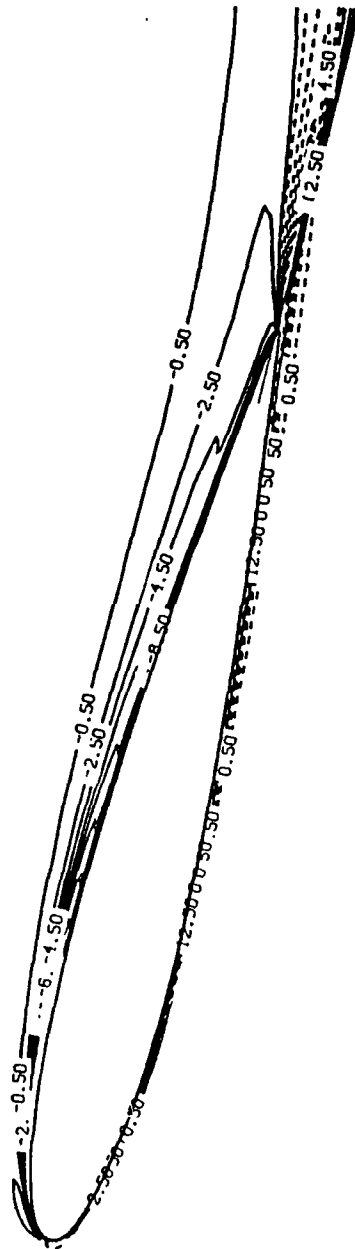


Figure 22. Vorticity Contours, NACA 0012-63, $M=0.3$, $k=0.01$, $\alpha=14.0^\circ$

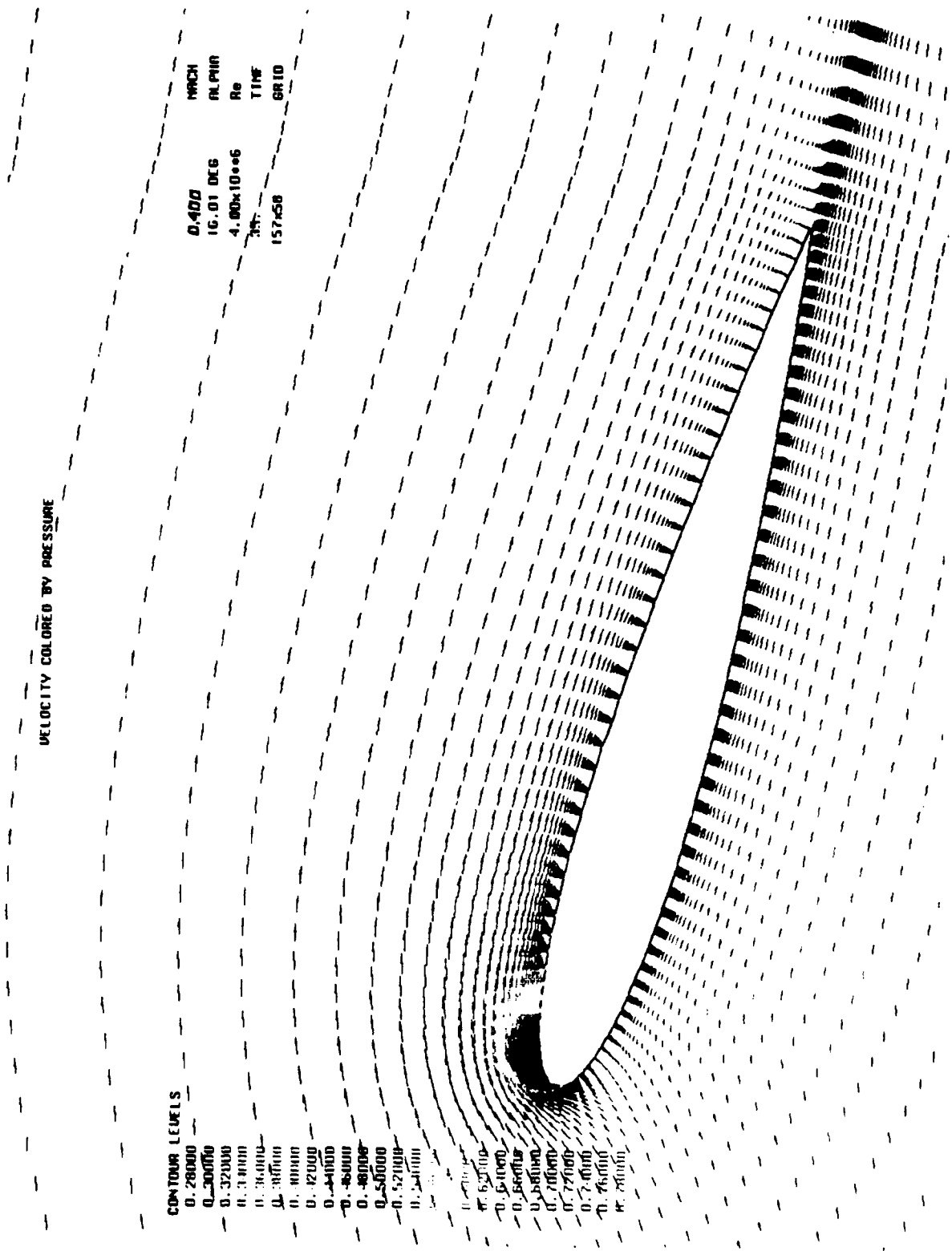


Figure 23. Velocity Field, NACA 0012-63, M=0.4, k=0.01, $\alpha=16.0^\circ$

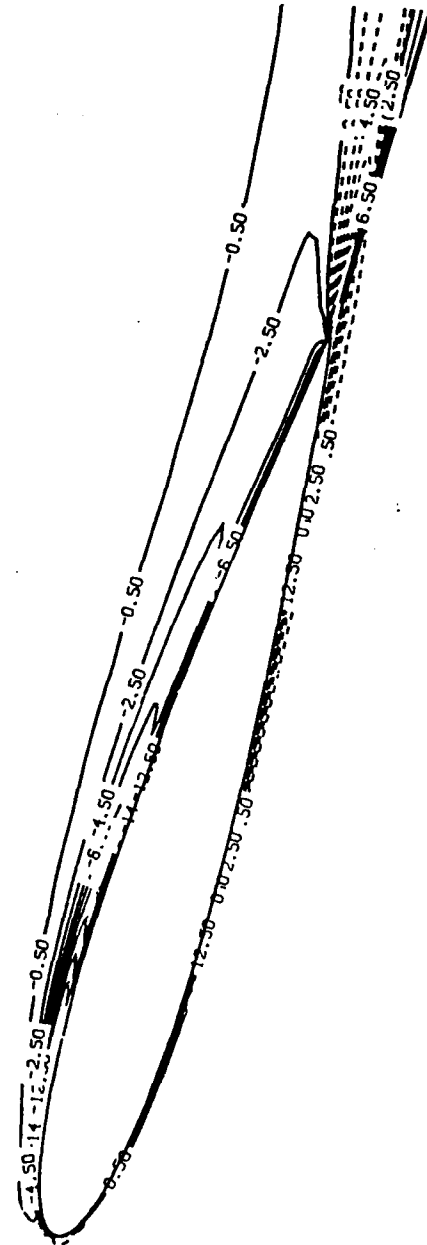


Figure 24. Vorticity Contours, NACA 0012-63, $M=0.4$, $k=0.01$, $\alpha=16.0^\circ$

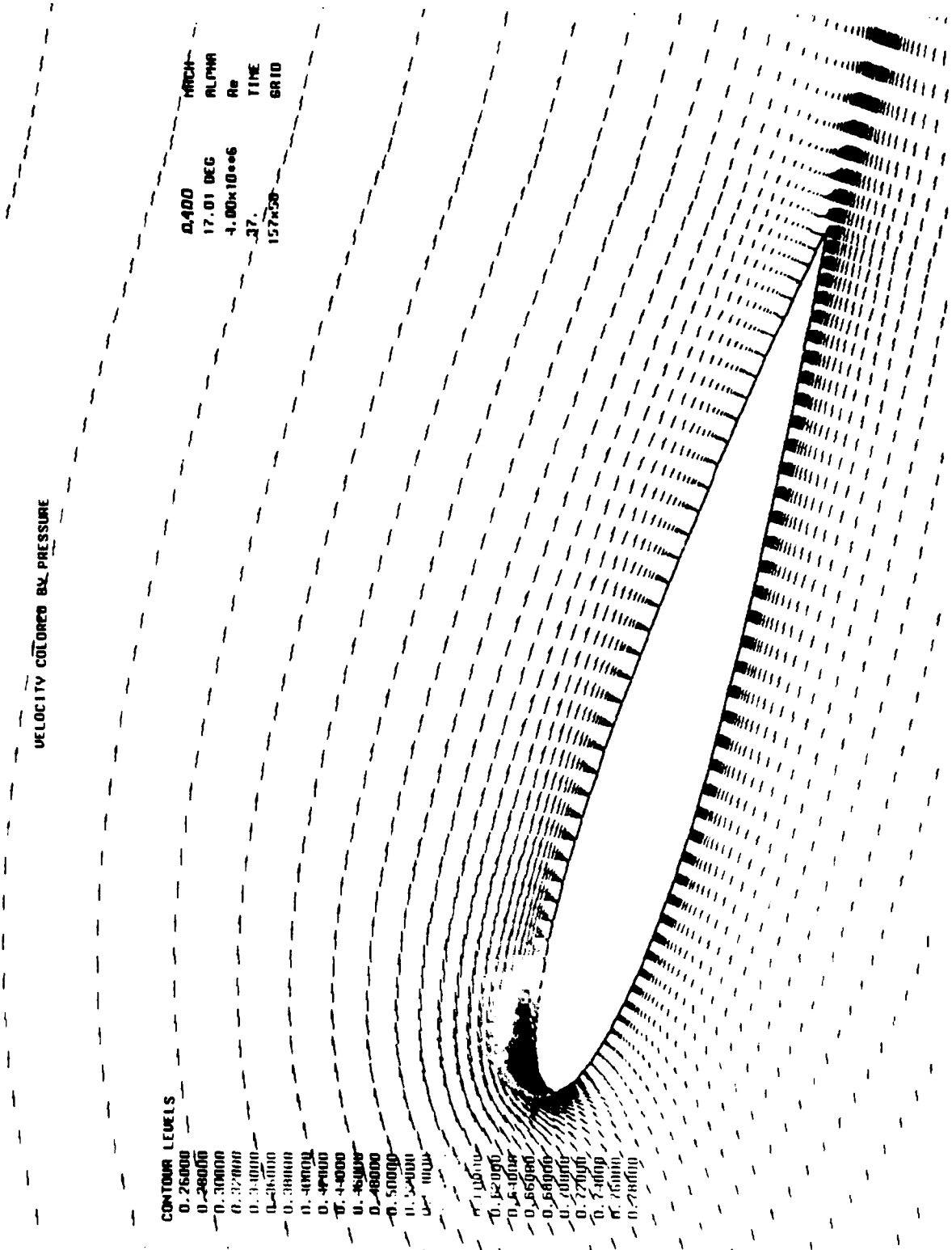


Figure 25. Velocity Field, NACA 0012-63, $M=0.4$, $k=0.01$, $\alpha=17.0^\circ$

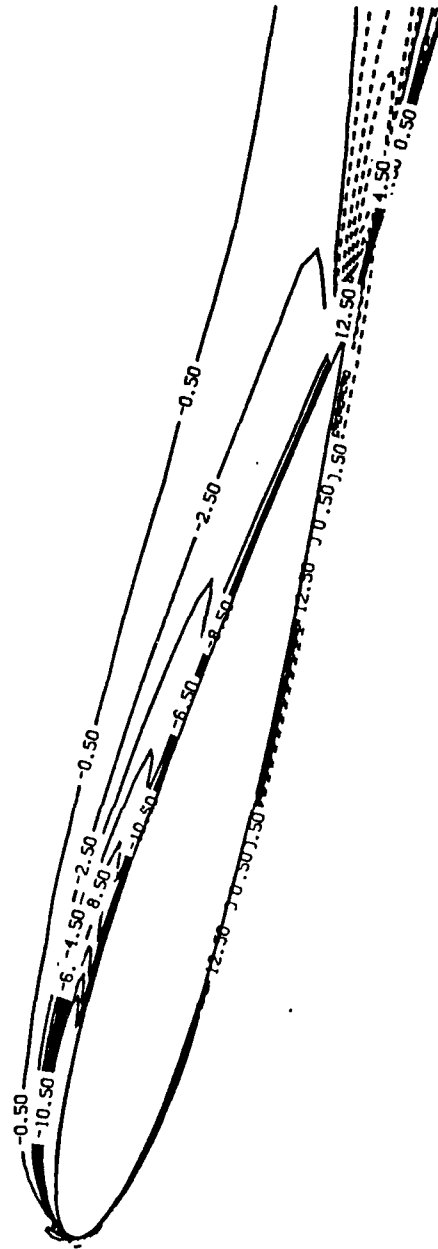


Figure 26. Vorticity Contours, NACA 0012-63, $M=0.3$, $k=0.01$, $\alpha=17.0^\circ$

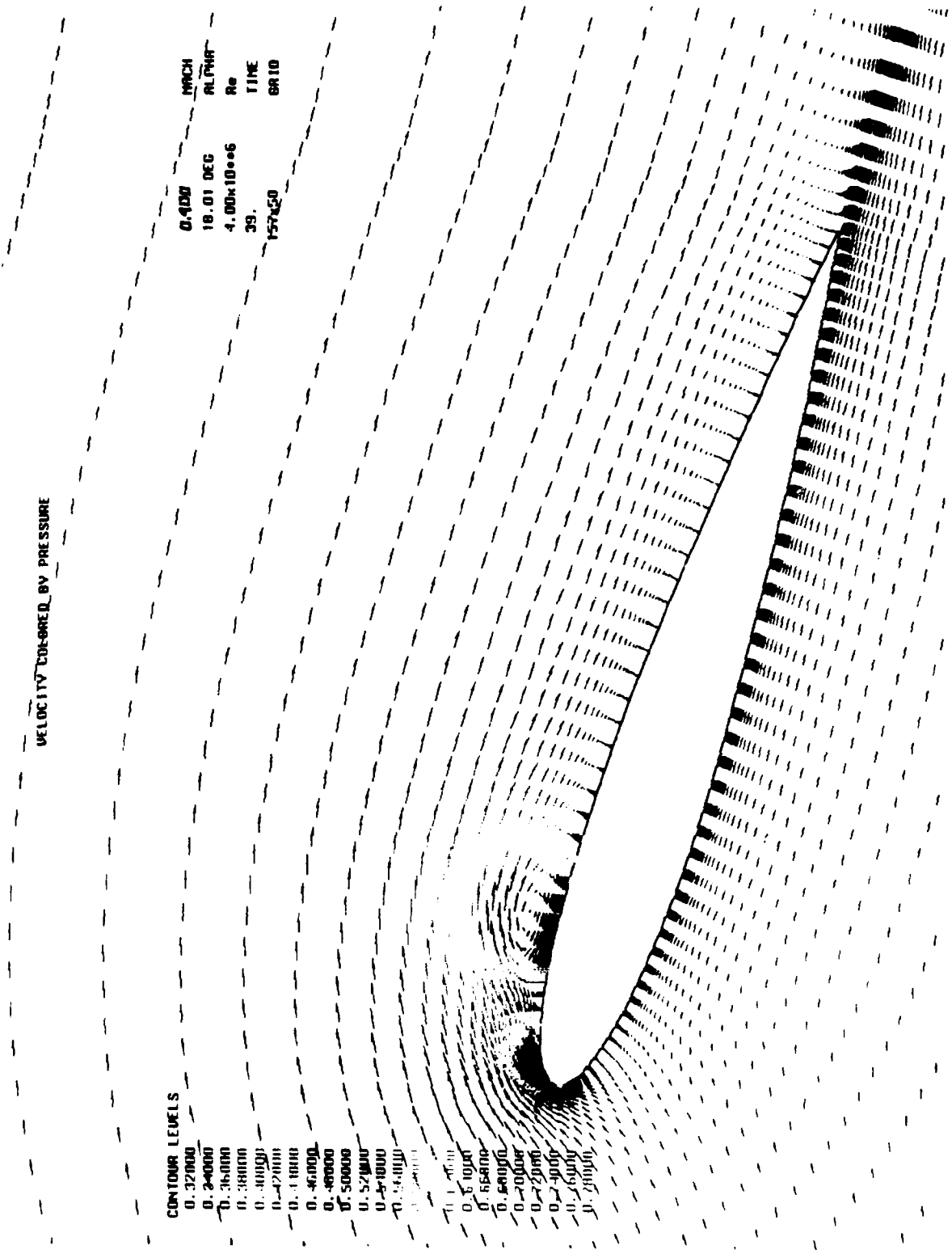


Figure 27. Velocity Field, NACA 0012-63, M=0.4, k=0.01, $\alpha=18.0^\circ$

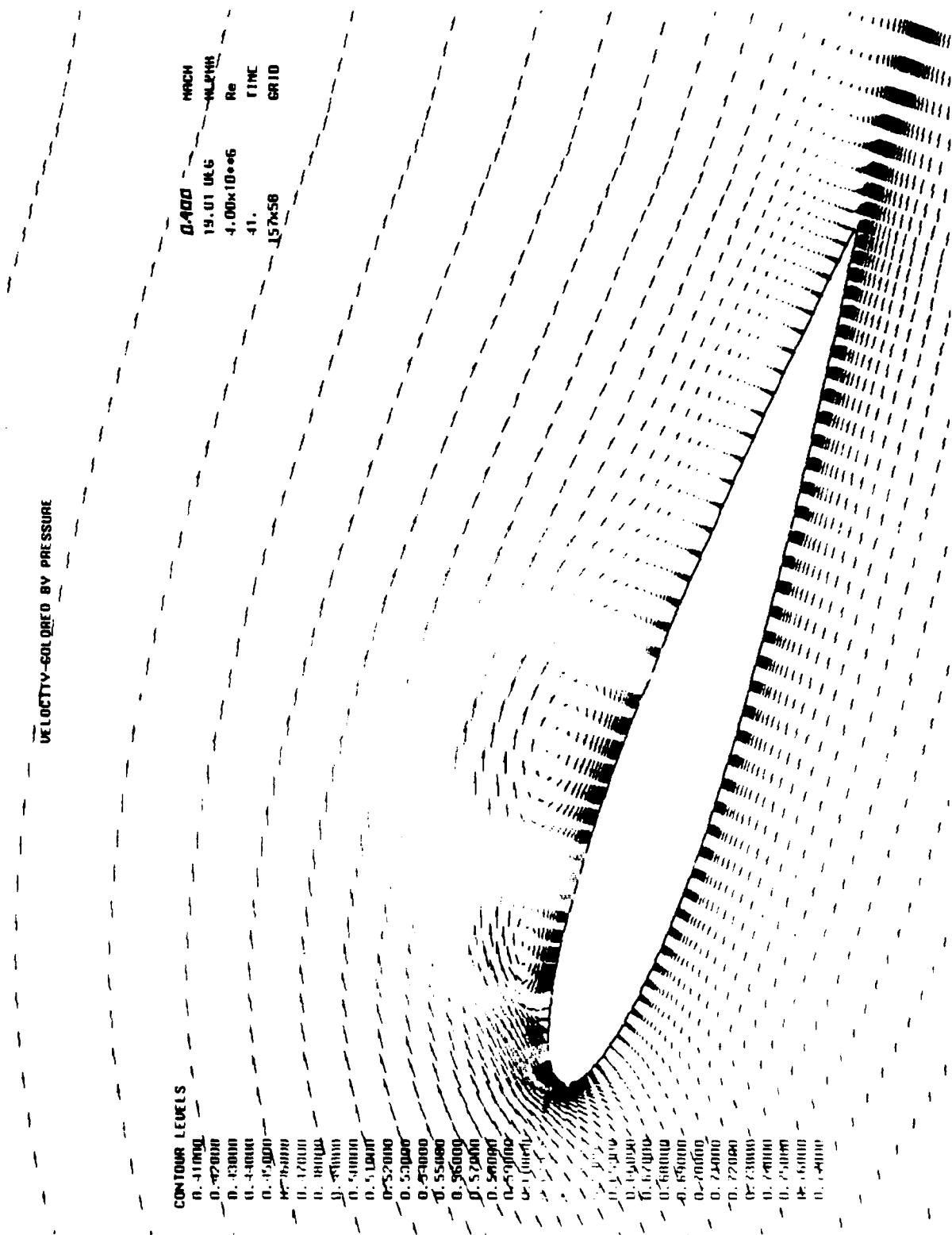


Figure 28. Velocity Field, NACA 0012-63, M=0.4. k=0.01, $\alpha=19.0^\circ$

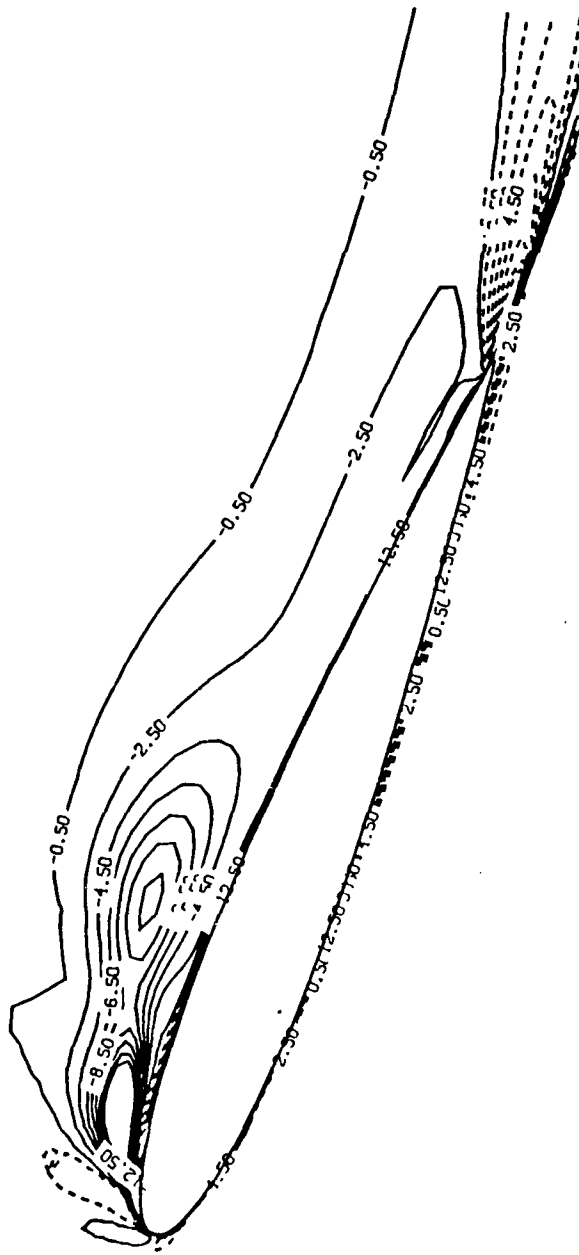


Figure 29. Vorticity Contours, NACA 0012-63, $M=0.4$, $k=0.01$, $\alpha=19.0^\circ$

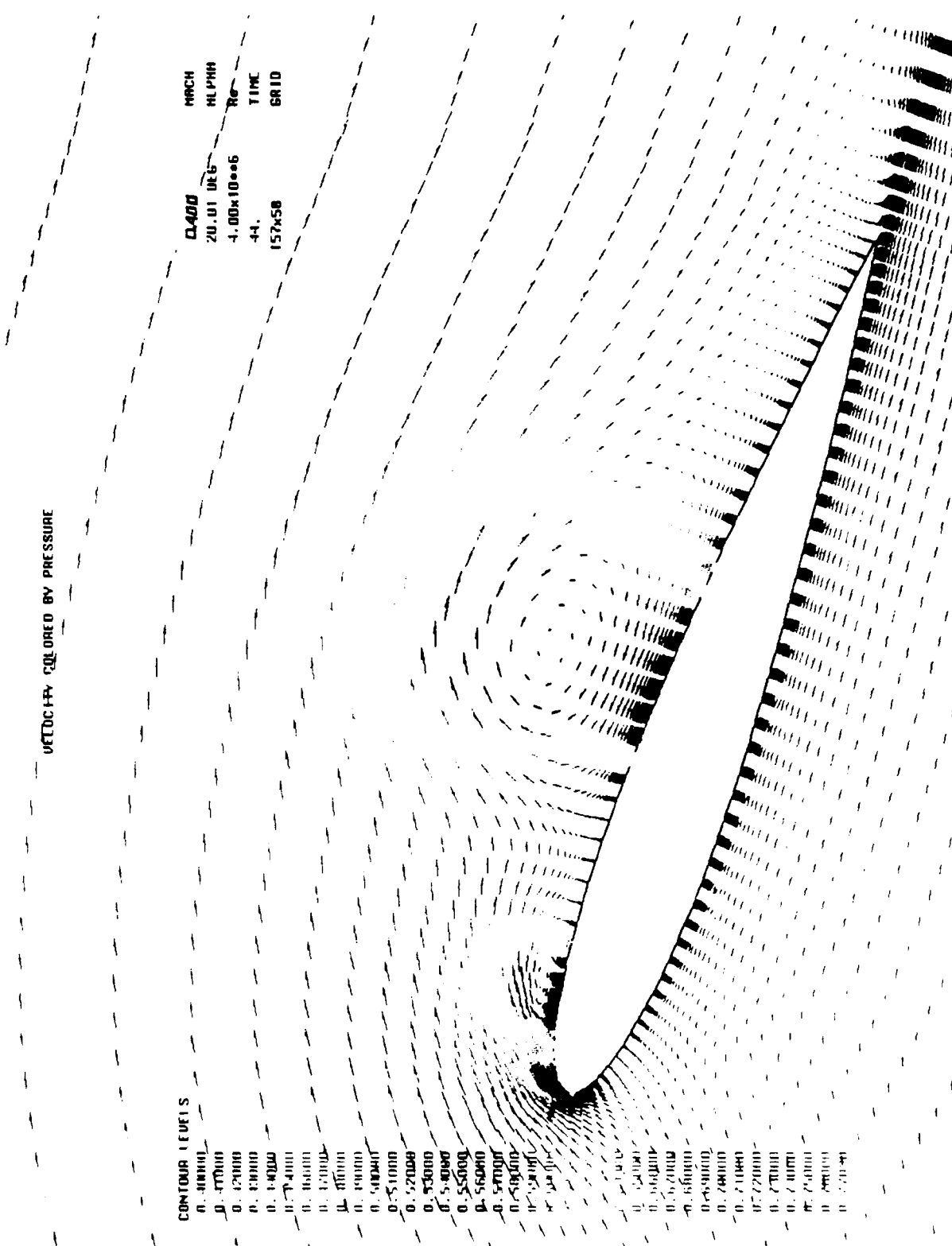


Figure 30. Velocity Field, NACA 0012-63, M=0.4, k=0.01, $\alpha=20.0^\circ$

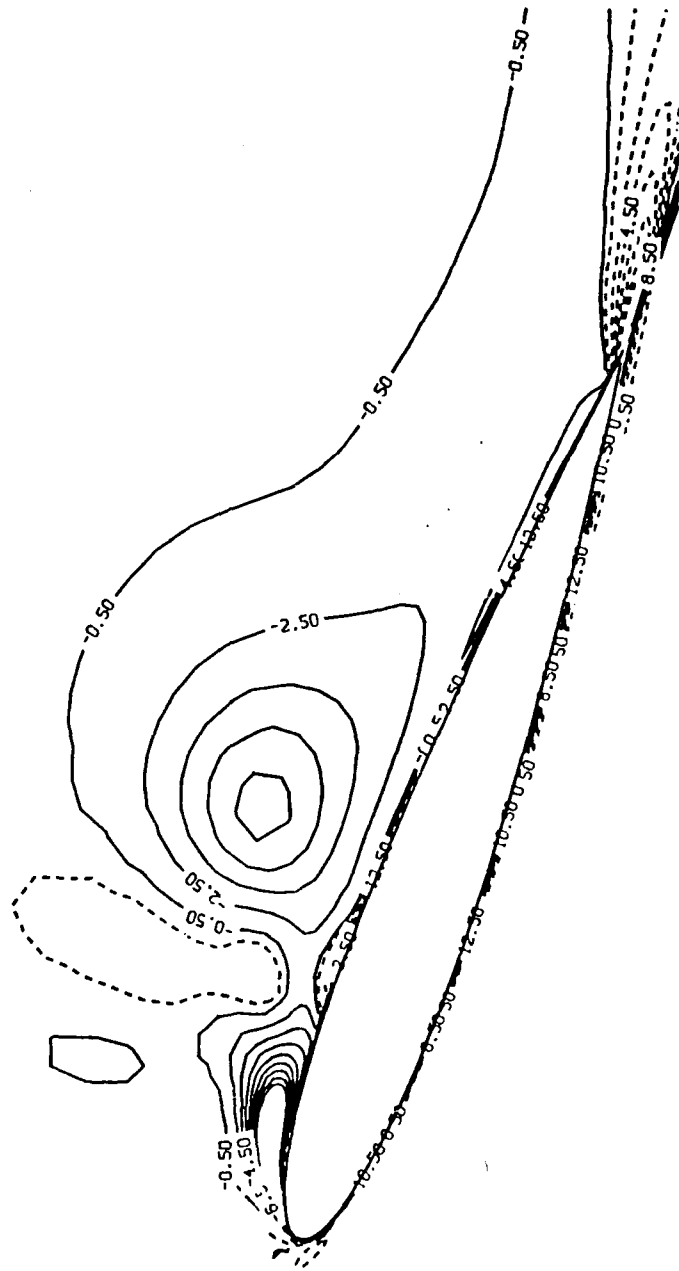


Figure 31. Vorticity Contours, NACA 0012-63, $M=0.3$, $k=0.01$,
 $\alpha=20.0^\circ$

VELOCITY COLORED BY PRESSURE

CONTOUR LEVELS

- 0.461000
- 0.471000
- 0.481000
- 0.491000
- 0.501000
- 0.511000
- 0.521000
- 0.531000
- 0.541000
- 0.551000
- 0.561000
- 0.571000
- 0.581000
- 0.591000
- 0.601000
- 0.611000
- 0.621000
- 0.631000
- 0.641000
- 0.651000
- 0.661000
- 0.671000
- 0.681000
- 0.691000
- 0.701000
- 0.711000
- 0.721000
- 0.731000
- 0.741000
- 0.751000
- 0.761000
- 0.771000
- 0.781000
- 0.791000
- 0.801000
- 0.811000
- 0.821000
- 0.831000
- 0.841000
- 0.851000
- 0.861000
- 0.871000
- 0.881000
- 0.891000
- 0.901000
- 0.911000
- 0.921000
- 0.931000
- 0.941000
- 0.951000
- 0.961000
- 0.971000
- 0.981000
- 0.991000
- 1.001000

MACH 0.400
 ALPHA 21.0; DEG
 Re 4.00x10⁶
 TIME 46.
 GRID 157x58

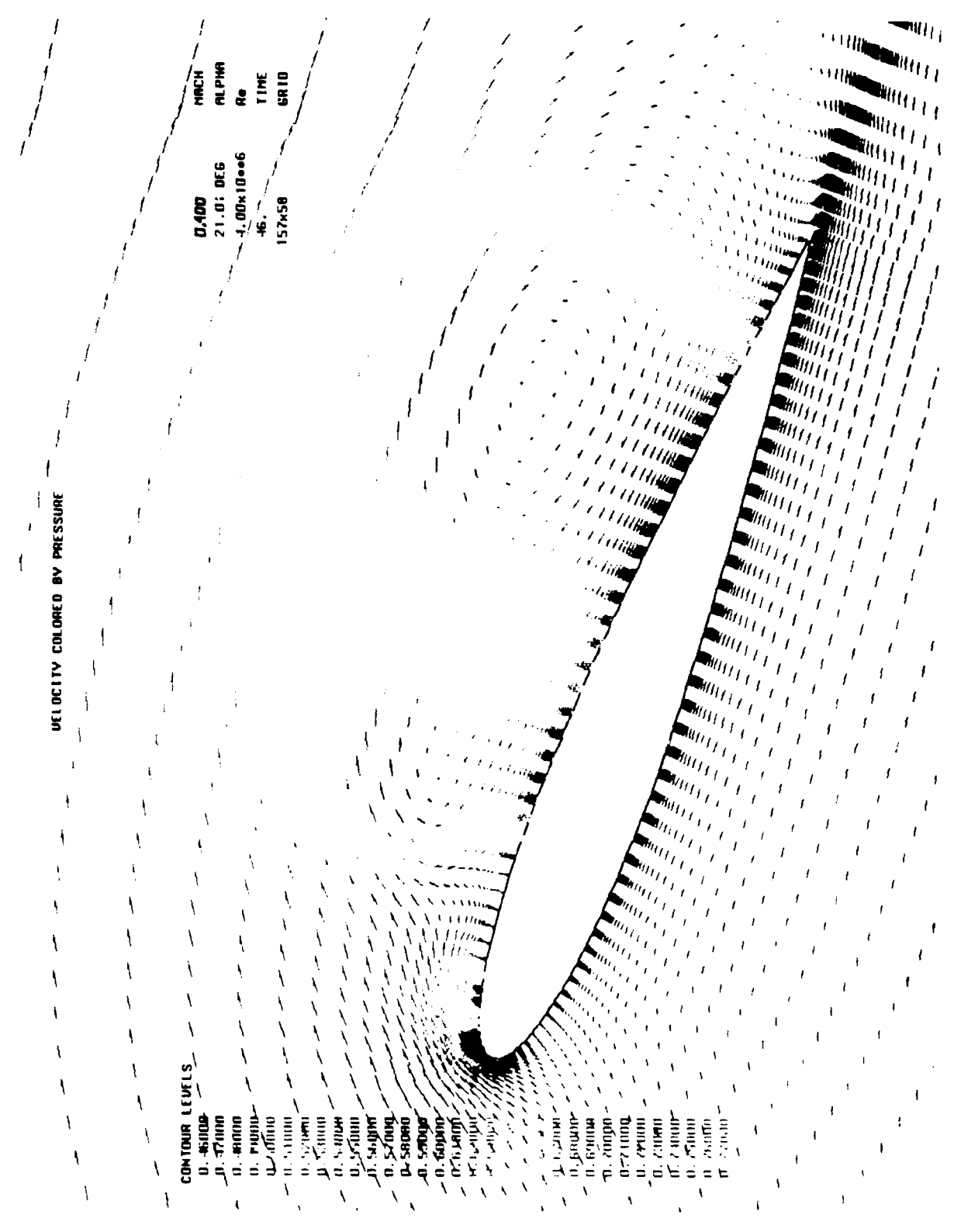


Figure 32. Velocity Field, NACA 0012-63, M=0.4, k=0.01, $\alpha=21.0^\circ$

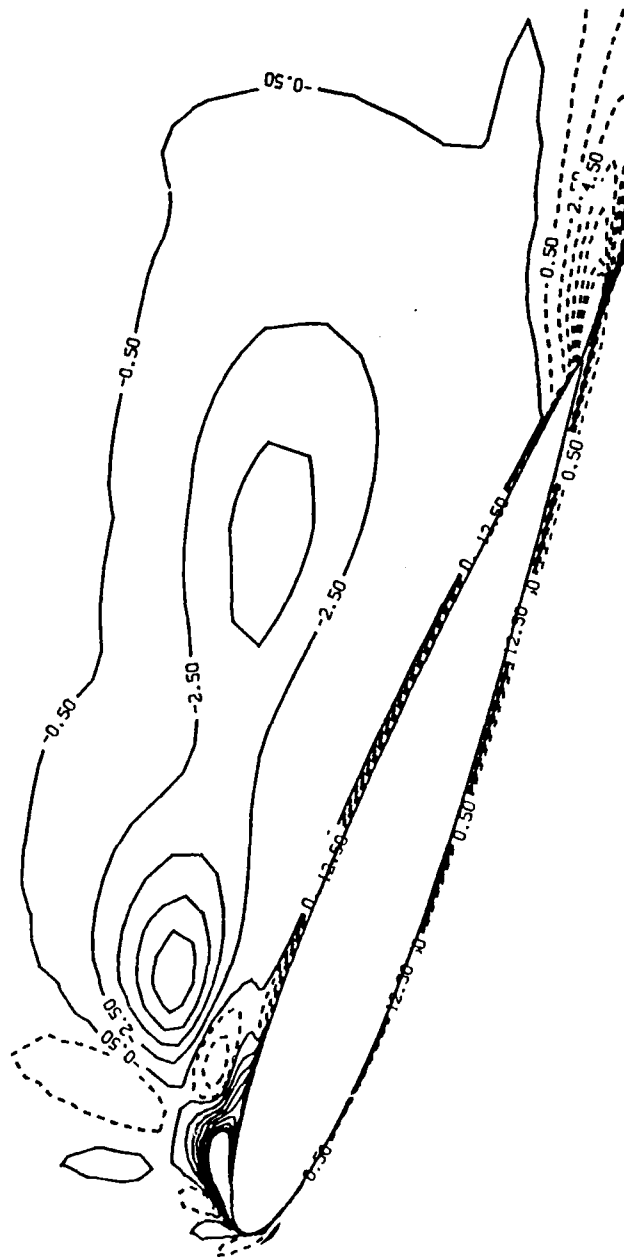


Figure 33. Vorticity Contours, NACA 0012-63, $M=0.4$, $k=0.01$, $\alpha=21.0^\circ$

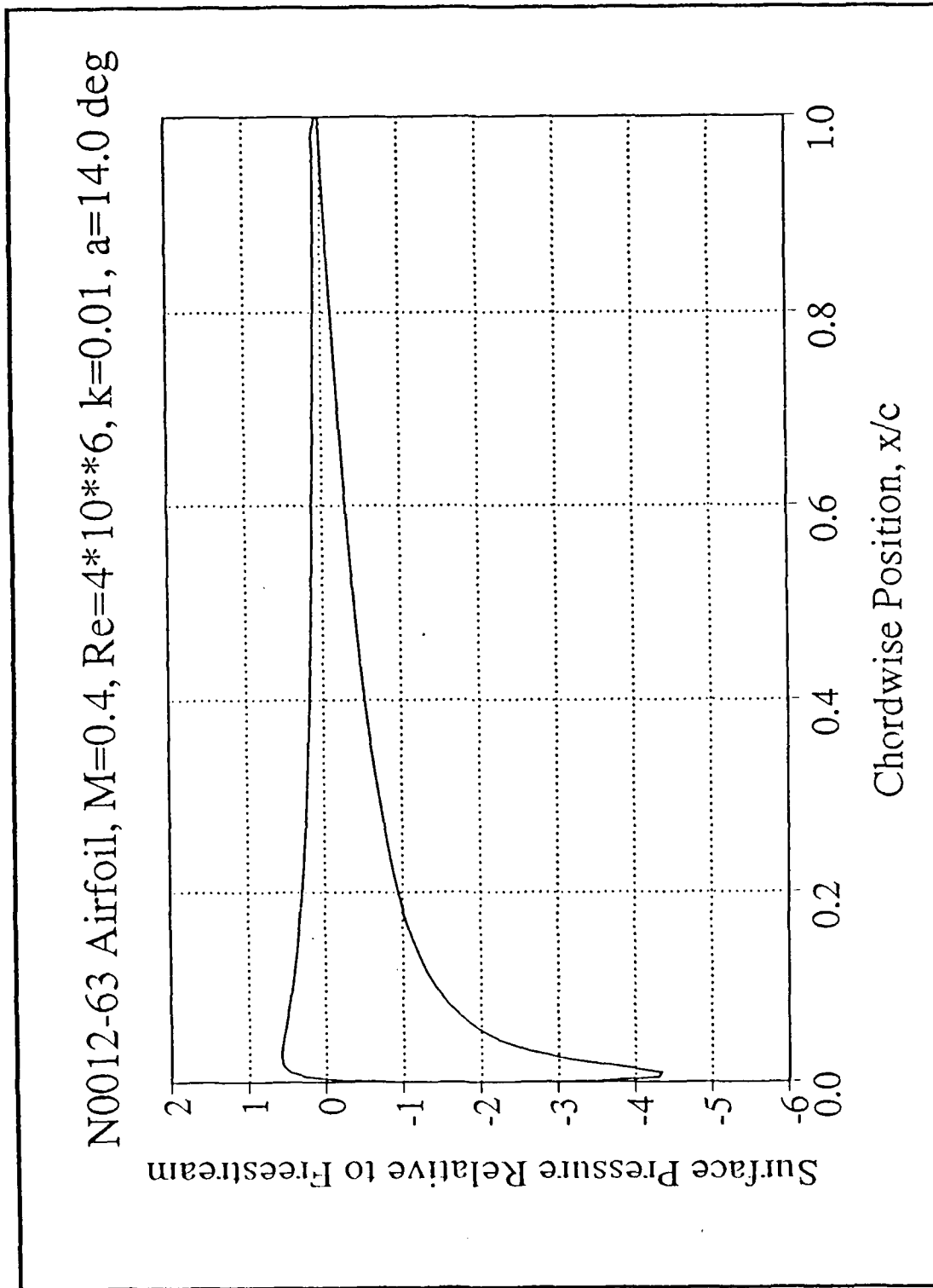


Figure 34. Surface Pressure, NACA 0012-63, $M=0.4$, $k=0.01$, $\alpha=14.0^\circ$

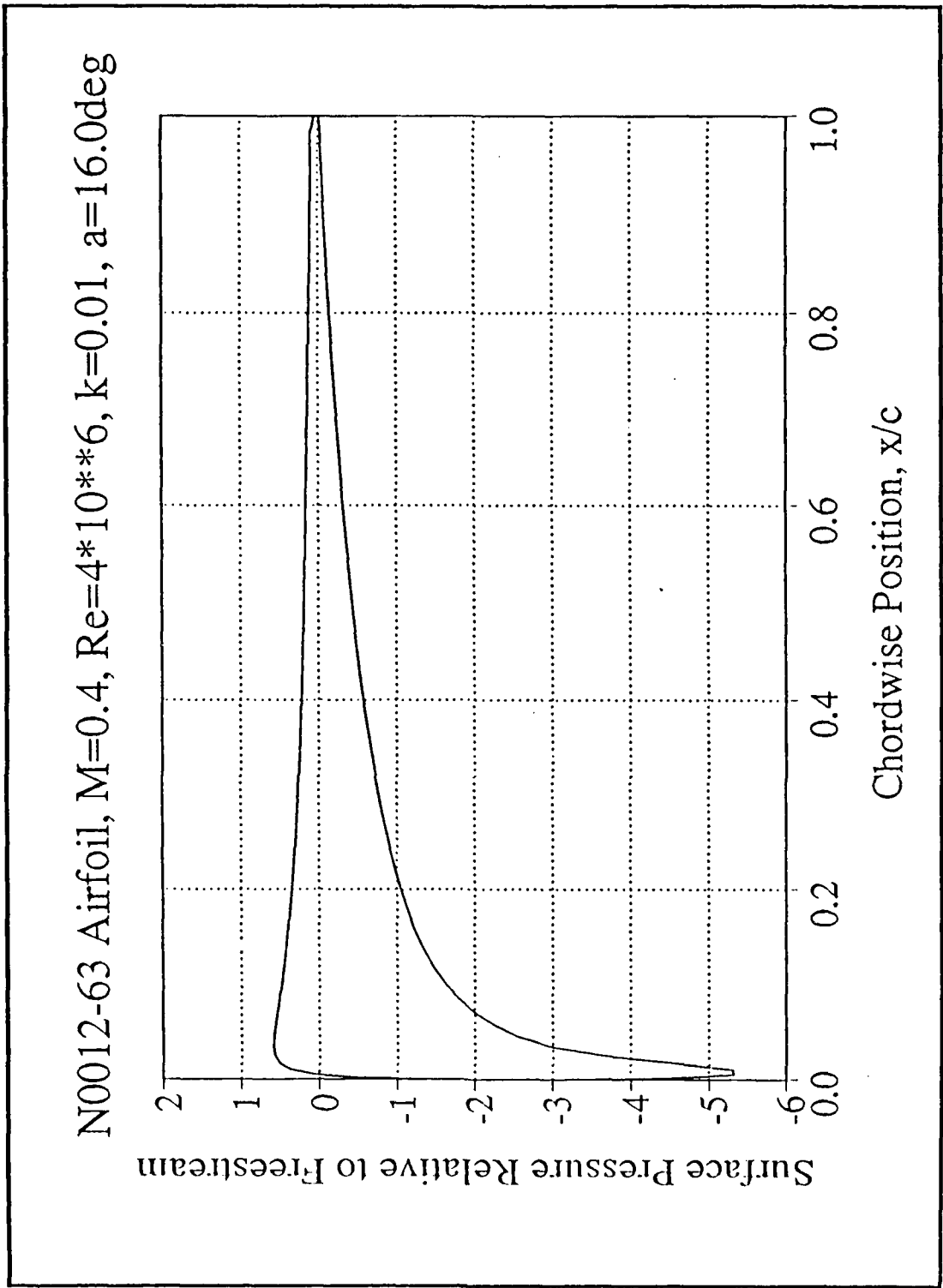


Figure 35. Surface Pressure, NACA 0012-63, $M=0.4$, $k=0.01$, $\alpha=16.0^\circ$

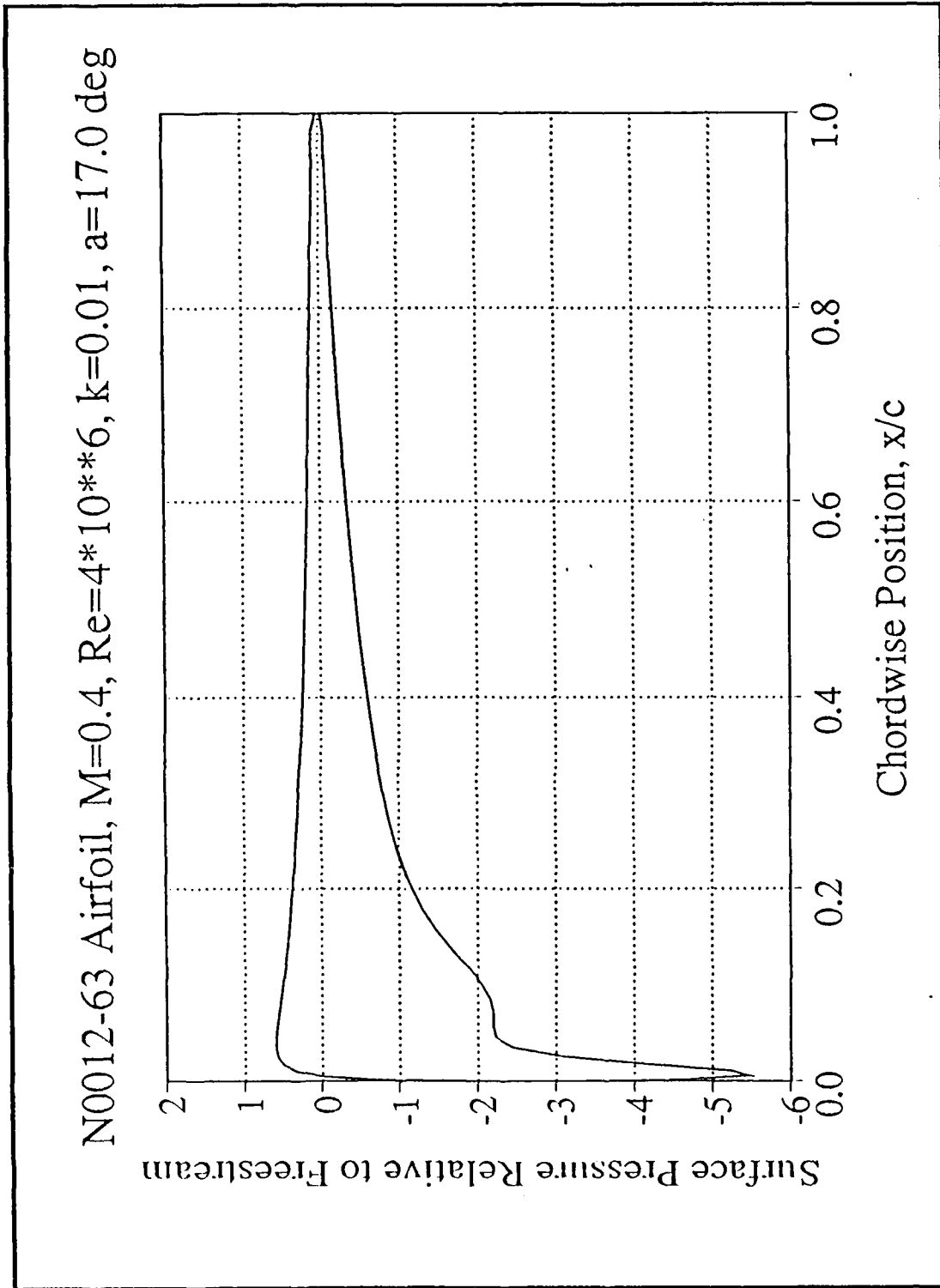


Figure 36. Surface Pressure, NACA 0012-63, $M=0.4$, $k=0.01$, $\alpha=17.0^\circ$

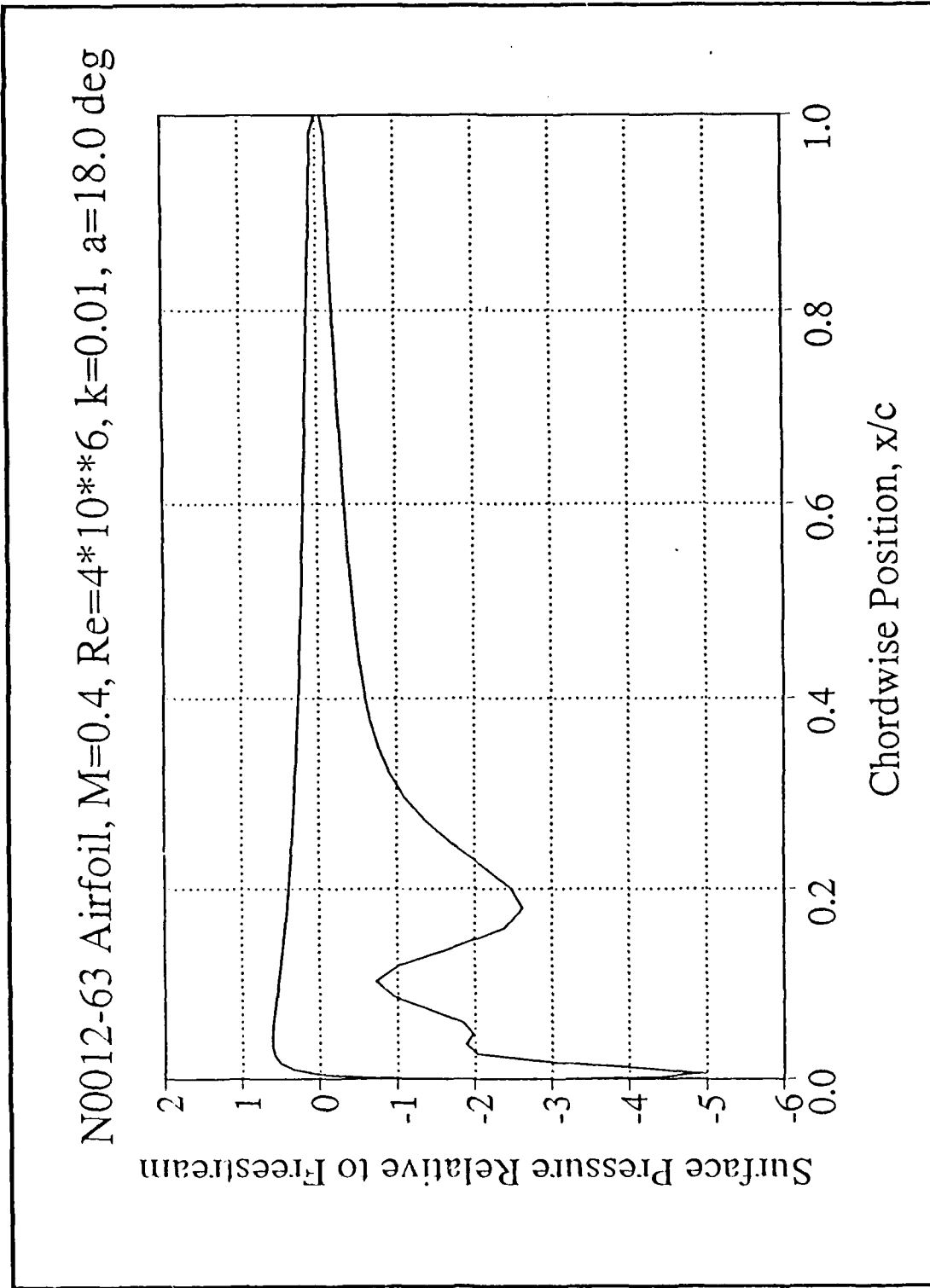


Figure 37. Surface Pressure, NACA 0012-63, $M=0.4$, $k=0.01$, $\alpha=18.0^\circ$

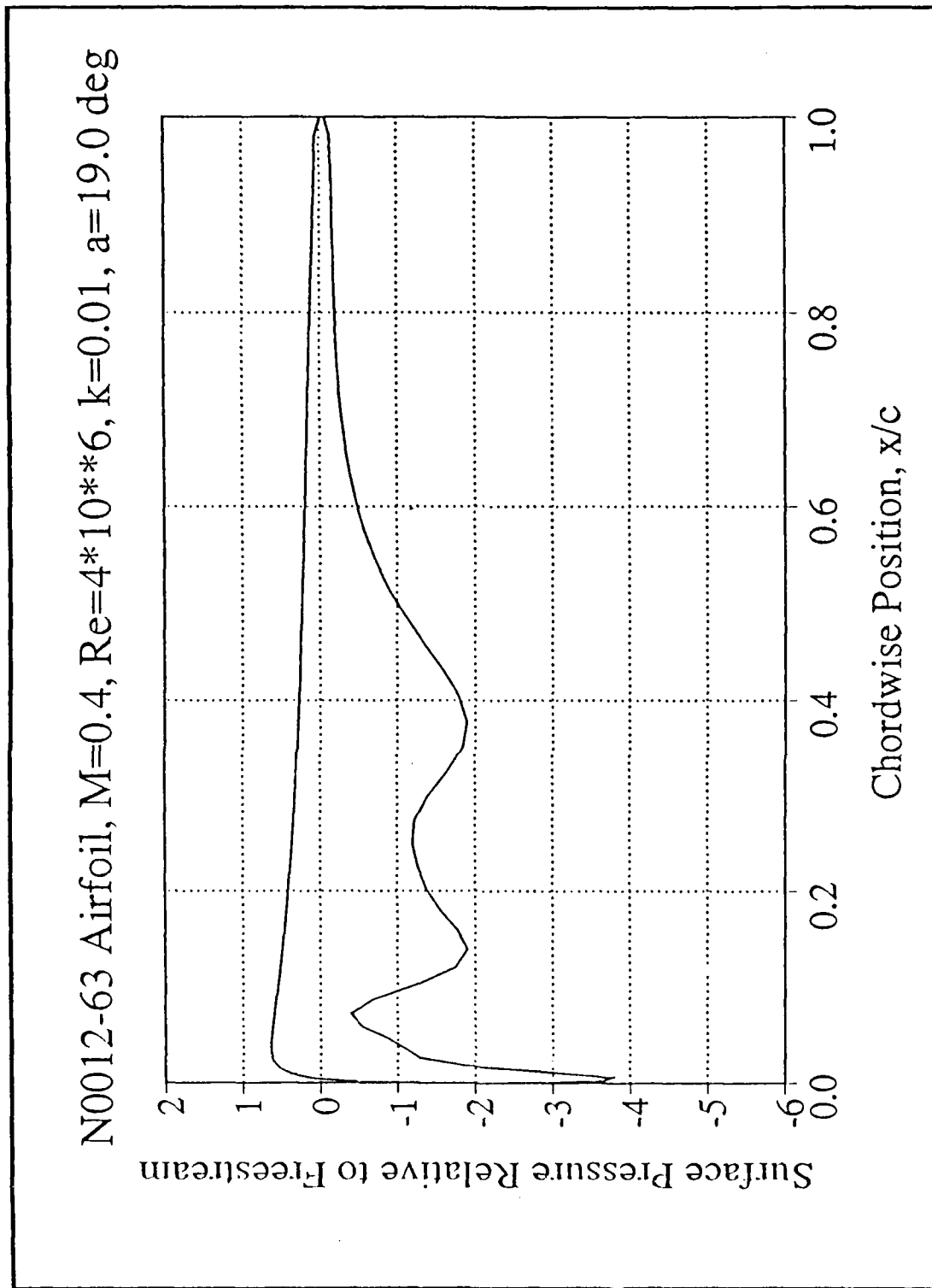


Figure 38. Surface Pressure, NACA 0012-63, $M=0.4$, $k=0.01$, $\alpha=19.0^\circ$

N0012-63 Airfoil, $M=0.4$, $Re=4 \times 10^6$, $k=0.01$, $\alpha=20.0$ deg

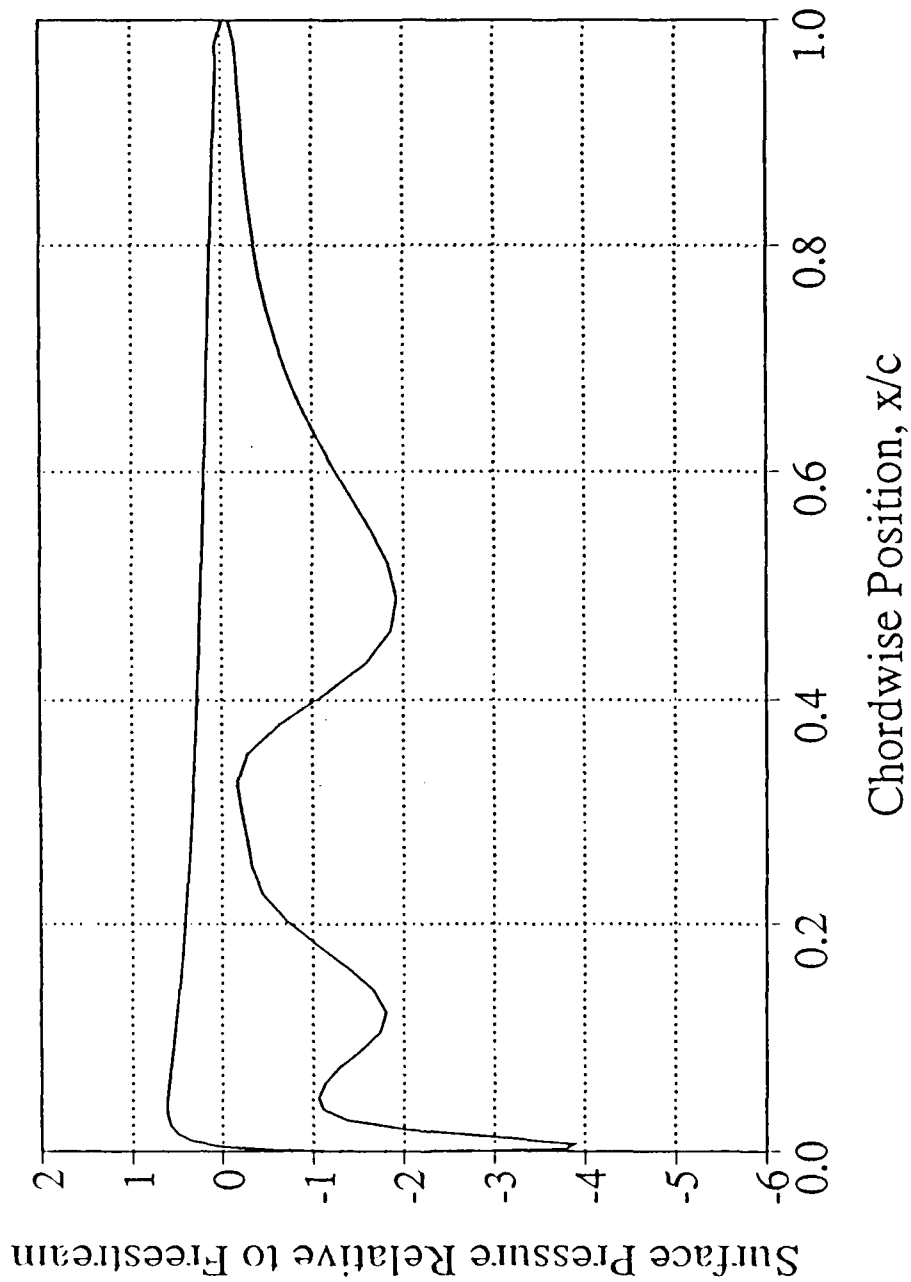


Figure 39. Surface Pressure, NACA 0012-63, $M=0.4$, $k=0.01$, $\alpha=20.0^\circ$

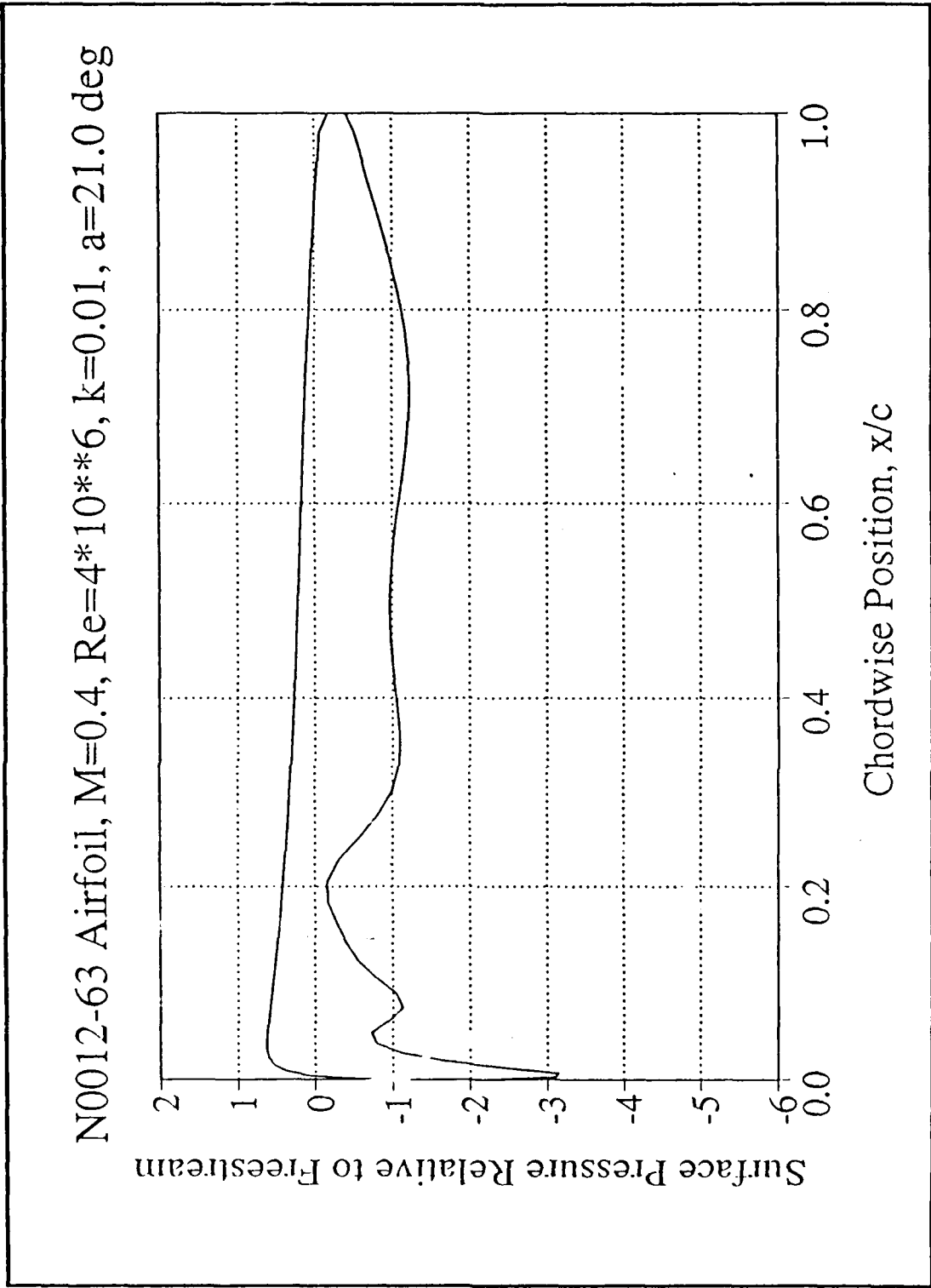


Figure 40. Surface Pressure, NACA 0012-63, $M=0.4$, $k=0.01$, $\alpha=21.0^\circ$

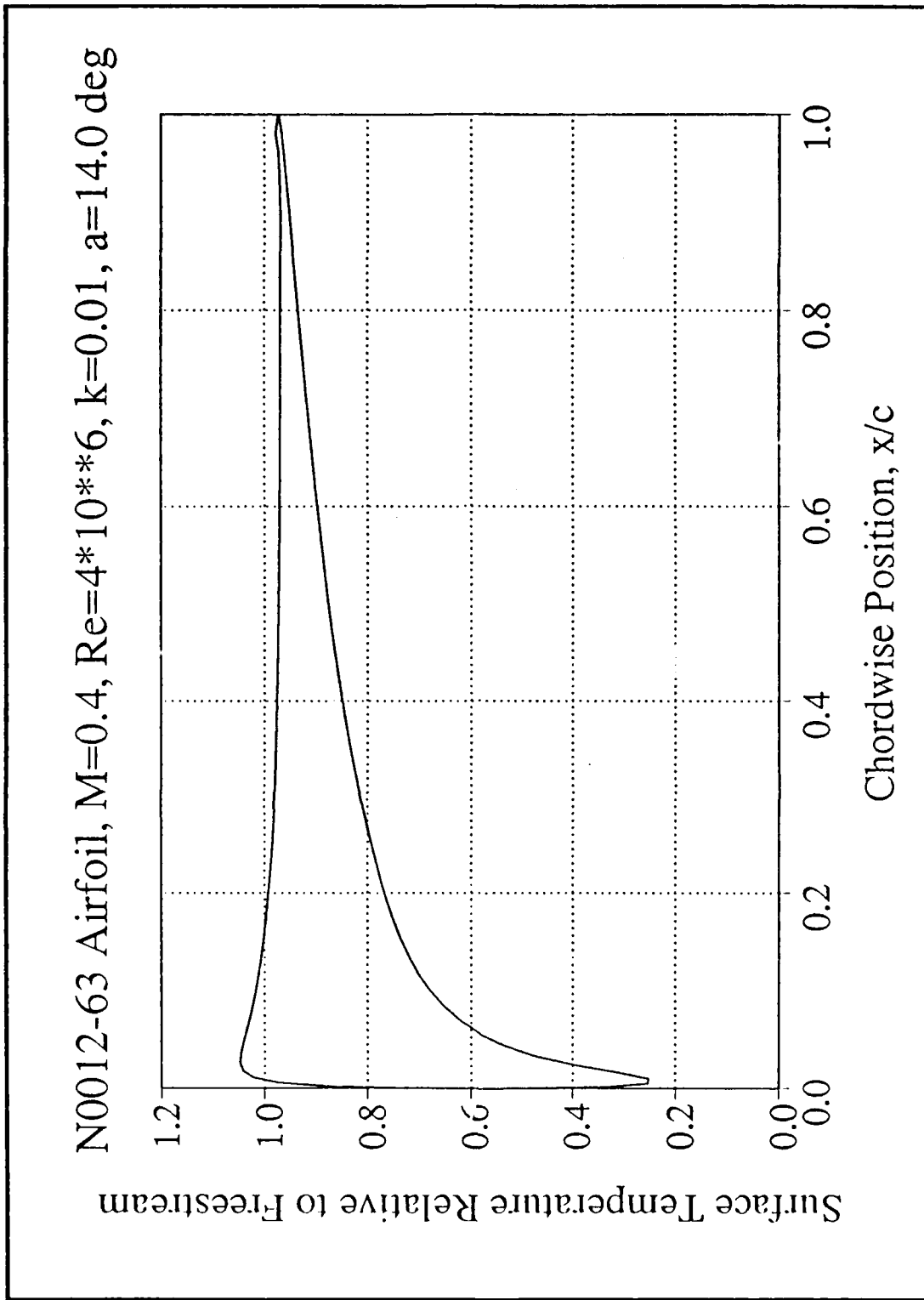


Figure 41. Surface Temperature, NACA 0012-63, $M=0.4$, $k=0.01$, $\alpha=14.0^\circ$

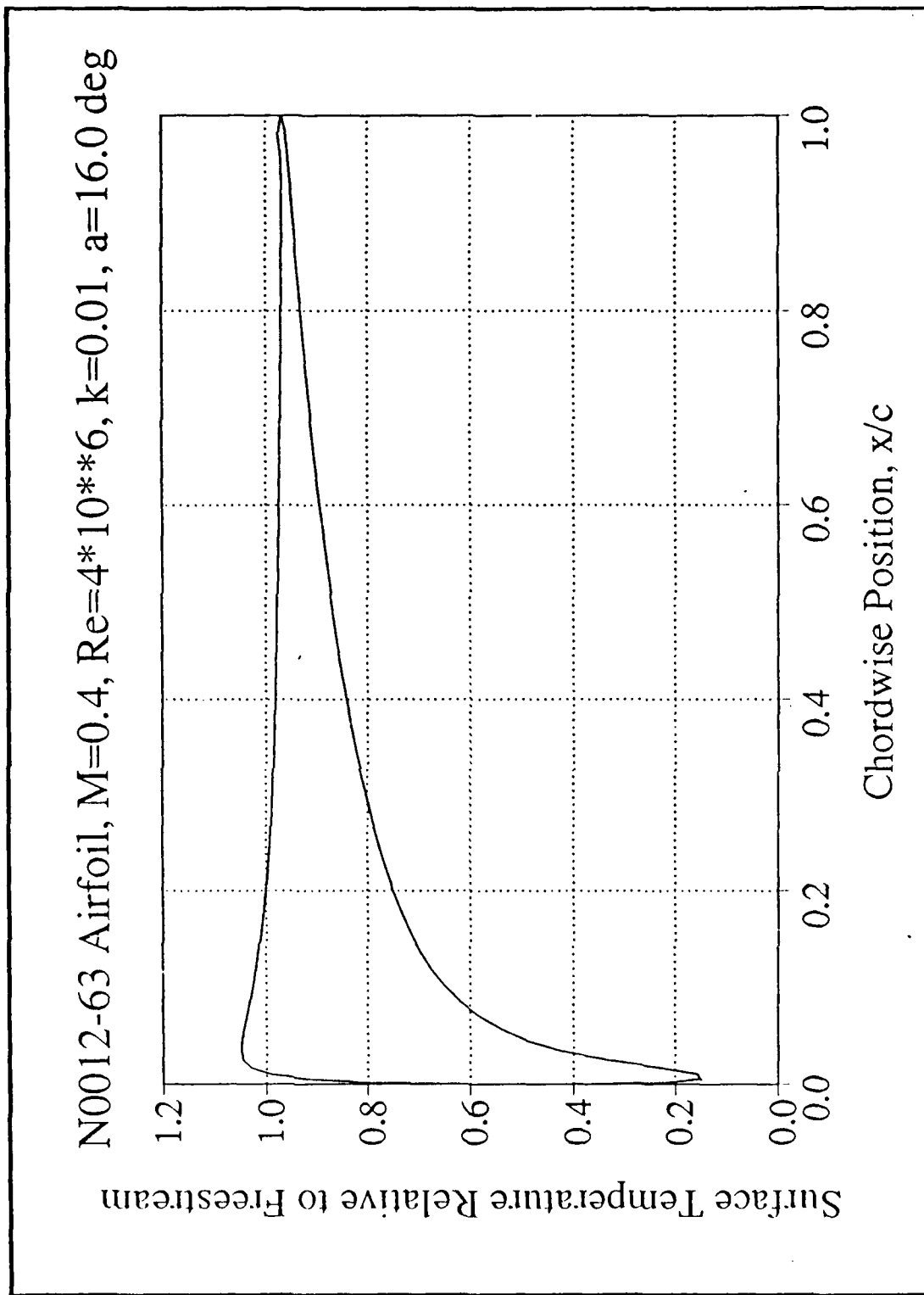


Figure 42. Surface Temperature, NACA 0012-63, $M=0.4$, $k=0.01$, $\alpha=16.0^\circ$

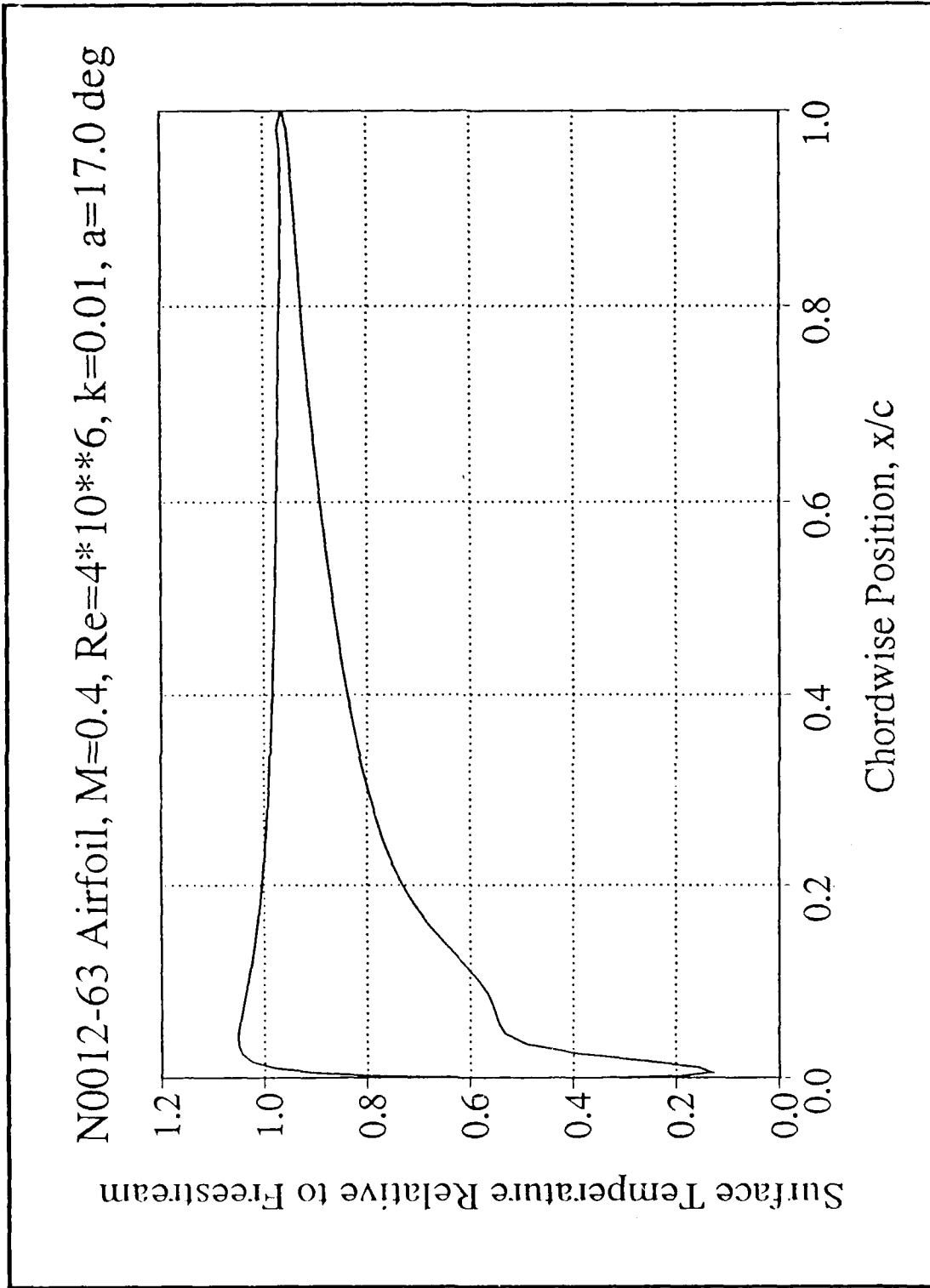


Figure 43. Surface Temperature, NACA 0012-63, $M=0.4$, $k=0.01$, $\alpha=17.0^\circ$

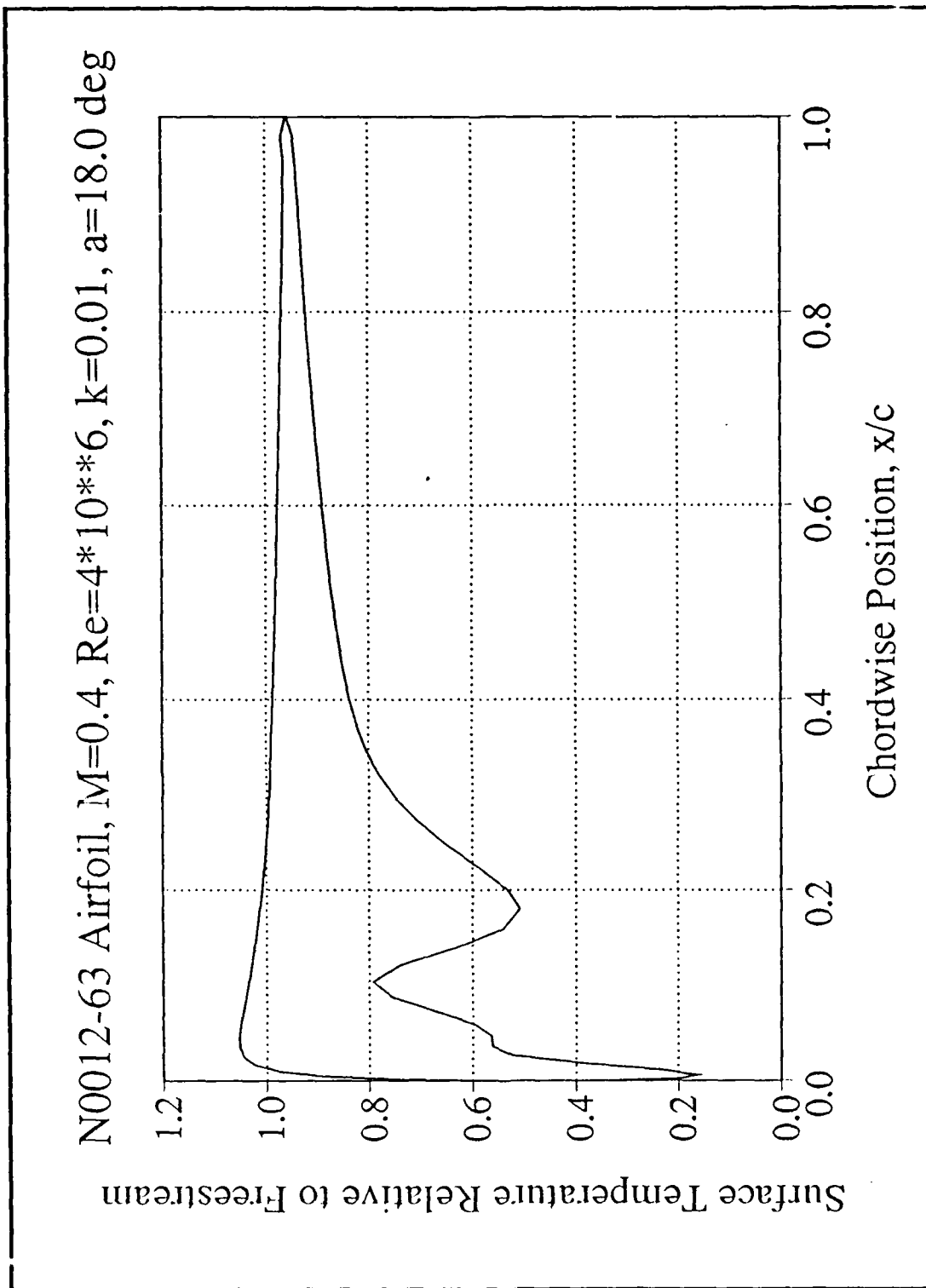


Figure 44. Surface Temperature, NACA 0012-63, $M=0.4$, $k=0.01$, $\alpha=18.0^\circ$

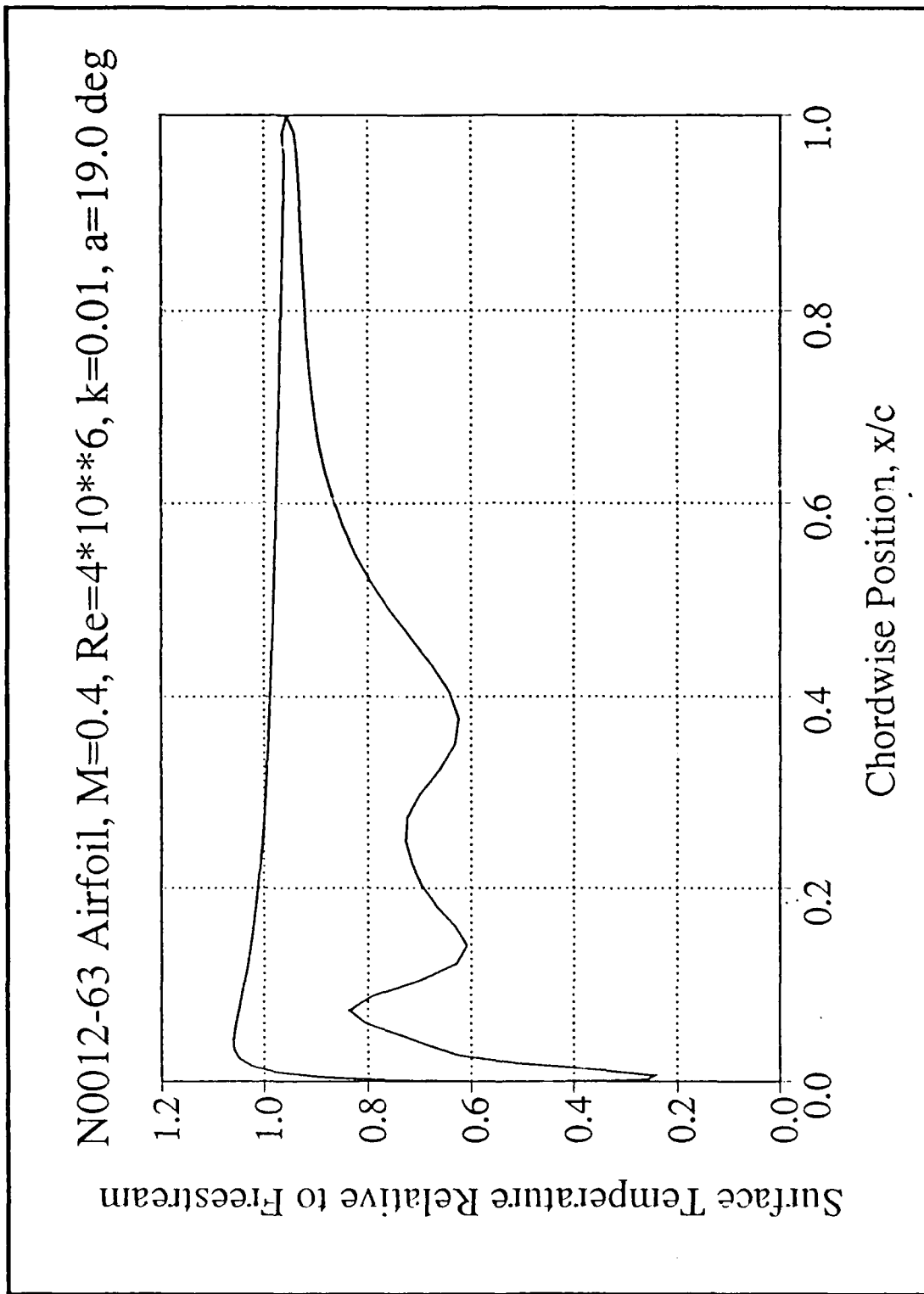


Figure 45. Surface Temperature, NACA 0012-63, $M=0.4$, $k=0.01$, $\alpha=19.0^\circ$

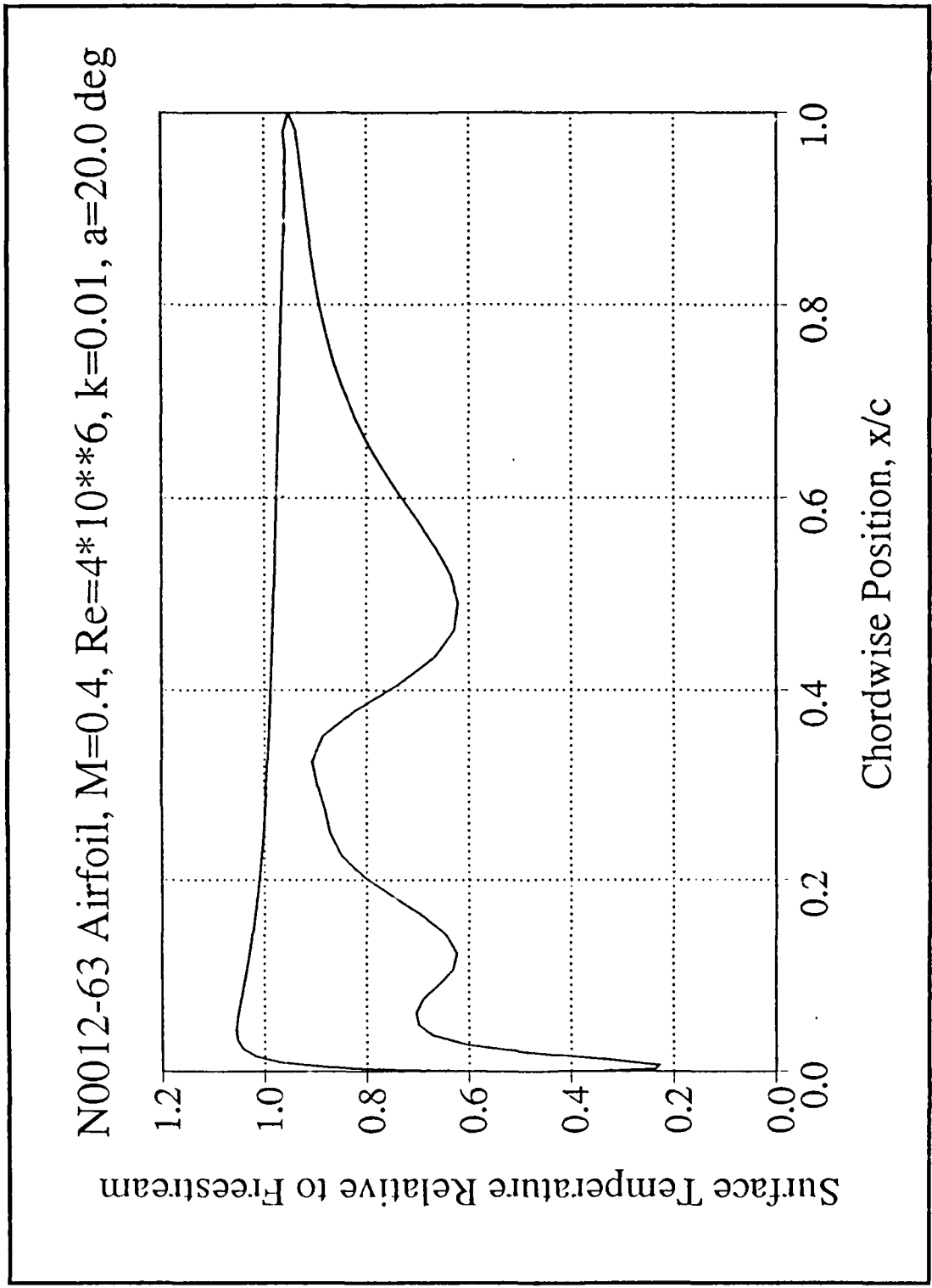


Figure 46. Surface Temperature, NACA 0012-63, $M=0.4$, $k=0.01$, $\alpha=20.0^\circ$

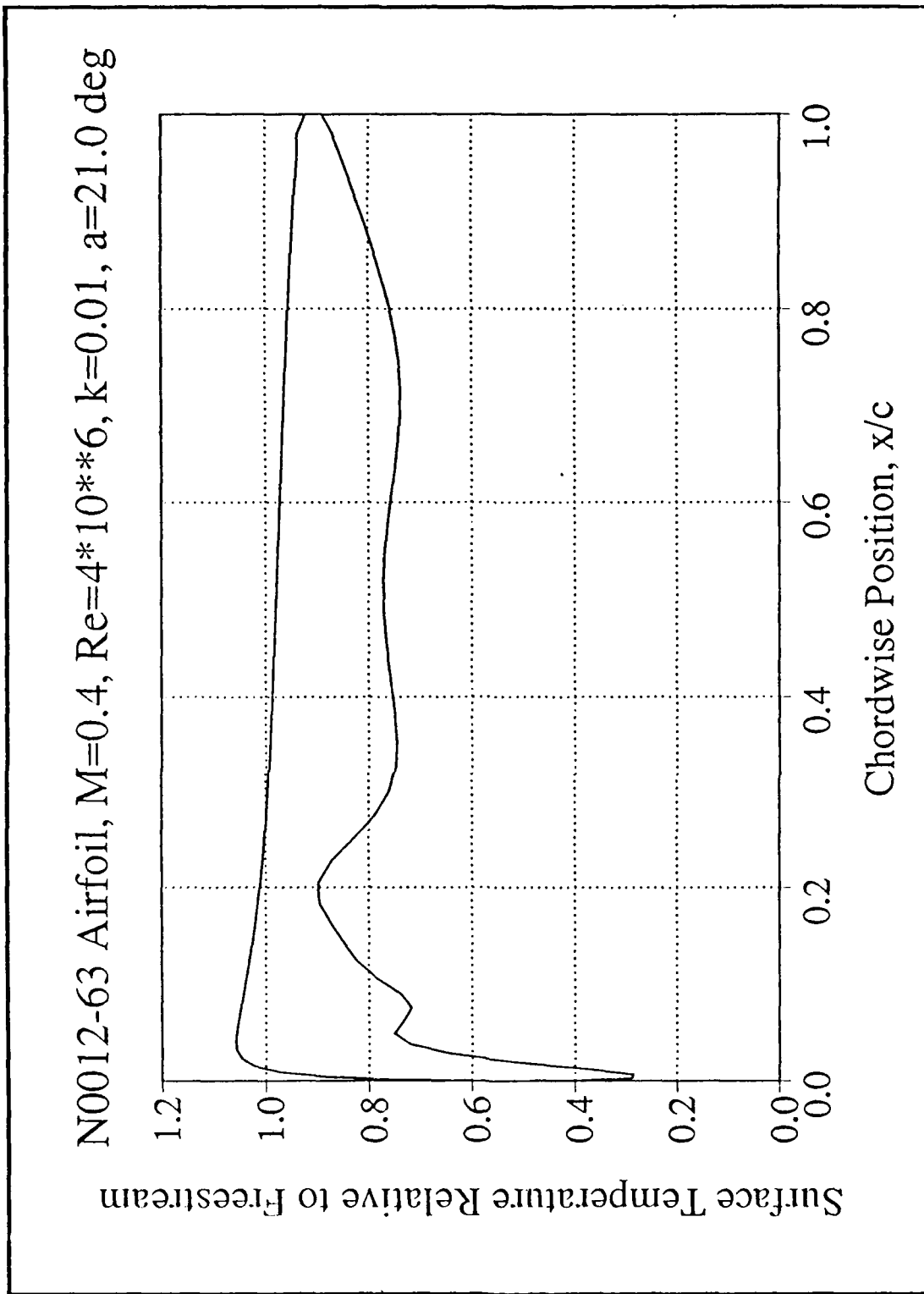


Figure 47. Surface Temperature, NACA 0012-63, $M=0.4$, $k=0.01$, $\alpha=21.0^\circ$

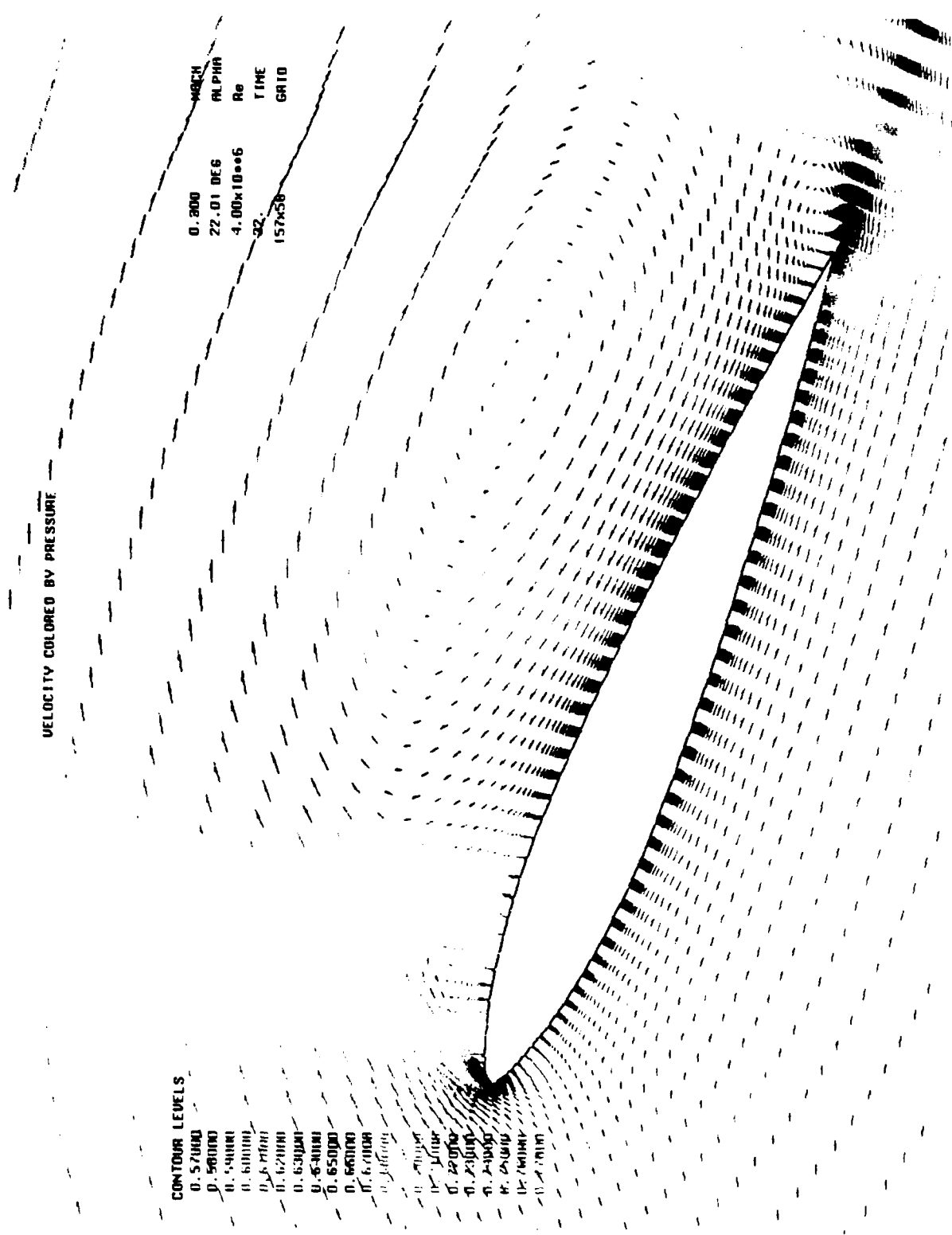


Figure 48. Velocity Field, NACA 0012-33, M=0.3, k=0.02, $Re=22.0 \times 10^6$

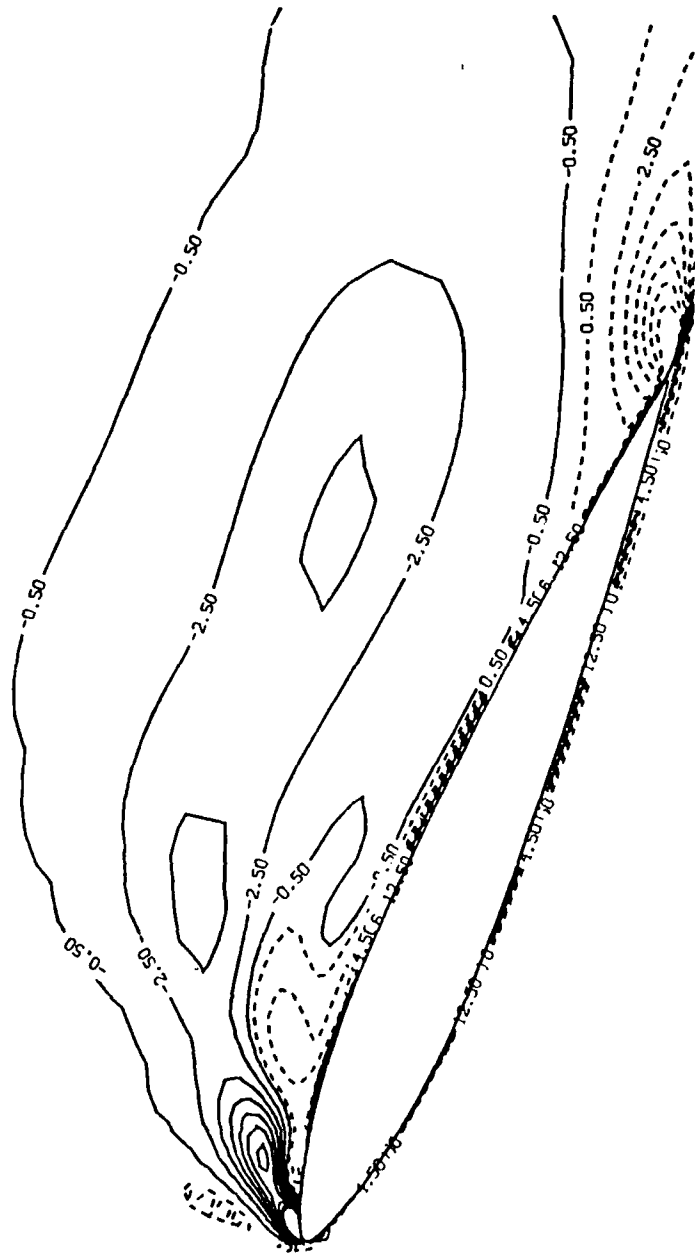


Figure 49. Vorticity Contours, NACA 0012-33, $M=0.3$, $k=0.02$, $\alpha=22.0^\circ$

2. Harmonically Oscillating Airfoil

The process of vortical flow development at the leading edge during the upstroke is similar to that of a rapidly pitching airfoil examined in the previous section. Although the pitching rate is not constant in the case of the harmonically oscillating airfoil, boundary layer separation and vortex development and shedding also occur during the upstroke.

The flow reattachment process during the downstroke involves the shedding of the large primary vortex into the wake and the diminishing intensity of the trailing edge vortex. Prior to the downstroke, the combination of the large clockwise primary vortex and the counter-clockwise trailing edge vortex cause extensive reverse flow, even outside the boundary layer, over the airfoil upper surface aft of 30% chord (Figure 50). As the angle of attack decreases further, flow over the leading edge upper surface rapidly reattaches, while the primary vortex is centered above the trailing edge (Figure 51). With further reduction in angle of attack, the primary vortex moves downstream of the airfoil, and the trailing edge vortex diminishes (Figure 52). Reverse flow at this time exists only on aft portions of the airfoil. As the angle of attack approaches $10-11^\circ$, the primary vortex has been swept downstream, the trailing edge vortex has diminished, and smooth, attached flow is established over the upper surface (Figure 53).

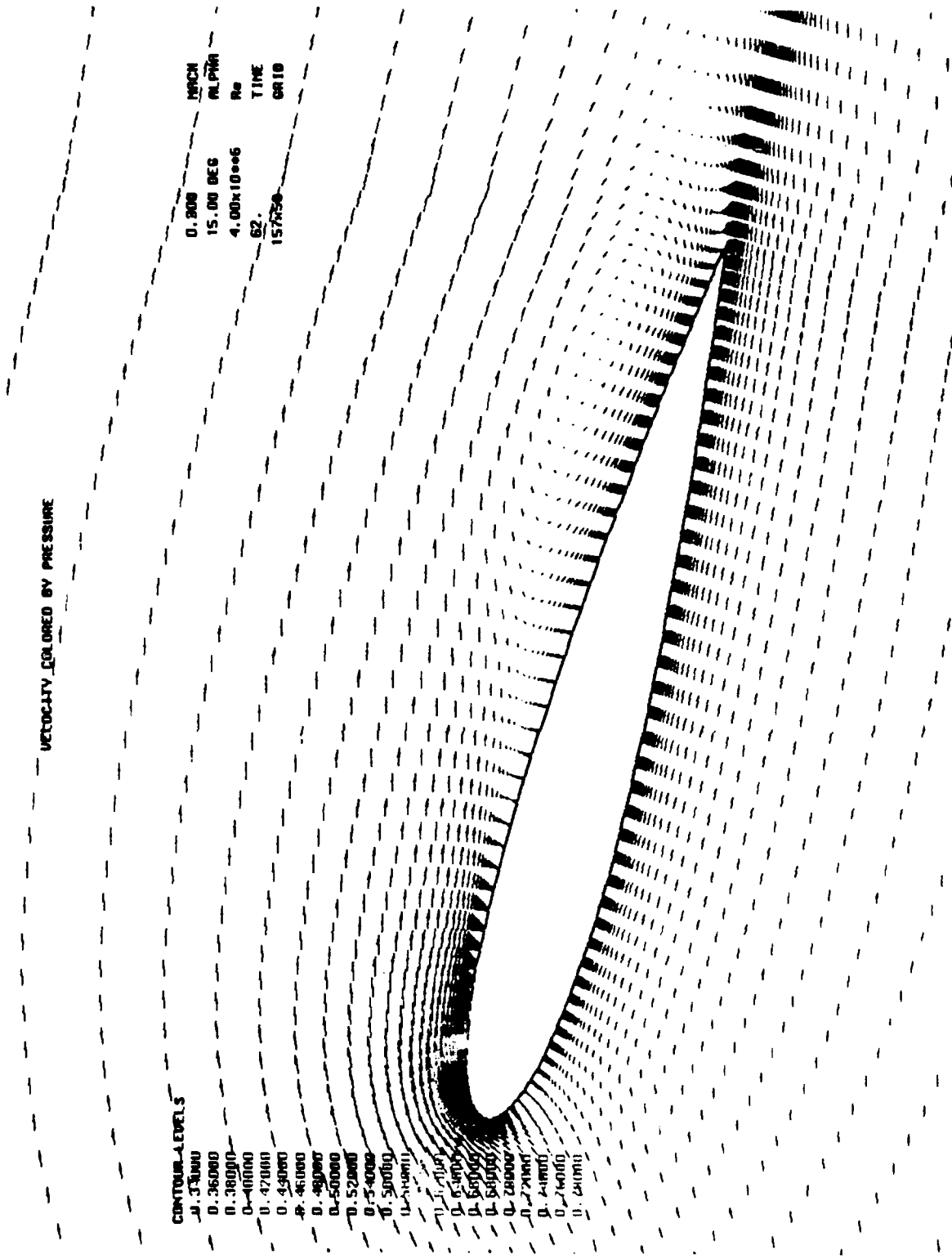


Figure 50. Velocity Field, NACA 0012, M=0.3, k=0.1, $\alpha=15.0^\circ$ downstroke

VELOCITY COLORED BY PRESSURE

0.2000 MACH
 13.00 DEG ALPHA
 4.00e+06 Re
 70 TIME
 157458 OR10

CONTOUR-LEVELS

0.40000
 0.45000
 0.50000
 0.51000
 0.52000
 0.53000
 0.54000
 0.55000
 0.56000
 0.57000
 0.58000
 0.59000
 0.60000
 0.61000
 0.62000
 0.63000
 0.64000
 0.65000
 0.66000
 0.67000
 0.68000
 0.69000
 0.70000
 0.71000
 0.72000
 0.73000
 0.74000
 0.75000
 0.76000

Figure 51. Velocity Field, NACA 0012, M=0.3, k=0.1, $\alpha=13.0^\circ$ downstroke

VELOCITY COLORED BY PRESSURE

MACH 0.300
 ALPHA 11.00 DEG
 Re 4.00x10+6
 TIME 76.
 GRAB 157x59

CONTOUR LEVELS
 0.520000
 0.530000
 0.540000
 0.550000
 0.560000
 0.570000
 0.580000
 0.590000
 0.600000
 0.610000
 0.620000
 0.630000
 0.640000
 0.650000
 0.660000
 0.670000
 0.680000
 0.690000
 0.700000
 0.710000
 0.720000
 0.730000
 0.740000
 0.750000
 0.760000
 0.770000
 0.780000
 0.790000
 0.800000
 0.810000
 0.820000
 0.830000
 0.840000
 0.850000
 0.860000
 0.870000
 0.880000
 0.890000
 0.900000
 0.910000
 0.920000
 0.930000
 0.940000
 0.950000
 0.960000
 0.970000
 0.980000
 0.990000
 1.000000

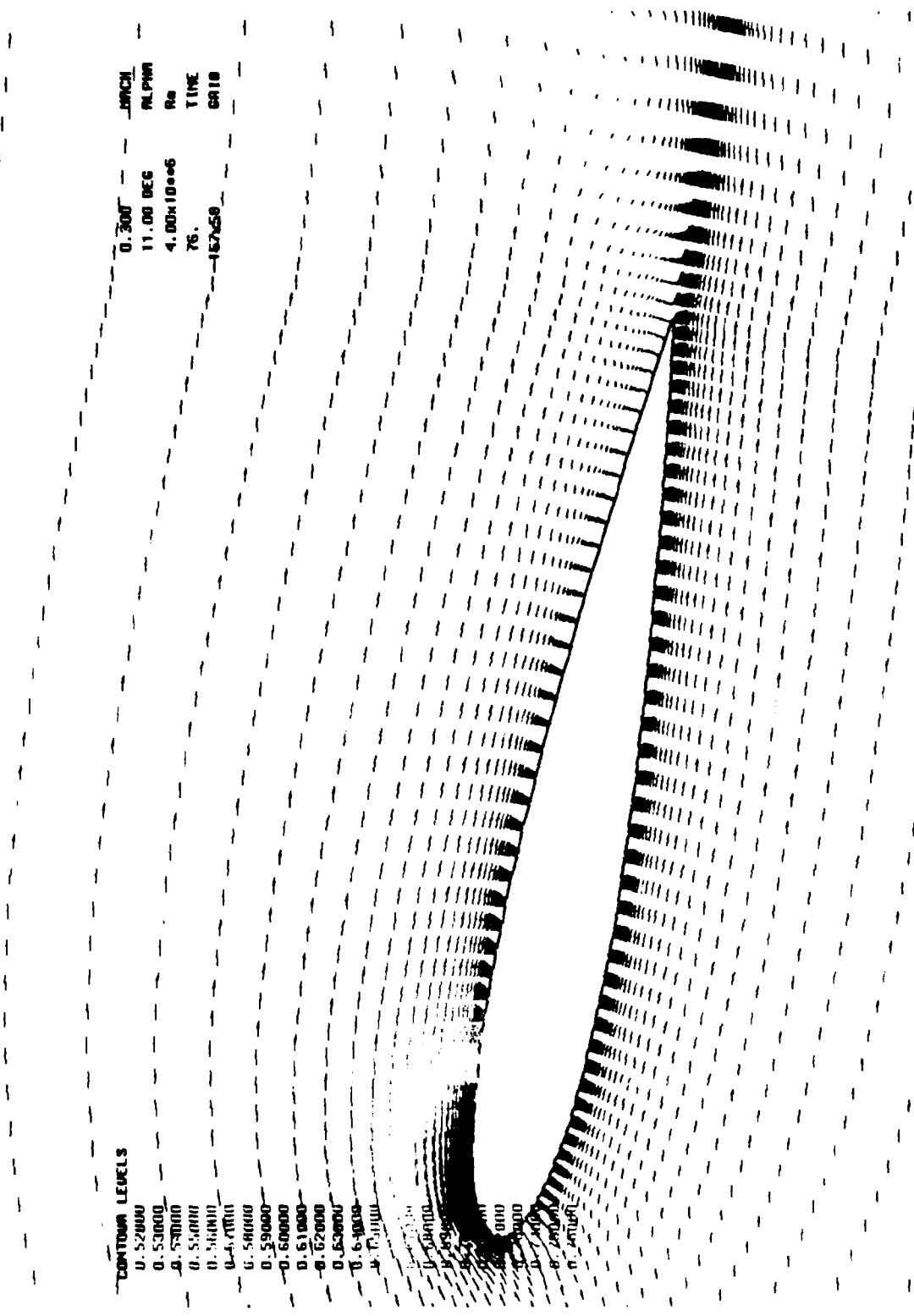


Figure 52. Velocity Field, NACA 0012, M=0.3, k=0.1, $\alpha=11.0^\circ$ downstroke

VELOCITY COLORED BY PRESSURE

CONTOUR LEVELS

- 0.520000
- 0.530000
- 0.540000
- 0.550000
- 0.560000
- 0.570000
- 0.580000
- 0.590000
- 0.600000
- 0.610000
- 0.620000
- 0.630000
- 0.640000
- 0.650000
- 0.660000
- 0.670000
- 0.680000
- 0.690000
- 0.700000
- 0.710000
- 0.720000
- 0.730000
- 0.740000
- 0.750000
- 0.760000
- 0.770000
- 0.780000
- 0.790000
- 0.800000
- 0.810000
- 0.820000
- 0.830000
- 0.840000
- 0.850000
- 0.860000
- 0.870000
- 0.880000
- 0.890000
- 0.900000
- 0.910000
- 0.920000
- 0.930000
- 0.940000
- 0.950000
- 0.960000
- 0.970000
- 0.980000
- 0.990000
- 1.000000
- 1.010000
- 1.020000
- 1.030000
- 1.040000
- 1.050000
- 1.060000
- 1.070000
- 1.080000
- 1.090000
- 1.100000
- 1.110000
- 1.120000
- 1.130000
- 1.140000
- 1.150000
- 1.160000
- 1.170000
- 1.180000
- 1.190000
- 1.200000
- 1.210000
- 1.220000
- 1.230000
- 1.240000
- 1.250000
- 1.260000
- 1.270000
- 1.280000
- 1.290000
- 1.300000
- 1.310000
- 1.320000
- 1.330000
- 1.340000
- 1.350000
- 1.360000
- 1.370000
- 1.380000
- 1.390000
- 1.400000
- 1.410000
- 1.420000
- 1.430000
- 1.440000
- 1.450000
- 1.460000
- 1.470000
- 1.480000
- 1.490000
- 1.500000
- 1.510000
- 1.520000
- 1.530000
- 1.540000
- 1.550000
- 1.560000
- 1.570000
- 1.580000
- 1.590000
- 1.600000
- 1.610000
- 1.620000
- 1.630000
- 1.640000
- 1.650000
- 1.660000
- 1.670000
- 1.680000
- 1.690000
- 1.700000
- 1.710000
- 1.720000
- 1.730000
- 1.740000
- 1.750000
- 1.760000
- 1.770000
- 1.780000
- 1.790000
- 1.800000
- 1.810000
- 1.820000
- 1.830000
- 1.840000
- 1.850000
- 1.860000
- 1.870000
- 1.880000
- 1.890000
- 1.900000
- 1.910000
- 1.920000
- 1.930000
- 1.940000
- 1.950000
- 1.960000
- 1.970000
- 1.980000
- 1.990000
- 2.000000
- 2.010000
- 2.020000
- 2.030000
- 2.040000
- 2.050000
- 2.060000
- 2.070000
- 2.080000
- 2.090000
- 2.100000
- 2.110000
- 2.120000
- 2.130000
- 2.140000
- 2.150000
- 2.160000
- 2.170000
- 2.180000
- 2.190000
- 2.200000
- 2.210000
- 2.220000
- 2.230000
- 2.240000
- 2.250000
- 2.260000
- 2.270000
- 2.280000
- 2.290000
- 2.300000
- 2.310000
- 2.320000
- 2.330000
- 2.340000
- 2.350000
- 2.360000
- 2.370000
- 2.380000
- 2.390000
- 2.400000
- 2.410000
- 2.420000
- 2.430000
- 2.440000
- 2.450000
- 2.460000
- 2.470000
- 2.480000
- 2.490000
- 2.500000
- 2.510000
- 2.520000
- 2.530000
- 2.540000
- 2.550000
- 2.560000
- 2.570000
- 2.580000
- 2.590000
- 2.600000
- 2.610000
- 2.620000
- 2.630000
- 2.640000
- 2.650000
- 2.660000
- 2.670000
- 2.680000
- 2.690000
- 2.700000
- 2.710000
- 2.720000
- 2.730000
- 2.740000
- 2.750000
- 2.760000
- 2.770000
- 2.780000
- 2.790000
- 2.800000
- 2.810000
- 2.820000
- 2.830000
- 2.840000
- 2.850000
- 2.860000
- 2.870000
- 2.880000
- 2.890000
- 2.900000
- 2.910000
- 2.920000
- 2.930000
- 2.940000
- 2.950000
- 2.960000
- 2.970000
- 2.980000
- 2.990000
- 3.000000

0.300 MACH
 10.00 DEG ALPHA
 4.00E+06 Re
 79. TIME
 157.50 JRI0

Figure 53. Velocity Field, NACA 0012, M=0.3, k=0.1, $\alpha=10.0^\circ$ downstroke

D. REDUCED FREQUENCY EFFECT

At a given Mach number the three airfoils exhibited higher peak lift coefficients at respectively higher angles of attack at a reduced frequency of $k=0.02$ when compared to that of $k=0.01$. Lift curve slopes for a given airfoil at the two reduced frequencies were nearly identical to the point of initial flow separation and subsequent dynamic stall at $k=0.01$. Lift coefficient at $k=0.02$ continued increasing, showing the increase in unsteady lift with higher pitching rate. The effect of increasing the reduced frequency at a freestream Mach number of 0.3 is shown in Figures 54 and 55 for the NACA 0012 and NACA 0012-33 airfoils, respectively. At the higher reduced frequency of 0.02, formation of the primary vortex occurred at angles of attack 0.7° to 1.6° higher than at a reduced frequency of 0.01 in all cases. As a result, the entire vortical flow development was delayed to progressively higher angles of attack. Dynamic stalling angle occurred 4.0° to 4.8° higher at the higher reduced frequency and the resulting peak lift coefficients were 15-20% higher compared to the $k=0.01$ cases (Table 3).

Experimental work by Chandrasekhara and Carr [Ref. 3] using the NACA 0012 airfoil demonstrated the same trends, wherein a higher reduced frequency resulted in retaining the vortex above the airfoil to higher angles of attack, thereby delaying dynamic stall.

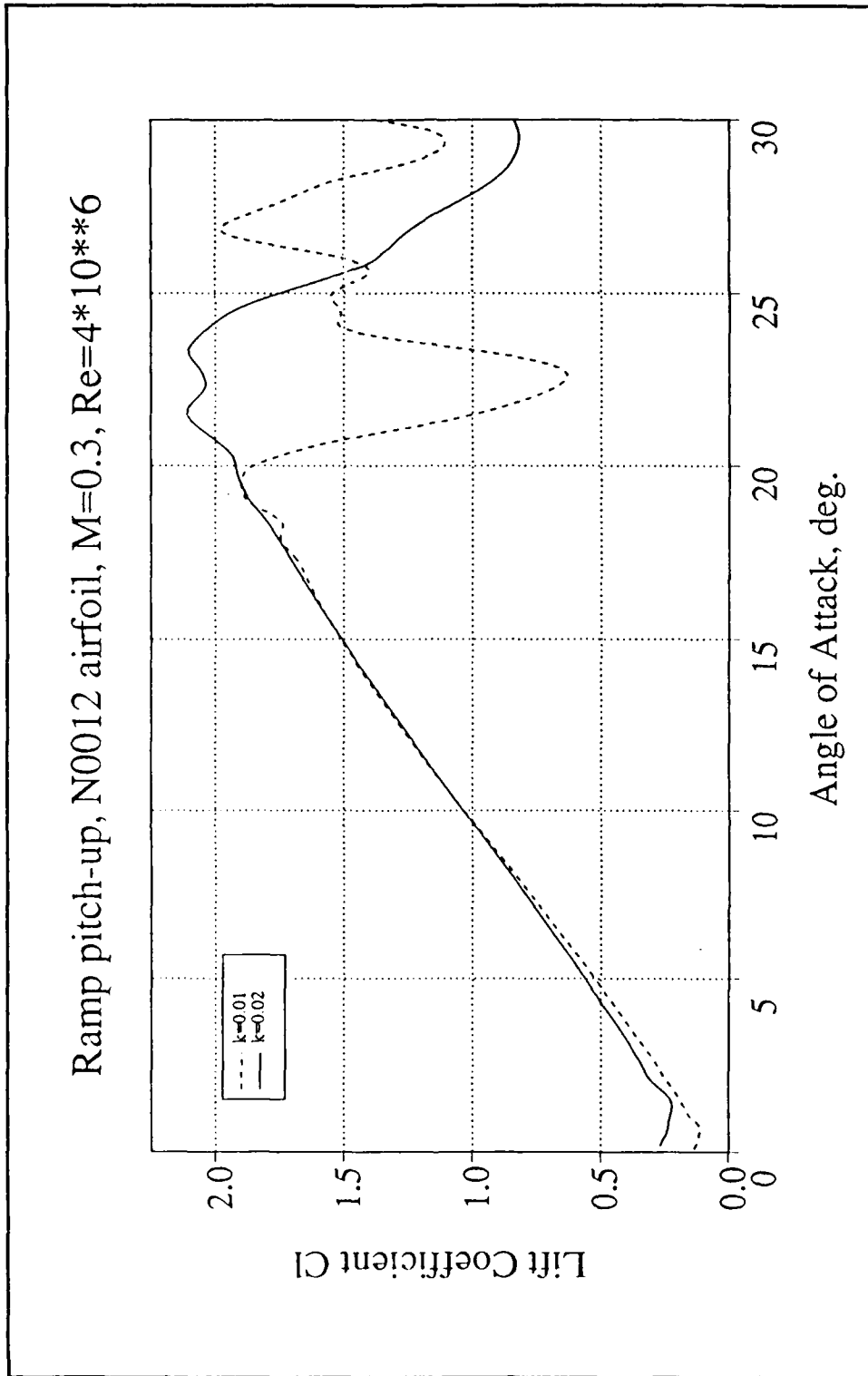


Figure 54. Reduced Frequency Effect, NACA 0012, $M=0.3$

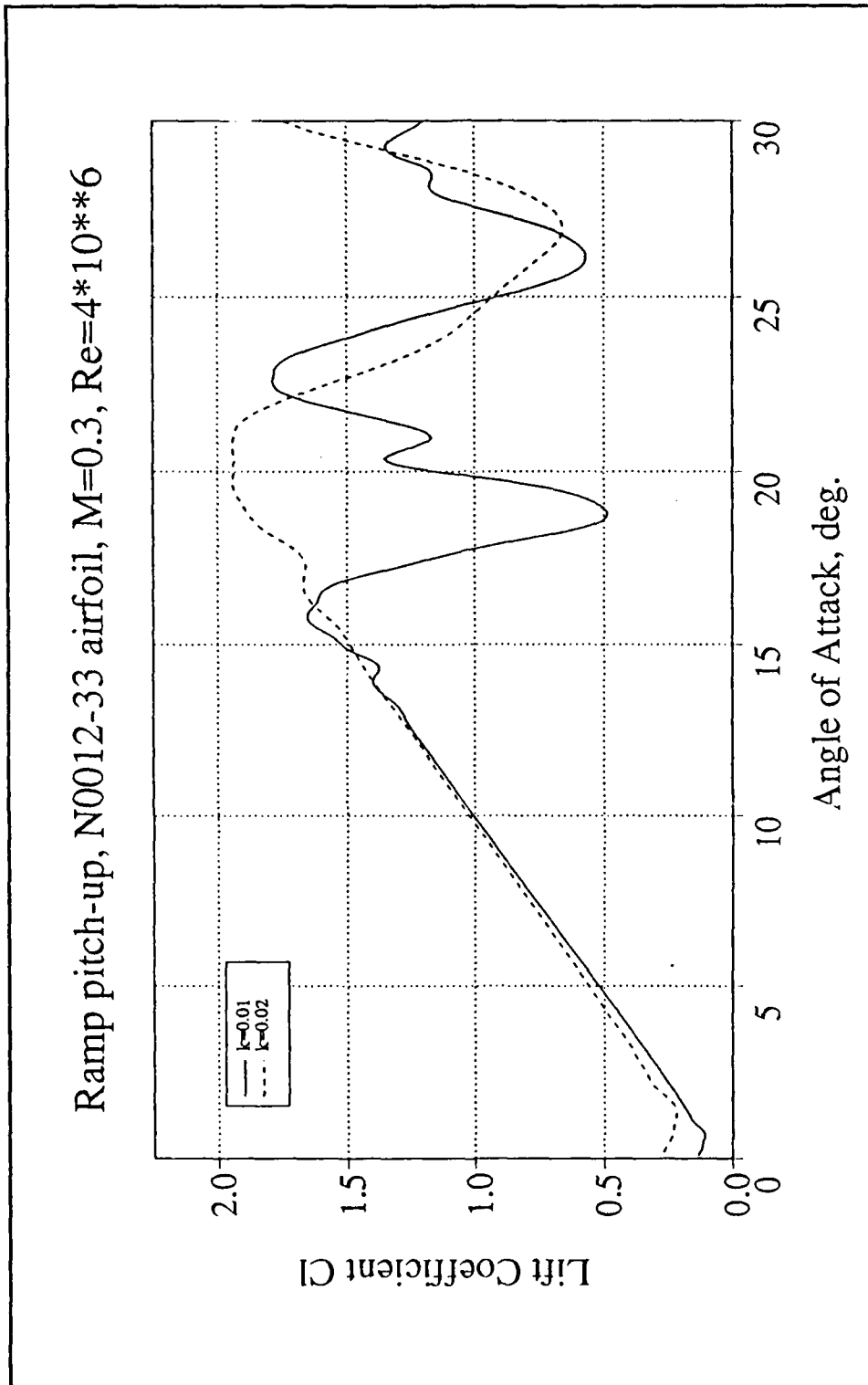


Figure 55. Reduced Frequency Effect, NACA 0012-33, $M=0.3$

The effect of the increased pitching rate in delaying the onset of dynamic stall and increasing the unsteady lift may prove to be of practical operational benefit as knowledge of the details of the flow development increases.

E. EFFECT OF FREESTREAM MACH NUMBER

The effect of increasing freestream Mach number from 0.3 to 0.4 resulted in slightly displacing the lift curve upward for the higher Mach number. The slope of the lift curve was unchanged. However, for a given angle of attack, a very slight increase in lift coefficient was observed at the higher Mach number before the onset of dynamic stall. Figures 56 and 57 show the effect of increasing Mach number for the NACA 0012 and 0012-33 airfoils at a reduced frequency of $k=0.02$. Flow at a Mach number of 0.4 resulted in slightly higher peak lift coefficients than at $M=0.3$. In addition, the peak lift coefficient at $M=0.4$ occurred $1-2^\circ$ higher angle of attack than at $M=0.3$.

The initial development of reverse flow regions and vorticity was largely independent of Mach number for a given airfoil in that the primary vortex originated at approximately the same angle of attack for the two Mach numbers. Subsequent growth of the primary vortex and development of the secondary, tertiary, and trailing edge vortices are delayed to slightly higher angles of attack at $M=0.4$ compared to the $M=0.3$ case. As a result, dynamic stall occurs at a higher angle of attack.

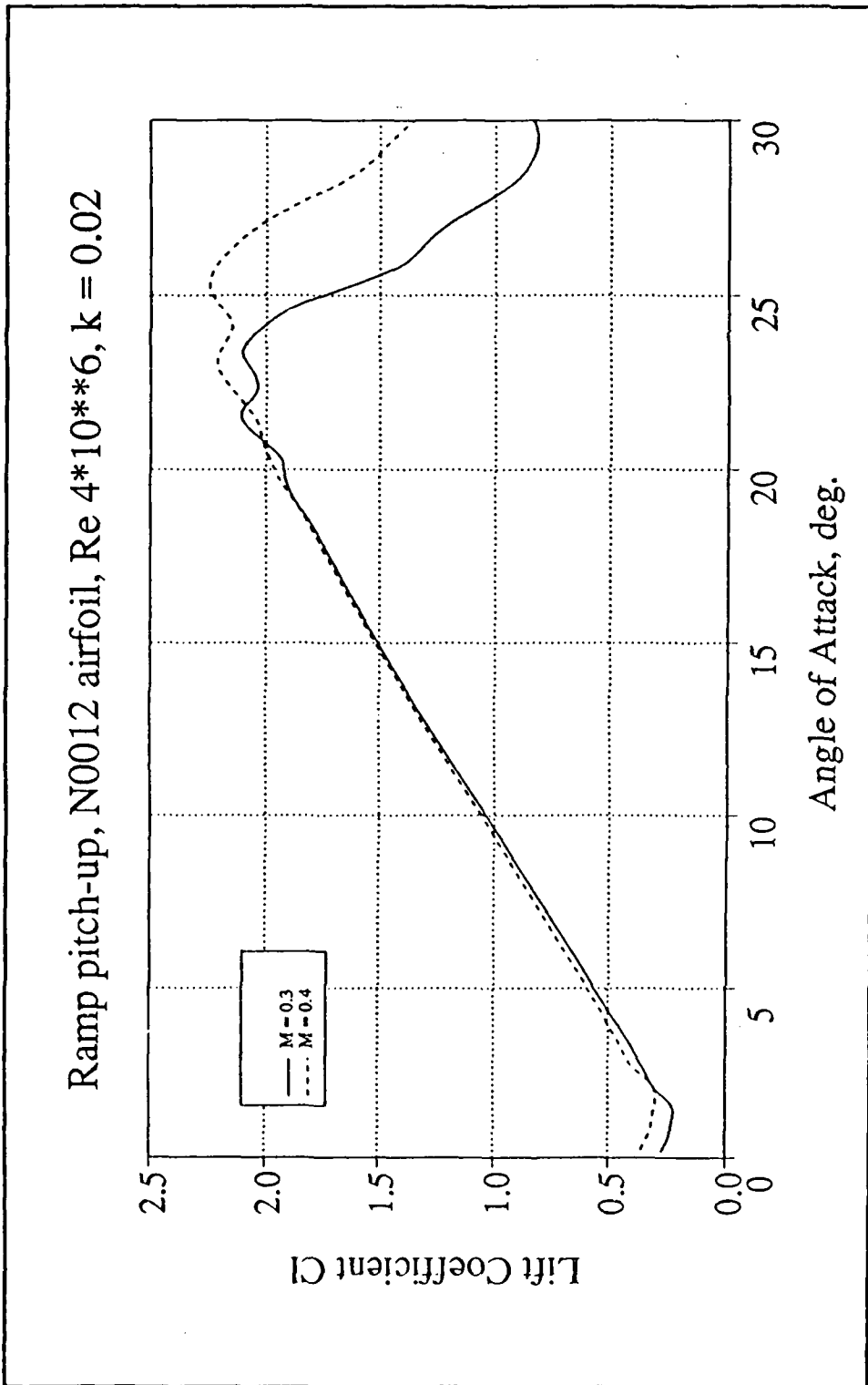


Figure 56. Freestream Speed Effect, NACA 0012, $k=0.02$

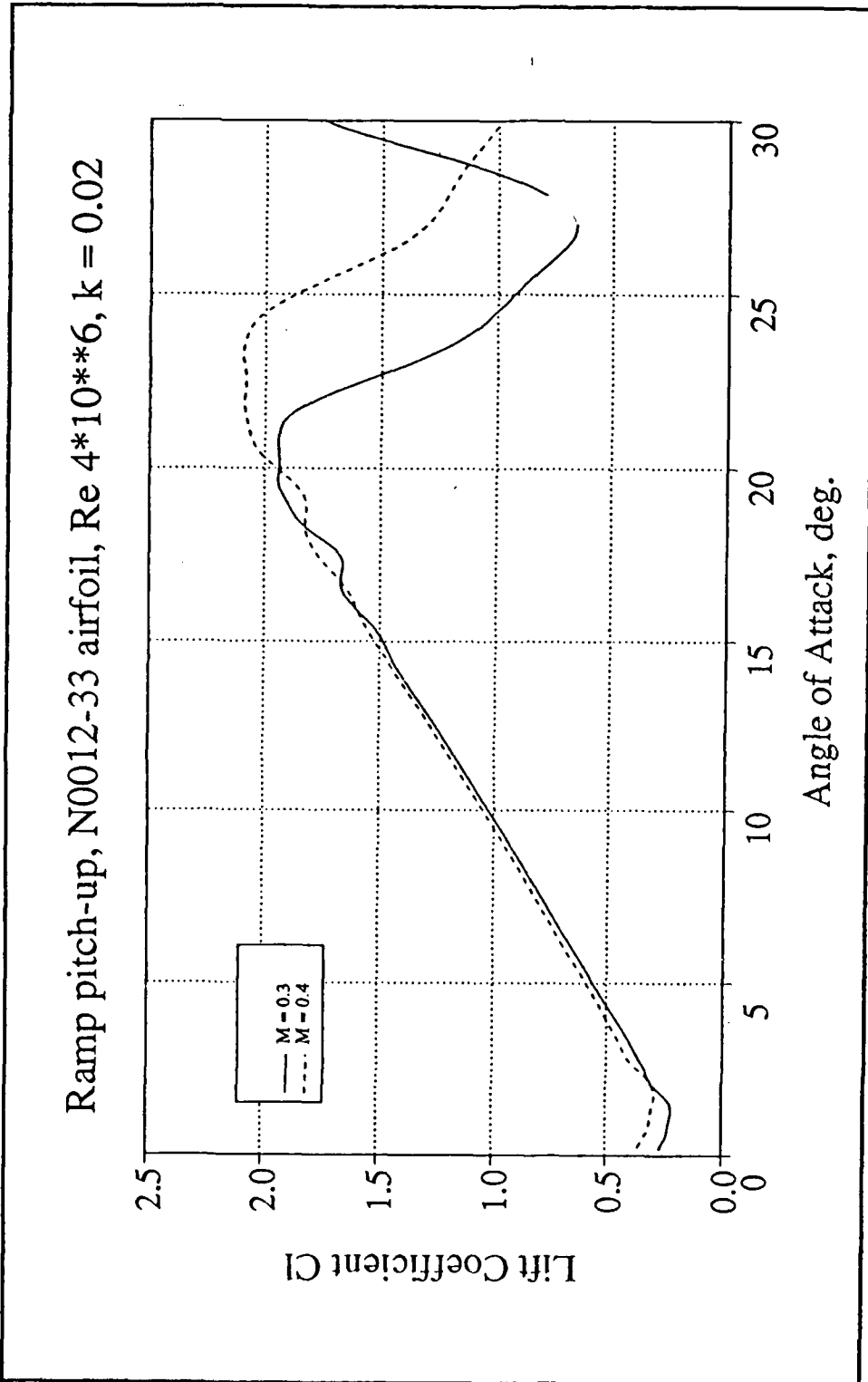


Figure 57. Freestream Speed Effect, NACA 0012-33, $k=0.02$

Ekatzerinaris [Ref. 11] found that for the SSC-a90 airfoil with 9% thickness ratio, increasing Mach number from 0.2 to 0.4 resulted in decreasing both lift coefficient and dynamic stalling angle of attack at a reduced frequency of 0.01. The experimental work by Chandrasekhara and Carr [Ref. 3] using a harmonically oscillating NACA 0012 airfoil also showed that increasing Mach number reduces the angle of attack at which dynamic stall occurred. Further experimental and computational investigation is required at comparable pitching rates to ascertain the accuracy of the computational model used at compressible flow Mach numbers. Further investigation into the influence of airfoil thickness ratio on Mach number effects is needed.

F. PRESSURE GRADIENT AT FLOW SEPARATION

The peak pressure gradient observed at initial flow separation occurring aft of the leading edge was investigated for the three airfoils at the reduced frequencies and Mach numbers listed in Table 2. Figure 58 displays a plot of streamwise pressure gradient along the airfoil chord for the NACA 0012-63 airfoil at different freestream conditions. The figure shows that, for the same airfoil, the peak pressure gradient encountered by the flow at initial flow separation is independent of freestream speed or pitching rate. Similar results were obtained for the other airfoils. Figure 59 shows the streamwise pressure gradient for the NACA 0012-33 airfoil.

Figure 60 displays pressure gradients at initial flow separation angle of attack for the three airfoils at the freestream condition of 0.4 Mach and reduced frequency of $k=0.01$. The peak pressure gradient observed at the instant of flow reversal was higher for the NACA 0012-33 airfoil than for the airfoils with larger leading edge radius. Similar results were obtained at other freestream conditions. The streamwise location of the peak pressure gradient for the NACA 0012-33 airfoil was slightly upstream of that for the NACA 0012-63 airfoil as shown in Figure 61. The higher peak pressure gradient observed for the NACA 0012-33 airfoil is an indication that flow momentum near the surface is higher around the smaller leading edge radius. The higher flow momentum combined with the relatively upstream location of the peak pressure gradient and sharper flow turning angle combined to cause the magnitude of the peak pressure gradient for the NACA 0012-33 airfoil to be 33% greater than that of the NACA 0012-63 airfoil. Thus, the critical pressure gradient required for flow reversal is dependent on leading edge radius, in that a smaller leading edge radius increases the peak pressure gradient at flow reversal.

The streamwise location of flow separation is, in turn, dependent on the location of the peak pressure gradient. The actual location of flow reversal on the airfoil surface occurred 1.0-1.5% chord length downstream of the location of the peak pressure gradient as shown in Figure 61. This delay

is attributed to the time lag in the aerodynamic response to the rapid increase in pressure gradient. The more downstream location of the peak pressure gradient of the NACA 0012-63 airfoil caused a similar relative location of the position of initial flow reversal compared the NACA 0012-33 airfoil.

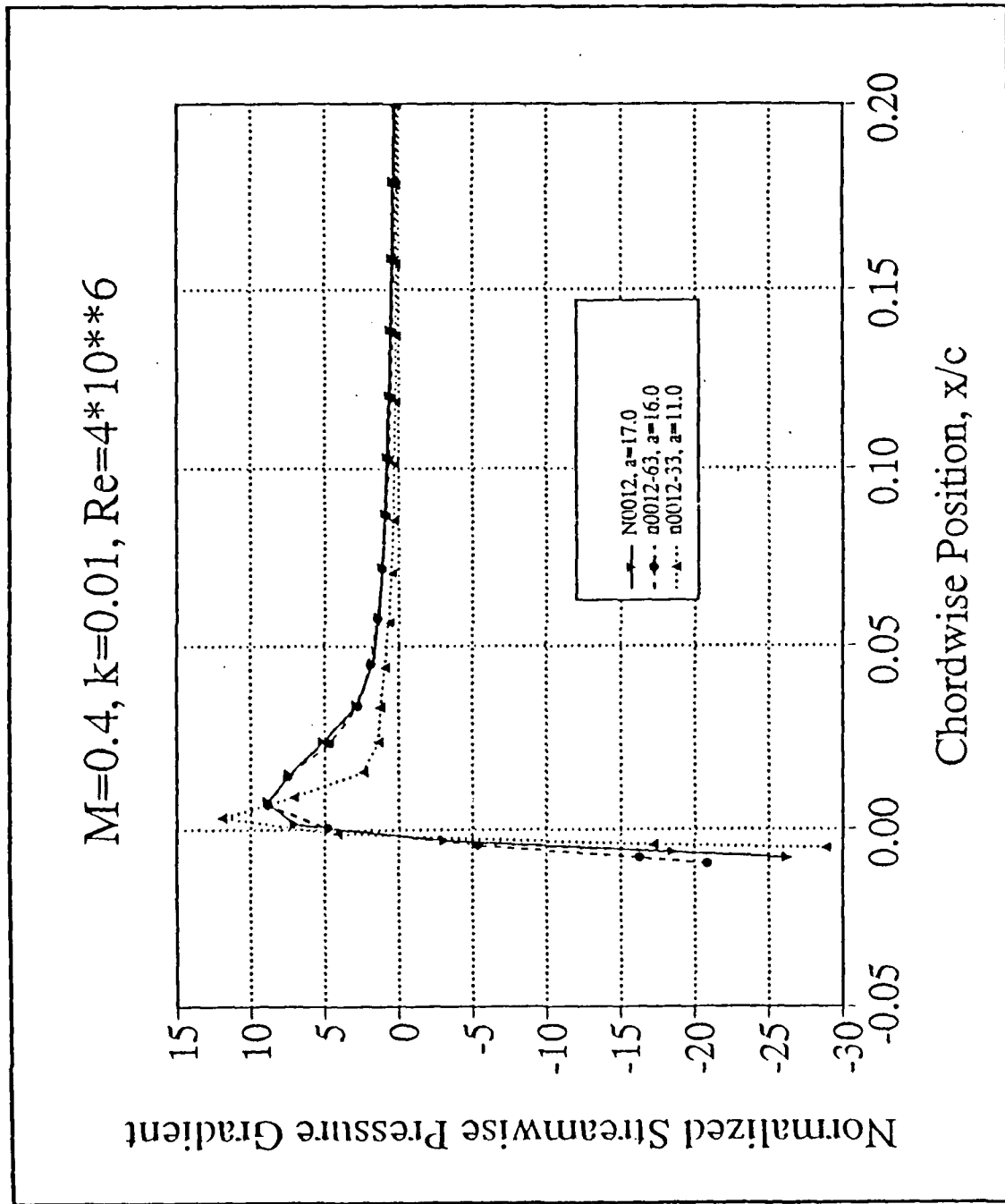


Figure 60. Pressure Gradient Comparison, $M=0.4, k=0.01$

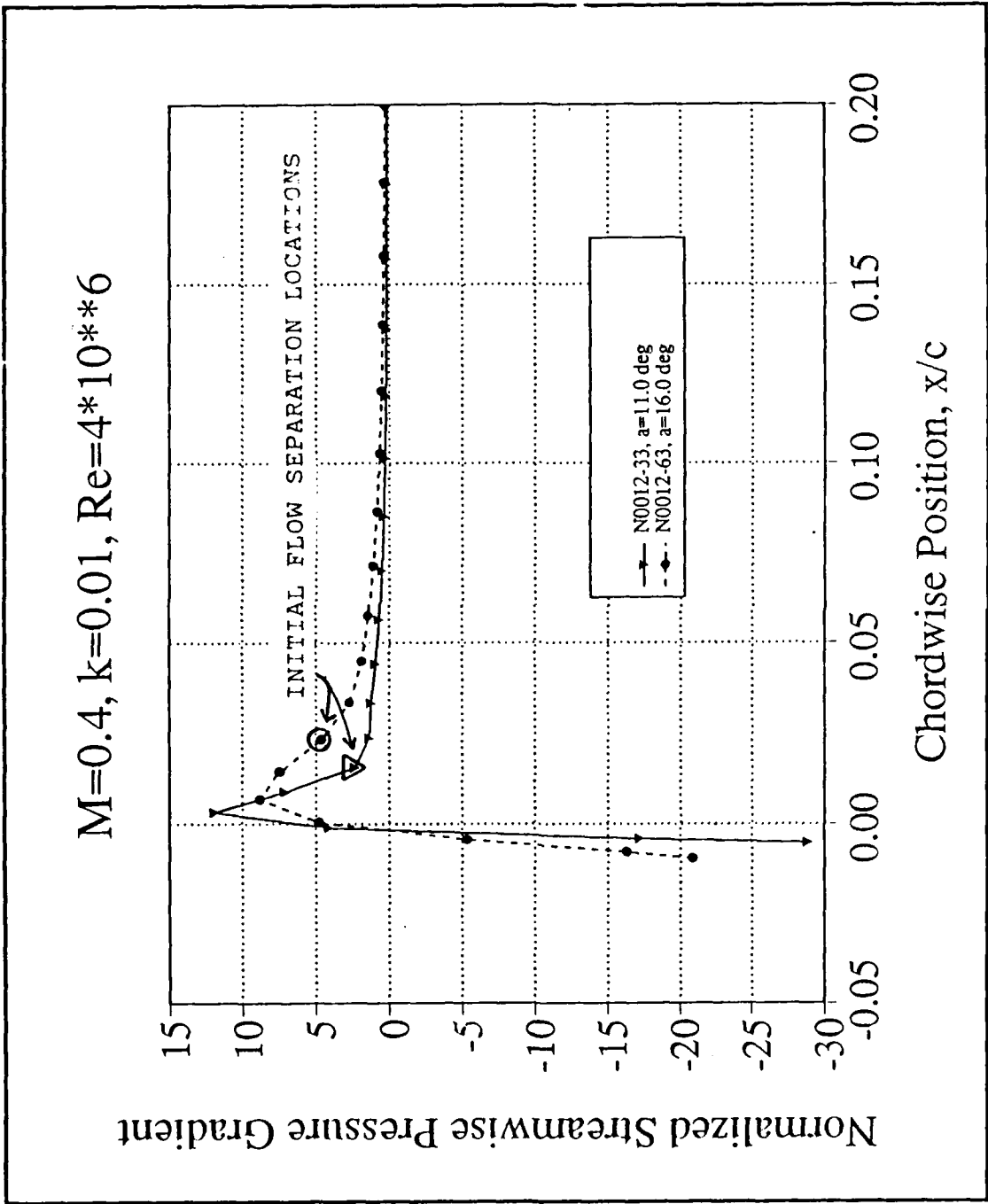


Figure 61. Flow Reversal Location, $M=0.4, k=0.01$

V. CONCLUSIONS AND RECOMMENDATIONS

A. CONCLUSIONS

1. The results of the unsteady flow solutions displayed good agreement with the experimental results for the harmonically oscillating airfoil at a reduced frequency of 0.1 and Mach number of 0.3. At a higher reduced frequency of 0.2, however, the agreement with experimental results was poor during the downstroke.
2. The leading edge geometry of an airfoil was found to have a significant effect on the development of the vortical flowfield and dynamic stall characteristics of the airfoil. Of primary importance is the size of the leading edge radius. A larger leading edge radius delays development of the adverse pressure gradient necessary for boundary layer separation and eventual vortex formation. Of secondary importance is the contouring of the airfoil aft of the leading edge. Thicker contouring forward of the location of maximum thickness contributes to delaying flow separation.
3. The effect of increasing the pitching rate of the airfoil is to enhance unsteady lift by delaying vortex formation to a higher angle of attack. The flow solutions presented in this study on the effects of reduced frequency are in good agreement with trends observed in experimental work.
4. The streamwise pressure gradient required for flow separation is a function of airfoil leading edge radius and is independent of reduced frequency or freestream speed.

B. RECOMMENDATIONS

1. Conduct further experimental and computational investigations to compare Mach number effects on flow development and dynamic stall. The investigations should be conducted at comparable Mach and Reynolds numbers.
2. Investigate the effect of airfoil thickness ratio on dynamic stall.

3. The understanding of harnessing the unsteady lift generated by rapidly pitching airfoils is only part of the knowledge required for practical implementation. Further investigations must include examining pitching moment development and how to minimize the adverse pitching moments produced.
4. Conduct further computational work at higher reduced frequencies and Mach number to check the validity of using this eddy-viscosity model at those flow conditions.

LIST OF REFERENCES

1. McCroskey, W. J., *The Phenomenon of Dynamic Stall*, National Aeronautics and Space Administration Technical Memorandum 81264, March 1981.
2. McCroskey, W. J., and Pucci, S. L., *Viscous-Inviscid Interaction on Oscillating Airfoils in Subsonic Flow*, American Institute of Aeronautics and Astronautics Paper 81-0051R, January 1981.
3. Chandrasekhara, M., and Carr, L., *Flow Visualization Studies of the Mach Number Effects on the Dynamic Stall of an Oscillating Airfoil*. American Institute of Aeronautics and Astronautics Paper 89-0023, January 1989.
4. Chandrasekhara, M. and Brydges, B., "Amplitude Effects on Dynamic Stall of an Oscillating Airfoil," paper presented at the Aerospace Sciences Meeting, 28th, Reno, NV, 9-12 January 1990.
5. Mehta, U. B., *Dynamic Stall of Oscillating Airfoils*, Advisory Group for Aerospace Research and Development Paper #23 CP-227, Unsteady Aerodynamics, September 1977.
6. Wu, J. C. and others, "Dynamic Stall of Oscillating Airfoils," paper presented at 42nd Annual Forum of American Helicopter Society, Washington, D.C., June 1986.
7. Beddoes, T. S., *Prediction Methods for Unsteady Separated Flows*, Advisory Group for Aerospace Research and Development Paper #15 CP-679, 1980.
8. Jang, H. M., Ekaterinaris, J. A., Platzler, M. F., and Cebeci, T., "Essential Ingredients for the Computation of Steady and Unsteady Blade Boundary Layers," ASME Paper 90-GT-160, June 1990.
9. Sankar, N. L., and Tang, W., *Numerical Solution of Unsteady Viscous Flow for Rotor Sections*, American Institute of Aeronautics and Astronautics Paper 85-0129, January 1985.
10. Visbal, M. R., *Effect of Compressibility on Dynamic Stall of a Pitching Airfoil*, American Institute of Aeronautics and Astronautics Paper 88-0132, January 1988.

11. Ekaterinaris, J. A. *Compressible Studies on Dynamic Stall*, American Institute of Aeronautics and Astronautics Paper 89-0024, January 1989.
12. Abbott, I. H. and Von Doenhoff, A. E., *Theory of Wing Sections*, Ch. 6, Dover Publications, Inc., 1959.
13. Schlichting, H., *Boundary Layer Theory*, McGraw-Hill Book Company, 1979.
14. Vivand, H., "Conservative Forms of Gas Dynamic Equations," *La Recherche Aerospatiale*, No. 1 pp. 65-68, January-February 1974.
15. Beam, R. M. and Warming, R. F., "An Implicit Factored Scheme for the Compressible Navier-Stokes Equations," *American Institute of Aeronautics and Astronautics Journal*, v. 16, no. 4, pp. 393-402, April 1978.
16. Baldwin, B. S. and Lomax, H., *Thin Layer Approximation and Algebraic Model for Separated Turbulent Flows*, American Institute of Aeronautics and Astronautics Paper 78-257, January 1978.
17. Cebeci, T., *Calculation of Compressible Turbulent Boundary Layers with Heat and Mass Transfer*, American Institute of Aeronautics and Astronautics Paper 70-741, June 1970.
18. Anderson, D. A., Tannehill, J. C., and Pletcher, R. H., *Computational Fluid Mechanics and Heat Transfer*, p. 490, Hemisphere Publishing Company, 1984.

APPENDIX A - USING THE PROGRAM

A. THE NAVIER-STOKES CODE FOR GENERATING FLOW SOLUTIONS

The main program *NSE2D* (listed in Appendix B for reference) reads input data as supplied by the input file *NSE.1d*, the grid files *fort.11* or *fort.21* as appropriate, and the flow file *fort.31*. The program forms the metrics and the Jacobian by calling the *METRIC* subroutine. After calling the *SLPS* subroutine to perform the computations, the main program outputs the rotated grid and the flow solution to the file *fort.20*, and outputs the data of lift, drag, moment and pressure coefficients, time, angle of attack, and rotational frequency to the loads file *fort.3*.

The subroutine *SLPS* is the primary subroutine, and it calls other subroutines to perform the steps in the ADI algorithm. The major subroutines that *SLPS* calls are:

<u>Subroutine</u>	<u>Function</u>
MATRIX1, MATRIX2	Form block tridiagonal matrices for the ξ and η directions
AMAT1, AMAT2	compute coefficient matrices $\partial F/\partial \xi$ and $\partial G/\partial \eta$
STRESS	supplies the viscous terms
DISSIP	adds fourth-order dissipation terms to the right-hand side of the Navier-Stokes Equations
EXPBC	applies boundary conditions

RES1 computes residuals from inviscid part of
 equations

EDDY applies Baldwin-Lomax model

B. DIRECTIONS FOR EDITING INPUT FILES FOR THE PURPOSE OF GENERATING FLOW SOLUTIONS

1. Generating a Grid

Initially, a grid must be generated as described in Chapter III in order to compute the flow about the airfoil in question. For this, it is necessary to use the *AIRFGR.F* program. With the rectangular coordinates of the desired airfoil, edit the input file *AIRFGR.IN* using the "ex" or the "vi" editors. Ensure that enough points are defined in regions of high curvature such as the leading edge regions. Then ensure that no *fort.21* file exists by renaming or deleting it. At this time, run the grid program by typing

```
AIRFGR < AIRFGR.IN
```

After the program has run, ensure that the grid is satisfactory by running *PLOT3D*. It may be necessary to define more coordinate points to ensure leading edge radius definition, upper or lower surface curvature, or trailing edge closure. Accuracy of trailing edge closure will determine wake thickness. The *AIRFGR.F* program is listed in Appendix C for reference.

2. Rotating a Grid

The grid generated in part 1 is for a zero degree angle of attack. Often it is desired to compute a steady flow or to

start an unsteady flow at an AOA other than zero. In order to do this the *ROTGR.F* program must be used. It is necessary to edit the *ROTGR.F* program and set the desired rotated grid angle by changing the α_1 value in line 10. After the program has been edited, then:

1. Compile *ROTGR.F* by typing "cf77 rotgr.f".
2. Compiling *ROTGR.F* results in an output file named *a.out*. Move *a.out* to *rotgr* by typing "mv a.out rotgr".
3. Execute the program by typing "rotgr".
4. The output file produced by *rotgr* is *fort.12*. It contains the desired grid rotation. Copy *fort.12* to *fort.11* or *fort.21* as necessary for future flow solutions.

The commands within the quotation marks should be typed, not the quotation marks themselves. Upper and lower case are not important.

3. Steady-State Solutions

Ensure that the grid is rotated to the desired angle of attack of the flow solution (part 2). The rotated grid should be copied to the file *fort.21*. The *fort.21* file must have the grid rotated to the desired angle of attack for the steady-state solution!

Modify the *NSE.IN* file as follows:

line 2:

- set desired computational time interval (DT)
- set ALFA, ALFAI, ALFA1 to zero
- set REDFRE to desired reduced frequency
- set AMINF to desired Mach number

line 8:

- set number of time steps (ISTP); usually 3000 are necessary for convergence at AOA \neq 0. In order to run interac-

tively and not exceed time limit, set ISTEP=1000 and run three times.

line 10:

- ensure that XREF=0.25
- set TSHIFT=0.0
- set REYREF to desired Reynolds number

line 14:

- For initial run, set RESTART OSCIL RAMP as FALSE TRUE TRUE. To restart (2nd and 3rd runs), set TRUE TRUE FALSE

line 22:

- Set time to 0.0 for 1st run. Set to preceding run time for restart.

To run interactively and observe output as it develops, type:

```
NSE < NSE.IN
```

To run in the background, type:

```
NSE < NSE.IN > NSE.OUT
```

When the run is finished the last time step solution will consist of grid and flow solutions in file *fort.20*. It will be necessary to separate the grid and flow solution to restart the second run. The command "SPLIT20" will move the grid solution to *fort.11* and the flow solution to *fort.31*, and will display the final run non-dimensional time. When restarting the second run, modify NSE.IN line 14 to RESTART=TRUE. A restarted solution uses grid file *fort.11* and flow file *fort.31*. Set time in NSE.IN to time specified for the previous run when SPLIT20 was executed. Execute the next run by the desired method as before.

After convergence, save the grid and flow files (SPLIT20 to *fort.11* and *fort.31*).

4. Unsteady Solutions

Both oscillatory and ramp (constant pitch rate) solutions can be obtained by the *NSE.F* program. One must ensure that the desired steady state initial angle of attack grid and flow solutions are obtained. The input file *NSE.IN* is modified as follows:

line 2:

- set time interval, freestream Mach number and reduced frequency, where $k = \dot{\alpha}c/2U_\infty$ for ramp solution and $k = \omega c/2U_\infty$ for oscillatory solution.
- For ramp response: set ALFAI to steady-state initial conditions; ALFA, ALFA1 are unused.
- For oscillatory response of form $\alpha = \alpha_0 + \alpha_1 \sin(\omega t)$, set ALFA= α_0 , ALFA1= α_1 , ALFAI=($\alpha_0 - \alpha_1$) since response will start at min α .

line 8:

- set ISTP 6000-12000 depending on length of response desired.

line 10:

- set REYREF to desired Reynolds number.
- set XREF=0.25
- set TSHIFT = -0.5 so that response starts at min α which is 1/4 cycle ($-\pi/2$ time shift as $\alpha = \alpha_0 + \alpha_1 \sin(\omega t - \pi/2)$) from mean α .

line 14:

- set RESTART to TRUE
- set OSCIL to TRUE for oscillatory response (else FALSE)
- set RAMP to TRUE for ramp response (else FALSE)

line 19:

- Program flow solution outputs can be selected for various angles of attack desired. Select desired AOA solutions by listing them multiplied by 100 (i.e. 11 degrees as 1100). The outputs are listed as files *fort.61* through *fort.72*.

line 22:

- Set time to 0.0 for initial run. For restart set time to the *fort.20* output from the last timestep of the last run.

Run the program by submitting it as a job to the queue by typing "qsub -lt 7200 subunst". The subunst file is a command file which will order the steps for the Cray when the job number comes up in the queue. With at least 1 1/2 hours in computation, go run 5 miles, eat lunch, or play with the kids. Upon returning, check on queue status by typing "mqs". If no entries, the run is finished and you can split the output files and continue, if desired.

Any of the output files *fort.61* through *fort.72* and *fort.20* can be split into grid solutions and flow solutions for further analysis. *Fort.20* file must be split to continue the response at further angles of attack, and to use the run time as the next run *NSE.IN* input in line 22. For continuous ramp or oscillatory responses, it is not necessary to reset ALFA, ALFAI, ALFA1, or RESTART; it is only necessary to reset desired AOA solutions to be recorded (line 19) and the time.

5. Example

As an example, to run an oscillatory solution for $\alpha=10+7\sin(t)$, it is necessary to get a steady flow solution at $\alpha=3^\circ$ ($3=10-7$). The grid developed for the airfoil must be rotated to 3° using the *ROTGR.F* program and input to *fort.21*. At this time a steady-state solution is obtained by modifying *NSE.IN* with the following inputs:

ALFA	0.0
ALFAI	0.0
ALFA1	0.0
REDFRE	as desired
AMINF	as desired
TIME	0.0
RESTART OSCIL RAMP	FALSE TRUE FALSE
XREF	0.25
TSHIFT	0.0

Run the program by typing " NSE < NSE.IN (>NSE.OUT) "

After 1000 timesteps, issue the command SPLIT20, so that the files *fort.11* and *fort.31* will be opened. Edit *NSE.IN* with the SPLIT20 time and set RESTART=TRUE. Run the program again, and then a third time, ensuring convergence (in lift coefficient, drag coefficient, etc.) Save the final *fort.11* and *fort.31* files.

Then, modify *NSE.IN* as follows

ALFA	10.0
ALFAI	3.0
ALFA1	7.0
ISTP	6000-12000
TIME	0.0
RESTART OSCIL RAMP	TRUE TRUE FALSE
XREF	0.25
TSHIFT	-0.5

ia1. ia2, ... ia12 as desired

Run the program by issuing the command "qsub -lt 7200 subunst". After completion, save the output files (*fort.61* through *fort.72*) and *fort.20*. Do a SPLIT20, note time and AOA, then input TIME into *NSE.IN* for further runs.

Graphs of the output files may be obtained by using the plot program *PLOT3D*. Observe output files (for example *fort.65*) and graph by typing the commands: "split" and then on

the next line "65". Outputs will be in files *fort.11* (grid) and *fort.31* (flow) which are read into the *PLOT3L* input.

A typical NSE.IN file for the unsteady solution of the example problem at $k=0.02$ and $M=0.4$ would be as follows.

```
IMAX  KMAX    DT      WW   ALFA  ALFA1  ALFAI  REDFRE  AMINF
 157   58  0.005   2.00  10.00   7.00   3.00   0.02   0.40
ISPEC (FLAG FOR CHOOSING DIFFERENT SPECTRAL RADIUS)
 3
WW2X, WW2Y, WW4X, WW4Y (EXPLICIT DISSIPATION COEF. FOR X AND Y)
 0.00    0.00    0.030   0.030
  ISTEP  NPER      NOUT      RES  STRUNST
 9000.   18000.   1000.    100.    0.
  REYREF  DMIN      XREF    TSHIFT
  4.00   0.00002   0.25    -0.5
TSTAR1
-1.0
RESTART, MULTIGRID OPTIONS SPECIFIED IN THE NEXT CARD
TRUE TRUE FALSE
CIRCOR ( CIRCULATION CORRECTION)
TRUE
 31  127
ITEL ITEU
0300 0400 0500 0600 0700 0800 0900 1000 1100 1200 1300 1400
 ia1  ia2  ia3  ia4  ia5  ia6  ia7  ia8  ia9 ia10 ia11 ia12
TIME
0.0
```

```

LINE # SOURCE TEXT
1 C*****
2 C
3 C
4 C MAIN PROGRAM
5 C*****
6 C
7 PROGRAM NSFMHAIN
8 PARAMETER (IX=180,KX=60)
9 COMMON/SURF/PSUR(IX)
10 COMMON/IX/OMEGA,BDOT
11 COMMON/MUTUR/CMU(IX,KX)
12 COMMON/SKINCF/CF(IX)
13 COMMON/GR/DL,X(IX,KX),Z(IX,KX)
14 COMMON/PAR/GAMMA,REYREF,ALFA,ALFAI,ALFAI,REDFRE,AMINF,ALFAI
15 COMMON/DGRID/DT,IMAX,KMAX,ITEL,ITEU
16 COMMON/GRID/YACOB(IX,KX)
17 COMMON/DAMP/WW,WMI,WW2X,WW2Y,WW4X,WW4Y
18 COMMON/FLOW/Q1(IX,KX),Q2(IX,KX),Q3(IX,KX),Q4(IX,KX)
19 COMMON/MTRIX/ X11(IX,KX),X12(IX,KX),ZETA(IX,KX),ZETAZ(IX,KX)
20 1 ,XIT(IX,KX),ZETAT(IX,KX)
21 COMMON/PLOT/TITLE(10),NSTPT,RES(3000),RES,CLB(3000),CDPH(3000)
22 DIMENSION DRBO(IX,KX)
23 COMMON/INITI/UINF,VINF
24 COMMON/BCLOG/CIRCOR
25 COMMON/LOGIC/RSTRT,PITCHE,RAMP
26 LOGICAL CIRCOR
27 LOGICAL RSTRT,PITCHE,RAMP
28 CHARACTER ITITLE*80
29 COMMON/TITL/ITITLE
30 COMMON/L2NORM/ RESDL2(10000)
31 PI = 4. * ATAN(1.)
32 C
33 C*** PROGRAM SOLVES TWO-DIMENSIONAL VISCOUS FLOW PAST ARBITRARY
34 C*** GEOMETRIES USING ADI PROCEDURE.
35 C
36 C TAPE5 = FILE CONTAINING INPUT DATA
37 C TAPE6 = OUTPUT
38 C TAPE8 = FILE THAT SAVES THE FLOW FIELD AT THE END OF A RUN
39 C IF THE CURRENT RUN IS A RESTART OF A PREVIOUS RUN, THEN
40 C TAPE7 IS USED TO READ THE FLOW FIELD INTO MEMORY
41 C*** READ INPUT DATA
42 C
43 READ *,ITITLE
44 READ (5,1) TITLE
45 READ(5,20(1))
46 READ (5,2) IMAX,KMAX,DT,WW,ALFA,ALFAI,ALFAI,REDFRE,AMINF
47 C
48 C ISPEC = FLAG TO SPECIFY DIFFERENT SPECTRAL RADIUS FOR SCALING
49 C WITH THE DISSIPATION
50 C
51 READ(5,20(1))
52 READ(5,2) ISPEC
53 READ(5,20(1))
54 READ(5,22(1)) WW2X,WW2Y,WW4X,WW4Y
55 C NSTP = NO. OF TIME STEPS TO BE DONE ON THIS RUN
56 READ(5,20(1))
57 READ (5,2,21) FNSTP, FNPER, FNOUT, RES
58 NPER = FNPER
59 NSTP = FNSTP
60 FNOUT = FNOUT
61 C
62 C REYREF= REYNOLDS NUMBER IN MILLIONS
63 C DNMIN = DISTANCE OF FIRST POINT OFF THE WALL
64 C FOR REYNOLDS NUMBERS UPTO 3 MILLION USE 0.00005
65 C XREF = REFERENCE VALUE AT X-AXIS
66 READ (5,2(01))
67 READ (5,22(1)) REYREF,DNMIN,XREF,TSBIFT
68 TSBIFT = TSBIFT * PI
69 REREAL = REYREF * 1000000.
70 REYREF = REYREF * 1.E+06
71 C
72 C TSTART = TIME THAT THE CALCULATIONS HAVE BEEN ADVANCED
73 C UPTO THE PPREVIOUS RUN. IF TSTART IS NEGATIVE THIS VALUE IS
74 C OBTAINED FROM THE TAPE 3.
75 READ (5,20(1))
76 READ (5,22(1)) TSTART
77 2221 FORMAT(4F10.0)
78 READ (5,2(01))
79 2001 FORMAT(1X)
80 READ (5,20(0)) RSTRT,PITCHE,RAMP
81 READ(5,20(1))
82 READ(5,20(0)) CIRCOR
83 2000 FORMAT(3I5)
84 read(5,*) ia1,ia2,ia3,ia4,ia5,ia6,ia7,ia8,ia9,ia10
85 @ ,ia11,ia12,ia13,ia14,ia15
86 ialfad = 100.*alfad
87 IF (PITCHE) DT = PI / (NPER*REDFRE*AMINF)
88 C NEGATIVE REYREF MEANS INVISCID FLOW
89 C
90 C*** PRINT OUT THE INPUT DATA
91 C
92 WWI = 3. * WW
93 WRITE (6,4) TITLE
94 WRITE (6,3) IMAX,KMAX,DT,WW,WMI,ALFA,ALFAI,ALFAI,REDFRE,AMINF,XREF
95 WRITE (6,6) NPER, NSTP, FNOUT
96 66 FORMAT(/,2X,5BNPER=,I8,5X,5BNSTP=,I8,5X,5BNOUT=,I8,/)
97 IF(REYREF.GT.0.) WRITE (6,3700) REYREF
98 WRITE(6,67) WW2X, WW2Y, WW4X, WW4Y
99 67 FORMAT(/,2X,5BNW2X=,F8.4,5X,5BNW2Y=,F8.4,5X,5BNW4X=,F8.4,5X,
100 1 5BNW4Y=,F8.4,/)
101 GAMMA=1.4
102 ITEL = 31
103 ITEU = 133
104 ILE = ( ITEU - ITEL ) / 2 + ITEL
105 C
106 ccc CALL A*RFOL(ITEU,ITEU,ILE)
107 ccc IF(REYREF.GT.0.) CALL CLUSTR(DNMIN)
108 C
109 READ(21) IMAX,KMAX
110 read(21) (( X(I,K),I=1,IMAX),K=1,KMAX ),
111 @ (( Z(I,K),I=1,IMAX),K=1,KMAX )
112 C
113 C***C STARTING CONDITIONS.
114 C*** DENSITY NORMALISED WITH RESPECT TO ROINF
115 C*** VELOCITIES NORMALISED WITH RESPECT TO AINF
116 C*** TOTAL ENERGY NORMALISED WITH RESPECT TO (ROINF*AINF*AINF)
117 C
118 TOTEN=AMINF*AMINF*0.5-1./(GAMMA*(GAMMA-1.))
119 ALFA = ALFA * PI / 180.
120 ALFAI = ALFAI * PI / 180

```

```

LINE # SOURCE TEXT
121 ALMEAN = ALFA
122 ALFA1 = ALFA1 * PI / 180.
123 ALFAMAX = ALFA1 + ALMEAN
124 ALFACR = ALFAMAX
125 C ALFA IS THE ANGLE OF AIRFOIL WITH RESPECT TO FREESTREAM AT STEADY-STATE
126 OR INITIAL POSITION OF UNSTEADY MOTION.
127 C IT SHOULD BE SET ACCORDING TO THE TYPE OF MOTION
128 ALFAS = ALMEAN - ALFA1 * COS(0.)
129 UINF = AMINF * COS(ALFA)
130 VINP = AMINF * SIN(ALFA)
131 C unif = aminf
132 C vinf = 0.0
133 C call rotgrid( imax,kmax,alfa )
134 DO 7 I=1,IMAX
135 DO 7 K=1,KMAX
136 Q1(I,K)=1.
137 Q2(I,K)=UINF
138 Q3(I,K)=VINP
139 Q4(I,K)=TOTEN
140 7 CONTINUE
141 IF(RSTRT) THEN
142 REWIND 11
143 READ (11) IMAX , KMAX
144 READ (11) ( ( X(I,K), I=1,IMAX ), K=1,KMAX ),
145 & ( ( Z(I,K), I=1,IMAX ), K=1,KMAX )
146 rewind 31
147 READ (31) IMAX , KMAX
148 READ (31) F5MACH, ALFAD, REREAL, TIME
149 READ (31) ( ( Q1(I,K), I=1,IMAX ), K=1,KMAX ) ,
150 & ( ( Q2(I,K), I=1,IMAX ), K=1,KMAX ) ,
151 & ( ( Q3(I,K), I=1,IMAX ), K=1,KMAX ) ,
152 & ( ( Q4(I,K), I=1,IMAX ), K=1,KMAX )
153 ENDIF
154 C
155 if( time .gt. 500. ) time = 0.
156 if( alfad .eq. 0 ) time = 0.
157 TSTART = TIME
158 IF(TSTART GE. 0.) TIME = TSTART
159 IF(.NOT.(RSTRT)) TIME = 0.
160 WRITE(6,62) TIME
161 68 FORMAT(/,40BTHE CALCULATIONS STARTED AT TIME T = ,F12.4,/)
162 ASTART = ALFA + ALFA1 * SIN( 2*REDFRE*AMINF * TIME + TSHIFT )
163 ASTART = ASTART * ( 180. / PI )
164 IDONE = TIME / DT
165 WRITE(6,661) ASTART, IDONE
166 681 FORMAT(2X,10HALFASTART=,F10.4,8X,15ITERATIONS DONE,5X,I6,/)
167 CALL METRIC
168 IMIN = ( ITEU - ITEL ) / 2 + ITEL
169 ILOW = 2 * IMIN
170 CBD = X(ITEL,1) - X(IMIN,1)
171 NSTPT = NSTP + NSTPP
172 C
173 C-----> STARTING FROM A STEADY-SATE SOLUTION AT CERTAIN ANGLE <Ao>
174 C GIVE A TIME SRIPT <TSHIFT> TO START FROM Ao AND SET INITIALLY
175 C TIME=0., KEEP TSHIFT THE SAME THROUGH THE GNST. CALCUL.
176 C
177 IF ( PITCH ) THEN
178 DTP = PI / (NPER*REDFRE*AMINF)
179 dt = dtp
180 endif
181 alfacr = pi / 9.
182 alfamax= almean + alfa1
183 IF( RAMP ) READ (5,*) TIME
184 DO 1000 ITN=1,NSTP
185 TIME = TIME + DT
186 C
187 C REDUCE THE TIME STEP TO HALF AT THE PEAK OF THE CYCLE
188 C
189 C IF (PITCH) THEN
190 C
191 C IF( ALFA .GT. ALFACR ) THEN
192 DT = DTP * ( 1. - .5*(ALFA-ALFACR)/(ALFAMAX-ALFACR) )
193 ELSE
194 DT = DTP
195 END IF
196 C
197 OMEGA = 2.*REDFRE*AMINF * COS( REDFRE* 2.*TIME*AMINF +TSHIFT)
198 1 *ALFA1
199 ALOLD = ALMEAN + ALFA1 * SIN( 2. * REDFRE * AMINF *
200 1(TIME - DT) + TSHIFT )
201 ALFA = ALMEAN + ALFA1 * SIN( REDFRF * 2. * TIME * AMINF
202 1 + TSHIFT )
203 ALFAD = ALFA * 45. / ATAN(1.)
204 DALFA = ALFA - ALOLD
205 CALL ROTGRID(IMAX,KMAX,DALFA)
206 CALL METRIC
207 END IF
208 IF (RAMP) THEN
209 OMEGA = 2. * REDFRE * AMINF
210 ALOLD = OMEGA * ( TIME - DT )
211 ALFA = OMEGA * TIME
212 ALFAD = ALFA * 45. / ATAN(1.)
213 DALFA = ALFA - ALOLD
214 CALL ROTGRID(IMAX,KMAX,DALFA)
215 CALL METRIC
216 END IF
217 ALFAD = ALFA * 45. / ATAN(1.)
218 C
219 CALL SLPS(ITN,ISPEC)
220 C
221 C APPLICATION OF BOUNDARY CONDITIONS
222 C
223 CALL EXPBC(CL)
224 C
225 CALL LOAD(CL,CDP,CDF,CM,ALFAS,XREF)
226 C
227 PRINT OUT PRESSURE AT THE SURFACE
228 C
229 IF(ITN/50*50.EQ.ITN) THEN
230 WRITE (6,19)
231 WRITE (6,33) ITN, TIME , DT
232 IF(PITCH OR. RAMP) WRITE (6,3500) ALFAD,OMEGA
233 IF(ITN/50*50.EQ.ITN)CALL CPPL0T(ITEU,ITEU,AMINF,X(1,1),Z(1,1))
234 IF(ITN/400*400.EQ.ITN) WRITE(6,12) [(I,CF(I),I=1,IMAX)
235 WRITE (6,3000) CL , CDP , CDF , CM
236 END IF
237 TIMPI = TIME / AMINF
238 IF(ITN/50*50.EQ.ITN)WRITE(3,8000)TIME,ALFAD,OMEGA,CL,CDP,CDF,CM
239 IF(ITN/1000*1000.EQ.ITN) THEN
240 DO 100 ? = IMIN , ITEU

```

LINE # SOURCE TEXT

```

241 C      XOC = ( X(I,1) - X(IMIN,1) ) / CND
242 C      WRITE(2,7000) XOC , PSUR(ILOW-I) , PSUR(I)
243 C      WRITE(9,7000) XOC , CF(ILOW-I) , CF(I)
244 C 100  CONTINUE
245 C
246 C      ENDIF
247 C      CMU TO CALCULATE THE AVERAGE VALUES OF CL, CD, CM
248 C      SCL = SCL + CL
249 C      SCDF = SCDF + CDF
250 C      SCDP = SCDP + CDP
251 C      SCM = SCM + CM
252 C      CMU TO NEXT CMU FOR USER SPECIFIED PLOTS
253 C      DO 984 K = 1 , KMAX
254 C      DO 984 I = 1 , IMAX
255 C 984 DRHO(I,K) = ABS( Q1(I,K) - DRHO(I,K) )
256 C      IRES = IFIX(RES)
257 C      IF (ITN/IRES.EQ.ITN) THEN
258 C      IPILOT = ( NSTPP + ITN ) / IRES
259 C      RESD(IPILOT) = 0.
260 C      CLB(IPILOT) = CL
261 C      CDPB(IPILOT) = CDP
262 C      DO 985 K = 1 , KMAX
263 C      DO 985 I = 1 , IMAX
264 C 985 RESD(IPILOT) = AMAX1(RESD(IPILOT),DRHO(I,K))
265 C      985 RESD(IPILOT) = RESDL2(ITN)
266 C      ENDIF
267 C
268 C      IF (ITN/NOUT.EQ.ITN) THEN
269 C      IF ( ITN .EQ. 1*NOUT ) IOUT = 31
270 C      IF ( ITN .EQ. 2*NOUT ) IOUT = 32
271 C      IF ( ITN .EQ. 3*NOUT ) IOUT = 33
272 C      IF ( ITN .EQ. 4*NOUT ) IOUT = 34
273 C      IF ( ITN .EQ. 5*NOUT ) IOUT = 35
274 C      IF ( ITN .EQ. 6*NOUT ) IOUT = 36
275 C      IF ( ITN .EQ. 7*NOUT ) IOUT = 37
276 C      IF ( ITN .EQ. 8*NOUT ) IOUT = 38
277 C      IF ( ITN .EQ. 9*NOUT ) IOUT = 39
278 C      IF ( ITN .EQ. 10*NOUT ) IOUT = 40
279 C      IF ( ITN .EQ. 11*NOUT ) IOUT = 41
280 C      IF ( ITN .EQ. 12*NOUT ) IOUT = 42
281 C      IF ( ITN .EQ. 13*NOUT ) IOUT = 43
282 C      IF ( ITN .EQ. 14*NOUT ) IOUT = 44
283 C      IF ( ITN .EQ. 15*NOUT ) IOUT = 45
284 C      IF ( ITN .EQ. 16*NOUT ) IOUT = 46
285 C
286 C      IOUT = 20
287 C      REWIND IOUT
288 C      WRITE (IOUT) IMAX , KMAX
289 C      WRITE (IOUT) ( ( X(I,K), I=1,IMAX ), K=1,KMAX ),
290 C      ( ( Z(I,K), I=1,IMAX ), K=1,KMAX )
291 C      WRITE (IOUT) IMAX , KMAX
292 C      WRITE (IOUT) AMINF, ALFAD, REREAL, TIME
293 C      WRITE (IOUT) ( ( Q1(I,K), I=1,IMAX ), K=1,KMAX ),
294 C      ( ( Q2(I,K), I=1,IMAX ), K=1,KMAX ),
295 C      ( ( Q3(I,K), I=1,IMAX ), K=1,KMAX ),
296 C      ( ( Q4(I,K), I=1,IMAX ), K=1,KMAX )
297 C
298 C      REWIND IOUT
299 C
300 C      ENDIF
301 C
302 C      ialfad = 100.*alfad
303 C      ia1 = 100
304 C      ia2 = 200
305 C      ia3 = 300
306 C      ia4 = 400
307 C      ia5 = 500
308 C      ia6 = 600
309 C      ia7 = 700
310 C      ia8 = 800
311 C      ia9 = 900
312 C      ia10 = 1000
313 C      ia11 = 1050
314 C      ia12 = 1100
315 C      IF( IALFAD .EQ. ia1 .OR.
316 C      @ IALFAD .EQ. ia2 .OR.
317 C      @ IALFAD .EQ. ia3 .OR.
318 C      @ IALFAD .EQ. ia4 .OR.
319 C      @ IALFAD .EQ. ia5 .OR.
320 C      @ IALFAD .EQ. ia6 .OR.
321 C      @ IALFAD .EQ. ia7 .OR.
322 C      @ IALFAD .EQ. ia8 .OR.
323 C      @ IALFAD .EQ. ia9 .OR.
324 C      @ IALFAD .EQ. ia10 .OR.
325 C      @ IALFAD .EQ. ia11 .OR.
326 C      @ IALFAD .EQ. ia12 ) THEN
327 C      IF( IALFAD .EQ. ia1 ) IAOUT = 61
328 C      IF( IALFAD .EQ. ia2 ) IAOUT = 62
329 C      IF( IALFAD .EQ. ia3 ) IAOUT = 63
330 C      IF( IALFAD .EQ. ia4 ) IAOUT = 64
331 C      IF( IALFAD .EQ. ia5 ) IAOUT = 65
332 C      IF( IALFAD .EQ. ia6 ) IAOUT = 66
333 C      IF( IALFAD .EQ. ia7 ) IAOUT = 67
334 C      IF( IALFAD .EQ. ia8 ) IAOUT = 68
335 C      IF( IALFAD .EQ. ia9 ) IAOUT = 69
336 C      IF( IALFAD .EQ. ia10 ) IAOUT = 70
337 C      IF( IALFAD .EQ. ia11 ) IAOUT = 71
338 C      IF( IALFAD .EQ. ia12 ) IAOUT = 72
339 C      REWIND IAOUT
340 C      WRITE (IAOUT) IMAX , KMAX
341 C      WRITE (IAOUT) ( ( X(I,K), I=1,IMAX ), K=1,KMAX ),
342 C      ( ( Z(I,K), I=1,IMAX ), K=1,KMAX )
343 C      WRITE (IAOUT) IMAX , KMAX
344 C      WRITE (IAOUT) AMINF, ALFAD, REREAL, TIME
345 C      WRITE (IAOUT) ( ( Q1(I,K), I=1,IMAX ), K=1,KMAX ),
346 C      ( ( Q2(I,K), I=1,IMAX ), K=1,KMAX ),
347 C      ( ( Q3(I,K), I=1,IMAX ), K=1,KMAX ),
348 C      ( ( Q4(I,K), I=1,IMAX ), K=1,KMAX )
349 C      REWIND IAOUT
350 C      ENDIF
351 C
352 C      1000 CONTINUE
353 C
354 C      REWIND 20
355 C      WRITE (20) IMAX , KMAX
356 C      WRITE (20) ( ( X(I,K), I=1,IMAX ), K=1,KMAX ),
357 C      ( ( Z(I,K), I=1,IMAX ), K=1,KMAX )
358 C      WRITE (20) IMAX , KMAX
359 C      WRITE (20) AMINF, ALFAD, REREAL, TIME
360 C      WRITE (20) ( ( Q1(I,K), I=1,IMAX ), K=1,KMAX ),
361 C      ( ( Q2(I,K), I=1,IMAX ), K=1,KMAX ),
362 C      ( ( Q3(I,K), I=1,IMAX ), K=1,KMAX ),
363 C      ( ( Q4(I,K), I=1,IMAX ), K=1,KMAX )

```

LINE # SOURCE TEXT

```

361 C
362   alfa = alfa * (180/pi)
363   write(6,667) alfa, time
364 667 format('ANGLE OF ATTACK =,F15.10,5X,SBTIME=,F10.4,/')
365 C
366 C   PRINT OUT VELOCITY PROFILE
367 C
368   WRITE(6,668)
369 668 format('14X,2HUX,14X,2HUY,10X,8HDENSITY ,6X,8BPRESSURE,/')
370   CMUL = AMINF / REYREF
371   DO 4000 I = 70,130,2
372     S = 0.
373     DO 4000 K = 2, 20
374       S = S + SQRT( (X(I,K)-X(I,K-1))**2 + (Z(I,K)-Z(I,K-1))**2 )
375       U = ( Q2(I,K)/Q1(I,K) )
376       V = ( Q3(I,K)/Q1(I,K) )
377       UTOT = U*U + V*V
378       P = (GAMMA-1.)*( Q4(I,K) - .5*Q1(I,K)*UTOT )
379       WRITE (6,2002) I,K, U,V , Q1(I,K) , P
380 4000 CONTINUE
381 C   CALL OUTRVC(RERFAL)
382 C   STOP
383 C   1 FORMAT(12A6)
384 C   1 FORMAT(12A8)
385 C   2 FORMAT(215,7F10.0)
386 C   11 FORMAT(7F10.0)
387 C   3 FORMAT(/,5X,5HIMAX=,I10,/,5X,5HKMAX=,I10,
388 C   1/,5X,5H DT=,F20.8,/,5X,5HMM =,F20.8,/,5X,5HWWI =,F20.8,
389 C   2/,5X,5HALFA=,F20.8,/,5X,6HALFAI=,F20.8,/,5X,6HALFAI=,F20.8,/,
390 C   +5X,7HREDFRE=,F18.8,/,5X,6HAMINF=,F20.8,/,5X,5HIREP=,F21.8)
391 C   4 FORMAT(1H1,5X,10A6)
392 C   12 FORMAT(8(14,F10.4))
393 C   19 FORMAT(/)
394 C   22 FORMAT(2F10.6,I5)
395 C   33 FORMAT(5X,5HISTP=,I5,5X,SBTIME=,F9.5,5X,3HDT=,F9.5)
396 2002 FORMAT(215,5E14.6)
397 3000 FORMAT(5X,3HCL=,F10.4,5X,4HCDP=,F10.4,5X,4HCDP=,F10.4,5X,3HCM=,
398 C   +F10.4)
399 3500 FORMAT(5X,5HALFA=,F10.4,5X,6HOMEGA=,F10.4,5X,2HB=,F10.4,5X,5HBDOT=
400 C   1,F10.4)
401 3700 FORMAT(5X,7HREYREF=,F20.4)
402 C5000 FORMAT(2110.6)
403 6000 FORMAT(8F14.8)
404 7000 FORMAT(3E16.9)
405 8000 FORMAT(9I13.6)
406 8001 FORMAT(3,8HCL(AVG)=,F12.7,4X,9HCDP(AVG)=,F12.7,4X,9HCDP(AVG)=,
407 C   +F12.7,4X,6HCM(AVG)=,F12.7)
408   END

```

```

LINE # SOURCE TEXT
409 SUBROUTINE AMAT1(K,IMX1,X1X,X1Z,X1T)
410 C.....
411 C
412 C SUBROUTINE AMAT1
413 C
414 C.....
415 PARAMETER (IX=180,KX=60)
416 COMMON/FLOW/Q1(IX,KX),Q2(IX,KX),Q3(IX,KX),Q4(IX,KX)
417 COMMON/PETR/DQ1(IX,KX),DQ2(IX,KX),DQ3(IX,KX),DQ4(IX,KX)
418 COMMON/AM A(4,4,IX)
419 COMMON/PAR/GAMMA,REYREF,ALFA,ALFA1,REDFRE,AMINF,ALFAI
420 DIMENSION X1T(IX,KX),X1X(IX,KX),X1Z(IX,KX)
421 REAL K0,K1,K2
422 C
423 C*** AMAT1 COMPUTES THE COEFFICIENT MATRIX DE/DQ DURING XI SWEEP
424 C
425 GM1 = GAMMA - 1.
426 DO 1000 I = 2, IMX1
427 K0 = X1T(I,K)
428 K1 = X1X(I,K)
429 K2 = X1Z(I,K)
430 U = Q2(I,K) / Q1(I,K)
431 W = Q3(I,K) / Q1(I,K)
432 EBYR = Q4(I,K) / Q1(I,K)
433 PHI2 = 0.5 * GM1 * (U * U + W * W)
434 THETA = K1 * U + K2 * W
435 A(1,1,I) = K0
436 A(1,2,I) = K1
437 A(1,3,I) = K2
438 A(1,4,I) = 0
439 A(2,1,I) = K1 * PHI2 - U * THETA
440 A(2,2,I) = K0 + THETA - K1 * (GM1 - 1.) * U
441 A(2,3,I) = K2 * U - GM1 * K1 * W
442 A(2,4,I) = K1 * GM1
443 A(3,1,I) = K2 * PHI2 - W * THETA
444 A(3,2,I) = K1 * W - K2 * GM1 * U
445 A(3,3,I) = K0 + THETA - K2 * (GM1 - 1.) * W
446 A(3,4,I) = K2 * GM1
447 A(4,1,I) = THETA * (2. * PHI2 - GAMMA * EBYR)
448 A(4,2,I) = K1 * (GAMMA * EBYR - PHI2) - GM1 * U * THETA
449 A(4,3,I) = K2 * (GAMMA * EBYR - PHI2) - GM1 * W * THETA
450 A(4,4,I) = K0 + GAMMA * THETA
451 1000 CONTINUE
452 RETURN
453 END

```

```

LINE # SOURCE TEXT
454 SUBROUTINE AMAT2(I, KM1, ZETAX, ZETAZ, ZETAT)
455 C.....
456 C*
457 C* SUBROUTINE AMAT2
458 C*
459 C.....
460 PARAMETER (IX=180, Ix=60)
461 COMMON /FLOM/Q1(IX, KX), Q2(IX, KX), Q3(IX, KX), Q4(IX, KX)
462 COMMON /PERTR/DQ1(IX, KX), DQ2(IX, KX), DQ3(IX, KX), DQ4(IX, KX)
463 COMMON /AM/A(4, 4, IX)
464 COMMON /PAR/GAMMA, REYRFF, ALFA, ALFN1, REDFFE, AMINF, ALFAI
465 DIMENSION ZETAX(IX, KX), ZETAZ(IX, KX), ZETAT(IX, KX)
466 REAL KO, K1, K2
467 C
468 C*** AMAT2 COMPUTES THE COEFFICIENT MATRIX DE/DQ DURING LTA SWEEP
469 C
470 GM1 = GAMMA - 1.
471 DO 1000 K = 2, KM1
472 K0 = ZETAT(I, K)
473 K1 = ZETAX(I, K)
474 K2 = ZETAZ(I, K)
475 U = Q2(I, K) / Q1(I, K)
476 W = Q3(I, K) / Q1(I, K)
477 EBYR = Q4(I, K) / Q1(I, K)
478 PHI2 = 0.5 * GM1 * (U * U + W * W)
479 THETA = K1 * U + K2 * W
480 A(1,1,K) = K0
481 A(1,2,K) = K1
482 A(1,3,K) = K2
483 A(1,4,K) = 0
484 A(2,1,K) = K1 * PHI2 - U * THETA
485 A(2,2,K) = K0 * THETA - K1 * (GM1-1.) * U
486 A(2,3,K) = K2 * U - GM1 * K1 * W
487 A(2,4,K) = K1 * GM1
488 A(3,1,K) = K2 * PHI2 - W * THETA
489 A(3,2,K) = K1 * W - K2 * GM1 * U
490 A(3,3,K) = K0 * THETA - K2 * (GM1-1.) * W
491 A(3,4,K) = K2 * GM1
492 A(4,1,K) = THETA * (2 * PHI2 - GAMMA * EBYR)
493 A(4,2,K) = K1 * (GAMMA * EBYR - PHI2) - GM1 * U * THETA
494 A(4,3,K) = K2 * (GAMMA * EBYR - PHI2) - GM1 * W * THETA
495 A(4,4,K) = K0 + GAMMA * THETA
496 1000 CONTINUE
497 RETURN
498 END

```

```

LINE # SOURCE TEXT
499 SUBROUTINE SLPS(ITN,ISPEC)
500 C*****
501 C*
502 C* SUBROUTINE SLPS
503 C*
504 C*****
505 PARAMETER (IX=180,KX=60)
506 COMMON/FLG/Q1(IX,KX),Q2(IX,KX),Q3(IX,KX),Q4(IX,KX)
507 COMMON/PIX/OMEGA,BDOT
508 COMMON/PERTR/DQ1(IX,KX),DQ2(IX,KX),DQ3(IX,KX),DQ4(IX,KX)
509 COMMON/AM A(4,4,IX)
510 COMMON/TRID1/DD(4,4,IX,KX)
511 COMMON/TRID2/MM(4,4,IX,KX)
512 COMMON/TRID3/EE(4,4,IX,KX)
513 COMMON/TRID4/GG(4,IX,KX)
514 COMMON/PAR/GAMMA,REYREF,ALFA,ALFAL,REDFRE,AMINF,ALFAI
515 COMMON/DGRID/DT,IMAX,KMAX,ITEL,ITEU
516 COMMON/GRID/YACOB(IX,KX)
517 COMMON/DAMP/NW,WW1,WW2X,WW2Y,WW4X,WW4Y
518 COMMON/MTRIX/ XIX(IX,KX),XIZ(IX,KX),ZETAX(IX,KX),ZETAZ(IX,KX)
519 1,XIT(IX,KX),ZETAT(IX,KX)
520 COMMON/RADIUS/ SPECX(IX,KX),SPECY(IX,KX)
521 COMMON/L2NORM/ RESDL2(10000)
522 REAL MM,DELTAT(IX,KX)
523 C
524 C*** THE SUBROUTINE SLPS DOES THE BULK OF THE WORK FOR THE ADI ALGORITHM.
525 C*** IT CALLS FLUX AND COMPUTES RIGHT HAND SIDE DURING THE TWO SWEEPS,
526 C*** ASSEMBLES THE COEFFICIENT MATRICES, ADDS IMPLICIT AND EXPLICIT
527 C*** DISSIPATION AND CALLS THE TRIDIAGONAL SOLVER TO OBTAIN THE FINAL
528 C*** SOLUTION.
529 IM1 = IMAX - 1
530 IM2 = IMAX - 2
531 KM1 = KMAX - 1
532 KM2 = KMAX - 2
533 C
534 C*** THE DISSIPATION TERMS ARE CONSTRUCTED AND STORED IN THE ARRAYS DQ1,
535 C*** DQ2,DQ3 AND DQ4.
536 C
537 CALL SPECX(ISPEC)
538 CALL DISSIP
539 C
540 C*** ON TO DQ1,DQ2,DQ3 AND DQ4.
541 C*** THE RIGHT HAND SIDE AT KNOWN TIME LEVEL IS NOW COMPUTED AND ADDED
542 CALL RESI
543 C
544 DO 8999 K = 2 , KM1
545 DO 8999 I = 2 , IM1
546 DELTAT(I,K) = .
547 IF((REDFRE.LT.0.001).AND.ITN.EQ.1) THEN
548 DO 1 K = 2 , KM1
549 DO 1 I = 2 , IM1
550 1 DELTAT(I,K) = 1.0 / ( 1. + SQRT(ABS(YACOB(I,K)) ) )
551 ENDIF
552 C
553 C*** IF VISCOUS FLOW IS COMPUTED THE VISCOUS TERMS ARE ADDED TO DQ1 ETC. HERE.
554 C
555 IF(REYREF.EQ.0.) CALL STRESS(ITN)
556 I-SWEEP.
557 DTH = DT * 0.5
558 DTW = DT * WW1
559 DO 3 K = 2 , KM1
560 CALL AMAT1(K,IMAX-1,XIX,XIZ,XIT)
561 DO 4 I1 = 1 , 4
562 DO 4 I2 = 1 , 4
563 DO 5 I = 2 , IM1
564 EE(I1,I2,I-1,K) = A(I1,I2,I+1) * DTH * DELTAT(I,K)
565 DD(I1,I2,I-1,K) = - A(I1,I2,I-1) * DTH * DELTAT(I,K)
566 5 CONTINUE
567 4 CONTINUE
568 C
569 C*** IMPLICIT DAMPING ADDED HERE.
570 C
571 DO 6 I = 2 , IM1
572 DT1 = SPECX(I,K) * DTW * DELTAT(I,K)
573 DTW1 = 2. * SPECX(I,K) * YACOB(I,K) * DTW*DELTAT(I,K)
574 DD(1,1,I-1,K) = DD(1,1,I-1,K) - DT1 * YACOB(I-1,K)
575 DD(2,2,I-1,K) = DD(2,2,I-1,K) - DT1 * YACOB(I-1,K)
576 DD(3,3,I-1,K) = DD(3,3,I-1,K) - DT1 * YACOB(I-1,K)
577 DD(4,4,I-1,K) = DD(4,4,I-1,K) - DT1 * YACOB(I-1,K)
578 EE(1,1,I-1,K) = EE(1,1,I-1,K) - DT1 * YACOB(I+1,K)
579 EE(2,2,I-1,K) = EE(2,2,I-1,K) - DT1 * YACOB(I+1,K)
580 EE(3,3,I-1,K) = EE(3,3,I-1,K) - DT1 * YACOB(I+1,K)
581 EE(4,4,I-1,K) = EE(4,4,I-1,K) - DT1 * YACOB(I+1,K)
582 MM(1,1,I-1,K) = 1. + DTW1
583 MM(2,2,I-1,K) = 1. + DTW1
584 MM(3,3,I-1,K) = 1. + DTW1
585 MM(4,4,I-1,K) = 1. + DTW1
586 6 CONTINUE
587 3 CONTINUE
588 DO 890 K = 2 , KM1
589 DO 890 I = 2 , IM1
590 GG(1,I-1,K) = DQ1(I,K) * DELTAT(I,K)
591 GG(2,I-1,K) = DQ2(I,K) * DELTAT(I,K)
592 GG(3,I-1,K) = DQ3(I,K) * DELTAT(I,K)
593 GG(4,I-1,K) = DQ4(I,K) * DELTAT(I,K)
594 890 CONTINUE
595 C
596 C PERFORM BLOCK TRIDIAGONAL MATRIX INVERSION FOR THE ENTIRE PLANE
597 C
598 CALL MATRX1(IMAX,KMAX)
599 DO 991 K = 2 , KM1
600 DO 991 I = 2 , IM1
601 DQ1(I,K) = GG(1,I-1,K)
602 DQ2(I,K) = GG(2,I-1,K)
603 DQ3(I,K) = GG(3,I-1,K)
604 DQ4(I,K) = GG(4,I-1,K)
605 991 CONTINUE
606 C
607 C K-SWEEP BEGINS HERE.
608 C
609 DO 13 I = 2 , IM1
610 CALL AMAT2(I,KMAX-1,ZETAX,ZETAZ,ZETAT)
611 DO 15 I1 = 1 , 4
612 DO 15 I2 = 1 , 4
613 DO 15 K = 2 , KM1
614 EE(I1,I2,I,K-1) = A(I1,I2,K-1)*DTH * DELTAT(I,K)
615 DD(I1,I2,I,K-1) = -A(I1,I2,K-1)*DTH * DELTAT(I,K)
616 15 CONTINUE
617 C
618 C*** SECOND ORDER DAMPING ADDED HERE.

```

```

LINE # SOURCE TEXT
619 C
620 DO 16 K = 2, KM1
621 DT1 = SPECY(I,K) * DTW * DELTAT(I,K)
622 DTW = 2. * SPECY(I,K) * YACOB(I,K) * DTW*DELTAT(I,K)
623 DD(1,1,I,K-1) = DD(1,1,I,K-1) - DT1 * YACOB(I,K-1)
624 DD(2,2,I,K-1) = DD(2,2,I,K-1) - DT1 * YACOB(I,K-1)
625 DD(3,3,I,K-1) = DD(3,3,I,K-1) - DT1 * YACOB(I,K-1)
626 DD(4,4,I,K-1) = DD(4,4,I,K-1) - DT1 * YACOB(I,K-1)
627 EE(1,1,I,K-1) = EE(1,1,I,K-1) - DT1 * YACOB(I,K+1)
628 EE(2,2,I,K-1) = EE(2,2,I,K-1) - DT1 * YACOB(I,K+1)
629 EE(3,3,I,K-1) = EE(3,3,I,K-1) - DT1 * YACOB(I,K+1)
630 EE(4,4,I,K-1) = EE(4,4,I,K-1) - DT1 * YACOB(I,K+1)
631 MM(1,1,I,K-1) = 1. + DTW1
632 MM(2,2,I,K-1) = 1. + DTW1
633 MM(3,3,I,K-1) = 1. + DTW1
634 16 MM(4,4,I,K-1) = 1. + DTW1
635 13 CONTINUE
636 DO 17 K = 2, KM1
637 DO 17 I = 2, IM1
638 GG(1,I,K-1) = DQ1(I,K)
639 GG(2,I,K-1) = DQ2(I,K)
640 GG(3,I,K-1) = DQ3(I,K)
641 GG(4,I,K-1) = DQ4(I,K)
642 17 CONTINUE
643 C
644 C PERFORM BLOCK TRIDIAGONAL MATRIX INVERSION FOR THE ENTIRE PLANE
645 C
646 CALL MATR2(IMAX,KMAX)
647 DO 18 K = 2, KM1
648 DO 18 I = 2, IM1
649 DQ1(I,K) = GG(1,I,K-1)
650 DQ2(I,K) = GG(2,I,K-1)
651 DQ3(I,K) = GG(3,I,K-1)
652 DQ4(I,K) = GG(4,I,K-1)
653 18 CONTINUE
654 C
655 C*** UPDATE FLOW VARIABLES AT INTERIOR POINTS.
656 967 CONTINUE
657 RMAX = 0.
658 RUMAX = 0.
659 RVMAX = 0.
660 EMAX = 0.
661 DO 995 K = 2, KM1
662 DO 19 I = 2, IM1
663 Q1(I,K) = Q1(I,K) + DQ1(I,K) * YACOB(I,K)
664 Q2(I,K) = Q2(I,K) + DQ2(I,K) * YACOB(I,K)
665 Q3(I,K) = Q3(I,K) + DQ3(I,K) * YACOB(I,K)
666 Q4(I,K) = Q4(I,K) + DQ4(I,K) * YACOB(I,K)
667 19 CONTINUE
668 DO 995 I = 2, IM1
669 IF (RMAX.LT.ABS(DQ1(I,K)*YACOB(I,K))) THEN
670 IR = I
671 KR = K
672 END IF
673 RMAX = AMAX1(RMAX,ABS(DQ1(I,K) * YACOB(I,K)))
674 RUMAX = AMAX1(RUMAX,ABS(DQ2(I,K) * YACOB(I,K)))
675 RVMAX = AMAX1(RVMAX,ABS(DQ3(I,K) * YACOB(I,K)))
676 EMAX = AMAX1(EMAX,ABS(DQ4(I,K) * YACOB(I,K)))
677 995 CONTINUE
678 C
679 C COMPUTE L2 NORM OF Q1, Q2, Q3, AND Q4 RESIDUAL
680 C
681 RL2 = 0.
682 RUL2 = 0.
683 RVL2 = 0.
684 EL2 = 0.
685 DO 996 K = 2, KM1
686 DO 996 I = 2, IM1
687 RL2 = RL2 + DQ1(I,K)**2
688 RUL2 = RUL2 + DQ2(I,K)**2
689 RVL2 = RVL2 + DQ3(I,K)**2
690 EL2 = EL2 + DQ4(I,K)**2
691 996 CONTINUE
692 RL2 = RL2 / ( IM2*KM2 )
693 RUL2 = RUL2 / ( IM2*KM2 )
694 RVL2 = RVL2 / ( IM2*KM2 )
695 EL2 = EL2 / ( IM2*KM2 )
696 RL2 = SQRT(RL2)
697 RUL2 = SQRT(RUL2)
698 RVL2 = SQRT(RVL2)
699 EL2 = SQRT(EL2)
700 RESDL2(ITN) = RL2
701 IF((ITN-1)/500*500.EQ.(ITN-1)) WRITE (6,3002)
702 IF(ITN/50*50.EQ.ITN) WRITE (6,3001) RMAX,RUMAX,RVMAX,EMAX,IR,KR
703 IF(ITN/50*50.EQ.ITN) WRITE (6,6004) RL2 ,RUL2 ,RVL2 ,EL2
704 RETURN
705 3002 FORMAT(/,5X,'DRMAX',11X,'DUMAX',11X,'DVMAX',11X,'DEMAX',9X,
706 'IR',3X,'KR')
707 3001 FORMAT(4(E14.8,2X),2I5)
708 6004 FORMAT(4(E14.8,2X) )
709 END

```

```
LINE # SOURCE TEXT
710 SUBROUTINE MATRIX1(IMAX,KMAX)
711 C.....
712 C
713 C SUBROUTINE MATRIX1
714 C
715 C.....
716 PARAMETER (IX=180,KX=60)
717 COMMON/TRID1/DD(4,4,IX,KX)
718 COMMON/TRID2/MM(4,4,IX,KX)
719 COMMON/TRID3/EE(4,4,IX,KX)
720 COMMON/TRID4/GG(4,4,IX,KX)
721 COMMON/CONST/A(4,IX),EH(4,4,IX),C(4,5,IX)
722 REAL MM
723 REAL L11,L21,L31,L41,L22,L32,L42,L33,L43,L44
724 2,L11,L21,L31,L41
725 C
726 THIS SUBROUTINE PERFORMS THE BLOCK TRIDIAGONAL MATRIX INVERSION FOR
727 AN ENTIRE PLANE DURING THE XI- SWEEP
728 C
729 KM1 = KMAX - 1
730 DO 1 I1 = 1, 4
731 DO 1 K = 2, KM1
732 AI = 1. / MM(1,1,1,K)
733 GG(11,1,1,K) = GG(11,1,K) * AI
734 EH(11,1,1,K) = EE(11,1,1,K) * AI
735 EH(11,2,1,K) = EE(11,2,1,K) * AI
736 EH(11,3,1,K) = EE(11,3,1,K) * AI
737 EH(11,4,1,K) = EE(11,4,1,K) * AI
738 1 CONTINUE
739 C
740 DO 1000 I = 2, IMAX - 2
741 DO 5 I1 = 1, 4
742 DO 2 K = 2, KM1
743 C(11,1,K) = GG(11,1,K) - DD(11,1,1,K) * GG(1,1-1,K)
744 1 - DD(11,2,1,K) * GG(2,1-1,K)
745 2 - DD(11,3,1,K) * GG(3,1-1,K)
746 3 - DD(11,4,1,K) * GG(4,1-1,K)
747 2 CONTINUE
748 DO 5 I2 = 1, 4
749 DO 5 K = 2, KM1
750 A(11,I2,K) = MM(11,I2,1,K) - DD(11,1,I,K) * EH(1,12,I-1,K)
751 1 - DD(11,2,I,K) * EH(2,12,I-1,K)
752 2 - DD(11,3,I,K) * EH(3,12,I-1,K)
753 3 - DD(11,4,I,K) * EH(4,12,I-1,K)
754 C(11,I2+1,K) = EE(11,I2,1,K)
755 5 CONTINUE
756 DO 3 K = 2, KM1
757 L11 = A(1,1,K)
758 L11 = 1. / L11
759 U12 = A(1,2,K) * L11
760 U13 = A(1,3,K) * L11
761 U14 = A(1,4,K) * L11
762 L21 = A(2,1,K)
763 L31 = A(3,1,K)
764 L41 = A(4,1,K)
765 L22 = A(2,2,K) - L21 * U12
766 L21 = 1. / L22
767 U23 = (A(2,3,K) - L21 * U13) * L21
768 U24 = (A(2,4,K) - L21 * U14) * L21
769 L32 = A(3,2,K) - L31 * U12
770 L42 = A(4,2,K) - L41 * U12
771 L33 = A(3,3,K) - L31 * U13 - L32 * U23
772 L31 = 1. / L33
773 U34 = (A(3,4,K) - L31 * U14 - L32 * U24) * L31
774 L43 = A(4,3,K) - L41 * U13 - L42 * U23
775 L44 = A(4,4,K) - L41 * U14 - L42 * U24 - L43 * U34
776 L41 = 1. / L44
777 C(1,1,K) = C(1,1,K) * L11
778 C(2,1,K) = (C(2,1,K) - L21 * C(1,1,K)) * L21
779 C(3,1,K) = (C(3,1,K) - L31 * C(1,1,K)
780 1 - L32 * C(2,1,K)) * L31
781 C(4,1,K) = (C(4,1,K) - L41 * C(1,1,K) - L42 * C(2,1,K)
782 1 - L43 * C(3,1,K)) * L41
783 C(1,2,K) = C(1,2,K) * L11
784 C(2,2,K) = (C(2,2,K) - L21 * C(1,2,K)) * L21
785 C(3,2,K) = (C(3,2,K) - L31 * C(1,2,K)
786 1 - L32 * C(2,2,K)) * L31
787 C(4,2,K) = (C(4,2,K) - L41 * C(1,2,K) - L42 * C(2,2,K)
788 1 - L43 * C(3,2,K)) * L41
789 C(1,3,K) = C(1,3,K) * L11
790 C(2,3,K) = (C(2,3,K) - L21 * C(1,3,K)) * L21
791 C(3,3,K) = (C(3,3,K) - L31 * C(1,3,K)
792 1 - L32 * C(2,3,K)) * L31
793 C(4,3,K) = (C(4,3,K) - L41 * C(1,3,K) - L42 * C(2,3,K)
794 1 - L43 * C(3,3,K)) * L41
795 C(1,4,K) = C(1,4,K) * L11
796 C(2,4,K) = (C(2,4,K) - L21 * C(1,4,K)) * L21
797 C(3,4,K) = (C(3,4,K) - L31 * C(1,4,K)
798 1 - L32 * C(2,4,K)) * L31
799 C(4,4,K) = (C(4,4,K) - L41 * C(1,4,K) - L42 * C(2,4,K)
800 1 - L43 * C(3,4,K)) * L41
801 C(1,5,K) = C(1,5,K) * L11
802 C(2,5,K) = (C(2,5,K) - L21 * C(1,5,K)) * L21
803 C(3,5,K) = (C(3,5,K) - L31 * C(1,5,K)
804 1 - L32 * C(2,5,K)) * L31
805 C(4,5,K) = (C(4,5,K) - L41 * C(1,5,K) - L42 * C(2,5,K)
806 1 - L43 * C(3,5,K)) * L41
807 C(3,1,K) = C(3,1,K) - U34 * C(4,1,K)
808 C(2,1,K) = C(2,1,K) - U24 * C(4,1,K)
809 1 - U23 * C(3,1,K)
810 C(1,1,K) = C(1,1,K) - U14 * C(4,1,K)
811 1 - U13 * C(3,1,K) - U12 * C(2,1,K)
812 C(3,2,K) = C(3,2,K) - U34 * C(4,2,K)
813 C(2,2,K) = C(2,2,K) - U24 * C(4,2,K)
814 1 - U23 * C(3,2,K)
815 C(1,2,K) = C(1,2,K) - U14 * C(4,2,K)
816 1 - U13 * C(3,2,K) - U12 * C(2,2,K)
817 C(3,3,K) = C(3,3,K) - U34 * C(4,3,K)
818 C(2,3,K) = C(2,3,K) - U24 * C(4,3,K)
819 1 - U23 * C(3,3,K)
820 C(1,3,K) = C(1,3,K) - U14 * C(4,3,K)
821 1 - U13 * C(3,3,K) - U12 * C(2,3,K)
822 C(3,4,K) = C(3,4,K) - U34 * C(4,4,K)
823 C(2,4,K) = C(2,4,K) - U24 * C(4,4,K)
824 1 - U23 * C(3,4,K)
825 C(1,4,K) = C(1,4,K) - U14 * C(4,4,K)
826 1 - U13 * C(3,4,K) - U12 * C(2,4,K)
827 C(3,5,K) = C(3,5,K) - U34 * C(4,5,K)
828 C(2,5,K) = C(2,5,K) - U24 * C(4,5,K)
829 1 - U23 * C(3,5,K)
```

```

LINE # SOURCE TEXT
830 C(1,5,K) = C(1,5,K) - U14 * C(4,5,K)
831 1 - U13 * C(3,5,K) - U12 * C(2,5,K)
832 3 CONTINUE
833 C
834 DO 6 I1 = 1, 4
835 DO 9 K = 2, KM1
836 9 GG(I1,I,K) = C(I1,I,K)
837 DO 6 I2 = 1, 4
838 DO 6 K = 2, KM1
839 HH(I1,I2,I,K) = C(I1,I2+1,K)
840 6 CONTINUE
841 1000 CONTINUE
842 C C C
843 BACKWARD SUBSTITUTION
844 DO 7 I = IMAX - 3, 1, - 1
845 DO 7 I1 = 1, 4
846 DO 7 K = 2, KM1
847 GG(I1,I,K) = GG(I1,I,K) - HH(I1,1,I,K) * GG(1,I+1,K)
848 1 - HH(I1,2,I,K) * GG(2,I+1,K)
849 2 - HH(I1,3,I,K) * GG(3,I+1,K)
850 3 - HH(I1,4,I,K) * GG(4,I+1,K)
851 7 CONTINUE
852 RETURN
853 END
854

```

LINE #	SOURCE TEXT
855	SUBROUTINE MATRI2(IMAX,KMAX)
856	C*****
857	C*
858	C* SUBROUTINE MATRI2
859	C*
860	C*****
861	PARAMETER (IX=180,KX=60)
862	COMMON/TRID1/DD(4,4,IX,KX)
863	COMMON/TRID2/MM(4,4,IX,KX)
864	COMMON/TRID3/EE(4,4,IX,KX)
865	COMMON/TRID4/GG(4,4,IX,KX)
866	COMMON/SCRAT/A(4,4,IX),HH(4,4,IX,KX),C(4,5,IX)
867	REAL MM
868	REAL L11,L21,L31,L41,L22,L32,L42,L33,L43,L44
869	2,L11,L21,L31,L41
870	C
871	C THIS SUBROUTINE PERFORMS THE BLOCK TRIDIAGONAL MATRIX INVERSION FOR
872	C AN ENTIRE J=CONSTANT PLANE DURING THE ZETA- SWEEP
873	C
874	IM1 = KMAX - 1
875	IM1 = IMAX - 1
876	DO 1 I1 = 1, 4
877	DO 1 I = 2, IM1
878	AI = 1. / MM(1,1,I,1)
879	GG(I1,I,1) = GG(I1,I,1) * AI
880	HH(I1,1,1,1) = EE(I1,1,1,1) * AI
881	HH(I1,2,1,1) = EE(I1,2,1,1) * AI
882	HH(I1,3,1,1) = EE(I1,3,1,1) * AI
883	HH(I1,4,1,1) = EE(I1,4,1,1) * AI
884	1 CONTINUE
885	C
886	DO 1000 F = 2, KMAX - 2
887	DO 5 I1 = 1, 4
888	DO 2 I = 2, IM1
889	C(I1,1,I) = GG(I1,I,K) - DD(I1,1,I,K) * GG(1,I,K-1)
890	1 - DD(I1,2,I,K) * GG(2,I,K-1)
891	2 - DD(I1,3,I,K) * GG(3,I,K-1)
892	3 - DD(I1,4,I,K) * GG(4,I,K-1)
893	2 CONTINUE
894	DO 5 I2 = 1, 4
895	DO 5 I = 2, IM1
896	A(I1,I2,I) = MM(I1,I2,I,K) - DD(I1,1,I,K) * HH(1,I2,I,K-1)
897	1 - DD(I1,2,I,K) * HH(2,I2,I,K-1)
898	2 - DD(I1,3,I,K) * HH(3,I2,I,K-1)
899	3 - DD(I1,4,I,K) * HH(4,I2,I,K-1)
900	C(I1,I2+1,I) = EE(I1,I2,I,K)
901	5 CONTINUE
902	DO 3 I = 2, IM1
903	L11 = A(1,1,I)
904	L11 = 1. / L11
905	U12 = A(1,2,I) * L11
906	U13 = A(1,3,I) * L11
907	U14 = A(1,4,I) * L11
908	L21 = A(2,1,I)
909	L31 = A(3,1,I)
910	L41 = A(4,1,I)
911	L22 = A(2,2,I) - L21 * U12
912	L21 = 1. / L22
913	U23 = (A(2,3,I) - L21 * U13) * L21
914	U24 = (A(2,4,I) - L21 * U14) * L21
915	L32 = A(3,2,I) - L31 * U12
916	L42 = A(4,2,I) - L41 * U12
917	L33 = A(3,3,I) - L31 * U13 - L32 * U23
918	L31 = 1. / L33
919	U34 = (A(3,4,I) - L31 * U14 - L32 * U24) * L31
920	L43 = A(4,3,I) - L41 * U13 - L42 * U23
921	L44 = A(4,4,I) - L41 * U14 - L42 * U24 - L43 * U34
922	L41 = 1. / L44
923	C(1,1,I) = C(1,1,I) * L11
924	C(2,1,I) = (C(2,1,I) - L21 * C(1,1,I)) * L21
925	C(3,1,I) = (C(3,1,I) - L31 * C(1,1,I))
926	1 - L32 * C(2,1,I)) * L31
927	C(4,1,I) = (C(4,1,I) - L41 * C(1,1,I) - L42 * C(2,1,I)
928	1 - L43 * C(3,1,I)) * L41
929	C(1,2,I) = C(1,2,I) * L11
930	C(2,2,I) = (C(2,2,I) - L21 * C(1,2,I)) * L21
931	C(3,2,I) = (C(3,2,I) - L31 * C(1,2,I))
932	1 - L32 * C(2,2,I)) * L31
933	C(4,2,I) = (C(4,2,I) - L41 * C(1,2,I) - L42 * C(2,2,I)
934	1 - L43 * C(3,2,I)) * L41
935	C(1,3,I) = C(1,3,I) * L11
936	C(2,3,I) = (C(2,3,I) - L21 * C(1,3,I)) * L21
937	C(3,3,I) = (C(3,3,I) - L31 * C(1,3,I))
938	1 - L32 * C(2,3,I)) * L31
939	C(4,3,I) = (C(4,3,I) - L41 * C(1,3,I) - L42 * C(2,3,I)
940	1 - L43 * C(3,3,I)) * L41
941	C(1,4,I) = C(1,4,I) * L11
942	C(2,4,I) = (C(2,4,I) - L21 * C(1,4,I)) * L21
943	C(3,4,I) = (C(3,4,I) - L31 * C(1,4,I))
944	1 - L32 * C(2,4,I)) * L31
945	C(4,4,I) = (C(4,4,I) - L41 * C(1,4,I) - L42 * C(2,4,I)
946	1 - L43 * C(3,4,I)) * L41
947	C(1,5,I) = C(1,5,I) * L11
948	C(2,5,I) = (C(2,5,I) - L21 * C(1,5,I)) * L21
949	C(3,5,I) = (C(3,5,I) - L31 * C(1,5,I))
950	1 - L32 * C(2,5,I)) * L31
951	C(4,5,I) = (C(4,5,I) - L41 * C(1,5,I) - L42 * C(2,5,I)
952	1 - L43 * C(3,5,I)) * L41
953	C(3,1,I) = C(3,1,I) - U34 * C(4,1,I)
954	C(2,1,I) = C(2,1,I) - U24 * C(4,1,I)
955	1 - U23 * C(3,1,I)
956	C(1,1,I) = C(1,1,I) - U14 * C(4,1,I)
957	1 - U13 * C(3,1,I) - U12 * C(2,1,I)
958	C(3,2,I) = C(3,2,I) - U34 * C(4,2,I)
959	C(2,2,I) = C(2,2,I) - U24 * C(4,2,I)
960	1 - U23 * C(3,2,I)
961	C(1,2,I) = C(1,2,I) - U14 * C(4,2,I)
962	1 - U13 * C(3,2,I) - U12 * C(2,2,I)
963	C(3,3,I) = C(3,3,I) - U34 * C(4,3,I)
964	C(2,3,I) = C(2,3,I) - U24 * C(4,3,I)
965	1 - U23 * C(3,3,I)
966	C(1,3,I) = C(1,3,I) - U14 * C(4,3,I)
967	1 - U13 * C(3,3,I) - U12 * C(2,3,I)
968	C(3,4,I) = C(3,4,I) - U34 * C(4,4,I)
969	C(2,4,I) = C(2,4,I) - U24 * C(4,4,I)
970	1 - U23 * C(3,4,I)
971	C(1,4,I) = C(1,4,I) - U14 * C(4,4,I)
972	1 - U13 * C(3,4,I) - U12 * C(2,4,I)
973	C(3,5,I) = C(3,5,I) - U34 * C(4,5,I)
974	C(2,5,I) = C(2,5,I) - U24 * C(4,5,I)

LINE #	SOURCE TEXT
975	1 - U23 = C(3,5,I)
976	C(1,5,I) = C(1,5,I) - U14 * C(4,5,I)
977	1 - U13 = C(3,5,I) - U12 * C(2,5,I)
978	3 CONTINUE
979	C
980	DO 6 I1 = 1, 4
981	DO 9 I = 2, IM1
982	9 GG(11,I,K) = C(11,1,I)
983	DO 6 I2 = 1, 4
984	DO 6 I = 2, IM1
985	HH(11,I2,I,*) = C(11,I2+1,I)
986	6 CONTINUE
987	1000 CONTINUE
988	C
989	BACKWARD SUBSTITUTION
990	C
991	DO 7 K = KMAX - 3, 1, - 1
992	DO 7 I1 = 1, 4
993	DO 7 I = 2, IM1
994	GG(11,1,K) = GG(11,I,K) - HH(11,1,I,K) * GG(1,I,K+1)
995	1 - HH(11,2,I,K) * GG(2,I,K+1)
996	2 - HH(11,3,I,K) * GG(3,I,K+1)
997	3 - HH(11,4,I,K) * GG(4,I,K+1)
998	7 CONTINUE
999	RETURN
1000	END

```

LINE #          SOURCE TEXT
1001  SUBROUTINE METRIC
1002  C.....
1003  C*
1004  SUBROUTINE METRIC
1005  C*
1006  C.....
1007  PARAMETER (IX=180,KX=60)
1008  COMMON/FIX/OMEGA,HDOT
1009  COMMON/DGRID/DT,IMAX,KMAX,ITEL,ITEU
1010  COMMON/GRID1/X(IX,KX),Z(IX,KX)
1011  COMMON/GRID/YACOB(IX,KX)
1012  COMMON/MTRIX/XIX(IX,KX),XIZ(IX,KX),ZETA1(IX,KX),ZETA2(IX,KX),
1013  XIT(IX,KX),ZETAT(IX,KX)
1014  C
1015  C*** THE SUBROUTINE METRIC COMPUTES THE METRICS IN ALL THE TWO DIRECTIONS AND
1016  C THE UNSTEADY COEFFICIENTS ETAT ETC.
1017  C
1018  DO 1000 K = 1 , KMAX
1019  DO 1000 I = 1 , IMAX
1020  XTAU = OMEGA * Z(I,K)
1021  YTAU = OMEGA * (-X(I,K)) - HDOT
1022  C*** PRESENT SET UP IS FOR FLOW PAST AN AIRFOIL.
1023  C
1024  IF(I.EQ.1.OR.I.EQ.IMAX) GO TO 10
1025  XXI = .5 * (X(I+1,K)-X(I-1,K))
1026  XZI = .5 * (Z(I+1,K)-Z(I-1,K))
1027  GO TO 15
1028  10 IF(I.EQ.IMAX) GO TO 16
1029  XXI = 1.0 * (X(2,K) - X(1,K))
1030  XZI = 1.0 * (Z(2,K) - Z(1,K))
1031  GO TO 15
1032  16 XXI = 1.0 * (X(IMAX,K) - X(IMAX-1,K))
1033  XZI = 1.0 * (Z(IMAX,K) - Z(IMAX-1,K))
1034  15 CONTINUE
1035  IF(K.EQ.1.OR.K.EQ.KMAX) GO TO 17
1036  XZET = .5 * (X(I,K+1)-X(I,K-1))
1037  ZZET = .5 * (Z(I,K+1)-Z(I,K-1))
1038  GO TO 20
1039  17 IF(K.EQ.KMAX) GO TO 18
1040  XZET = 2. * X(I,2)-1.5 * X(I,1) - .5 * X(I,3)
1041  ZZET = 2. * Z(I,2) - 1.5 * Z(I,1) - .5 * Z(I,3)
1042  GO TO 20
1043  18 XZET = 1.5 * X(I,KMAX)-2. * X(I,KMAX-1)+.5*X(I,KMAX-2)
1044  ZZET = 1.5 * Z(I,KMAX)-2. * Z(I,KMAX-1)+.5*Z(I,KMAX-2)
1045  20 CONTINUE
1046  YACOBI = XXI * ZZET - XZET * XZI
1047  YACOB(I,K) = 1. / YACOBI
1048  XIX(I,K) = ZZET * YACOB(I,K)
1049  XIZ(I,K) = -XZET * YACOB(I,K)
1050  XTAU = OMEGA * Z(I,K)
1051  YTAU = - OMEGA * X(I,K) - HDOT
1052  XIT(I,K) = - XIX(I,K) * XTAU - XIZ(I,K) * YTAU
1053  ZETA1(I,K) = -XZI * YACOB(I,K)
1054  ZETA2(I,K) = XXI * YACOB(I,K)
1055  ZETAT(I,K) = - ZETA1(I,K) * XTAU - ZETA2(I,K) * YTAU
1056  1000 CONTINUE
1057  RETURN
1058  END

```

Program

```

LINE # SOURCE TEXT
1059 SUBROUTINE DISSIP
1060 C*****
1061 C*
1062 C* SUBROUTINE DISSIP
1063 C*
1064 C*****
1065 PARAMETER (IX=180,KX=60)
1066 COMMON/FLOW/Q1(IX,KX),Q2(IX,KX),Q3(IX,KX),Q4(IX,KX)
1067 COMMON/MTRIX/X1X(IX,KX),X12(IX,KX),ZETAX(IX,KX),ZETAZ(IX,KX),
1068 L1X(IX,KX),ZETAT(IX,KX)
1069 COMMON/PERTR/DQ1(IX,KX),DQ2(IX,KX),DQ3(IX,KX),DQ4(IX,KX)
1070 COMMON/DGRID/DT,IMAX,KMAX,ITEL,ITEU
1071 COMMON/PAR/GAMMA,REYREF,ALFA,ALFA1,REDFRE,AMINF,ALFAI
1072 COMMON/GRID/YACOB(IX,KX)
1073 COMMON/DAMP/WW,WM1,WN2X,WN2Y,WM4X,WM4Y
1074 COMMON/RADIUS/ SPECX(IX,KX),SPECY(IX,KX)
1075 COMMON/SPEED/ U(IX,KX),V(IX,KX),AA(IX,KX)
1076 DIMENSION P(IX),EPS(IX),DIS1(IX,4),DIS2(IX,4),DIS3(IX,4)
1077 DIMENSION QQ(4)
1078 C
1079 C THIS SUBROUTINE ADDS THE FOURTH ORDER DISSIPATION TERMS TO THE
1080 C RIGHT HAND SIDE
1081 C
1082 C
1083 IM1 = IMAX - 1
1084 IM2 = IMAX - 2
1085 KM1 = KMAX - 1
1086 KM2 = KMAX - 2
1087 WDT = WM*DT
1088 GM1 = GAMMA - 1.
1089 DO 20 K = 2 , KM1
1090 C
1091 C COMPUTE SWITCHING FUNCITON BASED ON SECOND DERIVATIVE OF PRESSURE
1092 C
1093 DO 1 I = 1 , IMAX
1094 1 P(I) = GM1 * (Q4(I,K) - 0.5*Q1(I,K)*(U(I,K)**2 + V(I,K)**2))
1095 DO 3 I = 2 , IM1
1096 PS1 = P(I+1) - 2.*P(I) + P(I-1)
1097 PS2 = P(I+1) + 2.*P(I) + P(I-1)
1098 EPS(I) = ABS(PS1/PS2)
1099 3 CONTINUE
1100 EPS(1) = EPS(2)
1101 EPS(IMAX) = EPS(IM1)
1102 C
1103 C SMOOTH OUT PRESSURE COEFFICIENT
1104 C
1105 DO 4 I = 2 , IM1
1106 P(I) = AMAX1( EPS(I+1),EPS(I),EPS(I-1) )
1107 4 CONTINUE
1108 P(1) = P(2)
1109 P(IMAX) = P(IM1)
1110 C
1111 DO 10 I = 2 , IM1
1112 C2 = WN2X * P(I)
1113 C4 = WM4X - AMIN1(WM4X,C2)
1114 C22 = C2*WDT * ( SPECX(I,K) + SPECX(I+1,K) )
1115 C44 = -C4*WDT* SPECX(I,K)
1116 HPM = Q4(I-1,K) + P(I-1)
1117 HP = Q4(I,K) + P(I)
1118 HPP = Q4(I+1,K) + P(I+1)
1119 DIS1(I,1) = C22 * ( Q1(I+1,K) - Q1(I,K) )
1120 DIS1(I,2) = C22 * ( Q2(I+1,K) - Q2(I,K) )
1121 DIS1(I,3) = C22 * ( Q3(I+1,K) - Q3(I,K) )
1122 DIS1(I,4) = C22 * ( Q4(I+1,K) - Q4(I,K) )
1123 10 CONTINUE
1124 DIS2(I,1) = C44 * ( Q1(I+1,K) - 2.*Q1(I,K) + Q1(I-1,K) )
1125 DIS2(I,2) = C44 * ( Q2(I+1,K) - 2.*Q2(I,K) + Q2(I-1,K) )
1126 DIS2(I,3) = C44 * ( Q3(I+1,K) - 2.*Q3(I,K) + Q3(I-1,K) )
1127 DIS2(I,4) = C44 * ( Q4(I+1,K) - 2.*Q4(I,K) + Q4(I-1,K) )
1128 DIS2(I,4) = C44 * ( HPP - 2.*HP + HPM )
1129 C
1130 C B. C. TREATMENT
1131 QQ(1) = Q1(2,K) - Q1(1,K)
1132 QQ(2) = Q2(2,K) - Q2(1,K)
1133 QQ(3) = Q3(2,K) - Q3(1,K)
1134 QQ(4) = Q4(2,K) - Q4(1,K)
1135 C
1136 DO 15 N4 = 1 , 4
1137 C2 = WN2X*P(1)
1138 C22 = C2 * WDT * ( SPECX(1,K) + SPECX(2,K) )
1139 DIS1(1,N4) = C22 * QQ(N4)
1140 DIS2(1,N4) = 0.
1141 15 DIS2(IMAX,N4) = 0.
1142 C
1143 DO 16 I = 1 , IM1
1144 DIS3(I,1) = DIS1(I,1) + DIS2(I+1,1) - DIS2(I,1)
1145 DIS3(I,2) = DIS1(I,2) + DIS2(I+1,2) - DIS2(I,2)
1146 DIS3(I,3) = DIS1(I,3) + DIS2(I+1,3) - DIS2(I,3)
1147 DIS3(I,4) = DIS1(I,4) + DIS2(I+1,4) - DIS2(I,4)
1148 16 CONTINUE
1149 C
1150 C FILL IN DISSIPATION TERMS
1151 C
1152 DO 18 I = 2 , IM1
1153 DQ1(I,K) = DIS3(I,1) - DIS3(I-1,1)
1154 DQ2(I,K) = DIS3(I,2) - DIS3(I-1,2)
1155 DQ3(I,K) = DIS3(I,3) - DIS3(I-1,3)
1156 DQ4(I,K) = DIS3(I,4) - DIS3(I-1,4)
1157 18 CONTINUE
1158 20 CONTINUE
1159 C
1160 C K DIRECTION
1161 C
1162 DO 100 I = 2 , IM1
1163 C
1164 C COMPUTE SWITCHING FUNCTION BASED ON SECOND DERIVATIVE OF PRESSURE
1165 C
1166 DO 31 K = 2 , KMAX
1167 31 P(K) = GM1 * (Q4(I,K) - 0.5*Q1(I,K) * (U(I,K)**2 + V(I,K)**2))
1168 P(1) = ( 4.*P(2) - P(3) ) / 3.
1169 DO 33 K = 2 , KM1
1170 PS1 = P(K-1) - 2.*P(K) + P(K-1)
1171 PS2 = P(K-1) + 2.*P(K) + P(K-1)
1172 EPS(K) = ABS(PS1/PS2)
1173 33 CONTINUE
1174 EPS(1) = EPS(2)
1175 EPS(KMAX) = EPS(KM1)
1176 C
1177 C SMOOTH OUT PRESSURE COEFFICIENT
1178 C

```

LINE # SOURCE TEXT

```

1179 DO 34 K = 2 , KM1
1180 P(K) = AMAX1( EPS(K+1),EPS(K),EPS(K-1) )
1181 34 CONTINUE
1182 P(1) = P(2)
1183 P(KMAX) = P(KM1)
1184 C
1185 DO 52 K = 2 , KM1
1186 C2 = WN2Y * P(K)
1187 C4 = WN4Y - AMIN1(WN4Y,C2)
1188 C22 = C2 * WDT * ( SPECY(I,K) + SPECY(I,K+1) )
1189 C44 = -C4*WDT* SPECY(I,K)
1190 C HPM = Q4(I,K-1) + P(K-1)
1191 C HP = Q4(I,K) + P(K)
1192 C HPP = Q4(I,K+1) + P(K+1)
1193 DIS1(K,1) = C22 * ( Q1(I,K+1) - Q1(I,K) )
1194 DIS1(K,2) = C22 * ( Q2(I,K+1) - Q2(I,K) )
1195 DIS1(K,3) = C22 * ( Q3(I,K+1) - Q3(I,K) )
1196 DIS1(K,4) = C22 * ( Q4(I,K+1) - Q4(I,K) )
1197 C DIS1(K,4) = C22 * ( HPP - HP )
1198 DIS2(K,1) = C44 * ( Q1(I,K+1) - 2.*Q1(I,K) + Q1(I,K-1) )
1199 DIS2(K,2) = C44 * ( Q2(I,K+1) - 2.*Q2(I,K) + Q2(I,K-1) )
1200 DIS2(K,3) = C44 * ( Q3(I,K+1) - 2.*Q3(I,K) + Q3(I,K-1) )
1201 DIS2(K,4) = C44 * ( Q4(I,K+1) - 2.*Q4(I,K) + Q4(I,K-1) )
1202 C DIS2(K,4) = C44 * ( HPP - 2.*HP + HPM )
1203 52 CONTINUE
1204 C B.C. TREATMENT
1205 QQ(1) = Q1(I,2) - Q1(I,1)
1206 QQ(2) = Q2(I,2) - Q2(I,1)
1207 QQ(3) = Q3(I,2) - Q3(I,1)
1208 QQ(4) = Q4(I,2) - Q4(I,1)
1209 C QQ(4) = Q4(I,2) + P(2) - Q4(I,1) - P(1)
1210 DO 59 N4 = 1 , 4
1211 C2 = WN2Y * P(1)
1212 C22 = C2 * WDT * ( SPECY(I,1) + SPECY(I,2) )
1213 DIS1(I,N4) = C22 * QQ(N4)
1214 DIS2(I,N4) = 0.
1215 59 DIS2(KMAX,N4) = 0.
1216 C
1217 DO 60 K = 1 , KM1
1218 DIS3(K,1) = DIS1(K,1) + DIS2(K+1,1) - DIS2(K,1)
1219 DIS3(K,2) = DIS1(K,2) + DIS2(K+1,2) - DIS2(K,2)
1220 DIS3(K,3) = DIS1(K,3) + DIS2(K+1,3) - DIS2(K,3)
1221 DIS3(K,4) = DIS1(K,4) + DIS2(K+1,4) - DIS2(K,4)
1222 60 CONTINUE
1223 C
1224 C FILL IN DISSIPATION TERMS
1225 C
1226 DO 65 K = 2 , KM1
1227 DQ1(I,K) = DQ1(I,K) + DIS3(K,1) - DIS3(K-1,1)
1228 DQ2(I,K) = DQ2(I,K) + DIS3(K,2) - DIS3(K-1,2)
1229 DQ3(I,K) = DQ3(I,K) + DIS3(K,3) - DIS3(K-1,3)
1230 DQ4(I,K) = DQ4(I,K) + DIS3(K,4) - DIS3(K-1,4)
1231 65 CONTINUE
1232 100 CONTINUE
1233 RETURN
1234 END

```

Program	SOURCE TEXT
---------	-------------

```

1235 SUBROUTINE SPECR(ISPEC)
1236 C*****
1237 C*
1238 C* SUBROUTINE SPECR
1239 C*
1240 C*****
1241 PARAMETER (IX=180,KX=60)
1242 COMMON/PAR/GAMMA,REYREF,ALFA,ALFA1,REDFRE,AMINF,ALFAI
1243 COMMON/DGR:ID,DT,IMAX,KMAX,ITEL,ITEU
1244 COMMON/MTRIX/ XIX(IX,KX),XIZ(IX,KX),ZETAX(IX,KX),ZETAZ(IX,KX)
1245 1 ,XIT(IX,KX),ZETAT(IX,KX)
1246 COMMON/FLOW/Q1(IX,KX),Q2(IX,KX),Q3(IX,KX),Q4(IX,KX)
1247 COMMON/RADIUS/ SPECX(IX,KX),SPECY(IX,KX)
1248 COMMON/SPEED/ U(IX,KX),V(IX,KX),AA(IX,KX)
1249 COMMON/GRID/YACOB(IX,KX)
1250 C
1251 C THIS SUBROUTINE COMPUTE THE SPECTRAL RADIUS FOR SCALING THE
1252 C EXPLICIT AND IMPLICIT DISSIPATIONS
1253 C
1254 IMI = IMAX - 1
1255 IKI = KMAX - 1
1256 GAM = GAMMA * ( GAMMA - 1. )
1257 DO 5 K = 1 , KMAX
1258 DO 5 I = 1 , IMAX
1259 U(I,K) = Q2(I,K) / Q1(I,K)
1260 V(I,K) = Q3(I,K) / Q1(I,K)
1261 AA(I,K) = GAM * ( Q4(I,K)/Q1(I,K) - 0.5*(U(I,K)**2 + V(I,K)**2) )
1262 IF(AA(I,K).LT.0.) PRINT*, 'NEGATIVE A*A = ',AA(I,K), ' AT ',I,K
1263 5 CONTINUE
1264 C
1265 C COMPUTE IMPLICIT DISSIPATION SCALING
1266 C SPECX = SPECTRAL RADIUS FOR XI-DIRECTION
1267 C SPECY = SPECTRAL RADIUS FOR ZETA-DIRECTION
1268 C
1269 IF(ISPEC.EQ.1) THEN
1270 DO 20 K = 1 , KMAX
1271 DO 20 I = 1 , IMAX
1272 SPECX(I,K) = 1. / YACOB(I,K)
1273 SPECY(I,K) = 1. / YACOB(I,K)
1274 20 CONTINUE
1275 ELSEIF(ISPEC.EQ.2) THEN
1276 DO 30 K = 1 , KMAX
1277 DO 30 I = 1 , IMAX
1278 UCON = U(I,K)*XIX(I,K) + V(I,K)*XIZ(I,K) + XIT(I,K)
1279 VCON = U(I,K)*ZETAX(I,K) + V(I,K)*ZETAZ(I,K) + ZETAT(I,K)
1280 SPECX(I,K) = ABS(UCON) / YACOB(I,K)
1281 SPECY(I,K) = ABS(VCON) / YACOB(I,K)
1282 30 CONTINUE
1283 ELSEIF(ISPEC.EQ.3) THEN
1284 DO 40 K = 1 , KMAX
1285 DO 40 I = 1 , IMAX
1286 UCON = U(I,K)*XIX(I,K) + V(I,K)*XIZ(I,K) + XIT(I,K)
1287 VCON = U(I,K)*ZETAX(I,K) + V(I,K)*ZETAZ(I,K) + ZETAT(I,K)
1288 XI2 = XIX(I,K)**2 + XIZ(I,K)**2
1289 ZETA2 = ZETAX(I,K)**2 + ZETAZ(I,K)**2
1290 SPECX(I,K) = (ABS(UCON) + SQRT(AA(I,K)*XI2) ) / YACOB(I,K)
1291 SPECY(I,K) = (ABS(VCON) + SQRT(AA(I,K)*ZETA2) ) / YACOB(I,K)
1292 40 CONTINUE
1293 ENDIF
1294 RETURN
1295 END
1296

```

```

LINE # SOURCE TEXT
1297 SUBROUTINE EXPEC(CL)
1298 C*****
1299 C*
1300 C* SUBROUTINE EXPEC
1301 C*
1302 C*****
1303 PARAMETER (IX=180,KX=60)
1304 COMMON/SURF/PSUR(IX)
1305 COMMON/GRID1/X(IX,KX),Z(IX,KX)
1306 COMMON/PAR/GAMMA,REYREF,ALFA,ALFAL,REDFRE,AMINF
1307 COMMON/DGRID/DT,IMAX,KMAX,ITEL,ITEU
1308 COMMON/GRID/YACOB(IX,KX)
1309 COMMON/DAMP/WW,WW1,WW2X,WW2Y,WW4X,WW4Y
1310 COMMON/MTRIX/XIX(IX,KX),XIZ(IX,KX),ZETAX(IX,KX),ZETAZ(IX,KX),
1311 IXIT(IX,KX),ZETAT(IX,KX)
1312 COMMON/FLOW/Q1(IX,KX),Q2(IX,KX),Q3(IX,KX),Q4(IX,KX)
1313 COMMON/SPEED/ U(IX,KX),V(IX,KX),AA(IX,KX)
1314 COMMON/INITI/UINF,VINF
1315 COMMON/BC/LOG/CIRCOR
1316 COMMON/LOGIC/RSTRT,PITCH,RAMP
1317 LOGICAL RSTRT,PITCH,RAMP
1318 LOGICAL CIRCOR
1319 DIMENSION CL(4)
1320 DIMENSION A(2,2),RHS(2)
1321 DATA PI/3.1415927/
1322 DATA CHORD/1./
1323 C
1324 GAMI = 1. / GAMMA
1325 GAMM = GAMMA - 1.
1326 GAMMI = 1. / GAMM
1327 C
1328 INVISCID AND VISCOUS B.C. ON SOLID WALL
1329 C
1330 DO 1 I= ITEL , ITEU
1331 K = 3
1332 C1(1) = XIT(I,K)
1333 C1(2) = XIX(I,K)
1334 C1(3) = XIZ(I,K)
1335 UCON3 = (Q2(I,K)*C1(2)+Q3(I,K)*C1(3))
1336 1/Q1(I,K)
1337 K = 2
1338 C1(1) = XIT(I,K)
1339 C1(2) = XIX(I,K)
1340 C1(3) = XIZ(I,K)
1341 UCON2 = (Q2(I,K)*C1(2)+Q3(I,K)*C1(3))
1342 1/Q1(I,K)
1343 RHS(1) = 2. * UCON2 - UCON3 - XIT(I,1)
1344 FOR VISCOUS FLOWS SET UCON TO ZERO ALSO
1345 IF(REYREF GT.0.) RHS(1) = - XIT(I,1)
1346 A(1,1) = XIX(I,1)
1347 A(1,2) = XIZ(I,1)
1348 A(2,1) = ZETAX(I,1)
1349 A(2,2) = ZETAZ(I,1)
1350 RHS(2) = - ZETAT(I,1)
1351 TEMP1 = A(1,1)
1352 TEMP2 = A(1,2)
1353 TEMP3 = A(2,1)
1354 TEMP4 = A(2,2)
1355 DEN = 1. / (TEMP1 * TEMP4 - TEMP2 * TEMP3)
1356 A(1,1) = A(2,2) * DEN
1357 A(1,2) = - TEMP2 * DEN
1358 A(2,1) = - TEMP3 * DEN
1359 A(2,2) = TEMP1 * DEN
1360 Q1(I,1) = 2. * Q1(I,2) - Q1(I,3)
1361 Q2(I,1) = Q1(I,1)*A(1,1)*RHS(1)+A(1,2)*RHS(2)
1362 Q3(I,1) = Q1(I,1) * (A(2,1)*RHS(1)+A(2,2)*RHS(2))
1363 1 CONTINUE
1364 DO 10 I=ITEL,ITEU
1365 P2=GAMM*(Q4(I,2)-0.5*Q1(I,2)*(U(I,2)**2+V(I,2)**2))
1366 P3=GAMM*(Q4(I,3)-0.5*Q1(I,3)*(U(I,3)**2+V(I,3)**2))
1367 P1=(4.*P2-P3)/3.
1368 PSUR(I)=(GAMMA*P1-1.)/(.*AMINF**2)
1369 10 Q4(I,1)=P1/GAMM+0.5*Q1(I,1)*(U(I,1)**2+V(I,1)**2)
1370 C
1371 FAR FIELD BOUNDARY CONDITION ONLY FOR STEADY FLOW
1372 C
1373 CIRC = 0
1374 IF(PITCH.OR.RAMP) GO TO 999
1375 IF(AMINF.GT.1.) GO TO 65
1376 C
1377 CIRCULATION CORRECTION AT THE FAR FIELD IS BASED ON POTENTIAL
1378 VORTEX
1379 C
1380 BETA = SORT( 1. - AMINF**2 )
1381 IF(CIRCOR) CIRC = 0.25 * CHORD * CL * BETA * AMINF / PI
1382 C
1383 COSAL = COS(ALFA)
1384 SINAL = SIN(ALFA)
1385 AINF = 1.
1386 BINF = GAMMI + 0.5 * AMINF**2
1387 C
1388 CIRCQ = CIRCULATION CORRECTION QUANTITY
1389 C
1390 K = IMAX
1391 DO 60 I = 2 , IMAX-1
1392 XLOC = X(I,K) - XREF
1393 ZLOC = Z(I,K)
1394 RADIUS = SQRT( XLOC**2 + ZLOC**2 )
1395 ANGLE = ATAN2(ZLOC,XLOC)
1396 CIRCQ = CIRC / ( RADIUS * ( 1. - (AMINF*SIN(ANGLE-ALFA))**2 ) )
1397 UF = UINF + CIRCQ * SIN(ANGLE)
1398 VF = VINF - CIRCQ * COS(ANGLE)
1399 AFSQ = GAMM * ( BINF - 0.5*( UF**2 + VF**2 ) )
1400 AF = SQRT(AFSQ)
1401 C
1402 NONREFLECTING B.C. BASE ON 1-D RIEMANN INVARIANTS
1403 ZETXN, ZETZN = NORMALIZED NORMAL VECTOR
1404 C
1405 ANOR = 1. / SQRT( ZETAX(I,K)**2 + ZETAZ(I,K)**2 )
1406 ZETXN = ZETAX(I,K) * ANOR
1407 ZETZN = ZETAZ(I,K) * ANOR
1408 C
1409 CHECK FOR INFLOW OR OUTFLOW
1410 FOR INFLOW: R1, VOLT, ENTROPY ARE SPECIFIED AS FREE STREAM VALUES
1411 R2 IS EXTRAPOLATED
1412 FOR OUTFLOW: R1 IS SPECIFIED AS FREE STREAM VALUE
1413 R2, VOLT, ENTROPY ARE EXTRAPOLATED
1414 C
1415 RBOEXT = Q1(I,K-1)
1416 RBO: = 1. Q1(I,K-1)

```

```

LINE #          SOURCE TEXT
1417          UEXT = Q1(I,K-1) * RHO1
1418          VEXT = Q3(I,K-1) * RHO1
1419          EEXT = Q4(I,K-1)
1420          PEXT = GAMM * ( EEXT - 0.5*RHOEXT*( UEXT**2 + VEXT**2 ) )
1421
1422          SET RIEMANN INVARIANTS R1, AND R2
1423          VELN = NORMAL VELOCITY, VELT = TANGENTIAL VELOCITY
1424
1425          R1 = ZETXN * UF + ZETZN * VF - 2. * AF * GAMMI
1426          R2 = ZETXN * UEXT + ZETZN * VEXT + 2. * SQRT( GAMMA * PEXT /
1427          1          RHOEXT ) * GAMMI
1428
1429          VELN = ( R1 + R2 ) * 0.5
1430          SPSQ = ( R2 - R1 ) * GAMM * 0.25
1431          A2 = SPSQ**2
1432
1433          SET OTHER FIXED OR EXTRAPOLATED VARIABLES
1434
1435          IF(VELN.LE.0.) THEN
1436              VELT = ZETZN * UF - ZETXN * VF
1437              ENTRO = GAMMA
1438          ELSE
1439              VELT = ZETZN * UEXT - ZETXN * VEXT
1440              ENTRO = RHOEXT**GAMMA / PEXT
1441          ENDIF
1442
1443          NOW COMPUTE FLOW VARIABLES
1444
1445          U(I,K) = ZETXN * VELN + ZETZN * VELT
1446          V(I,K) = ZETZN * VFLN - ZETXN * VELT
1447          Q1(I,K) = ( A2 * ENTRO * GAMMI ) ** GAMMI
1448          PRESS = A2 * Q1(I,K) * GAMMI
1449          Q2(I,K) = Q1(I,K) * U(I,K)
1450          Q3(I,K) = Q1(I,K) * V(I,K)
1451          Q4(I,K) = PRESS*GAMMI + 0.5 * Q1(I,K) * ( U(I,K)**2 + V(I,K)**2 )
1452          60 CONTINUE
1453          GO TO 67
1454          65 CONTINUE
1455
1456          B.C. FOR SUPERSONIC FLOW
1457
1458          K = KMAX
1459          DO 66 I = 2 , IMAX-1
1460              RHO1 = 1. / Q1(I,K)
1461              U(I,K) = Q2(I,K) * RHO1
1462              V(I,K) = Q3(I,K) * RHO1
1463              ANOR = 1. / SQRT( ZETAX(I,K)**2 + ZETAZ(I,K)**2 )
1464              ZETXN = ZETAX(I,K) * ANOR
1465              ZETZN = ZETAZ(I,K) * ANOR
1466              VELN = ZETXN * U(I,K) + ZETZN * V(I,K)
1467              IF(VELN.GE.0.) THEN
1468                  Q1(I,K) = Q1(I,K-1)
1469                  Q2(I,K) = Q2(I,K-1)
1470                  Q3(I,K) = Q3(I,K-1)
1471                  Q4(I,K) = Q4(I,K-1)
1472              ENDIF
1473          66 CONTINUE
1474
1475          67 CONTINUE
1476
1477          OUTFLOW B.C. AT THE DOWNSTREAM OF C-GRID ONLY FOR INVISCID FLOW
1478
1479          IF(REYREF.LT.0.) THEN
1480              I = 1
1481              IP1 = 1
1482              SIGN = -1.
1483
1484          CHECK FOR SUPERSONIC FLOW
1485
1486          IF(AMINF.GT.1.) GO TO 75
1487
1488          72 CONTINUE
1489          DO 74 K = 1 , KMAX
1490
1491          CORRECT FREE STREAM VALUES WITH CIRCULATION CORRECTION
1492
1493          XLOC = X(I,K) - XREF
1494          ZLOC = Z(I,K)
1495          RADIUS = SQRT( XLOC**2 + ZLOC**2 )
1496          ANGLE = ATAN2(ZLOC,XLOC)
1497          CIRCO = CIRC / ( RADIUS * ( 1. - (AMINF*SIN(ANGLE-ALFA))**2 ) )
1498          UF = UINF + CIRCO * SIN(ANGLE)
1499          VF = VINF - CIRCO * COS(ANGLE)
1500          AFSQ = GAMM * ( BINF - 0.5*( UF**2 + VF**2 ) )
1501          AF = SQRT(AFSQ)
1502
1503          XIXB, XIZB = NORMALIZED HORIZONTAL VECTOR
1504
1505          ANOR = 1. / SQRT( XIX(I,K)**2 + XIZ(I,K)**2 )
1506          XIXB = XIX(I,K) * ANOR
1507          XIZB = XIZ(I,K) * ANOR
1508
1509          RHOEXT = Q1(I+IP1,K)
1510          RHO1 = 1. / Q1(I+IP1,K)
1511          UEXT = Q2(I+IP1,K)
1512          VEXT = Q3(I+IP1,K)
1513          EEXT = Q4(I+IP1,K)
1514          PEXT = GAMM * ( EEXT - 0.5*RHOEXT*( UEXT**2 + VEXT**2 ) )
1515
1516          SET RIEMANN INVARIANTS R1, AND R2
1517
1518          R1 = XIXB * UF + XIZB * VF - SIGN * 2. * AF * GAMMI
1519          R2 = XIXB * UEXT + XIZB * VEXT + SIGN * 2. * SQRT( GAMMA * PEXT /
1520          1          RHOEXT ) * GAMMI
1521
1522          VELN = ( R1 + R2 ) * 0.5
1523          SPSQ = SIGN * ( R2 - R1 ) * GAMM * 0.25
1524          A2 = SPSQ**2
1525
1526          SET OTHER FILED OR EXTRAPOLATED VARIABLES
1527
1528          IF(SIGN*VELN.LE.0.) THEN
1529              VELT = -XIZB * UF + XIXB * VF
1530              ENTRO = GAMMA
1531          ELSE
1532              VELT = -XIZB * UEXT + XIXB * VEXT
1533              ENTRO = RHOEXT**GAMMA / PEXT
1534          ENDIF
1535
1536          COMPUTE FLOW VARIABLES

```

```
LINE # SOURCE TEXT
1537 C
1538 U(I,K) = XIXH * VELN - XIZH * VELT
1539 V(I,K) = XIZH * VELN + XIXH * VELT
1540 Q1(I,K) = ( A2 * ENTRO * GAMI ) ** GAMMI
1541 PRESS = A2 * Q1(I,K) * GAMI
1542 Q2(I,K) = Q1(I,K) * U(I,K)
1543 Q3(I,K) = Q1(I,K) * V(I,K)
1544 Q4(I,K) = PRESS * GAMMI + 0.5 * Q1(I,K) * ( U(I,K)**2 + V(I,K)**2 )
1545
1546 74 CONTINUE
1547 IF(I.EQ.IMAX) GO TO 79
1548 I = IMAX
1549 IP1 = -1
1549 SIGN = 1.
1550 GO TO 72
1551 79 CONTINUE
1552 GO TO 89
1553
1554 C
1555 C
1556 C
1557 75 CONTINUE
1558 DO 84 K = 1 , KMAX
1559
1560 RBOI = 1. / Q1(I,K)
1561 U(I,K) = Q2(I,K) * RBOI
1562 V(I,K) = Q3(I,K) * RBOI
1563 ANOR = 1. / SQRT( XIX(I,K)**2 + XIZ(I,K)**2 )
1564 XIXH = XIX(I,K) * ANOR
1565 XIZH = XIZ(I,K) * ANOR
1566 VELN = SIGN * ( XIXH * U(I,K) + XIZH * V(I,K) )
1567
1568 IF(VELN.GE.0.) THEN
1568 Q1(I,K) = Q1(I-IP1,K)
1569 Q2(I,K) = Q2(I-IP1,K)
1570 Q3(I,K) = Q3(I-IP1,K)
1571 Q4(I,K) = Q4(I-IP1,K)
1572 ENDIF
1573 84 CONTINUE
1574 IF(I.EQ.IMAX) GO TO 89
1575 I = IMAX
1576 IP1 = -1.
1577 SIGN = 1.
1578 GO TO 75
1579 89 CONTINUE
1580
1581 C
1582 C
1583 C
1584 C
1585 C
1586 C
1587 C
1588 C
1589 C
1590 DO 100 K = 1 , KMAX
1591 I = 1
1591 Q1(I,K) = Q1(I+1,K)
1592 Q2(I,K) = Q2(I+1,K)
1593 Q3(I,K) = Q3(I+1,K)
1594 PEXT = GAMM * ( Q4(I+1,K) - 0.5 * ( Q2(I+1,K)**2 + Q3(I+1,K)**2 )
1595 / Q1(I+1,K) )
1596 Q4(I,K) = PEXT / GAMM + 0.5 * ( Q2(I,K)**2 + Q3(I,K)**2 ) / Q1(I,K)
1597 I = IMAX
1598 Q1(I,K) = Q1(I-1,K)
1599 Q2(I,K) = Q2(I-1,K)
1600 Q3(I,K) = Q3(I-1,K)
1601 PEXT = GAMM * ( Q4(I-1,K) - 0.5 * ( Q2(I-1,K)**2 + Q3(I-1,K)**2 )
1602 / Q1(I-1,K) )
1603 Q4(I,K) = PEXT / GAMM + 0.5 * ( Q2(I,K)**2 + Q3(I,K)**2 ) / Q1(I,K)
1604 100 CONTINUE
1605 C
1606 C
1607 C
1608 C
1609 C
1610 999 CONTINUE
1611 DO 120 J = 1 , ITEL - 1
1612 IU = IMAX + 1 - I
1613 Q1AVG = 0.5 * ( Q1(I,2) + Q1(IU,2) )
1614 Q2AVG = 0.5 * ( Q2(I,2) + Q2(IU,2) )
1615 Q3AVG = 0.5 * ( Q3(I,2) + Q3(IU,2) )
1616 Q1(I,1) = Q1AVG
1617 Q1(IU,1) = Q1AVG
1618 Q2(I,1) = Q2AVG
1619 Q2(IU,1) = Q2AVG
1620 Q3(I,1) = Q3AVG
1621 Q3(IU,1) = Q3AVG
1622 PSLOW = GAMM * ( Q4(I,2) - 0.5 * ( Q2(I,2)**2 + Q3(I,2)**2 ) /
1623 Q1(I,2) )
1624 PSUPP = GAMM * ( Q4(IU,2) - 0.5 * ( Q2(IU,2)**2 + Q3(IU,2)**2 ) /
1625 Q1(IU,2) )
1626 PSAVG = 0.5 * ( PSLOW + PSUPP )
1627 Q4AVG = PSAVG / GAMM + 0.5 * ( Q2(I,1)**2 + Q3(I,1)**2 ) /
1628 Q1(I,1)
1629 Q4(I,1) = Q4AVG
1630 Q4(IU,1) = Q4AVG
1631 120 CONTINUE
1632 RETURN
1633 END
```

```
LINE # SOURCE TEXT
1634 SUBROUTINE STRESS(ITN)
1635 C.....
1636 C*
1637 C* SUBROUTINE STRESS
1638 C*
1639 C.....
1640 PARAMETER (IX=1*0,KX=60)
1641 COMMON/FLWQ/Q1 (IX,KX),Q2 (IX,KX),Q3 (IX,KX),Q4 (IX,KX)
1642 COMMON/DGRID/DT,IMAX,IMAXI,ITEL,ITEU
1643 COMMON/GRD1/X (IX,KX),Z (IX,KX)
1644 COMMON/PAR/GAMMA,REYREF,ALFA,ALFAI,REDFRE,AMINF,ALFAI
1645 COMMON/SPEED/ U (IX,KX),V (IX,KX),AA (IX,KX)
1646 COMMON/PERTR/DQ1 (IX,KX),DQ2 (IX,KX),DQ3 (IX,KX),DQ4 (IX,KX)
1647 COMMON/MUTUR/CMU (IX,KX)
1648 DIMENSION RB1 (IX),RB2 (IX),RB3 (IX),RB4 (IX)
1649 COMMON/LOGIC/RSTRT,PITCHE,RAMP
1650 LOGICAL RSTRT,PITCHE,RAMP
1651 C THIS SUBROUTINE ADDS VISCOUS TERMS TO THE RIGHT HAND SIDE
1652 C
1653 C CMUL = LAMINAR OR MOLECULAR VISCOSITY
1654 C
1655 C CMUL = AMI. / REYREF
1656 C CALL EDDY(CMUL)
1657 C KMAXMI = KMAX - 1
1658 C IMAXMI = IMAX - 1
1659 C PR = 1.
1660 C
1661 C COMPUTE TXX,TTY AND VISCOUS DISSIPATION AT I - 1 / 2
1662 C
1663 DO 30 K = 2, KMAXMI
1664 DO 20 I = 2, IMAX
1665 UX1 = U (I,K) - U (I-1,K)
1666 VX1 = V (I,K) - V (I-1,K)
1667 AX1 = AA (I,K) - AA (I-1,K)
1668 UZET = .25 * (U (I,K+1) - U (I,K) + U (I-1,K+1) - U (I-1,K))
1669 VZET = .25 * (V (I,K+1) - V (I,K) + V (I-1,K+1) - V (I-1,K))
1670 AZET = .25 * (AA (I,K+1) - AA (I,K) + AA (I-1,K+1) - AA (I-1,K))
1671 ZX1 = X (I,K) - X (I-1,K)
1672 ZXI = Z (I,K) - Z (I-1,K)
1673 XZET = .25 * (X (I,K+1) - X (I,K) + X (I-1,K+1) - X (I-1,K))
1674 ZZET = .25 * (Z (I,K+1) - Z (I,K) + Z (I-1,K+1) - Z (I-1,K))
1675 YAC = XX1 * ZZET - ZXI * XZET
1676 YAC = 1. / YAC
1677 XIX = ZZET * YAC
1678 ZETAX = - ZXI * YAC
1679 XIZ = - XZET * YAC
1680 ZETAZ = XAI * YAC
1681 CNM = (.5 * (CMU (I,K) + CMU (I-1,K)) + CMUL) * DT
1682 UX = UX1 * XIX - UZET * ZETAX
1683 VX = VX1 * XIX - VZET * ZETAX
1684 AX = AX1 * XIX + AZET * ZETAX
1685 UZ = UX1 * XIZ + UZET * ZETAZ
1686 VZ = VX1 * XIZ - VZET * ZETAZ
1687 AZ = AX1 * XIZ - AZET * ZETAZ
1688 TXX = (-.4 * UX + 2. * VZ) * CNM / 3.
1689 TXY = CNM * (UZ + VX)
1690 TTY = -CNM / 3. * (-.4 * VZ + 2. * UX)
1691 C R4 = ((U (I,K) + U (I-1,K)) * TXX + (V (I,K) + V (I-1,K)) * TXY) * 0.5
1692 C 1 + CNM / PR / (GAMMA - 1.) * AX
1693 C S4 = ((V (I,K) + V (I-1,K)) * TXY + (U (I,K) + U (I-1,K)) * TTY) * 0.5
1694 C 1 - CNM / PR / (GAMMA - 1.) * AZ
1695 C
1696 C DEBUG
1697 C TURN OFF ENRGY DISSIPATION AND DIFFUSION
1698 R4 = 0.
1699 S4 = 0.
1700 RB1 (I) = 0.
1701 RB2 (I) = (XIX * TXX + XIZ * TXY) / YAC
1702 RB3 (I) = (XIX * TXY + XIZ * TTY) / YAC
1703 RB4 (I) = (XIX * R4 + XIZ * S4) / YAC
1704 DO 30 I = 2, IMAXMI
1705 DQ1 (I,K) = DQ1 (I,K) + RB1 (I-1) - RB1 (I)
1706 DQ2 (I,K) = DQ2 (I,K) + RB2 (I-1) - RB2 (I)
1707 DQ3 (I,K) = DQ3 (I,K) + RB3 (I-1) - RB3 (I)
1708 DQ4 (I,K) = DQ4 (I,K) + RB4 (I-1) - RB4 (I)
1709 C 30 CONTINUE
1710 C IN THE Z DIRECTION
1711 DO 70 I = 2, IMAXMI
1712 DO 60 K = 2, KMAX
1713 UX1 = .25 * (U (I+1,K) - U (I-1,K) + U (I+1,K-1) - U (I-1,K-1))
1714 VX1 = .25 * (V (I+1,K) - V (I-1,K) + V (I+1,K-1) - V (I-1,K-1))
1715 AX1 = .25 * (AA (I+1,K) - AA (I-1,K) + AA (I+1,K-1) - AA (I-1,K-1))
1716 ZX1 = .25 * (X (I+1,K) - X (I-1,K) + X (I+1,K-1) - X (I-1,K-1))
1717 ZXI = .25 * (Z (I+1,K) - Z (I-1,K) + Z (I+1,K-1) - Z (I-1,K-1))
1718 UZET = U (I,K) - U (I,K-1)
1719 VZET = V (I,K) - V (I,K-1)
1720 AZET = AA (I,K) - AA (I,K-1)
1721 XZET = X (I,K) - X (I,K-1)
1722 ZZET = Z (I,K) - Z (I,K-1)
1723 YAC = XX1 * ZZET - ZXI * XZET
1724 YAC = 1. / YAC
1725 XIX = ZZET * YAC
1726 ZETAX = - ZXI * YAC
1727 XIZ = - XZET * YAC
1728 ZETAZ = XAI * YAC
1729 CNM = (.5 * (CMU (I,K) + CMU (I,K-1)) + CMUL) * DT
1730 UX = UX1 * XIX + UZET * ZETAX
1731 VX = VX1 * XIX + VZET * ZETAX
1732 AX = AX1 * XIX + AZET * ZETAX
1733 UZ = UX1 * XIZ + UZET * ZETAZ
1734 VZ = VX1 * XIZ + VZET * ZETAZ
1735 AZ = AX1 * XIZ + AZET * ZETAZ
1736 TXX = (-.4 * UX + 2. * VZ) * CNM / 3.
1737 TXY = CNM * (UZ + VX)
1738 TTY = -CNM / 3. * (-.4 * VZ + 2. * UX)
1739 C R4 = ((U (I,K) + U (I,K-1)) * TXX + (V (I,K) + V (I,K-1)) * TXY) * 0.5
1740 C 1 + CNM / PR / (GAMMA - 1.) * AX
1741 C S4 = ((V (I,K) + V (I,K-1)) * TXY + (U (I,K) + U (I,K-1)) * TTY) * 0.5
1742 C 1 - CNM / PR / (GAMMA - 1.) * AZ
1743 R4 = 0.
1744 S4 = 0.
1745 RB1 (K) = 0.
1746 RB2 (K) = (ZETAX * TXX + ZETAZ * TXY) / YAC
1747 RB3 (K) = (ZETAX * TXY + ZETAZ * TTY) / YAC
1748 RB4 (K) = (ZETAX * R4 + ZETAZ * S4) / YAC
1749 DO 70 K = 2, KMAXMI
1750 DQ1 (I,K) = DQ1 (I,K) + RB1 (K+1) - RB1 (K)
1751 DQ2 (I,K) = DQ2 (I,K) + RB2 (K+1) - RB2 (K)
1752 DQ3 (I,K) = DQ3 (I,K) + RB3 (K+1) - RB3 (K)
1753 DQ4 (I,K) = DQ4 (I,K) + RB4 (K+1) - RB4 (K)
1754 DO 70 I = 2, IMAXMI
```

LINE #	SOURCE TEXT
1754 1755 1756	C RETURN END

LINE #	SOURCE TEXT
1757	SUBROUTINE LOAD(CL,CDP,CF,CM ALFAS,XREF)
1758	C.....
1759	C*
1760	C* SUBROUTINE LOAD
1761	C*
1762	C.....
1763	PARAMETER (IX=180,KX=60)
1764	COMMON/GRID1/X(IX,KX),Y(IX,KX)
1765	COMMON/SKINCF/CF(IX)
1766	COMMON/DGRID/DT,IMAX,EMAX,ITEL,ITEU
1767	COMMON/SURF/PSUR(IX)
1768	C
1769	THIS SUBROUTINE COMPUTES THE INVISCID CONTRIBUTIONS
1770	TO LOADS ON THE AIRFOIL SURFACE
1771	C
1772	CL = 0.
1773	CD = 0.
1774	CDP = 0.
1775	CM = 0.
1776	DO 300 I = ITEL , ITEU - 1
1777	DX = X(I+1,1) - X(I,1)
1778	300 CDF = CDF + (CF(I) + CF(I+1)) * 0.5 * DX
1779	DO 400 J = ITEL , ITEU - 1
1780	XL = .5 * (X(I,1)+X(I+1,1))
1781	YL = .5 * (Y(I,1)+Y(I+1,1))
1782	DX = X(I+1,1) - X(I,1)
1783	DY = Y(I+1,1) - Y(I,1)
1784	CPA = PSUR(I+1) * .5 + PSUR(J) * .5
1785	DCL = CPA * (-DX)
1786	DCD = CPA * DY
1787	CL = CL + DCL
1788	CD = CD + DCD
1789	400 CM = CM + DCD * YL - DCL * (XL - XREF)
1790	C
1791	DCL = CL * COS(ALFAS) - CD * SIN(ALFAS)
1792	CDP = CL * SIN(ALFAS) + CD * COS(ALFAS)
1793	CL = DCL
1794	RETURN
1795	END

```

LINE # SOURCE TEXT
1796 SUBROUTINE WRAP(II,JJ,XSING,YSING,XP,YP,SO,AO,YO)
1797 C.....
1798 C*
1799 C* SUBROUTINE WRAP
1800 C*.....
1801 C.....
1802 PARAMETER (IX=180,KX=60)
1803 DIMENSION SO(IX,4),YO(60,4),AO(IX,4),XP(1),YP(1)
1804 C
1805 C THIS SUBROUTINE UNWRAPS THE AIRFOIL AND STORES THE UNWRAPPED
1806 C SURFACE IN ARRAYS AO AND EO. IT ALSO DETERMINES THE STRETCHING
1807 C IN THE ETA DIRECTION.
1808 C
1809 C IMID = (II + 1) / 2
1810 C DY = .8 / (JJ - 2)
1811 C DO 1 J = 2 , JJ
1812 C Y = FLOAT(J-2) * DY
1813 C 1 YO(J,1) = 1.25 * Y / (1. - Y * Y)
1814 C YO(1,1) = - YO(3,1)
1815 C PI = 4. * ATAN ( 1.)
1816 C ANGL = PI * PI
1817 C U = XP(1) - XSING
1818 C V = YP(1) - YSING
1819 C U = 1.
1820 C V = 0.
1821 C IIM1 = II - 1
1822 C DO 2 I = 1 , IIM1
1823 C X11 = XP(I) - XSING
1824 C Y11 = YP(I) - YSING
1825 C ANGL = ANGL + ATAN2((U*Y11-V*X11),(U*X11+V*Y11))
1826 C R = SQRT(X11**2 + Y11**2)
1827 C U = X11
1828 C V = Y11
1829 C R = SQRT(R)
1830 C AO(I,1) = R * COS(.5 * ANGL)
1831 C 2 SO(I,1) = R * SIN(.5 * ANGL)
1832 C WRITE (6,1000)
1833 C WRITE (6,2000) (I,AO(I,1),SO(I,1),I = 1 , IIM1)
1834 C RETURN
1835 1000 FORMAT(1X,'UNWRAPPED COORDINATES IN THE TRANSFORMED PLANE')
1836 2000 FORMAT(15 , 2F20.8)
1837 C END

```

LINE #	SOURCE TEXT
1838	SUBROUTINE TABINT(XP,YP,XSING,YSING,N)
1839	C.....
1840	C*
1841	C* SUBROUTINE TABINT
1842	C*
1843	C.....
1844	PARAMETER (IX=180,KM=60)
1845	DIMENSION XP(IX),YP(IX),SO(IX),AO(IX)
1846	U = XP(1) - XSING
1847	V = YP(1) - YSING
1848	U = 1.
1849	V = 0.
1850	ANGL = 8. * ATAN(1.)
1851	DO 1 I = 1,N
1852	X11 = XP(I) - XSING
1853	Y11 = YP(I) - YSING
1854	ANGL = ANGL + ATAN2((U*Y11-V*X11),(U*X11+V*Y11))
1855	R = SQRT(X11**2 + Y11 ** 2)
1856	D = X11
1857	V = Y11
1858	R = SQRT(R)
1859	AO(I) = R * COS(ANGL * .5)
1860	1 SO(I) = R * SIN(ANGL * .5)
1861	DX = (AO(N)-AO(1))/96.
1862	AOST = AO(1)
1863	DO 3 I = 1 , 97
1864	IX = FLOAT(I-1) * DX + AOST
1865	CALL TAINI(AO,SO,IX,YY,N,3,NER,MON)
1866	XP(I) = XX * IX - YY * YI + XSING
1867	3 YP(I) = 2. * IX * YI + YSING
1868	RETURN
1869	END

LINE #	SOURCE TEXT
870	SUBROUTINE TAINT(XTAB,FTAB,X,FX,N,K,NER,MON)
871	C.....
872	C*
873	C* SUBROUTINE TAINT
874	C*
875	C.....
876	PARAMETER (IX=180,KX=50)
877	DIMENSION XTAB(1),FTAB(1),T(10),C(10)
878	C
879	C NASA - AMES SUBROUTINE FOR POLYNOMIAL INTERPOLATION
880	C OF A TABULATED FUNCTION
881	C
882	IF(N-K) 1, 1, 2
883	1 NER = 2
884	RETURN
885	2 IF(K-9) 3,3,1
886	3 IF(MON) 4,4,5
887	5 IF(MON-2) 6,7,4
888	4 J = 0
889	NM1 = N - 1
890	DO 8 I = 1, NM1
891	IF(XTAB(I) - XTAB(I+1)) 9,11,10
892	11 NER = 3
893	RETURN
894	9 J = J-1
895	GO TO 8
896	10 J = J+1
897	8 CONTINUE
898	MON = 1
899	IF(J) 12, 6, 6
900	12 MON = 2
901	7 DO 13 I = 1, N
902	IF(X - XTAB(I)) 14,14,13
903	14 J = I
904	GO TO 18
905	13 CONTINUE
906	GO TO 15
907	6 DO 16 I = 1, N
908	IF(X-XTAB(I)) 16,17,17
909	17 J = I
910	GO TO 18
911	16 CONTINUE
912	15 J = N
913	18 J = J - (K+1) / 2
914	IF(J) 19,19,20
915	19 J = 1
916	20 M = J + K
917	IF(M - N) 21,21,22
918	22 J = J - 1
919	GO TO 20
920	21 KP1 = K + 1
921	JSAVE = J
922	26 DO 23 L = 1, KP1
923	C(L) = X - XTAB(J)
924	T(L) = FTAB(J)
925	23 J = J+1
926	DO 24 J = 1,K
927	I = J-1
928	25 T(I) = (C(J)*T(I)-C(I)*T(J))/(C(J)-C(I))
929	I = I+1
930	IF(I-KP1) 25,25,24
931	24 CONTINUE
932	FX = T(KP1)
933	NER = 1
934	RETURN
935	END

LINE #	SOURCE TEXT
936	SUBROUTINE SING(N2,N,X,Z,XLE,YLE,TEA,TES,XSING,YSING,CBD)
937
938	C.....
939	C.....
940	C.....
941	C.....
942	PARAMETER (IX=180,kx=60)
943	C.....
944	C.....
945	C.....
946	C.....
947	THIS SUBROUTINE COMPUTES SINGULAR POINT LOCATIONS.
948	C.....
949	DIMENSION X(2) , Z(2)
950	NU = N2
951	N1 = N2 + 1
952	N3 = N2 - 1
953	X1 = X(N1)
954	Z1 = Z(N1)
955	X2 = X(N2)
956	Z2 = Z(N2)
957	X3 = X(N3)
958	Z3 = Z(N3)
959	D1 = X2 ** 2 - X1 ** 2
960	D2 = Z2 ** 2 - Z1 ** 2
961	D3 = X2 - X1
962	D4 = Z2 - Z1
963	D5 = X3 ** 2 - X1 ** 2
964	D6 = Z3 ** 2 - Z1 ** 2
965	D7 = X3 - X1
966	D8 = Z3 - Z1
967	B = (D7 * (D1 + D2) - D3*(D5+D6))/(2.*(D7*D4-D3*D8))
968	IF(ABS(D3).LT.ABS(D7)) GO TO 10
969	A = (D1 + D2 - 2. * B * D4) / (2. * D3)
970	GO TO 20
971	10 A = (D5 + D6 - 2. * B * D8) / (2. * D7)
972	20 CONTINUE
973	R = SQRT((X2-A)** 2 + (Z2-B)**2)
974	XLE = X(N1)
975	YLE = Z(N1)
976	CHD = X(1) - X(NU)
977	A2 = (Z(2)-Z(1))/(X(2) - X(1))
978	A1 = (Z(N)-Z(N-1))/(X(N)-X(N-1))
979	TES = .5 * (A1 + A2)
980	TEA = A2 - A1
981	TEA = TEA + 57.29578
982	XSING = (X-XLE) / 2.
983	YSING = (B-YLE) / 2.
984	RETURN
985	END

LINE #	SOURCE TEXT
984	SUBROUTINE AIRPOL(IT,IE,ILE)
985	C.....
986	C* SUBROUTINE AIRPOL
987	C.....
988	PARAMETER (IX=180,KX=60)
989	COMMON/DGRID/I(IX,KX),Z(IX,KX)
990	COMMON/DGRID/DT,IMAX,KMAX,ITEL,ITEU
991	COMMON/YSYM/ISYM
992	DIMENSION SO(IX,4),AO(IX,4),YO(60,4),XP(IX),YP(IX),
993	IE(IX),F(IX),BO(49)
994	DIMENSION XL(IX),XU(IX),YL(IX),YU(IX),
995	Z(IX),ZY(IX)
996	C
997	DATA (BO(I),I=1,32)/1.,1.0414,1.0836,1.1270,1.1715,1.2175,1.2651,
998	11.3145,1.3659,1.4199,1.4755,1.5349,1.5973,1.6636,1.7342,1.8099,
999	21.8914,1.9799,2.0764,2.1829,2.3012,2.4341,2.5653,2.7597,2.9646,
1000	33.2106,3.5141,3.9019,4.4219,5.1687,6.3632,8.6809/
1001	C
1002	READ(5,*) IBMAX,ISYM
1003	IF(ISYM .EQ. 0) THEN
1004	DO 101 I=1,IBMAX
1005	READ(5,*) XU(I), YU(I), YL(I)
1006	101 CONTINUE
1007	ELSE
1008	DO 102 I = 1,IBMAX
1009	102 READ(5,*) XU(I), YU(I)
1010	DO 103 I = 1,IBMAX
1011	103 YL(I) = - YU(I)
1012	ENDIF
1013	C
1014	DO 1000 I=1,IBMAX
1015	IC = I + IBMAX
1016	XX(IU) = XU(I)
1017	YY(IU) = YU(I)
1018	IL = IBMAX - I + 1
1019	XX(IL) = XU(IL)
1020	YY(IL) = YL(IL)
1021	1000 CONTINUE
1022	C
1023	IBMAX2 = 2*IBMAX
1024	DO 1010 I=1,IBMAX2
1025	XP(I) = XX(I)
1026	YP(I) = YY(I)
1027	1010 CONTINUE
1028	FNU = IBMAX
1029	FNL = IBMAX
1030	C
1031	THIS SUBROUTINE GENERATES SHEAR PARABOLIC C-GRID
1032	THE FOLLOWING SUBROUTINES ARE RELATED TO THE GRID GENERATION
1033	WRAP SING
1034	TABINT CLUSTR
1035	TAINT STRTC
1036	C
1037	DO 8 I = 1 , 32
1038	8 AO(I,1) = BO(I)
1039	II = IMAX
1040	JJ = KMAX-1
1041	IT = 31
1042	IE = 31
1043	IIP1 = II + 1
1044	IIM1 = II - 1
1045	IJJJ = II * JJ
1046	IJJJ2 = II * (JJ-2)
1047	ILE = (IT + IE) / 2
1048	PI = 4. * ATAN(1.)
1049	NU = FNU
1050	NL = FNL
1051	N = NU + NL
1052	SCALE = 1. / (XP(1) - XP(NL))
1053	DO 3333 I=1,N
1054	XP(I) = XP(I) * SCALE
1055	YP(I) = YP(I) * SCALE
1056	3333 CONTINUE
1057	CALL SING(NU,N,XP,YP,ILE,ZLE,TEA,TES,XSING,YSING,CBD)
1058	CALL TABINT(XP,YP,XSING,YSING,N)
1059	NBODY = IE + 1 - IT
1060	DO 6791 I = 1 , NBODY
1061	L = I - 1
1062	E(IT+L) = XP(I)
1063	6791 F(IT-L) = YP(I)
1064	IEP1 = IE + 1
1065	SLOPT = TES * .75
1066	DO 438 I = IEP1 , II
1067	II = I + 1 - IE
1068	E(I) = AO(II,1)
1069	DII = 1. / 48.
1070	D = 4. / 3. * (E(I) - .25)
1071	F(I) = F(IE) + SLOPT * ALOG(D) / D
1072	L = IIP1 - I
1073	E(L) = E(I)
1074	438 F(L) = F(IT) + SLOPT * ALOG(D)/D
1075	C
1076	WRITE (6,439)
1077	439 FORMAT(2X,3H I,19X,1EX,19X,1HY)
1078	WRITE (6,37) (I,E(I),F(I),I = 1 , II)
1079	CALL WRAP(II,JJ,XSING,YSING,E,F,SO,AO,YO)
1080	DO 10 J = 2 , JJ
1081	DO 10 I = 1 , II
1082	X(I,J-1) = AO(I,1)**2 - (SO(I,1)+YO(J,1))**2
1083	10 Z(I,J-1) = 2. * AO(I,1) * (SO(I,1)+YO(J,1))
1084	RETURN
1085	37 FORMAT(15.2F20.8)
	END

LINE #	SOURCE TEXT
2086	SUBROUTINE CLUSTR(DS)
2087
2088	C*
2089	C* SUBROUTINE CLUSTR
2090	C*
2091
2092	PARAMETER (IX=180,KX=60)
2093	COMMON/GRID1/X(IX,KX),Z(IX,KX)
2094	COMMON/GRID/DT,IMAX,KMAX,ITEL,ITEU
2095	DIMENSION S(60),XP(60),YP(60),R(60)
2096	C
2097	C THIS SUBROUTINE CLUSTERS A GIVEN X,Z GRID SUCH THAT THE FIRST POINT IS AT
2098	C
2099	DO 100 I = 1 , IMAX
2100	S(I) = 0.
2101	XP(I) = X(I,1)
2102	YP(I) = Z(I,1)
2103	DO 10 K = 2 , KMAX
2104	XP(K) = X(I,K)
2105	YP(K) = Z(I,K)
2106	10 S(K) = SQRT((XP(K)-XP(K-1))**2+(YP(K)-YP(K-1))**2)
2107	1+S(K-1)
2108	SUMDX = S(KMAX)
2109	CALL STRTCH(SUMDX,DS,F1,KMAX,FACTOR)
2110	C WRITE (6,200) I,FACTOR
2111	R(1) = 0.
2112	DR = DS
2113	DO 20 K = 2 , KMAX
2114	R(K) = R(K-1) + DR
2115	DR = DR * FACTOR
2116	20 CONTINUE
2117	RLAST = 1. / R(KMAX)
2118	DO 30 K = 2 , KMAX
2119	R1 = R(K) * RLAST * S(KMAX)
2120	CALL TAINI(S,XP,R1,XP1,KMAX,3,NER,MON)
2121	X(I,K) = XP1
2122	CALL TAINI(S,YP,R1,YP1,KMAX,3,NER,MON)
2123	Z(I,K) = YP1
2124	30 CONTINUE
2125	100 CONTINUE
2126	C WRITE (6,115)
2127	DO 110 I = 1 , IMAX
2128	DX = X(I,2) - X(I,1)
2129	DY = Z(I,2) - Z(I,1)
2130	DN = SQRT(DX*DX+DY*DY)
2131	C WRITE(6,120) I , DX , DY , DN
2132	110 CONTINUE
2133	RETURN
2134	115 FORMAT(5X,6HNORMAL,1X,8HDISTANCE,3E AT,4E THE,5E WALL,/ 1,5E 1,8X,2HDX,8X,2HDY,8X,2HDN,///)
2135	120 FORMAT(15,3F10.5)
2136	200 FORMAT(15,3F10.5)
2137	END
2138	END

```
LINE # SOURCE TEXT
2139 SUBROUTINE STATCH(SUMDX,DX1,F1,N1,R)
2140 C.....
2141 C
2142 C SUBROUTINE STATCH
2143 C.....
2144 C
2145 C PARAMETER (IX=180,kx=60)
2146 C
2147 C THIS SUBROUTINE DETERMINES A GEOMETRIC
2148 C PROGRESSION OF GRID SPACING BETWEEN 1 AND N1 SUCH THAT
2149 C SUMDX) EQUALS SUMDX. THE RATIO BETWEEN SUCCESSIVE
2150 C SPACINGS IS R.
2151 C N = N1 - 1
2152 C R = 1.5
2153 C E1 = 1.E-04
2154 C E2 = 1.E-04
2155 C DO 10 L = 1, 50
2156 C F = (R-1) * SUMDX - DX1*(R**N-1)
2157 C FP = SUMDX - DX1 * FLOAT(N) * R ** (N-1)
2158 C RITER = F - F/FP
2159 C IF(1.E-02.LT.RITER.AND.RITER.LT.1.) RITER = 1.
2160 C IF(1..LT.RITER.AND.RITER.LT.100.) RITER=.01
2161 C IF(ABS(R-RITER).LT.R*E1) GO TO 1
2162 C R = RITER
2163 C 10 CONTINUE
2164 C R = 1.0001
2165 C DX1 = DXTOT/LOAT(N1-1)
2166 C RETURN
2167 C 1 R= RITER
2168 C RETURN
2169 C END
```

```

LINE # SOURCE TEXT
2170 SUBROUTINE EDDY(CMUL)
2171 C*****
2172 C*
2173 C* SUBROUTINE EDDY
2174 C*
2175 C*****
2176 PARAMETER (IX=180,KX=60)
2177 COMMON/FLON/Q1(IX,KX),Q2(IX,KX),Q3(IX,KX),Q4(IX,KX)
2178 COMMON/MUTUR/CMU(IX,KX)
2179 COMMON/SKINCF/CF(IX)
2180 COMMON/DGRID/DT,IMAX,KMAX,ITEL,ITEU
2181 COMMON/PAR/GAMMA,REYREF,ALFA,ALFAL,REDPRE,AMINF,ALFAI
2182 COMMON/GRID1/X(IX,KX),Z(IX,KX)
2183 COMMON/SPEED/ U(IX,KX),V(IX,KX),AA(IX,KX)
2184 DIMENSION TIN(KX),TOUT(KX),Y(KX),TRANS(IX),S(IX),UD(KX),UE(IX)
2185 C
2186 CMUPP = 1000. * CMUL
2187 KEDGE = KMAX
2188 ILE = ( ITEL + ITEU ) / 2
2189 CHORD = X(ITEU,1) - X(ILE,1)
2190 DO 100 I = 2 , IMAX - 1
2191 C IF( ABS(X(I,1)),LT.( ABS(X(ILE,1)) + 0.05 * CHORD ; ) GO TO 100
2192 UDIF = 0.
2193 UMAX = 0.
2194 UMIN = 9999.
2195 FMAX = 0.1E-06
2196 YMAX = .1E-06
2197 FYMAX = 0.1E-06
2198 Y(1) = 0.
2199 C COMPUTE TAU AT THE WALL
2200 UET = U(I,2) - U(I,1)
2201 VET = V(I,2) - V(I,1)
2202 XXI = X(I-1,1) - X(I-1,1)
2203 ZXI = Z(I-1,1) - Z(I-1,1)
2204 XET = 4. * X(I,2) - 3. * X(I,1) - X(I,3)
2205 ZET = 4. * Z(I,2) - 3. * Z(I,1) - Z(I,3)
2206 XXI = .5 * XXI
2207 ZXI = .5 * ZXI
2208 XET = .5 * XET
2209 ZET = .5 * ZET
2210 YAC = 1. / (XXI * ZET - ZXI * XET)
2211 OMEGA = (UET * XXI + VET * ZXI) * YAC
2212 TWALL = AMINF * OMEGA / REYREF
2213 CF(I) = 2. * TWALL / (AMINF**2)
2214 FACT = SQRT(Q1(I,1) * ABS(TWALL)) * REYREF / (26. * AMINF)
2215 DO 10 K = 2 , KEDGE-1
2216 UXI = U(I-1,K) - U(I-1,K)
2217 VXI = V(I-1,K) - V(I-1,K)
2218 UET = U(I,K-1) - U(I,K-1)
2219 VET = V(I,K-1) - V(I,K-1)
2220 XXI = X(I-1,K) - X(I-1,K)
2221 ZXI = Z(I-1,K) - Z(I-1,K)
2222 XET = X(I,K-1) - X(I,K-1)
2223 ZET = Z(I,K-1) - Z(I,K-1)
2224 YAC = 1. / (XXI * ZET - ZXI * XET)
2225 OMEGA = ABS(UET*XXI-VET*ZXI-UXI*XET-VXI*ZET) * YAC
2226 UTOT = SQRT(U(I,K)**2 + V(I,K)**2)
2227 UMAX = A*MAX1(UTOT,UMAX)
2228 UMIN = A*MIN1(UTOT,UMIN)
2229 Y(K) = SQRT((X(I,K)-X(I,K-1))**2+(Z(I,K)-Z(I,K-1))**2)+Y(K-1)
2230 F = Y(K) * OMEGA
2231 IF((Y(K)*FACT).GT.20.) GO TO 31
2232 IF(I.GT.ITEL.AND.I.LT.ITEU) F = F * (1. - EXP(-Y(K)*FACT))
2233 31 CONTINUE
2234 C
2235 IF(F.GT.FMAX) THEN
2236 FMAX = F
2237 YMAX = Y(K)
2238 ENDIF
2239 FCT = Y(K) * FACT
2240 IF(FCT.GT.20.) FCT = 20.
2241 FCT = ABS(FCT)
2242 EL = .4 * Y(K) * (1. - EXP(-FCT))
2243 TIN(K) = Q1(I,K) * EL * EL * OMEGA
2244 TIN(K) = ABS(TIN(K))
2245 10 CONTINUE
2246 UDIF = ABS(UMAX-UMIN)
2247 KSWTCH = 0
2248 FWAKE = YMAX * FMAX
2249 FI = 0.25 * YMAX * UDIF **2 / FMAX
2250 IF(FI.LT.FWAKE) FWAKE = FI
2251 DO 20 K = 2 , KEDGE - 1
2252 FKLEB = 0
2253 IF(ABS(Y(K)/YMAX).LT.1.E+04) THEN
2254 FKLEB = 1. / (1. + 5.5 * (0.3 * Y(K)/YMAX) ** 6)
2255 END IF
2256 TOUT(K) = .0168 * 1.6 * Q1(I,K) * FWAKE * FKLEB
2257 TOUT(K) = ABS(TOUT(K))
2258 IF(KSWTCH.NE.0) GO TO 20
2259 IF(TIN(K).GT.TOUT(K)) KSWTCH = K - 1
2260 20 CONTINUE
2261 DO 30 K = 2 , KEDGE - 1
2262 IF(K.LE.KSWTCH) THEN
2263 CMU(I,K) = ABS(TIN(K))
2264 ELSE
2265 CMU(I,K) = ABS(TOUT(K))
2266 END IF
2267 30 CONTINUE
2268 C
2269 C FROZE THE VALUE OF EDDY VISCOSITY TO AN UPPER LIMIT
2270 C
2271 R = 1
2272 C 734 R = R + 1
2273 C IF(R.GT.KEDGE) GO TO 736
2274 C 735 IF(CMU(I,K).LE.CMUPP) GO TO 734
2275 C CMU(I,K) = CMUPP
2276 C I = K + 1
2277 C IF(K.LE.KEDGE) GO TO 735
2278 C 736 CONTINUE
2279 100 CONTINUE
2280 RETURN
2281 END

```

```

LINE #          SOURCE TEXT
2282 SUBROUTINE RESI
2283 C.....
2284 C C
2285 C C      SUBROUTINE RESI
2286 C C
2287 C.....
2288 PARAMETER (IX=180,KX=60)
2289 COMMON/FIX/OMEGA,EDOT
2290 COMMON/PERTR/DQ1(IX,KX),DQ2(IX,KX),DQ3(IX,KX),DQ4(IX,KX)
2291 COMMON/GRID1/X(IX,KX),Z(IX,KX)
2292 COMMON/DGFID/DT,IMAX,KMAX,ITEL,ITEU
2293 COMMON/FLOW/Q1(IX,KX),Q2(IX,KX),Q3(IX,KX),Q4(IX,KX)
2294 COMMON/SPEED/ U(IX,KX),V(IX,KX),AA(IX,KX)
2295 COMMON/PAR/GAMMA,REYREF,ALFA,ALFAL,REDFRE,AMINF,ALFAI
2296 COMMON/COMRRS/ RRS(IX,4)
2297 XTAU(I,K) = OMEGA * Z(I,K)
2298 YTAU(I,K) = - OMEGA * X(I,K) - EDOT
2299 THIS SUBROUTINE COMPUTES THE RESIDUAL ON THE RIGHT HAND
2300 SIDE ARISING FROM THE EULER- PART OF THE GOVERNING EQUATIONS
2301 C C C C
2302 C C C C  FLUX TERMS WITHIN THE XI- DERIVATIVE
2303 DO 100 K = 2 , KMAX - 1
2304 DO 10 I = 1 , IMAX
2305 UCON = U(I,K) * (Z(I,K+1)-Z(I,K-1))
2306 1 - V(I,K) * (X(I,K+1)-X(I,K-1))
2307 UCON = 0.25 * DT * UCON
2308 XIT = - XTAU(I,K) * (Z(I,K+1)-Z(I,K-1))
2309 1 + YTAU(I,K) * (X(I,K+1) - X(I,K-1))
2310 XIT = XIT * DT * 0.25
2311 UCON = UCON + XIT
2312 RRS(I,1) = UCON * Q1(I,K)
2313 P = (GAMMA-1.) * (Q4(I,K) - .5*Q1(I,K)*(U(I,K)**2 + V(I,K)**2) )
2314 RRS(I,2) = Q2(I,K) * UCON + P * DT * 0.25 * (Z(I,K+1) - Z(I,K-1))
2315 RRS(I,3) = Q3(I,K) * UCON - P * DT * 0.25 * (X(I,K+1)-X(I,K-1))
2316 RRS(I,4) = UCON * (Q4(I,K)+P) - XIT * P
2317 10 CONTINUE
2318 DO 11 I = 2 , IMAX - 1
2319 DQ1(I,K) = DQ1(I,K) - RRS(I+1,1) + RRS(I-1,1)
2320 DQ2(I,K) = DQ2(I,K) - RRS(I+1,2) + RRS(I-1,2)
2321 DQ3(I,K) = DQ3(I,K) - RRS(I+1,3) + RRS(I-1,3)
2322 11 DQ4(I,K) = DQ4(I,K) - RRS(I+1,4) + RRS(I-1,4)
2323 100 CONTINUE
2324 C C C C
2325 C C C C  FLUX TERMS WITHIN THE ETA- DERIVATIVE
2326 DO 200 I = 2 , IMAX - 1
2327 DO 20 K = 1 , KMAX
2328 VCON = U(I,K) * (Z(I-1,K)-Z(I+1,K))
2329 1 - V(I,K) * (X(I+1,K)-X(I-1,K))
2330 VCON = VCON * 0.25 * DT
2331 ETAT = -XTAU(I,K) * (Z(I-1,K)-Z(I+1,K)) - YTAU(I,K)*
2332 (X(I+1,K)-X(I-1,K))
2333 1
2334 ETAT = ETAT * 0.25 * DT
2335 VCON = VCON + ETAT
2336 RRS(K,1) = VCON * Q1(I,K)
2337 P = (GAMMA-1.) * (Q4(I,K) - 0.5 * Q1(I,K)*(U(I,K)**2 + V(I,K)**2) )
2338 RRS(K,2) = VCON * Q2(I,K) + P * DT * .25 * (Z(I-1,K)-Z(I+1,K))
2339 RRS(K,3) = VCON * Q3(I,K) + P * DT * .25 * (X(I+1,K) - X(I-1,K))
2340 RRS(K,4) = VCON * (Q4(I,K)+P) - ETAT * P
2341 20 CONTINUE
2342 DO 21 K = 2 , KMAX - 1
2343 DQ1(I,K) = DQ1(I,K) - RRS(K+1,1) + RRS(K-1,1)
2344 DQ2(I,K) = DQ2(I,K) - RRS(K+1,2) + RRS(K-1,2)
2345 DQ3(I,K) = DQ3(I,K) - RRS(K+1,3) + RRS(K-1,3)
2346 21 DQ4(I,K) = DQ4(I,K) - RRS(K+1,4) + RRS(K-1,4)
2347 200 CONTINUE
2348 C 300 FORMAT(216,4E14.6)
2349 RETURN
2350 END

```

Program

LINE #	SOURCE TEXT
2351	SUBROUTINE ROTGRID(IMAX,KMAX,DALFA)
2352
2353	C
2354	SUBROUTINE ROTGID
2355
2356	C
2357	PARAMETER (IX=180,KX=60)
2358	ROTATE GRID IN THE CLOCKWISE DIRECTION BY AN AMOUNT DALFA
2359	COMMON/GRID1/X(IX,KI),Z(IX,KX)
2360	CA = COS(DALFA)
2361	SA = - SIN(DALFA)
2362	DO 20 K = 1 , KMAX
2363	DO 20 I = 1 , IMAX
2364	X1 = X(I,K)
2365	Z1 = Z(I,K)
2366	X(I,K) = X1 * CA - Z1 * SA
2367	20 Z(I,K) = Z1 * CA + X1 * SA
2368	RETURN
2369	END

```
LINE # SOURCE TEXT
2370 SUBROUTINE CP PLOT(I1,I2,FMACH,X,Y)
2371 C.....
2372 C*
2373 C* SUBROUTINE CP PLOT
2374 C*
2375 C*.....
2376 PARAMETER (IX=180,kx=60)
2377 C
2378 C THIS SUBROUTINE PLOTS CP AT EQUAL INTERVALS IN THE MAPPED PLANE
2379 C
2380 COMMON/SURF/PSUR(IX)
2381 DIMENSION KODE(4),LINE(90),X(IX),Y(IX)
2382 DATA KODE/18,18*,181,18*/
2383 WRITE (6,2)
2384 2 FORMAT(50BOPLOT OF CP AT EQUAL INTERVALS IN THE MAPPED PLANE/
2385 1 10B0 X,10H X/C,10H CPL,10H CPL )
2386 CP0 = (1. + .2 * FMACH **2) ** 3.5 - 1.
2387 CP0 = CP0 / (.7 * FMACH **2)
2388 K0 = 30. * CP0 + 4.5
2389 IMIN = (I2-I1)/2 + I1
2390 ILOW = 2 * IMIN
2391 CHD=X(I1) - X(IMIN)
2392 DO 12 I = 1, 90
2393 12 LINE(I) = KODE(1)
2394 DO 34 I = IMIN, I2
2395 K = 30. * (CP0 - PSUR(I)) + 4.5
2396 K1 = 30. * (CP0 - PSUR(ILOW-I)) + 4.5
2397 IF(K.LT.1) K = 1
2398 IF(K1.LT.1) K1 = 1
2399 IF(K.GT.90) K = 90
2400 IF(K1.GT.90) K1 = 90
2401 LINE(K0) = KODE(3)
2402 LINE(K) = KODE(2)
2403 LINE(K1) = KODE(4)
2404 XOC = (X(I) - X(IMIN)) / CHD
2405 WRITE (6,610) X(I),XOC,PSUR(ILOW-I),PSUR(I),LINE
2406 LINE(K1) = KODE(1)
2407 34 LINE(K) = KODE(1)
2408 RETURN
2409 600 FORMAT(4F10.4)
2410 610 FORMAT(4F10.4,90A1)
2411 END
```

LINE #	SOURCE TEXT
2412	SUBROUTINE OTRVC(REREAL)
2413	C*****
2414	C*
2415	C* SUBROUTINE OTRVC
2416	C*
2417	C*****
2418	PARAMETER (IX=180,KX=60)
2419	COMMON/PLOT/TITLE(10),NSTPT,RESD(3000),RES,CLB(3000),CDPB(3000)
2420	COMMON/DGRID/DT,IMAX,KMAX,ITEL,ITEU
2421	COMMON/FLOW/Q1(IX,KX),Q2(IX,KX),Q3(IX,KX),Q4(IX,KX)
2422	COMMON/PAR/GAMMA,REYREF,ALFA,ALFAI,REDFRE,AMINF,ALFAI
2423	COMMON/SURF/PSUR(IX)
2424	COMMON/SKINCF/CF(IX)
2425	COMMON/MUTUR/CMU(IX,KX)
2426	COMMON/TITL/ITITLE
2427	CHARACTER ITITLE*80
2428	DIMENS ON FY(IX,KX)
2429	DUM = 0.
2430	CODE = 0.
2431	IRIS = IFIX(RES)
2432	ALFAD = ALFA * 45. / ATAN(1.)
2433	CMUL = AMINF / REYREF
2434	DO 10 K = 1 , KMAX
2435	DO 10 I = 1 , IMAX
2436	FY(I,K) = 0.
2437	10 CMU(I,K) = CMU(I,K) / CMUL
2438	WRITE(4) ITITLE
2439	WRITE(4) IMAX,KMAX,ITEL,ITEU,AMINF,ALFAD,REREAL,DUM,NSTPT,GAMMA,
2440	+ CODE,RES,DUM
2441	WRITE(4) Q1,Q2,Q3,Q4
2442	WRITE(4) RESD
2443	WRITE(4) PSUR
2444	WRITE(4) CF
2445	WRITE(4) CLB,CDPB
2446	WRITE(4) CMU
2447	WRITE(4) FY
2448	WRITE(4) TK
2449	WRITE(4) TE
2450	RETURN
2451	END

```

LINE # SOURCE TEXT
2452 SUBROUTINE OUTNT(NOUT,NSTPP,TIME,REREAL)
2453 PARAMETER (IX=180,KX=60)
2454 COMMON/GRID1/X(IX,K),Z(IX,KX)
2455 COMMON/PAR/GAMMA,REYREF,ALFA,ALFAL,REDFRE,AMINF,ALFAL
2456 COMMON/DGRID/DT,IMAX,KMAX,ITEL,ITEU
2457 COMMON/FLOW/Q1(IX,KX),Q2(IX,KX),Q3(IX,KX),Q4(IX,KX)
2458 ITN = NSTPP
2459 PI = 4.*ATAN(1.)
2460 ALFAD=ALFA*(180./PI)
2461 IF (ITN.EQ.1*NOUT) THEN
2462 REWIND 31
2463 WRITE (31) IMAX , KMAX
2464 WRITE (31) ( ( X(I,K), I=1,IMAX ), K=1,KMAX )
2465 WRITE (31) ( ( Z(I,K), I=1,IMAX ), K=1,KMAX )
2466 WRITE (31) IMAX , KMAX
2467 WRITE (31) AMINF, ALFAD, REREAL, TIME
2468 WRITE (31) ( ( Q1(I,K), I=1,IMAX ), K=1,KMAX )
2469 WRITE (31) ( ( Q2(I,K), I=1,IMAX ), K=1,KMAX )
2470 WRITE (31) ( ( Q3(I,K), I=1,IMAX ), K=1,KMAX )
2471 WRITE (31) ( ( Q4(I,K), I=1,IMAX ), K=1,KMAX )
2472 REWIND 31
2473 END IF
2474 IF (ITN.EQ.2*NOUT) THEN
2475 REWIND 32
2476 WRITE (32) IMAX , KMAX
2477 WRITE (32) ( ( X(I,K), I=1,IMAX ), K=1,KMAX )
2478 WRITE (32) ( ( Z(I,K), I=1,IMAX ), K=1,KMAX )
2479 WRITE (32) IMAX , KMAX
2480 WRITE (32) AMINF, ALFAD, REREAL, TIME
2481 WRITE (32) ( ( Q1(I,K), I=1,IMAX ), K=1,KMAX )
2482 WRITE (32) ( ( Q2(I,K), I=1,IMAX ), K=1,KMAX )
2483 WRITE (32) ( ( Q3(I,K), I=1,IMAX ), K=1,KMAX )
2484 WRITE (32) ( ( Q4(I,K), I=1,IMAX ), K=1,KMAX )
2485 REWIND 32
2486 END IF
2487 IF (ITN.EQ.3*NOUT) THEN
2488 REWIND 33
2489 WRITE (33) IMAX , KMAX
2490 WRITE (33) ( ( X(I,K), I=1,IMAX ), K=1,KMAX )
2491 WRITE (33) ( ( Z(I,K), I=1,IMAX ), K=1,KMAX )
2492 WRITE (33) IMAX , KMAX
2493 WRITE (33) AMINF, ALFAD, REREAL, TIME
2494 WRITE (33) ( ( Q1(I,K), I=1,IMAX ), K=1,KMAX )
2495 WRITE (33) ( ( Q2(I,K), I=1,IMAX ), K=1,KMAX )
2496 WRITE (33) ( ( Q3(I,K), I=1,IMAX ), K=1,KMAX )
2497 WRITE (33) ( ( Q4(I,K), I=1,IMAX ), K=1,KMAX )
2498 REWIND 33
2499 END IF
2500 IF (ITN.EQ.4*NOUT) THEN
2501 REWIND 34
2502 WRITE (34) IMAX , KMAX
2503 WRITE (34) ( ( X(I,K), I=1,IMAX ), K=1,KMAX )
2504 WRITE (34) ( ( Z(I,K), I=1,IMAX ), K=1,KMAX )
2505 WRITE (34) IMAX , KMAX
2506 WRITE (34) AMINF, ALFAD, REREAL, TIME
2507 WRITE (34) ( ( Q1(I,K), I=1,IMAX ), K=1,KMAX )
2508 WRITE (34) ( ( Q2(I,K), I=1,IMAX ), K=1,KMAX )
2509 WRITE (34) ( ( Q3(I,K), I=1,IMAX ), K=1,KMAX )
2510 WRITE (34) ( ( Q4(I,K), I=1,IMAX ), K=1,KMAX )
2511 REWIND 34
2512 END IF
2513 IF (ITN.EQ.5*NOUT) THEN
2514 REWIND 35
2515 WRITE (35) IMAX , KMAX
2516 WRITE (35) ( ( X(I,K), I=1,IMAX ), K=1,KMAX )
2517 WRITE (35) ( ( Z(I,K), I=1,IMAX ), K=1,KMAX )
2518 WRITE (35) IMAX , KMAX
2519 WRITE (35) AMINF, ALFAD, REREAL, TIME
2520 WRITE (35) ( ( Q1(I,K), I=1,IMAX ), K=1,KMAX )
2521 WRITE (35) ( ( Q2(I,K), I=1,IMAX ), K=1,KMAX )
2522 WRITE (35) ( ( Q3(I,K), I=1,IMAX ), K=1,KMAX )
2523 WRITE (35) ( ( Q4(I,K), I=1,IMAX ), K=1,KMAX )
2524 REWIND 35
2525 END IF
2526 IF (ITN.EQ.6*NOUT) THEN
2527 REWIND 36
2528 WRITE (36) IMAX , KMAX
2529 WRITE (36) ( ( X(I,K), I=1,IMAX ), K=1,KMAX )
2530 WRITE (36) ( ( Z(I,K), I=1,IMAX ), K=1,KMAX )
2531 WRITE (36) IMAX , KMAX
2532 WRITE (36) AMINF, ALFAD, REREAL, TIME
2533 WRITE (36) ( ( Q1(I,K), I=1,IMAX ), K=1,KMAX )
2534 WRITE (36) ( ( Q2(I,K), I=1,IMAX ), K=1,KMAX )
2535 WRITE (36) ( ( Q3(I,K), I=1,IMAX ), K=1,KMAX )
2536 WRITE (36) ( ( Q4(I,K), I=1,IMAX ), K=1,KMAX )
2537 REWIND 36
2538 END IF
2539 IF (ITN.EQ.7*NOUT) THEN
2540 REWIND 37
2541 WRITE (37) IMAX , KMAX
2542 WRITE (37) ( ( X(I,K), I=1,IMAX ), K=1,KMAX )
2543 WRITE (37) ( ( Z(I,K), I=1,IMAX ), K=1,KMAX )
2544 WRITE (37) IMAX , KMAX
2545 WRITE (37) AMINF, ALFAD, REREAL, TIME
2546 WRITE (37) ( ( Q1(I,K), I=1,IMAX ), K=1,KMAX )
2547 WRITE (37) ( ( Q2(I,K), I=1,IMAX ), K=1,KMAX )
2548 WRITE (37) ( ( Q3(I,K), I=1,IMAX ), K=1,KMAX )
2549 WRITE (37) ( ( Q4(I,K), I=1,IMAX ), K=1,KMAX )
2550 REWIND 37
2551 END IF
2552 IF (ITN.EQ.8*NOUT) THEN
2553 REWIND 38
2554 WRITE (38) IMAX , KMAX
2555 WRITE (38) ( ( X(I,K), I=1,IMAX ), K=1,KMAX )
2556 WRITE (38) ( ( Z(I,K), I=1,IMAX ), K=1,KMAX )
2557 WRITE (38) IMAX , KMAX
2558 WRITE (38) AMINF, ALFAD, REREAL, TIME
2559 WRITE (38) ( ( Q1(I,K), I=1,IMAX ), K=1,KMAX )
2560 WRITE (38) ( ( Q2(I,K), I=1,IMAX ), K=1,KMAX )
2561 WRITE (38) ( ( Q3(I,K), I=1,IMAX ), K=1,KMAX )
2562 WRITE (38) ( ( Q4(I,K), I=1,IMAX ), K=1,KMAX )
2563 REWIND 38
2564 END IF
2565 IF (ITN.EQ.9*NOUT) THEN
2566 REWIND 39
2567 WRITE (39) IMAX , KMAX
2568 WRITE (39) ( ( X(I,K), I=1,IMAX ), K=1,KMAX )
2569 WRITE (39) ( ( Z(I,K), I=1,IMAX ), K=1,KMAX )
2570 WRITE (39) IMAX , KMAX
2571 WRITE (39) AMINF, ALFAD, REREAL, TIME

```

LINE #	SOURCE TEXT
--------	-------------

2572	WRITE (39) ((Q1(I,K), I=1,IMAX), K=1,KMAX)
2573	WRITE (39) ((Q2(I,K), I=1,IMAX), K=1,KMAX)
2574	WRITE (39) ((Q3(I,K), I=1,IMAX), K=1,KMAX)
2575	WRITE (39) ((Q4(I,K), I=1,IMAX), K=1,KMAX)
2576	END IF
2577	IF(ITN .EQ. 10*NOUT) THEN
2578	REWIND 40
2579	WRITE (40) IMAX , KMAX
2580	WRITE (40) ((X(I,K), I=1,IMAX), K=1,KMAX)
2581	WRITE (40) ((Z(I,K), I=1,IMAX), K=1,KMAX)
2582	WRITE (40) IMAX , KMAX
2583	WRITE (40) AMINF, ALFAD, REREAL, TIME
2584	WRITE (40) ((Q1(I,K), I=1,IMAX), K=1,KMAX)
2585	WRITE (40) ((Q2(I,K), I=1,IMAX), K=1,KMAX)
2586	WRITE (40) ((Q3(I,K), I=1,IMAX), K=1,KMAX)
2587	WRITE (40) ((Q4(I,K), I=1,IMAX), K=1,KMAX)
2588	END IF
2589	IF(ITN .EQ. 11*NOUT) THEN
2590	REWIND 41
2591	WRITE (41) IMAX , KMAX
2592	WRITE (41) ((X(I,K), I=1,IMAX), K=1,KMAX)
2593	WRITE (41) ((Z(I,K), I=1,IMAX), K=1,KMAX)
2594	WRITE (41) IMAX , KMAX
2595	WRITE (41) AMINF, ALFAD, REREAL, TIME
2596	WRITE (41) ((Q1(I,K), I=1,IMAX), K=1,KMAX)
2597	WRITE (41) ((Q2(I,K), I=1,IMAX), K=1,KMAX)
2598	WRITE (41) ((Q3(I,K), I=1,IMAX), K=1,KMAX)
2599	WRITE (41) ((Q4(I,K), I=1,IMAX), K=1,KMAX)
2600	END IF
2601	IF(ITN .EQ. 12*NOUT) THEN
2602	REWIND 42
2603	WRITE (42) IMAX , KMAX
2604	WRITE (42) ((X(I,K), I=1,IMAX), K=1,KMAX)
2605	WRITE (42) ((Z(I,K), I=1,IMAX), K=1,KMAX)
2606	WRITE (42) IMAX , KMAX
2607	WRITE (42) AMINF, ALFAD, REREAL, TIME
2608	WRITE (42) ((Q1(I,K), I=1,IMAX), K=1,KMAX)
2609	WRITE (42) ((Q2(I,K), I=1,IMAX), K=1,KMAX)
2610	WRITE (42) ((Q3(I,K), I=1,IMAX), K=1,KMAX)
2611	WRITE (42) ((Q4(I,K), I=1,IMAX), K=1,KMAX)
2612	END IF
2613	IF(ITN .EQ. 13*NOUT) THEN
2614	REWIND 43
2615	WRITE (43) IMAX , KMAX
2616	WRITE (43) ((X(I,K), I=1,IMAX), K=1,KMAX)
2617	WRITE (43) ((Z(I,K), I=1,IMAX), K=1,KMAX)
2618	WRITE (43) IMAX , KMAX
2619	WRITE (43) AMINF, ALFAD, REREAL, TIME
2620	WRITE (43) ((Q1(I,K), I=1,IMAX), K=1,KMAX)
2621	WRITE (43) ((Q2(I,K), I=1,IMAX), K=1,KMAX)
2622	WRITE (43) ((Q3(I,K), I=1,IMAX), K=1,KMAX)
2623	WRITE (43) ((Q4(I,K), I=1,IMAX), K=1,KMAX)
2624	END IF
2625	IF(ITN .EQ. 14*NOUT) THEN
2626	REWIND 44
2627	WRITE (44) IMAX , KMAX
2628	WRITE (44) ((X(I,K), I=1,IMAX), K=1,KMAX)
2629	WRITE (44) ((Z(I,K), I=1,IMAX), K=1,KMAX)
2630	WRITE (44) IMAX , KMAX
2631	WRITE (44) AMINF, ALFAD, REREAL, TIME
2632	WRITE (44) ((Q1(I,K), I=1,IMAX), K=1,KMAX)
2633	WRITE (44) ((Q2(I,K), I=1,IMAX), K=1,KMAX)
2634	WRITE (44) ((Q3(I,K), I=1,IMAX), K=1,KMAX)
2635	WRITE (44) ((Q4(I,K), I=1,IMAX), K=1,KMAX)
2636	END IF
2637	RETURN
2638	END

```

LINE # SOURCE TEXT
1 PROGRAM AIRFGRID
2 PARAMETER (IX=100,KX=100)
3 COMMON/GRID1/X(IX,KX),Z(IX,KX)
4 COMMON/DGRID/DT,IMAX,KMAX,ITEL,ITEU
5 LOGICAL VISCOUS
6 READ(5,10)
7 READ(5,100) IMAX,KMAX
8 READ(5,10)
9 READ(5,100) ITEL,ITEU
10 READ(5,10)
11 READ(5,200) VISCOUS
12 READ(5,10)
13 READ(5,300) DMIN
14 READ(5,10)
15 READ(5,*) AORAT , AOEXP , sdispl
16 ILE = ( ITEU + ITEL ) / 2
17 IUP = ( ITEU - ITEL ) / 2
18 WRITE(6,1000) IMAX,KMAX,ITEL,ITEU,ILE,IUP,DMIN,AORAT
19 1000 FORMAT('Imax = ',I10,10x,'kmax = ',I10,5x,/,
20 1 'Trailing edge lower = ',I10,/,
21 2 'Trailing edge upper = ',I10,/,
22 2 'Leading edge = ',I10,/,
23 2 'Upper = llower = ',I10,/,
24 3 'Distanse of the first point = ',F20.10,/,
25 4 'Strechbing ratio = ',F20.10,/)
26 CALL AIRFOL( AORAT , AOEXP , sdispl )
27 IF( VISCOUS ) CALL CLUSTR( DMIN )
28 C
29 WRITE(6,1100)
30 1100 FORMAT(//,'GRID BOUNDARIES',/)
31 RTEOUT = ABS( X(1,1) - X(ITEL,1) )
32 RLEIN = ABS( X(ILE,KMAX) - X(ILE,1) )
33 IUP = ILE + ( ITEU - ILE ) / 2
34 RUP = ABS( Z(IUP,KMAX) - Z(IUP,1) )
35 WRITE(6,1200) RTEOUT , RLEIN , RUP
36 1200 FORMAT(5X,'Distanse between trailing edge ans outflow = ',F20.10,/,
37 1 5x,'Distanse " leading edge and inflow = ',F20.10,/,
38 2 5x,'Distanse of the body from the upper boudary=',F20.10,/)
39 REWIND 21
40 WRITE (21) IMAX,KMAX
41 WRITE (21) (( X(I,K), I=1,IMAX), K=1,KMAX ),
42 1 (( Z(I,F), I=1,IMAX), K=1,KMAX )
43 STOP
44 10 FORMAT(1X)
45 100 FORMAT(2I5)
46 200 FORMAT(3L5)
47 300 FORMAT(4F10.0)
48 END

```

```

LINE # SOURCE TEXT
49 SUBROUTINE METRIC
50 C.....
51 C*
52 C* SUBROUTINE METRIC
53 C*
54 C.....
55 PARAMETER (IX=300,KX=100)
56 COMMON/PIX/OMEGA,HDOT
57 COMMON/DGRID/DT,IMAX,KMAX,ITEL,ITEU
58 COMMON/GRID1/X(IX,KX),Z(IX,KX)
59 COMMON/GRID/YACOB(IX,KX)
60 COMMON/MTRIX/XIX(IX,KX),XIZ(IX,KX),ZETAX(IX,KX),ZETAZ(IX,KX),
61 IXIT(IX,KX),ZETAT(IX,KX)
62 C
63 C*** THE SUBROUTINE METRIC COMPUTES THE METRICS IN ALL THE TWO DIRECTIONS AND
64 C THE UNSTEADY COEFFICIENTS ETAT ETC.
65 C
66 DO 1000 K = 1 , KMAX
67 DO 1000 I = 1 , IMAX
68 XTAU = OMEGA * Z(I,K)
69 YTAU = OMEGA * (-X(I,K))- HDOT
70 C*** PRESENT SET UP IS FOR FLOW PAST AN AIRFOIL.
71 C
72 IF(I.EQ.1.OR.I.EQ.IMAX) GO TO 10
73 XXI = .5 * (X(I+1,K)-X(I-1,K))
74 ZXI = .5 * (Z(I+1,K)-Z(I-1,K))
75 GO TO 15
76 10 IF(I.EQ.IMAX) GO TO 16
77 XXI = 1.0 * (X(2,K) - X(1,K))
78 ZXI = 1.0 * (Z(2,K) - Z(1,K))
79 GO TO 15
80 16 XXI = 1.0 * (X(IMAX,K) - X(IMAX-1,K))
81 ZXI = 1.0 * (Z(IMAX,K) - Z(IMAX-1,K))
82 15 CONTINUE
83 IF(K.EQ.1.OR.K.EQ.KMAX) GO TO 17
84 XZET = .5 * (X(I,K+1)-X(I,K-1))
85 ZZET = .5 * (Z(I,K+1)-Z(I,K-1))
86 GO TO 20
87 17 IF(K.EQ.KMAX) GO TO 18
88 XZET = 2. * X(I,2)-1.5 * X(I,1) - .5 * X(I,3)
89 ZZET = 2. * Z(I,2) - 1.5 * Z(I,1) - .5 * Z(I,3)
90 GO TO 20
91 18 XZET = 1.5 * X(I,KMAX)-2. * X(I,KMAX-1)+.5*X(I,KMAX-2)
92 ZZET = 1.5 * Z(I,KMAX)-2. * Z(I,KMAX-1)+.5*Z(I,KMAX-2)
93 20 CONTINUE
94 YACOBI = XXI * ZZET - XZET * ZXI
95 YACOB(I,K) = 1. / YACOBI
96 XIX(I,K) = ZZET * YACOB(I,K)
97 XIZ(I,K) = -XZET * YACOB(I,K)
98 XTAU = OMEGA * Z(I,K)
99 YTAU = - OMEGA * X(I,K)- HDOT
100 XIX(I,K) = - XIX(I,K) * XTAU - XIZ(I,K) * YTAU
101 ZETAX(I,K) = -ZXI * YACOB(I,K)
102 ZETAZ(I,K) = XXI * YACOB(I,K)
103 ZETAT(I,K) = - ZETAX(I,K) * XTAU - ZETAZ(I,K) * YTAU
104 1000 CONTINUE
105 RETURN
106 END

```

```
LINE # SOURCE TEXT
107 SUBROUTINE WRAP(II,JJ,XSING,YSING,XP,YP,S0,A0,Y0)
108 .....
109 C*
110 C* SUBROUTINE WRAP
111 C*
112 .....
113 PARAMETER (IX=300,KX=100)
114 DIMENSION S0(IX,4),Y0(IX,4),A0(IX,4),XP(1),YP(1)
115 C
116 THIS SUBROUTINE UNWRAPS THE AIRFOIL AND STORES THE UNWRAPPED
117 SURFACE IN ARRAYS A0 AND S0. IT ALSO DETERMINES THE STRETCHING
118 IN THE ETA DIRECTION.
119 C
120 IMID = (II + 1) / 2
121 DY = .8 / (JJ - 2)
122 DO 1 J = 2, JJ
123 Y = FLOAT(J-2) * DY
124 1 Y0(J,1) = 1.25 * Y / (1. - Y * Y)
125 Y0(1,1) = - Y0(3,1)
126 PI = 4. * ATAN ( 1.)
127 ANGL = PI + PI
128 U = XP(1) - XSING
129 V = YP(1) - YSING
130 U = 1.
131 V = 0.
132 IIM1 = II - 1
133 DO 2 I = 1, II
134 X11 = XP(I) - XSING
135 Y11 = YP(I) - YSING
136 ANGL = ANGL + ATAN2((U*Y11-V*X11),(U*X11+V*Y11))
137 R = SORT(X11**2 + Y11**2)
138 U = X11
139 V = Y11
140 R = SORT(R)
141 A0(I,1) = R * COS(.5 * ANGL)
142 2 S0(I,1) = R * SIN(.5 * ANGL)
143 WRITE (6,1000)
144 C WRITE (6,2000) (I,A0(I,1),S0(I,1),I = 1, II)
145 RETURN
146 C
147 1000 FORMAT(IX,'UNWRAPPED COORDINATES IN THE TRANSFORMED PLANE')
148 2000 FORMAT(I5, 2F20.8)
149 END
```

```

LINE #          SOURCE TEXT
149          SUBROUTINE TABINT(XP,YP,XSING,YSING,N,sdispl)
150          C*****
151          C*
152          C*          SUBROUTINE TABINT
153          C*
154          C*****
155          PARAMETER (IX=300,KX=100)
156          DIMENSION XP(IX),YP(IX),SO(IX),A0(IX),DTHXI(IX),DXW(IX),DX(IX)
157          COMMON/DGRID/DT,IMAX,KMAX,ITEL,ITEU,ILE
158          PI = 4.*ATAN(1.)
159          U = XP(1) - XSING
160          V = YP(1) - YSING
161          U = 1.
162          V = 0.
163          ANGL = 8. * ATAN(1.)
164          DO 1 I = 1,N
165          X11 = XP(I) - XSING
166          Y11 = YP(I) - YSING
167          ANGL = ANGL + ATAN2((U*Y11-V*X11),(U*X11+V*Y11))
168          R = SQRT(X11**2 + Y11 ** 2)
169          U = X11
170          V = Y11
171          R = SQRT(R)
172          A0(I) = R * COS(ANGL * .5)
173          1 SO(I) = R * SIN(ANGL * .5)
174          C
175          A0L = A0(N) - A0(1)
176          DXWS = 0.0
177          C
178          AOST = A0(1)
179          idiv = 1 + ( iteu - itel )
180          C
181          THDX = 0.
182          DTHXI(1) = 0.
183          DTHXI(2) = pi* SDISPL/2.
184          DTHX = (1.- SDISPL ) * PI / (IDIV-1)
185          DO 9 I= 3, IDIV
186          9 DTHXI(I) = DTHXI(I-1) + DTHX
187          DO 10 I = 1, IDIV
188          THDX = (I-1)*DTHX
189          if( i .eq. 2 .or. i .eq. idiv ) then          tbdx = .5*sdispl * pi + thdx
190          if( i .eq. 2 )                                tbdx = ( 1.-sdispl)*pi
191          if( i .eq. idiv )
192          else
193          tbdx = tdx
194          endif
195          THDX = DTHXI(I)
196          c          tbdxd = (180/pi)*thdx
197          c          write(6,*) I, tbdxd
198          DXW(I) = abs ( SIN( THDX ) )
199          10 DXWS = DXWS + DXW(I)
200          DO 20 I = 1, IDIV
201          20 DX(I) = DXW(I) * A0L / DXWS
202          DXI = 0.
203          DO 3 I = 1 , IDIV
204          DXI = DXI + DX(I)
205          XX = DXI + AOST
206          CALL TAINT(A0,SO,XX,YY,N,3,NER,MON)
207          XP(I) = XX * XX - YY * YY + XSING
208          3 YP(I) = 2. * XX * YY + YSING
209          RETURN
210          END

```

LINE # SOURCE TEXT

```
211 C
212 SUBROUTINE TAIN(TAB,FTAB,X,FX,N,K,NER,MON)
213 .....
214 C
215 SUBROUTINE TAIN
216 .....
217 C
218 PARAMETER (IX=300,KX=100)
219 DIMENSION XTAB(1),FTAB(1),T(10),C(10)
220
221 NASA - AMES SUBROUTINE FOR POLYNOMIAL INTERPOLATION
222 OF A TABULATED FUNCTION
223 C
224 IF(N-K) 1, 1, 2
225 1 NER = 2
226 RETURN
227 2 IF(K-9) 3,3,1
228 3 IF(MON) 4,4,5
229 5 IF(MON-2) 6,7,4
230 4 J = 0
231 NML = N - 1
232 DO 8 I = 1, NML
233 IF(XTAB(I) - XTAB(I+1)) 9,11,10
234 11 NER = 3
235 RETURN
236 9 J = J-1
237 GO TO 8
238 10 J = J+1
239 8 CONTINUE
240 MON = 1
241 IF(J) 12, 6, 6
242 12 MON = 2
243 7 DO 13 I = 1, N
244 IF(X - XTAB(I)) 14,14,13
245 14 J = I
246 GO TO 18
247 13 CONTINUE
248 GO TO 15
249 6 DO 16 I = 1, N
250 IF(X-XTAB(I)) 16,17,17
251 17 J = I
252 GO TO 18
253 16 CONTINUE
254 15 J = N
255 18 J = J - (K-1) / 2
256 IF(J) 19,19,20
257 19 J = 1
258 20 M = J + K
259 IF(M - N) 21,21,22
260 22 J = J - 1
261 GO TO 20
262 21 KP1 = K + 1
263 JSAVE = J
264 26 DO 23 L = 1, KP1
265 C(L) = X - XTAB(J)
266 T(L) = FTAB(J)
267 J = J+1
268 DO 24 J = 1,K
269 I = J+1
270 T(I) = (C(J)*T(I)-C(I)*T(J))/(C(J)-C(I))
271 I = I-1
272 IF(I-FP1) 25,25,24
273 24 CONTINUE
274 FX = T(KP1)
275 NER = 1
276 RETURN
277 END
```

LINE #	SOURCE TEXT
278	SUBROUTINE SING(N2,N,X,Z,XLE,YLE,TEA,TES,XSING,YSING,CHD)
279	C.....
280	C*
281	C* SUBROUTINE SING
282	C*
283	C.....
284	PARAMETER (IX=300,KX=100)
285	C
286	C
287	C THIS SUBROUTINE COMPUTES SINGULAR POINT LOCATIONS.
288	C
289	C
290	DIMENSION X(2) , Z(2)
291	NU = N2
292	N1 = N2 + 1
293	N3 = N2 - 1
294	X1 = X(N1)
295	Z1 = Z(N1)
296	X2 = X(N2)
297	Z2 = Z(N2)
298	X3 = X(N3)
299	Z3 = Z(N3)
300	D1 = X2 ** 2 - X1 ** 2
301	D2 = Z2 ** 2 - Z1 ** 2
302	D3 = X2 - X1
303	D4 = Z2 - Z1
304	D5 = X3 ** 2 - X1 ** 2
305	D6 = Z3 ** 2 - Z1 ** 2
306	D7 = X3 - X1
307	D8 = Z3 - Z1
308	B = (D7 * (D1 + D2) - D3*(D5+D6))/(2. * (D7*D4-D3*D8))
309	IF(ABS(D3) .LT. ABS(D7)) GO TO 10
310	A = (D1 + D2 - 2. * B * D4) / (2. * D3)
311	GO TO 20
312	10 A = (D5 + D6 - 2. * B * D8) / (2. * D7)
313	20 CONTINUE
314	R = SQRT((X2-A)** 2 + (Z2-B)**2)
315	XLE = X(NU)
316	YLE = Z(NU)
317	CHD = X(1) - X(NU)
318	A2 = (Z(2)-Z(1)) / (X(2) - X(1))
319	A1 = (Z(N)-Z(N-1)) / (X(N)-X(N-1))
320	TES = .5 * (A1 + A2)
321	TEA = A2 - A1
322	TEA = TEA + 57.29578
323	XSING = (A+XLE) / 2.
324	YSING = (B+YLE) / 2.
325	RETURN
	END

```

LINE # SOURCE TEXT
326 SUBROUTINE AIRPOL( AORAT , a0exp ,sd1spl)
327 C.....
328 C* SUBROUTINE AIRPOL
329 C.....
330 PARAMETER (IX=300,KX=100)
331 COMMON/GRID1/X(IX,KX),Z(IX,KX)
332 COMMON/DGRID/DT,IMAX,KMAX,ITEL,ITEU
333 COMMON/YSYM/ISYM
334 DIMENSION SO(IX,4),AO(IX,4),YO(IX,4),XP(IX),YP(IX),
335 1E(IX),F(IX),BO(IX)
336 DIMENSION XL(IX), XU(IX), YL(IX), YU(IX),
337 2 XX(IX), YY(IX)
338
339 C
340 DATA (BO(I),I=1,32)/1.,1.8414,1.8836,1.1270,1.1715,1.2175,1.2651,
341 11.3145,1.3659,1.4199,1.4755,1.5349,1.5973,1.6636,1.7342,1.8099,
342 21.8914,1.9799,2.0764,2.1829,2.3012,2.4341,2.5853,2.7597,2.9646,
343 33.2106,3.5141,3.9019,4.4219,5.1687,6.3632,8.6809/
344
345 C
346 READ(5,*) ISYM, IBMAX
347 IF( ISYM .EQ. 1 ) THEN
348 DO 101 I=1,IBMAX
349 101 READ(5,*) XU(I), YU(I)
350 ELSE
351 DO 102 I=1,IBMAX
352 102 READ(5,*) XU(I), YU(I), YL(I)
353 CONTINUE
354 ENDIF
355 IF( ISYM .EQ. 1 ) THEN
356 DO 103 I=1,IBMAX
357 103 YL(I) = - YU(I)
358 ENDIF
359 C
360 DO 1000 I=1,IBMAX
361 IU = I + IBMAX
362 IX(IU) = XU(I)
363 YI(IU) = YU(I)
364 IL = IBMAX - I + 1
365 IX(IL) = XU(IL)
366 YI(IL) = YL(IL)
367 1000 CONTINUE
368 C
369 IBMAX2 = 2*IBMAX
370 DO 1010 I=1,IBMAX2
371 XP(I) = XX(I)
372 YP(I) = YY(I)
373 1010 CONTINUE
374 C
375 FNU = IBMAX
376 FNL = IBMAX
377 C
378 THIS SUBROUTINE GENERATES SHEAR PARABOLIC C-GRID
379 THE FOLLOWING SUBROUTINES ARE RELATED TO THE GRID GENERATION
380 C
381 WRAP SING
382 TABINT CLUSTR
383 TAINI STRIC
384 C
385 AO(1,1) = 1.
386 DO 8 I = 2 , IBMAX
387 B AO(I,1) = ( AO(I-1,1) * AORAT )**AOEXP
388 PI = 4. * ATAN(1.)
389 NU = FNU
390 NL = FNL
391 N = NU + NL
392 IT = ITEL
393 IE = ITEU
394 ILE = ( ITEL + ITEU ) / 2
395 II = IMAX
396 JJ = KMAX-1
397 IIP1 = II + 1
398 IIM1 = II - 1
399 IIJJ = II * JJ
400 IIJJ2 = II * ( JJ-2)
401 C
402 SCALE = 1. / ( XP(1) - XP(NL) )
403 DO 3333 I=1,N
404 XP(I) = XP(I) * SCALE
405 YP(I) = YP(I) * SCALE
406 3333 CONTINUE
407 CALL SING(NU,N,XP,YP,XLE,ZLE,TEA,TES,XSING,YSING,CBD)
408 CALL TABINT(XP,YP,XSING,YSING,N,sd1spl)
409 NBODY = IE + 1 - IT
410 DO 6791 I = 1 , NBODY
411 L = I - 1
412 E(IT+L) = XP(I)
413 6791 F(IT+L) = YP(I)
414 IEPI = IE + 1
415 SLOPT = TES * .75
416 DO 438 I = IEPI , II
417 I1 = I + 1 - IE
418 E(I) = AO(I1,1)
419 DXI = 1. / 48.
420 D = 4. / 3. * (E(I) - .25)
421 F(I) = F(IE) + SLOPT * ALOG(D) / D
422 L = IIP1 - I
423 E(L) = E(I)
424 F(L) = F(IT) + SLOPT * ALOG(D)/D
425 C
426 WRITE (6,439)
427 C439 FORMAT(2X,3B I,19X,19X,19X,19X)
428 WRITE (6,37) (I,E(I),F(I),I = 1 , II)
429 CALL WRAP(II,JJ,XSING,YSING,E,F,SO,AO,YO)
430 DO 10 J = 2 , JJ
431 DO 10 I = 1 , II
432 X(I,J-1) = AO(I,1)**2 - (SO(I,1)+YO(J,1))**2
433 10 Z(I,J-1) = 2. * AO(I,1) * (SO(I,1)+YO(J,1))
434 RETURN
435 37 FORMAT(15,2F20.8)
436 END

```

```

LINE #          SOURCE TEXT
432          SUBROUTINE CLUSTR(DS)
433          C.....
434          C*
435          C*          SUBROUTINE CLUSTR
436          C*
437          C.....
438          PARAMETER (IX=300,KX=100)
439          COMMON/GRID1/X(IX,KX),Z(IX,KX)
440          COMMON/DGRID/DT,IMAX,KMAX,ITEL,ITEU
441          DIMENSION S(IX),XP(IX),YP(IX),R(IX)
442
443          C
444          C          THIS SUBROUTINE CLUSTERS A GIVEN X,Z GRID SUCH THAT THE FIRST POINT IS AT
445          C
446          DO 100 I = 1 , IMAX
447          S(I) = 0.
448          XP(I) = X(I,1)
449          YP(I) = Z(I,1)
450          DO 10 K = 2 , KMAX
451          XP(K) = X(I,K)
452          YP(K) = Z(I,K)
453          10 S(K) = SQRT((XP(K)-XP(K-1))**2+(YP(K)-YP(K-1))**2)
454          1+S(K-1)
455          SUMDX = S(KMAX)
456          C          CALL STRTCH(SUMDX,DS,F1,KMAX,FACTOR)
457          C          WRITE (6,200) I,FACTOR
458          R(I) = 0.
459          DR = DS
460          DO 20 K = 2 , KMAX
461          R(K) = R(K-1) + DR
462          DR = DR * FACTOR
463          20 CONTINUE
464          RLAST = 1. / R(KMAX)
465          DO 30 K = 2 , KMAX
466          R1 = R(K) * RLAST * S(KMAX)
467          CALL TAIN1(S,XP,R1,XP1,KMAX,3,NER,MON)
468          X(I,K) = XP1
469          CALL TAIN1(S,YP,R1,Y1,KMAX,3,NER,MON)
470          Z(I,K) = Y1
471          30 CONTINUE
472          100 CONTINUE
473          C          WRITE (6,115)
474          DO 110 I = 1 , IMAX
475          DX = X(I,2) - X(I,1)
476          DY = Z(I,2) - Z(I,1)
477          DN = SQRT(DX*DX+DY*DY)
478          C          WRITE(6,120) I , DX , DY , DN
479          110 CONTINUE
480          RETURN
481          115 FORMAT(5X,6HNORMAL,1X,8HDISTANCE,3B AT,4B THE,5H WALL,/,
482          1,5H      1,8X,2HDX,8X,2HDY,8X,2BDN,/)
483          120 FORMAT(15,3F10.5)
484          200 FORMAT(15,F10.5)
485          END

```

LINE # SOURCE TEXT

```

485 SUBROUTINE STRTCH(SUMDX,DX1,F1,N1,R)
486 C.....
487 C*
488 C* SUBROUTINE STRTCH
489 C*
490 C.....
491 PARAMETER (IX=300,IX=100)
492 C
493 C THIS SUBROUTINE DETERMINES A GEOMETRIC
494 C PROGRESSION OF GRID SPACING BETWEEN 1 AND N1 SUCH THAT
495 C SUMSDX) EQUALS SUMDX. THE RATIO BETWEEN SUCCESSIVE
496 C SPACINGS IS R.
497 C N = N1 - 1
498 C R = 1.5
499 C E1 = 1.E-04
500 C E2 = 1.E-04
501 C DO 10 L = 1, 50
502 C F= (R-1) * SUMDX - DX1*(R**N-1)
503 C FP = SUMDX - DX1 * FLOAT(N) * R ** (N-1)
504 C RITER = R - F/ FP
505 C IF(1.E-02.LT.RITER.AND.RITER.LT.1.) RITER = 1.
506 C IF(1. LT.RITER.AND.RITER.LT.100.) RITER=.01
507 C IF(ABS(R-RITER).LT. R*E1) GO TO 1
508 C R = RITER
509 C 10 CONTINUE
510 C R = 1.0001
511 C DX1 = DETOT/FLOAT(N1-1)
512 C RETURN
513 C 1 R= RITER
514 C RETURN
515 C END

```

LINE # SOURCE TEXT

```
516 SUBROUTINE ROTGRID(INAX,KMAX,DALFA)
517 C.....
518 C*
519 C* SUBROUTINE ROTGRID
520 C*
521 C.....
522 PARAMETER (IX=300,KI=100)
523 C ROTATE GRID IN THE CLOCKWISE DIRECTION BY AN AMOUNT DALFA
524 COMMON/GRID1/X(IX,KI),Z(IX,KI)
525 CA = COS(DALFA)
526 SA = - SIN(DALFA)
527 DO 20 K = 1 , KMAX
528 DO 20 I = 1 , INAX
529 X1 = X(I,K)
530 Z1 = Z(I,K)
531 X(I,K) = X1 * CA - Z1 * SA
532 Z(I,K) = Z1 * CA + X1 * SA
533 RETURN
534 END
```

20. Ms. L. Cowles 1
 Naval Air Développement Center
 Street Road
 Warminster, PA 18974-5000
21. Dr. W. Tseng 1
 Naval Air Development Center
 Street Road
 Warminster, PA 18974-5000
22. Mr. D. Findlay 1
 Naval Air Development Center
 Street Road
 Warminster, PA 18974-5000
23. Mr. M. Walters 1
 Naval Air Development Center
 Street Road
 Warminster, PA 18974-5000
24. Mr. W. J. King 1
 Technology Area Manager, Aircraft
 Code 212
 Office of Naval Technology
 Arlington, VA 22217-5000
25. Dr. T. Cebeci 1
 Professor and Chairman
 Dept. of Aerospace Engineering
 California State University
 Long Beach, CA 90840
26. Capt. H. Helin 1
 Program Manager, Directorate of Aerospace Sciences
 AFOSRNA
 Bolling AFB
 Washington, D.C. 20332-6448
27. Dr. T. L. Doligalski 1
 Chief, Fluid Mechanics Division
 Army Research Office
 P.O. Box 1221
 Research Triangle Park, NC 27709-2211
29. Lt. Col. Steven Grohsmeyer 2
 P.O. Box 732
 Venice, FL 34284

10. Dr. R. M. Howard 1
Dept. of Aeronautics and Astronautics, Code 67HO
Naval Postgraduate School
Monterey, CA 93943
11. Dr. S. K. Hebbar 1
Dept. of Aeronautics and Astronautics, Code 67HB
Naval Postgraduate School
Monterey, CA 93943
12. Dr. M. S. Chandrasekhara 1
NASA Ames Research Center (M.S. 260-1)
Moffet Field, CA 94035
13. Dr. L. W. Carr 1
NASA Ames Research Center (M.S. 260-1)
Moffet Field, CA 94035
14. Dr. L. E. Schiff 1
NASA Ames Research Center (M.S. 258-1)
Moffet Field, CA 94035
15. Mr. D. P. Bencze 1
Chief, Applied Aerodynamics Branch
NASA Ames Research Center (M.S. 227-6)
Moffet Field, CA 94035
16. Dr. S. Davis 1
NASA Ames Research Center (M.S. 260-1)
Moffet Field, CA 94035
17. Mr. T. S. Momiyama 1
Director, Aircraft Division
Code AIR-931
Naval Air Systems Command
Washington, D.C. 20631-9320
18. Mr. E. Neuman 1
Aircraft Division
Code AIR-931
Naval Air Systems Command
Washington, D.C. 20631-9320
19. Mr. G. Derderian 1
Aircraft Division
Code AIR-931
Naval Air Systems Command
Washington, D.C. 20631-9320

INITIAL DISTRIBUTION LIST

		No. Copies
1.	Commandant of the Marine Corps Code TE 06 Headquarters, U.S. Marine Corps Washington, D.C. 20380-0001	1
2.	Library, Code 52 Naval Postgraduate School Monterey, CA 93943-5002	2
3.	Dr. J. A. Ekaterinaris NASA Ames Research Center (M.S. 260-1) Moffet Field, CA 94035	5
4.	Defense Technical Information Center Cameron Station Alexandria, VA 22304-6145	2
5.	Dr. E. R. Wood Chairman Dept. of Aeronautics and Astronautics, Code 67WD Naval Postgraduate School Monterey, CA 93943-5002	1
6.	Dr. M. F. Platzler Dept. of Aeronautics and Astronautics, Code 67PL Naval Postgraduate School Monterey, CA 93943-5002	5
7.	Dr. L. V. Schmidt Dept. of Aeronautics and Astronautics, Code 67SC Naval Postgraduate School Monterey, CA 93943-5002	1
8.	Dr. R. P. Shreeve Dept. of Aeronautics and Astronautics, Code 67SF Naval Postgraduate School Monterey, CA 93943-5002	1
9.	Dr. R. Kolar Dept. of Aeronautics and Astronautics, Code 67KJ Naval Postgraduate School Monterey, CA 93943-5002	1